



**University of
Nottingham**

UK | CHINA | MALAYSIA

**Cell-free protein synthesis for on-site and
on-demand biomanufacturing in extreme
and low resource environments**

Tejasvi Shivakumar

University of Nottingham

Thesis submitted to the University of Nottingham for the degree of Doctor of
Philosophy

August 2023

Declaration

I confirm that the work presented in this thesis is my own. Information derived from other sources has been indicated, where necessary. The work described in this thesis was performed under the guidance of the following supervisors:

Professor Phil Williams

Dr Ingrid Dreveny

Dr Anna Croft

Professor Alex Conradie (now at University College London)

This work was supported by the following funding: Engineering and Physical Sciences Research Council [EP/R513283/1] and the University of Nottingham.

Abstract

Humans are starting to explore extreme environments such as space due to advancements in Science and Technology. Although current manned missions have involved short-durations with emergency supply or return to earth, future long-duration space travel will not have this luxury. Moreover, 87% of current spaceflight medications have a limited shelf-life of less than 2 years. Therefore, there is a severely limited capacity to supply a pharmacy for human exploration of Mars, which is a combined goal of 15 space agencies in the next decade. This research project, under the theme 'astropharmacy', aims to address this challenge through on-demand and on-site synthesis of biopharmaceuticals.

The increasing share of biologics in the pharmaceutical market can be attributed to their therapeutic abilities against challenging targets, but they are conventionally produced in centralized, large-scale facilities using living cells, and typically require cold chain storage and transportation. This severely limits their applicability in low-resource and extreme environments, where a largely untreated human population are present. A platform based on cell-free protein synthesis (CFPS) technology is capable of surpassing many limitations of cell-based expression and is the system of choice for the astropharmacy vision in this thesis.

This thesis begins by describing the development and optimisation of an in-house CFPS system, which was optimised for high-level protein production, using chromogenic reporter superfolder green fluorescent protein (*sfGFP*) as a model. Next, the system was benchmarked against commercial systems such as the NEB PURExpress and Promega *E.coli* S30A extract system for circular DNA, with *sfGFP* yields increasing and surpassing commercial systems and others reported in literature. The *sfGFP* yield improvements are seen from 0.8 mg/mL in experiments described in the initial chapter to > 5 mg/mL in that of the final chapters.

Experimentation with freeze-drying, microglassificationTM and cellulose stacks were carried out in order to explore platforms with ease-of-storage and distribution. Lyophilised pellets and cellulose stacks were two main approaches that met some astropharmacy goals. The latter platform was composed of lyophilised CFPS components on cellulose discs, which were layered and rehydrated to kickstart protein synthesis. Such paper-encompassed reactions were shown to be capable of robust expression after drying, and the system can be modulated by simply changing the DNA element.

To further address the gap in our knowledge of storing and transporting active CFPS compounds for longer periods of time, stability studies were conducted. This was particularly important for VITA (Visualising In-situ Tx-TI Astropharmaceuticals); a student payload being developed with the European Space Agency. VITA aims to become Nottingham's first astropharmacy technology demonstration mission on the International Space Station. The thesis finishes with a short, but final note on producing therapeutic proteins-of-interest using the developed platform, along with ideas and initial experiments for *in situ* purification. As this research progresses, numerous applications in healthcare for space and Earth, such as elimination of transport and provision in extreme environments, are hoped to be realized.

Keywords: Cell-free protein synthesis; on-demand biomanufacturing; protein therapeutics; freeze-drying; *sfGFP* reporter; stability testing; protein purification; quality control

Acknowledgments

This Astropharmacy PhD journey has been nothing short of 'weird and wonderful', to which this thesis is dedicated. Having spent countless hours spent exploring its mysteries, it is important to acknowledge the stellar individuals who have made the last few years an unforgettable cosmic voyage.

I would like to express my sincere gratitude to my supervisor, Professor Phil Williams. His unbounded creativity truly set the tone for this research - thank you for introducing me to Astropharmacy and encouraging orbits into realms of crazy ideas. Further thanks to Dr. Anna Croft, Dr. Ingrid Dreveny and Professor Alex Conradie for their guidance and expertise – your celestial wisdom, and ability to decipher my convoluted ideas were nothing short of miraculous. Dr. Valentine Anyanwu, you were truly an otherworldly mentor and I will always cherish the times we were trying to figure out extremophiles. I must extend further thanks to Dr. Nigel Savage and ESA Academy for providing the opportunity to actually lift-off a part of this thesis. Being able to send the science I developed (and therefore a part of my soul) to the ISS feels like something out of a movie!

A great deal of gratitude to my family, who provided unwavering support through the last 3.5 years. Your belief in me gave me the propulsion I needed - thank you for enduring my ramblings about esoteric scientific concepts and pretending to understand them. To my fellow doctoral comrades (you know who you are), you are the souls who have brightened the corners of this academic universe. Thank you for your ability to warp time, for challenging my assumptions, and for reminding me that it's okay to embrace the alien in us.

Lastly, I am indebted to the various coffee shops on our beautiful campus. Their strong gravitational pull was inescapable during moments of frustration and hangry/under-caffeinated meteor storms. Godspeed to all future pharmanauts!

Table of contents

Declaration	ii
Abstract	iii
Acknowledgments	v
List of Figures	x
List of Tables	xiii
Abbreviations	xiv
Impact statement	xvi
Chapter 1 Introduction	1
1.1 Astropharmacy and Astromedicine	1
1.1.1 Humans in extreme environments	1
1.1.2 Why astropharmacy?.....	3
1.2 Cell-free protein synthesis	5
1.2.1 An introduction to protein synthesis	5
1.2.2 Fundamentals of cell-free protein synthesis.....	6
1.2.3 Historical overview of CFPS.....	7
1.2.4 Cell-free components.....	8
1.2.5 CFPS formats	11
1.2.6 Applications of CFPS.....	14
1.3 On-demand biomanufacturing	16
1.3.1 The need for on-demand biomanufacturing.....	16
1.3.2 Examples of cell-based biomanufacturing methods	16
1.3.3 The advantages of cell-free biomanufacturing	17
1.3.4 Delivery of pure, functional, and approved products.....	18
1.4 Research opportunities.....	23
1.5 Aims and objectives	29
Chapter 2 Methodology	31
2.1 Materials	31
2.2 Methods in microbiology and molecular biology	31
2.2.1 Bacterial growth	31
2.2.2 <i>E. coli</i> strains and cryostock preparation	32

2.2.3 Plasmid design	33
2.3 CFPS reactions	37
2.3.1 Commercial kits.....	37
2.3.2 Extract preparation	37
2.3.3 CFPS buffer components preparation.....	38
2.3.4 Setting up a cell-free protein synthesis reaction	40
2.3.5 Freeze-dried CFPS on cellulose stacks	41
2.3.6 Microclassification of CFPS components	41
2.4 Analytical methods.....	42
2.4.1 Protein concentration.....	42
2.4.2 Quantification of fluorescence and protein yield	42
2.4.3 SDS-Page and western blotting.....	43
2.4.4 RT-qPCR analysis.....	44
2.4.5 FTIR spectra collective and data analysis	45
2.4.6 CD spectra collection	46
2.4.7 Statistical analysis and software	46
2.5 Other methods.....	46
2.5.1 Lyophilisation.....	46
2.5.2 Stability studies	47
2.5.3 Bead-based protein purification.....	47
2.5.4 ÄKTA start column-based protein purification.....	48
Chapter 3 Generation of in-house bacterial cell-free extract and DNA templates	49
3.1 Introduction and aims	49
3.2 Results and discussion	50
3.2.1 Development of the BL21 Star (DE3) – pAR1219 strain	50
3.2.2 Development of fluorescence reporter templates: sfGFP and sfGFP-His..	56
3.2.3 Generation of therapeutic protein constructs	61
3.3 Summary	63
Chapter 4 Development and optimisation of CFPS and experimenting with formats for on-demand manufacturing	65
4.1 Introduction	65
4.2 Results and discussion	66

4.2.1 Commercial kits provide a good understanding of highly efficient CFPS	66
4.2.2 Development and optimisation of a fully functional in-house CFPS system	69
4.2.3 CFPS formats that enable on-site, on-demand synthesis	75
4.3 Summary	92
Chapter 5 Improving stability of CFPS for VITA (Visualising In-Situ Tx-TL Astro pharmaceuticals)	94
5.1 Introduction	94
Results and discussion	95
5.1.1 Introduction to VITA (Visualising In-situ Tx-TL Astro pharmaceuticals)	95
5.1.2 Stability studies for CFPS shelf life determination	105
5.1.3 Impact of various supplements on CFPS kinetics	109
5.1.4 From short-term to long-term stability: An iterative process	115
5.2 Summary	124
Chapter 6 Towards obtaining functional and pure therapeutics from cell-free systems	126
6.1 Introduction	126
6.2 Results and discussion	127
6.2.1 Cell-free expression of therapeutic proteins	127
6.2.2 Purification of cell-free products	133
6.2.3 Structural and functional studies of cell-free synthesised proteins	136
6.2.4 Co-expression studies	146
6.3 Summary	150
Chapter 7 Conclusions	152
7.1 Recap of project objectives	152
7.2 Overall conclusions and achievement of research objectives	153
7.3 Recommendations for Future Research	155
7.4 Future work for addressing challenges of on-demand biomanufacturing	157
7.5 Meeting regulatory standards	158
References	160
Supplementary information	176
Synthetic DNA fragments	176

> sfGFP_His.....	176
> Reteplase_His	176
> Entolimod_His.....	177
> G-CSF_His.....	177
> Alfimeprase_His.....	178
> Teriparatide_His	178
> NBS07_His.....	178
Plasmid maps	179
> sfGFP_His.....	179
> Reteplase_His	180
> Entolimod_His.....	181
> G-CSF_His.....	182
> Alfimeprase_His.....	183
> Teriparatide_His	184
> NBS07_His.....	185
<i>In situ</i> purification templates (<i>In silico</i> designs).....	185
Cellulose binding domain linker strategies for <i>in situ</i> purification	186
Room temperature measurements for stability studies.....	187
Impact of refrigeration on post-flight cell-free samples until for the VITA mission	188

List of Figures

Figure 1.1: Effects of spaceflight on the human body.....	3
Figure 1.2: Illustration of transcription and translation and the various cellular machinery required.	5
Figure 1.3: Overview of Cell-Free Protein Synthesis (CFPS)	7
Figure 1.4: The role of ATP in protein synthesis	10
Figure 1.5: Summary of the components, formats and applications of cell-free systems	23
Figure 1.6: Swiss homology models of the five therapeutic proteins, created using SwissModel (Expasy) and images generated using PyMOL 2.5.5 (Schrödinger, Inc.)	26
Figure 3.1: A stained agarose gel showing DNA corresponding to plasmid purified from BL21 Star (DE3) – pAR1219 cells.....	51
Figure 3.2: SDS-Page analysis of (a) BL21 Star (DE3) and (b) BL21 Star (DE3)-pAR1219	52
Figure 3.3: Experimental set up for time course analysis of BL21 Star (DE3) – pAR1219.	53
Figure 3.4: SDS-Page analysis of (a) soluble and (b) insoluble BL21 Star (DE3)-pAR1219 cell extract	54
Figure 3.5: SDS-Page analysis of (a) soluble and (b) insoluble BL21 Star (DE3)-pAR1219 cell extract	55
Figure 3.6: SDS-Page analysis of (a) soluble and (b) insoluble BL21 Star (DE3)-pAR1219 cell extract	55
Figure 3.7: Structure of sfGFP.	56
Figure 3.8: Cloning of pET20b(+) – sfGFP.....	58
Figure 3.9: Verification of pET20b(+) – sfGFP	59
Figure 3.10: Cloning of pET20b(+) – sfGFP-His.....	60
Figure 3.11: Stained 1% agarose gel showing amplified pUC57 DNA.....	61
Figure 3.12: Stained 1% agarose gel showing restriction digested fragments.....	61
Figure 3.13: Stained 1% agarose gel showing plasmids extracted from various NEB5 α colonies transformed with ligated DNA	62
Figure 3.14: Stained 1% agarose gel.....	63

Figure 4.1: CFPS using commercial kits.....	67
Figure 4.2: In-house extract preparation.....	69
Figure 4.3: Higher energy mix concentration contributes to higher protein yield	70
Figure 4.4: Optimisation of magnesium glutamate (Mg-Glu) and DNA concentrations for CFPS.....	71
Figure 4.5: Effects of supplementation of PEG on CFPS	73
Figure 4.6: Development of an in-house cell-free system.....	75
Figure 4.7: Overview of the four formats explored for on-site and on-demand applications of CFPS.....	76
Figure 4.8: Overview of the microclassification procedure	77
Figure 4.9: Effect of microclassification on CFPS	79
Figure 4.10: Effect of RNA supplementation on CFPS using microclassified cell-free extract.....	81
Figure 4.11: Effect of gentler mixing methods of the viability of microclassified cell-free extract.....	82
Figure 4.12: Effect of microclassification on the proteins that make up the cell-free extract.....	83
Figure 4.13: Effect of lyophilisation on CFPS. End-point fluorescence readings from cell-free reactions under various conditions.	84
Figure 4.14: Overview of the paper-based platform	86
Figure 4.15: CFPS on paper enables protein expression upon rehydration.....	88
Figure 4.16: CFPS kinetics on cellulose is similar to that in liquid format.....	90
Figure 4.17: Concept of on-site and on-demand CFPS in a patch format	91
Figure 4.18: Cellulose stacks release sfGFP when loaded onto dissolving microneedles.....	92
Figure 5.1: VITA Concept of Operations	97
Figure 5.2: Computer Aided Diagram (CAD) of the VITA experiment cube	97
Figure 5.3: Image showing contents of one science unit.	98
Figure 5.4: Preliminary VITA instrumentation tests.	100
Figure 5.5: CFPS time course analysis of sfGFP using VITA instrumentation.....	102
Figure 5.6: Effect of VITA temperature (30 ° C) on CFPS kinetics	103
Figure 5.7: Impact of Scaling up reaction volumes on CFPS	104

Figure 5.8: Stability tests of in-house CFPS in cellulose stack format and lyophilised pellets.....	108
Figure 5.9: Impact of various supplements on CFPS.	111
Figure 5.10: Impact of secondary energy sources on CFPS.....	113
Figure 5.11: Impact of maltodextrin on short-term CFPS stability	115
Figure 5.12: Effect of sugar supplementation on short-term stability	117
Figure 5.13: Comparison of the VITA instrumentation with the Nanodrop™ 3300 spectrophotometer	119
Figure 5.14: Design of experiments approach for improving stability of lyophilised CFPS.....	121
Figure 5.15: Long term stability studies using newly identified supplements.	123
Figure 6.1: Cell-free expression of therapeutic proteins using the NEB PURExpress system.....	128
Figure 6.2: In-house cell-free expression of therapeutic proteins.....	130
Figure 6.3: Qualitative RT-qPCR analyses provides insights into cell-free mRNA levels	132
Figure 6.4: Purification of cell-free expressed sfGFP and Reteplase-His	134
Figure 6.5: Cell-free protein yield determination	135
Figure 6.6: Tertiary and quaternary structure analysis	138
Figure 6.7: Purification of proteins for secondary structure analysis.....	140
Figure 6.8: Unprocessed infrared spectra of purified proteins reteplase (black trendline), (b) sfGFP (cell-free; dark green trendline) and (c) sfGFP (cell-based; fluorescent green trendline).....	141
Figure 6.9: Infrared spectrum in the amide I region of (a) sfGFP (cell-based), (b) sfGFP (cell-free) and (c) reteplase.....	143
Figure 6.10: Raw Circular Dichroism (CD) spectra for purified sfGFP (cell-free and cell-based) and reteplase in D ₂ O shown at optimised concentrations	145
Figure 6.11: Co-expression studies.	148
Figure 6.12: SDS-Page and native PAGE analysis	149

List of Tables

Table 1.1: Comparison of cell-free and cell-based biomanufacturing routes for on-site and on-demand applications.....	18
Table 1.2: Examples of biologics with potential use in a space-born emergency; adapted from (Williams et al., 2022).....	24
Table 1.3: Description of the five chosen therapeutic proteins, their critical features and dosing information, summarised from literature	27
Table 2.1: Materials used in this thesis and supplier information	31
Table 2.2: YTPG media components.....	32
Table 2.3: Bacterial strains used in this thesis and their applications.....	32
Table 2.4: PCR reaction set-up.....	33
Table 2.5: PCR thermocycler settings	34
Table 2.6: PCR primer information sheet.....	34
Table 2.7: Restriction enzyme digestion reaction set-up	35
Table 2.8: Ligation reaction set-up.....	35
Table 2.9: NEB Hi-Fi DNA assembly reaction set-up	35
Table 2.10: S30A buffer components	37
Table 2.11: List of amino acid components.....	38
Table 2.12: List of energy components.....	39
Table 2.13: CFPS set-up for standard in-house reactions	40
Table 2.14: Cell-free reaction set-up for paper and microglassification reaction formats.....	41
Table 2.15: Primer information sheet for RT-qPCR.....	44
Table 2.16: RT-qPCR reaction set up	44
Table 2.17: qPCR thermocycler settings.....	45
Table 6.1: Extrapolation of pure sfGFP protein concentration from DC assay standard curve.....	135
Table 6.2: Example estimates of yields from previous experiments. Concentrations were extrapolated from standard curve shown in Figure 6.5, b and yield was calculated based on reaction volume. Examples from commercial systems and other research groups are provided for comparison.....	136

Abbreviations

3D	3 dimensional
3-PGA	3-phosphoglyceric acid
μL	Microlitre
mL	Millilitre
AA	Amino acid
AMP	Adenosine monophosphate
Amp	Ampicillin
ANOVA	Analysis of variance
ATP	Adenosine triphosphate
bp	Base pairs
c-AMP	Cyclic adenosine monophosphate
c-DNA	Complementary DNA
CAD	Computer aided diagram
CFPS	Cell-free protein synthesis
CHO	Chinese hamster ovary cells
CoA	Coenzyme A
CTP	Cytidine triphosphate
DARPA	Defense advanced research projects agency
DNA	Deoxyribonucleic acid
dNTP	Deoxyribonucleoside triphosphate
DoE	Design of experiments
DTT	Dithiothreitol
EC	Energy components
<i>E. coli</i>	<i>Escherichia coli</i>
ELISA	Enzyme-linked immunosorbent assay
EMA	European medicines agency
FDA	Food and drug administration
GCR	Galactic cosmic rays
G-CSF	Granulocyte colony stimulating factor
GFP	Green fluorescent protein
Glu	Glucose
GMP	Good manufacturing practice
GPCR	G-protein coupled receptor
GTP	Guanosine triphosphate
His	Histidine
Hr	Hour
IPTG	Isopropyl β- d-1-thiogalactopyranoside

IR	Ionising radiation
ISS	International space station
LB	Luria broth
LEO	Low earth orbit
kDa	Kilodalton
KOH	Potassium hydroxide
mRNA	Messenger RNA
MDX	Maltodextrin
NaCl	Sodium chloride
NAD	Nicotinamide adenine dinucleotide
NASA	National aeronautics and space administration
NTP	Nucleoside triphosphate
OD ₆₀₀	Optical density at 600 nm
PCR	Polymerase chain reaction
PEG	Polyethylene glycol
PEP	Phosphoenolpyruvate
PTM	Post-translational modification
qPCR	Quantitative polymerase chain reaction
RFU	Relative fluorescence units
ROS	Reactive oxygen species
RNA	Ribonucleic acid
RNase	Ribonuclease
RPM	Rotations per minute
RT-qPCR	Reverse transcriptase quantitative polymerase chain reaction
S30	Cell-free extract
SD	Standard deviation
SDS-Page	Sodium dodecyl sulphate-polyacrylamide gel electrophoresis
sfGFP	Super folder green fluorescent protein
TBS	Tris-buffered saline
tRNA	Transfer RNA
Tx-Tl	Transcription-translation
SPEs	Solar particle events
UTP	Uridine triphosphate
UV	Ultraviolet light
VITA	Visualising in-situ Tx-Tl astropharmaceuticals
VLP	Virus-like particle
w/v	Weight by volume
YTPG	Yeast tryptone phosphate glucose media

Impact statement

Book chapter

WILLIAMS, P. M., SHIVAKUMAR, T. & ANYANWU, V. 2022. Space Medicine and Countermeasures. In-Space Manufacturing and Resources.

Conference posters

SHIVAKUMAR, T., ANYANWU, V., CROFT, A., DREVENY, I., CONRADIE, A. & WILLIAMS, P. M. 2021. Cell-free synthetic biology enables on-demand, on-site expression of therapeutic proteins. The biochemical society synthetic biology conference. Nottingham, UK. (relates to Chapters 3 & 4)

SHIVAKUMAR, T., ANYANWU, V., CROFT, A., DREVENY, I., CONRADIE, A. & WILLIAMS, P. M. 2022. An 'Astropharmacy' based on bacterial cell-free technology. Microbiology society annual conference. Belfast, UK. (relates to Chapters 3 & 4)

Conference presentations

SHIVAKUMAR, T., CROFT, A., DREVENY, I., CONRADIE, A. & WILLIAMS, P. M. 2022. On-demand biopharmaceuticals in extreme environments. The IUBMB global biochemistry summit. Lisbon, Portugal. (relates to Chapters 4 & 6)

SHIVAKUMAR, T., GREEN, M., ROBSON, D., COPE, H. & WILLIAMS, P. M. 2022. Astropharmacy – Healthcare for Earth, the Moon, Mars and beyond. 27th ELGRA Biennial Symposium and General Assembly. Lisbon, Portugal. (relates to Chapter 5)

Competitions and programmes

Science lead of a student team selected to participate in the ESA Orbit Your Thesis!3 Programme, that will enable an experiment to be flown and tested on the International Space Station (ISS). The mission, ['VITA \(Visualizing In-Situ Tx-TI Astropharmaceuticals\)'](#) will test a cell-free expression system that was developed during this PhD (relates to Chapter 5), and will be Nottingham's first student-led experiment on the ISS.

[Winner of the 2021 Space4Youth competition](#) organized by UNOOSA and Space Generation Advisory Council (SGAC)

Invited speaker at the United Nation's Access2Space4All initiative [microgravity and hypergravity webinar series](#)

Presented at Pre-COP26- related workshops and at COP26, Glasgow with support from the UK Space Agency (UKSA) space4climate division and UNOOSA

Grants and awards

SHIVAKUMAR, T. & WILLIAMS, P. M. 2023. UK Space Agency grant (upto £5k) 'student experiments in microgravity'.

SHIVAKUMAR, T. 2022. Federation of European Biochemical Societies travel bursary (680 EUR) for the global biochemistry summit, Lisbon, 2022.

SHIVAKUMAR, T. 2022. ESA Academy sponsorship (1000 EUR) for the 27th biennial ELGRA symposium, Lisbon, 2022.

SHIVAKUMAR, T. 2021. Space4Climate travel bursary (£332) for COP26, Glasgow, 2021.

Outreach

The Brilliant Club tutor. 2021 - 2022. 'How to keep an astronaut healthy in space' key stage 4 course designed and delivered over a term in the following Nottinghamshire and Derbyshire schools: Frederick Gent School, Alfreton, Sutton Community academy, Sutton-in-Ashfield and Bramcote College, Bramcote.

'Pursuing Education, Research, Science and Innovation in Space Together' mentor. 2021 - 2022. U.S. Mission to International Organizations in Vienna and the University of Alabama.

Chapter 1 Introduction

1.1 Astropharmacy and Astromedicine

1.1.1 Humans in extreme environments

Extreme environments can be defined as hostile or harsh natural areas that typically do not support life (Rothschild and Mancinelli, 2001). Most life is present on Earth's superficial layers – deeper parts of the oceans do not receive sunlight and is highly pressurized. On land, extreme environments such as frozen, arid deserts and other latitudinal and topographical variations in temperature, water and nutrient availability make it difficult for species survival. A remarkable class of organisms, known as extremophiles, are perhaps the most complex capable of surviving and thriving in such extreme environments (Rampelotto, 2013).

Although human beings are adaptable organisms, survival is significantly low in extreme environments. This is attributed to the high complexity of the human body in comparison to relatively simpler microscopic extremophiles. Nevertheless, advancements in science and technology have improved our tolerance and made exploration of these areas, a reality (Piantadosi, 2003). Space is perhaps the most extreme environment that humans have ever faced. In the 1960s, the Apollo program marked the farthest and most extreme point humans have ever been from Earth – the far side of the Moon. Other advances include the International Space Station (ISS), an artificial research satellite in low earth orbit, launched on the 20th of November 1998 (NASA, 2018). The ISS is still in orbit with astronauts working onboard, contributing heavily to our scientific, geological and medical knowledge on Earth. Space exploration has advanced further in the 21st century; NASA (National Aeronautics and Space Agency, United States) and other agencies have already sent orbiters and landed rovers (“the Curiosity Rover”) for the surface exploration of Mars. Human exploration of Mars is now the combined long-term goal of 15 space agencies around the world (ISECG, 2018).

1.1.1.a Physiological effects of space travel on the human body

Although commercial spaceflight/tourism is emerging, current space missions are only embarked by well-trained, professional astronauts. Applicants undergo a strict ‘Psychological and Medical selection process’, ensuring that they possess minimum health requirements for enduring the physiological effects related to space exploration (Johnston *et al.*, 2014). ‘Space Medicine’ or ‘Astromedicine’ is a field of

science that aims to deliver healthcare to humans travelling to space, the need for which will increase considerably with more manned deep-space missions. Medical standards are classified based on the traveller and the type of spaceflight – Suborbital, Low Earth Orbit (LEO) and Exploration class missions. Suborbital flights are short journeys that do not complete one full orbit around the Earth (*e.g.* Virgin Galactic Unity flights). The ISS is in LEO, 250 miles above the Earth's surface. Lastly, Exploration class missions involve long-duration space travel through deep space (*e.g.* Mars) (Hodkinson *et al.*, 2017).

The group of symptoms observed by most astronauts within the initial three days in space are termed as the Space Adaptation Syndrome. This is primarily due to the body's response to microgravity (feeling of weightlessness). Most common symptoms include headaches, illusion, vertigo, nausea and disorientation (Hodkinson *et al.*, 2017). More complex bodily changes are observed in longer duration missions. A frequent complaint among US astronauts was sleep disturbance – sleep inducers such as zolpidem were the most used medications on the ISS followed by pain, congestion and allergy medications (Wotring, 2015).

Exposure to radiation is the number one concern for long-duration space travel; ionising radiation (IR) causes ionisation of atoms in molecules such as DNA, leading to cell damage and disrepair Galactic cosmic radiation (GCR) and solar particle events (SPEs) are the main sources of radiation in outer space (Hodkinson *et al.*, 2017). At the cellular level, IR causes damage through direct and indirect effects. Direct effects involve DNA damage caused by breakage of the phosphate-sugar backbone and/or chemical bonds within base pairs. Exposed cells try to repair the damage or otherwise undergo apoptosis, if irreversible. DNA is a crucial yet small part of the cell, therefore, the probability of direct IR exposure is also low. Other components like water, however, form a major part of cellular volume. IR causes disassociation of water molecules thereby releasing free radicals such as $O_2^{\bullet-}$, $O_2^{\bullet-2}$, $\bullet OH$, and OH^{\bullet} (Desouky *et al.*, 2015). These radicals are called reactive oxygen species (ROS) and they cause indirect damage by oxidizing biomolecules, leading to oxidative stress. The unstable unpaired electron in ROS readily interacts with biomolecules such as proteins, lipids, RNA and DNA leading to their breakdown. Further caspase activation, mitochondrial dysfunction and activation of cytokines (Interleukin 1/8, Tumour Necrosis Factor- α) lead to inflammation and result in apoptosis (Bai *et al.*, 2018).

In addition to the above, various other organ system-level changes take place in the human body in space, collectively summarised in Figure 1.1. Redistribution of fluid to the upper body is immediately recognisable in astronauts aboard the ISS ('puffy face' syndrome). In microgravity, the sensory systems register and adapt to the new

space environment, causing temporary disorientation. But the body again experiences changes upon re-entry, whether it be Earth or Mars, which can often be more dangerous (Hodkinson et al., 2017).

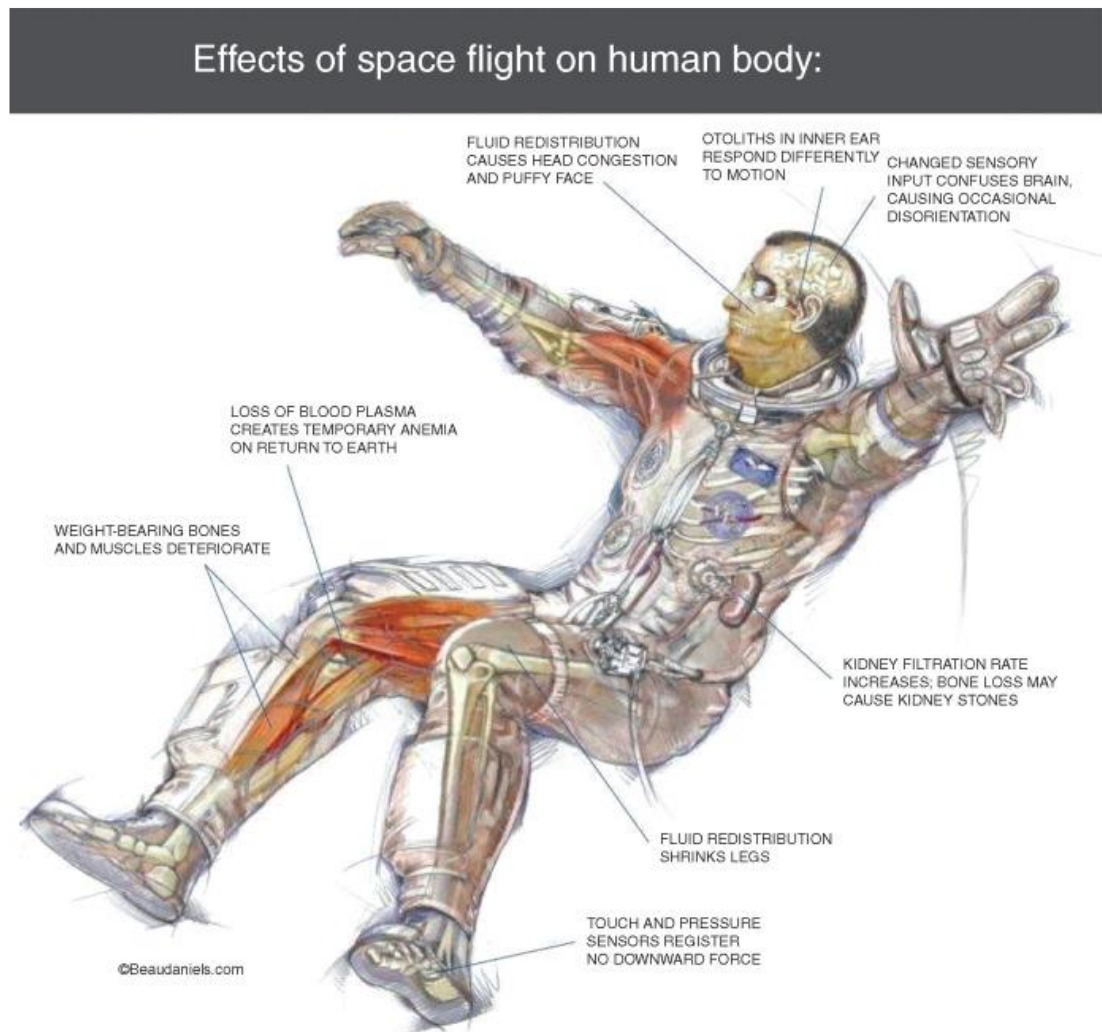


Figure 1.1: Effects of spaceflight on the human body, caused by exposure to radiation and/or microgravity. Adapted from Hodkinson et al., 2017), copyright Daniels and Daniels.

1.1.2 Why astropharmacy?

Medications for common ailments were carried on spaceflights for astronaut use on all previous manned missions. More number of medications are being provided to the ISS in recent years; medical kits on the ISS contained 78 medicines in 2014, whereas 107 medicines were available in 2017 (Eyal and Derendorf, 2019). This is due to increased research, newer treatments and drugs approved by the Food and Drug Administration (FDA). 87% of medicines supplied to the ISS have a shelf-life of less than 2 years (Blue et al., 2019). On that account, we have a severely limited ability to

supply an 'Astropharmacy' (pharmacy for space) for missions lasting more than 2 years.

All previous crewed spaceflight involved short durations with the safety net of emergency return to earth or resupply of food, oxygen, fuel, and medicine. Crew living and working aboard the ISS have an on-call doctor (practice termed 'telemedicine'). However, long distance space travel will mean moving further afield. Mars, the next target for a manned mission, is between 34 million and 240 million miles from Earth, in which case, telemedicine may not be feasible due to shuttle-Earth communication lag time. Astronauts will also have limited resources to take from Earth to sustain for a longer period of time (Hodkinson *et al.*, 2017). Furthermore, astronauts will have to endure exposure to extreme environments; in which all adverse events are unlikely to be predicted in advance. Therefore, it will be highly beneficial to develop a technology that will allow on-site production of therapeutics as and when needed.

In addition to outer space, there are humans living and working in numerous other extreme environments on Earth. The development of an on-site production system would be beneficial for conducting long duration expeditions to such places (*e.g.* research camps in Antarctica, submarine missions). Even today, particularly in rural areas, some communities do not receive a regular supply of therapeutics that require cold chain supply. Controlling the temperature during transport of temperature-sensitive products is important to preserve the integrity of the cargo. The cold chain logistics industry has boomed in the past decade primarily due to the demand for transport of insulin and vaccines. Together with rapid arrival of biologics on the market, cold chain for biopharma alone will be worth \$21.3 billion by 2024 (Shelley, 2022). With the advent of on-site production, cold chain may no longer be required to maintain integrity of biologics. This new avenue may potentially save the phenomenal amounts of energy consumed and the effects on the environment.

Conventionally, cells of many species (bacteria, yeast, insect and human) are used on Earth for the production of proteins through the recombinant protein technology (Fothergill-Gilmore, 1993). With the appropriate DNA input, such as plasmid containing the gene of interest, cells can be programmed to synthesize proteins of interest. The protein production pipeline, consisting of the above process, typically takes place in a laboratory. One way of synthesising therapeutics on-site is to adapt protein synthesis to take place outside the lab in a said environment. This new approach, with many advantages over cell-based recombinant protein expression, is termed cell-free protein synthesis (CFPS) and is the core technology that is researched in this project.

1.2 Cell-free protein synthesis

1.2.1 An introduction to protein synthesis

Proteins are a complex class of biomolecules that are essential to life. They contain a defined sequence of amino acids folded in specific 3-dimensional conformations that allow interactions with other biomolecules. Proteins play crucial roles inside cells, not limited to enzymes, switches, channels, receptors and signal molecules (Berg JM, 2002a). Biosynthesis of proteins is a common process in prokaryotes and eukaryotes; however, the more complex nature of eukaryotes gives rise to some key differences in the way proteins are made, changed, and processed. According to central dogma, a gene is first transcribed to messenger RNA by RNA polymerases, then translated into proteins, catalysed by ribosomes (Arnstein, 1965, Crick, 1970a). Both transcription and translation have three main steps, namely initiation, elongation, and termination, as summarised in Figure 1.1 below. Transcription initiation takes place when the RNA polymerase and transcription factors bind to the promoter region of the DNA (*e.g.* T7 promoter). During elongation, the polymerase moves along the DNA strand, unwinding the double helix and synthesizing a complementary RNA strand using a single DNA strand as template. Transcription continues until the RNA polymerase reaches a termination signal in the DNA (*e.g.* T7 terminator) following which the polymerase detaches and releases the synthesized RNA molecule. Transcription takes place in the nucleus in eukaryotic cells and translation takes place in the cytoplasm in both prokaryotic and eukaryotic cells.

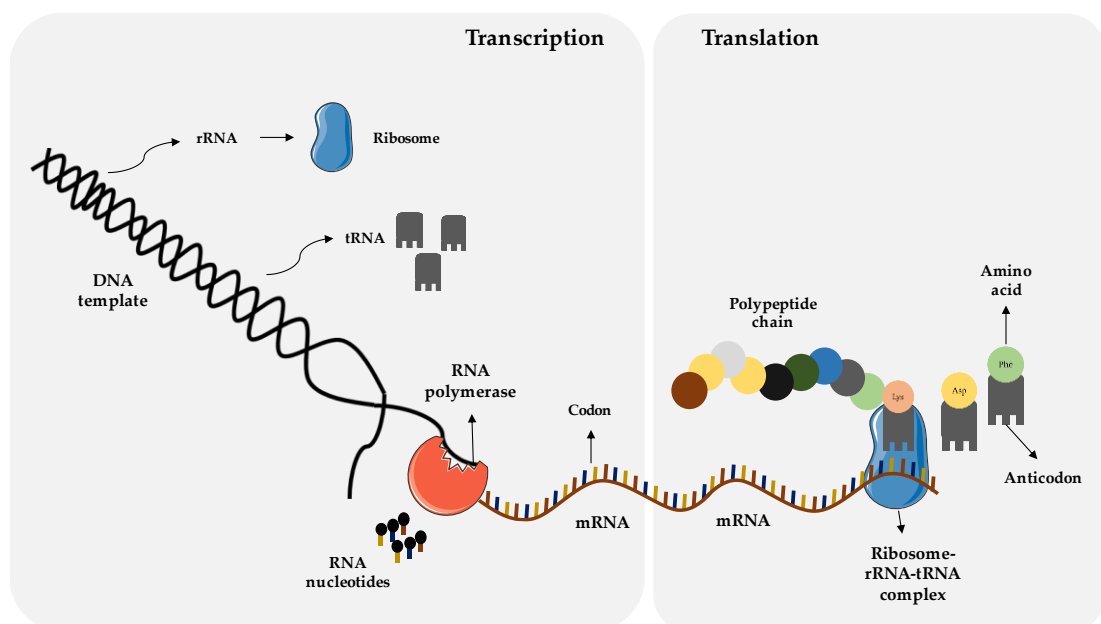


Figure 1.2: Illustration of transcription and translation and the various cellular machinery required. The central dogma of molecular biology involves transcription of a DNA template (double stranded; black) by the

enzyme RNA polymerase. The resulting single stranded RNA molecule (brown) is translated by a ribosome-rRNA-tRNA complex.

Translation is initiated when the ribosome, complexed with the starting tRNA and initiation factors, binds to the mRNA molecule at the start codon (typically AUG). During elongation, the ribosome complex moves along the codons sequentially, and as each codon is read, the corresponding amino acid is brought to the ribosome by corresponding tRNAs. Peptide bonds form between neighbouring amino acids, forming the polypeptide chain. This continues until the ribosome encounters a stop codon (typically UAA, UAG, or UGA) on the mRNA molecule. The polypeptide chain is released as the complex dissociates and translation is terminated.

In eukaryotic cells, there are additional steps for processing mRNA (*e.g.* splicing, 5' cap and PolyA tail). Prokaryotic cells have limited post-translational modifications, whereas, more complex modifications are present in eukaryotes (*e.g.* glycosylation, phosphorylation, acetylation, ubiquitination) (Berg JM, 2002b). Due to these differences, choice of organism is an important determinant in the intended application for synthesised protein (Brondyk, 2009). The four most common expression systems are based on bacterial (prokaryotic), yeast, insect, and mammalian (eukaryotic) cell types. By culturing cells with modified DNA templates, recombinant protein technology has allowed production of pure proteins in large quantities for commercial purposes (Fothergill-Gilmore, 1993). However, a new method of producing proteins, called cell-free protein synthesis is being used, due to its various advantages discussed below.

1.2.2 Fundamentals of cell-free protein synthesis

Cell free protein synthesis (CFPS) refers to the *in vitro* production of proteins using molecular machinery derived from cellular extracts. These cellular extracts (derived from prokaryotic or eukaryotic sources) contain most biomolecules that are required for translation of exogenic RNA/DNA templates. As discussed in Section 1.2.1, these include tRNA, ribosomes, initiation, elongation, and termination factors. Amino acids are supplemented to cell-free reactions for synthesis of the polypeptide chain and energy sources (such as adenosine triphosphate) are also supplemented along with cofactors (Mg^{2+} and K^{2+}) to maintain and sustain protein synthesis. CFPS is increasingly becoming the method of choice over cell-based systems for expression of cytotoxic, synthetic, and complex proteins. The numerous advantages of CFPS stems from its open, protean nature and free of concern over viability (Carlson *et al.*, 2012).

A cell free protein synthesis reaction is often broken down into three broad elements: cellular extract, template DNA, and reaction mixture (Figure 1.2). The extract strain

is initially grown in media followed by lysis to obtain the cellular extract. A variety of methods have been employed for cell lysis, including sonication, high pressure homogenization, freeze-thawing, bead-beating, and lytic enzymes. The reaction mixture consists of a cocktail of salts, nucleotides, amino acids, energy sources, transfer RNAs (tRNAs), and metabolic co-factors and additives that fuel expression. Lastly, linear or plasmid DNA or RNA serve as templates for gene expression. Protein synthesis occurs upon combining the above components and incubation at desired temperatures (typically between 25°C and 37°C) over a period of time (hours – days) (Gregorio *et al.*, 2019b).

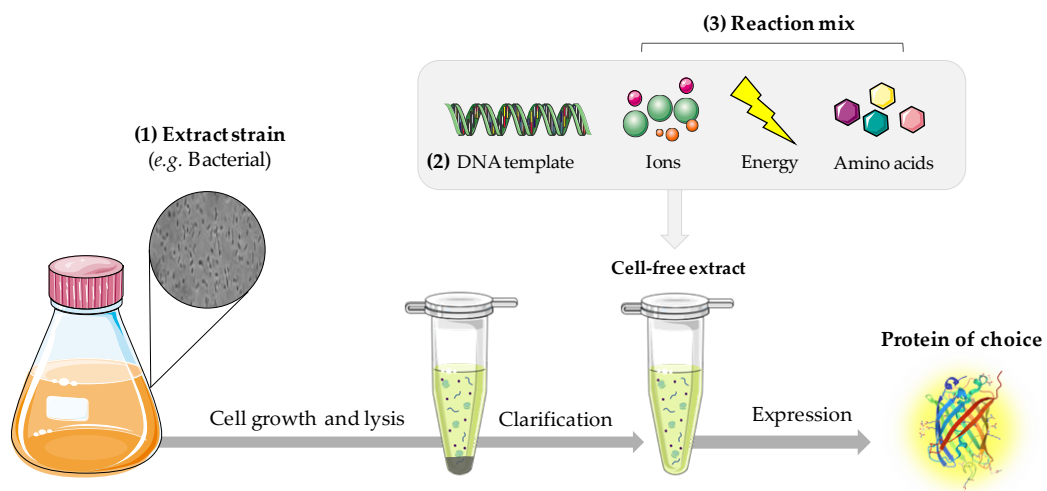


Figure 1.3: Overview of Cell-Free Protein Synthesis (CFPS). Cell extracts are first prepared by growing the extract strain and subjecting them to lysis. The lysate is clarified by centrifugation to obtain functional cell-free extract. Upon supplementing the extract with amino acids, ions, energy and DNA, the desired protein can be produced.

1.2.3 Historical overview of CFPS

The origins of CFPS can be traced back to the late 1940s, when scientists began to study incorporation of amino acids into proteins (Zamecnik *et al.*, 1948). The CFPS methodology played a role in many crucial discoveries during that decade. Perhaps the most notable is the Nobel Prize-winning work of Nirenberg and Matthaei in 1961. The duo first discovered that triplet nucleotides code for specific amino acids by establishing the cell-free synthesis of phenylalanine from poly-uridylic acid using *E.coli* extracts (Nirenberg and Matthaei, 1961). CFPS was employed in the following five years for successfully deciphering all such genetic codes (Crick, 1970b, Nirenberg, 2004).

The next breakthrough in CFPS was the development of a coupled transcription-translation (TxTl) system that enabled DNA-directed protein synthesis (Lederman

and Zubay, 1967). A major limitation with this “batch” approach was the rapid depletion of resources in the reaction mixture, which prevented reactions to exceed 20 minutes. In an effort to increase protein yields, scientists explored a continuous exchange format. This new format allowed continuous removal of products from reaction mixture in addition to a feed of fresh buffer, thereby improving reaction time and yield (Spirin *et al.*, 1988). Secondary energy sources such as glucose-6-phosphate and pyruvate were also explored for regeneration of ATP in the reaction (Kim and Swartz, 2001).

The onset of the 21st century saw various groups optimising cell-free extract preparation to create a protocol that was more efficient and cost-effective. This involved various lytic procedures, centrifugation steps and genome alterations such as the expression of T7 polymerase to enhance protein expression. Such continued optimization for tailored applications has produced efficacious methods for extract preparation (Kigawa *et al.*, 2004, Liu *et al.*, 2005, Kim *et al.*, 2006b, Didovyk *et al.*, 2017).

Mathematical modelling has been extensively used in the biosciences to investigate metabolic and regulatory biological processes. Recently, mathematical modelling of CFPS has created a better understanding of system capabilities, with regards to transcription and translation processes. By generating simple models using ordinary differential equations (ODEs), scientists are able to follow gene expression in cell-free systems in the first instance (Karzbrun *et al.*, 2011). Modelling has further enabled the identification of bottlenecks in CFPS reactions without the need for thorough experimentation (Nieß *et al.*, 2017). Other commonly used tools to study cellular metabolism such as flux balance analysis (FBA) and constrain based models have been used to increase CFPS efficiency. Dai *et al* admitted that although flux estimation remains a challenge for the future, modelling can greatly aid in predicting cell-free metabolite production. The authors discuss promising features of modelling for RNA and multi-protein circuits and even small-molecule production (Dai *et al.*, 2018). Initial efforts in metabolic and mathematical modelling have contributed to our understanding of the production limits of CFPS. There is promising potential and research advances will address these gaps and aid in the development of new technologies such as on-demand manufacturing of therapeutics.

1.2.4 Cell-free components

1.2.4.a Cell-free extract sources

The most common choice of prokaryotic extract for cell-free expression is *Escherichia coli*, owing to its simplicity and vast number of experimental tools available.

However, extracts from *Bacillus subtilis*, *Vibrio*, *Streptomyces* and *Pseudomonas* strains have also been explored (Rosano *et al.*, 2019, Dondapati *et al.*, 2020, Failmezger *et al.*, 2018). Achieving expression of proteins with complex post-translational modifications (PTMs) is a challenge in prokaryotic extracts. Nevertheless, recent efforts in cellular systems engineering have allowed incorporation of basic PTMs like glycosylation, thereby improving the cost-effectiveness of production (Jaroentomechai *et al.*, 2018). Eukaryotic extracts are typically chosen for expression of complex eukaryotic proteins. A majority of therapeutic proteins intended for human use are produced using Chinese hamster ovary (CHO) cells (Thoring and Kubick, 2018). This cell line is an attractive choice due to its ability to produce complex PTMs such as glycosylation, phosphorylation, and ubiquitination. Other extract sources come from insect cells (*Sf21*), yeast, wheat germ and tobacco have also been used for expression of complex proteins in high yields and quality (Ezure *et al.*, 2010, Hodgman and Jewett, 2013, Buntru *et al.*, 2014, Morita *et al.*, 2003).

1.2.4.b DNA templates

A great advantage of CFPS is the direct addition of the coding template to the reaction, in the form of plasmid DNA or linear expression templates. Plasmid DNA is easy to prepare from commercially available DNA extraction kits and was the template of choice in this work. With a well-designed plasmid, templates of any size can be used in cell-free reactions and is often the chosen method for expression of a designated protein (Stark *et al.*, 2018). On the other hand, for high throughput screening of proteins, linear expression templates are an ideal choice as PCR products can directly be added to the cell-free reactions, thereby decreasing the cloning-to-expression time (McSweeney and Styczynski, 2021). Recent work with strain modifications has increased the expression efficiency from linear expression templates by decreasing nuclease activity (Sato *et al.*, 2022). Furthermore, codon optimisation has been shown to play a key role in improving protein yields by improve translation efficiency through enhancing the rate of mRNA elongation (Yu *et al.*, 2015).

1.2.4.c Energy sources

Protein synthesis is perhaps the most energy intensive process in a cell (Buttgereit and Brand, 1995). The primary energy currency in biological systems is adenosine triphosphate (ATP), and ATP is required for various steps in CFPS (Figure 1.3). There are a variety of ways through which ATP can be supplied in cell-free reactions and perhaps the most popular method is through direct supplementation of nucleotide triphosphates (NTPs): ATP, GTP, CTP, and UTP (Levine *et al.*, 2019). An alternative

and cost-effective method is through the addition of glucose, which can generate ATP and other metabolites through glycolysis (Calhoun and Swartz, 2005). The use of phosphoenolpyruvate (PEP), creatine phosphate or acetyl phosphate as a secondary energy source is also popular, as ATP can be regenerated in simple substrate-level phosphorylation reactions. However, this requires kinases to be endogenously present in the cell-free extract or be supplemented to the reaction. Not only does this increase the cost of each reaction, but the accumulation of phosphate also inhibits protein synthesis due to precipitation of Mg^{2+} that is required for translation (Khambhati *et al.*, 2019).

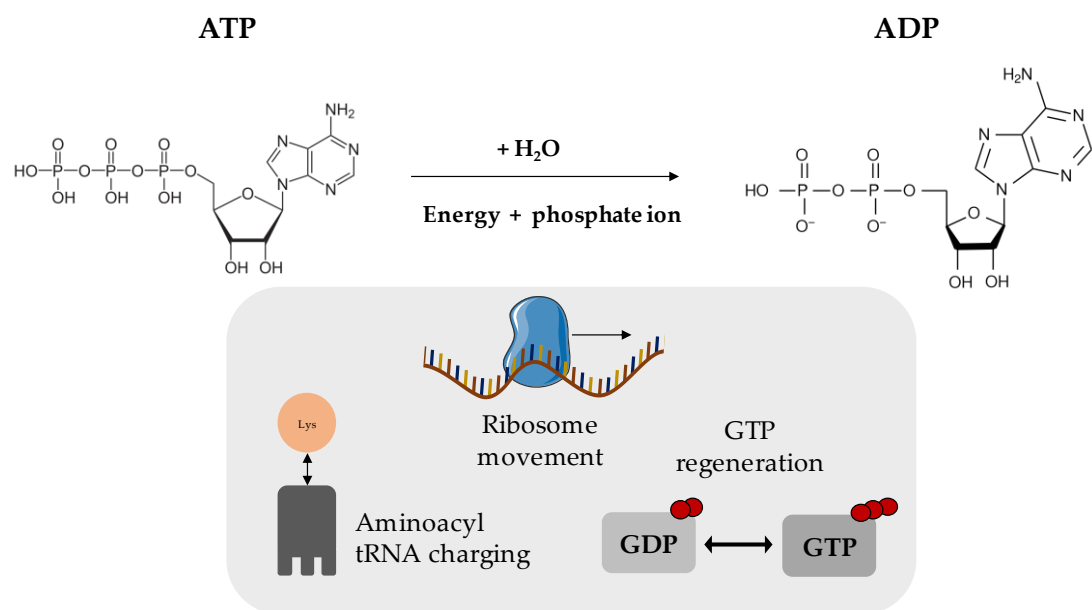


Figure 1.4: The role of ATP in protein synthesis. Hydrolysis of ATP, the cellular energy currency, results in the production of ADP, energy and a phosphate ion. The released energy is used by cells to fuel ribosome movement, aminoacyl tRNA charging (both essential for translation) and GTP regeneration (GTP plays a role in translation initiation, elongation and termination secondary to ATP).

Less popular carbon and energy sources such as 3-phosphoglycerate (3-PGA), fructose-1, 6-bisphosphate and other organic compounds have been utilised to produce ATP and fuel CFPS to varying degrees of successes in the past (Sitaraman *et al.*, 2004, Kim *et al.*, 2007). Due to its low cost and utilisation of inorganic phosphate in the reaction, maltodextrin (MDX) has gained popularity as a secondary energy compound in CFPS (Wang and Zhang, 2009). More recently, CFPS systems energised with MDX was shown to perform similarly to costlier PEP-based systems, making it more suitable for distribution in extreme/low resource environments and for educational projects (Guzman-Chavez *et al.*, 2022). In summary, the choice of energy systems for CFPS will vary depending on the application of the desired protein and the source of extract and should be optimised to achieve high protein yields. In this

project, nucleoside triphosphates (ATP, GTP, CTP and UTP) were chosen as the primary energy source along with 3-PGA and other cofactors (N-2-hydroxyethylpiperazine-N-2-ethane sulfonic acid, coenzyme A, nicotinamide adenine dinucleotide, cyclic adenosine monophosphate, folic acid, and spermidine), however, the suitability of PEP and MDX as secondary energy compounds was also further studied.

1.2.4.d A note on the importance of optimisation

Supplementing the cell-free reaction with chaperones such as DnaK/DnaJ/GrpE and GroES/EL has been shown to improve protein folding efficiency in cell-free expression using prokaryotic extracts (Jin *et al.*, 2019). Similarly, as a result of increased catalytic activity (including T7 RNA polymerase) in reactions supplemented with optimal concentrations of magnesium and potassium ions, an increase in protein yields was observed (Schwarz *et al.*, 2007, Thoring *et al.*, 2017). Many groups working in the area of cell-free synthetic biology have embraced optimisation of reaction conditions such as vessel volumes, freeze-thaw cycles, membrane disruption methods, temperature, template DNA concentration *etc.* (Hodgman and Jewett, 2013, Au - Levine *et al.*, 2019). Collectively, optimisation is necessary to achieve high protein yields in bespoke CFPS platforms and the open nature of CFPS allows for easier optimisation and manipulation compared to cell-based protein expression optimisation.

1.2.5 CFPS formats

1.2.5.a Formats for liquid CFPS reactions

There are two formats for implementing CFPS; batch, and continuous exchange. Batch-based formats are commonly chosen for fast and easy protein output. Protein yield in a cell-free batch format can range from the microgram to milligram scales, with prokaryotic extracts typically producing higher yields than eukaryotic extracts. Sutro Biopharma, one of the handful number of companies working on CFPS, recently showed bioactive cytokine production in batches of up to 100 litres, without compromise on yield (Zawada *et al.*, 2011). On the other hand, the continuous exchange format trades time for yield. The set-up consists of the reaction and feed chamber comprised of fresh buffer, separated by a semi-permeable membrane. This format allows inflow of fresh reaction components in exchange for removal of metabolites, thereby allowing prolonged expression over time. The continuous exchange format has been successfully applied to express proteins that are conventionally difficult to express (*e.g.* membrane proteins) (Stech *et al.*, 2014, Thoring

et al., 2017). Although the continuous exchange format has great potential for applications in well-equipped laboratories, they are not suitable for on-site and on-demand applications as they are difficult to set up and operate, hence, batch based methods were mainly studied in this project.

1.2.5.b Lyophilisation

Several anti-microbial peptides, with high yield and solubility, have been produced using *E. coli* based CFPS to target viruses, bacteria, fungi, and parasites. Such class of medications are important for elevation of human health, particularly in poor and low-resource environments. This led researchers to gain interest in the ability of extracts to retain viability following lyophilisation and kickstart protein synthesis for therapeutic applications in austere environments. Pardee *et al.* have shown production of anti-microbial peptides (Cecropin P1, Cecropin B *etc.*), vaccines (antigens for botulinum, diphtheria, and anthrax), and enzymes for synthesis of small-molecule pharmaceuticals in a portable on-demand biomanufacturing model. Their system consisted of freeze-dried cell-free extract that can be hydrated and made to express proteins upon addition of DNA up to a year subsequently (Pardee *et al.*, 2016b). In the same year, Salehi *et al.* showed the production of onconase, a cytotoxic cancer therapeutic, in a similar 'just-add-water' system. They went on to analysis different temperatures and time setting and concluded that soluble, active protein can be synthesised up to a year later when stored above -80°C (Salehi *et al.*, 2016a).

1.2.5.c Hydrogels

Hydrogels are made up of a polymeric network of hydrophilic monomers. Recently, crosstalk in the science of hydrogels and CFPS has brought about interesting thoughts and applications. Whitfield *et al.*, demonstrated cell-free expression of mCherry in hydrogels made from a variety of materials such as agarose, agar, hyaluronic acid, xanthan gum, alginate, Gelzan™, collagen, gelatin, HydroMatrix™, F-108, F-127, and polyacrylamide. It showed successful lyophilisation of hydrogel that was reconstituted with fresh CFPS components and vice versa, and further discussed both components in a hydrogel without a free liquid phase. The authors concluded that the gel acted as a structural molecular crowding agent, which positively impacted the CFPS reaction that was further enhanced through the addition of 2% polyethylene glycol (PEG) (Whitfield *et al.*, 2020).

In a different study, DNA hydrogels were fabricated with the DNA template (GFP) and polyethylene glycol diacrylate (PEGDA). It was shown that the hydrogel can be used repeatedly (10 times) with cell-free reaction buffer to induce protein synthesis with little effect on protein yields (Cui *et al.*, 2020). This strategy may work well with

batch and continued exchange cell-free systems and offers a safe and sustainable mode for carrying DNA templates for cell-free applications. This work could be further expanded to identify excipients that may confer DNA stability against environmental stressors such as temperature, humidity, and radiation for applications in extreme and low-resource environments.

Lastly, hydrogels have also been fabricated in a microchannel device for micro-compartmentalising CFPS which once again has the beneficial molecular crowding effect. CFPS components were casted in 2% alginate and the synthesised His-tagged protein was further extracted with agarose beads immobilised with cobalt (Benítez-Mateos *et al.*, 2020). This work could be expanded for synthesis of protein therapeutics and may benefit from functional studies, as this type of synthesis system coupled with purification is highly advantageous for on-site and on-demand applications.

1.2.5.d Microfluidic devices

Time consuming molecular cloning can be surpassed by the direct addition of PCR DNA templates. These attributes make CFPS an attractive method for implementation in high-throughput synthesis, which can be miniaturised in multi-well plates. CFPS is often coupled with microfluidic devices, in order to achieve high-throughput expression. This format allows simultaneous detection and rapid analysis of expressed proteins, thereby minimizing time and cost of protein synthesis. In a DARPA supported project, Jackson *et al.* describe a microfluidic device with continuous exchange, consisting of CFPS and nutrient reservoir in a chamber separated by a dialysis membrane. This 96-well microfluidic device produced up to 87 times more protein in comparison to the batch format (Jackson *et al.*, 2014). Fallah-Araghi *et al.* published an ultrahigh-throughput screening platform based on droplet-based microfluidics for directed evolution of proteins. A droplet containing PCR-amplified gene and one containing CFPS components were fused to initiate gene expression (Fallah-Araghi *et al.*, 2012). Batch based formats have also been utilised in microfluidic devices. One study reported coupling of CFPS with a microfluidic bioreactor in an effort to demonstrate higher synthesis rates of single-dose therapeutic proteins at point-of-care (Timm *et al.*, 2016).

A good example of the use of CFPS in microfluidic devices for production of protein therapeutics is the 'therapeutics on a chip' platform that showed the production of cecropin B (antimicrobial peptide) in < 5 hours and further in-chip purification in 40 minutes. A bead-based approach was taken for the purification procedure, where separate channels were fabricated for the various wash and elution steps (Murphy *et al.*, 2019). The parallelisation and multiplexing nature of microfluidics, as exploited in the previous work, can elevate CFPS capabilities by combining purification,

formulation, and delivery of produced protein in one device, hence, microfluidics contains promising potential for on-site and on-demand biomanufacturing.

1.2.6 Applications of CFPS

1.2.6.a Difficult to synthesise proteins – membrane proteins

Membrane proteins, such as G-protein coupled receptors (GPCRs), ion channels and transporters, contribute to more than a third of drug targets in the pharmaceutical industry (Santos *et al.*, 2017). Despite being popular targets, cell-based synthesis of membrane proteins gives rise to aggregation and improper folding, causing challenges in expression, purification and crystallisation (Sachse *et al.*, 2014). Cell-free systems have been thoroughly explored for expressing membrane proteins due to ease of solubilisation and reconstitution in liposomes and nanodiscs. Both prokaryotic and eukaryotic extracts have been used but lysates lacking microsomes require additional supplements in the form of detergents, whereas most eukaryotic lysates such CHO and *sf21* endogenously offer proper folding machinery (Zemella *et al.*, 2015b, Dondapati *et al.*, 2019).

1.2.6.b Virus-like particles

Virus-like particles (VLPs) are small proteins that self-assemble and mimic native viruses. Since they lack viral genome, these particles are effectively used as vaccines to elicit an innate immune response in humans. Higher yield and more soluble VLPs can be obtained using CFPS in comparison to cell-based methods, partly due to lower contamination from cellular proteins and membranes (Khambhati *et al.*, 2019). VLPs have served as delivery vehicles when encapsulated with DNA or protein, and particles are often fused with antigens. Therefore, VLPs have broad applications ranging from vaccination to gene therapy, drug delivery and nanotechnology (Shirbaghaee and Bolhassani, 2016). This expands the repertoire of products that can be synthesised through on-site and on-demand biomanufacturing platforms.

1.2.6.c Biosensors

CFPS has been employed for the development of biosensors for three broad applications, namely diagnostic, environmental, and food safety sensing. By combining CFPS-synthesised proteins with detection platforms, such as lateral flow kits or paper-based devices, rapid and sensitive diagnostic tests can be developed. Such biosensors have been used for detecting infectious diseases from pathogens, such as the Zika and Chikungunya viruses, and hormones, such as thyroid hormone

and estrogen, at point-of-care (Karlikow *et al.*, 2022, Hunt *et al.*, 2022). CFPS has been harnessed for biosensing applications related to environmental monitoring involving the detection of pollutants, heavy metals, and toxic compounds in environmental samples. CFPS can be programmed for synthesis receptors or enzymes that specifically bind to target molecules, enabling sensitive and selective detection through regulated genetic circuits. Many such sensors comprise of cell-free components freeze-dried and/or immobilised on paper, enabling the sensor to be stable and portable and detection capabilities range from heavy metal contaminants in water to bacterial quorum sensing signals (Lin *et al.*, 2020, Jung *et al.*, 2020). Thirdly, CFPS-based biosensors have also been developed for monitoring food safety and water quality. Also freeze-dried onto paper, one study discussed a platform for the detection of mercury in water, based on super folder green fluorescent protein (sfGFP) expression. The same study also developed a biosensor for the detection of gamma-hydroxybutyrate, a substance used as a date-rape drug, and further devised a 3D-printed cassette with a GFP filter for easy detection using a smartphone (Gräwe *et al.*, 2019). Such CFPS biosensors are gaining traction due to their ease-of-use and deployment where analytical facilities such as laboratories are scarce, and this evolving field may benefit from increased sensor stability in the future.

1.2.6.d CFPS in vesicles

Vesicles are influential in drug delivery owing to properties such as effective drug encapsulation and selective targeting. In addition, vesicles are currently gaining the spotlight in synthetic construction of artificial cells, where CFPS has an important role to play. Perhaps the first notable encapsulation in this field was that of Noireaux and Libchaber in 2004. The duo built an artificial cell-like bioreactor by encapsulating *E. coli* extracts in a phospholipid vesicle (Noireaux and Libchaber, 2004). Since then, the researchers have worked towards building artificial cells in the form of programmed vesicles that are also capable of self-organisation and reproduction, like living cells. Noireaux *et al.* share this vision and extensively discuss the advantages and bottlenecks of cell-free expression in encapsulated vesicles to achieve this. Briefly, the needs for higher protein synthesis rate, advanced promoter networks to create large DNA programs and methods to control inactivation of RNA and degradation of proteins (source-sink dynamics) are highlighted as bottle-necks (Noireaux *et al.*, 2011).

Peruzzi and colleagues report DNA 'barcoded' vesicles for the production of useful proteins, in a similar mission towards developing cell-mimetic structures. DNA oligonucleotides were cleverly used to tag vesicles which were shown to fuse upon hybridization. Methods to alter biophysical features on the vesicles were described to control extent of fusion using FRET (Förster resonance energy transfer). This

technique was then used to monitor delivery of DNA cargo to vesicles that initiated CFPS upon fusion; expression of a soluble and membrane reporter protein was shown for proof-of-concept (Peruzzi *et al.*, 2019). The bottom-up construction of artificial cells is an evolving area of research that aims to achieve complex biomanufacturing of useful compounds. CFPS is continuing to be explored in conventional vesicles such as liposomes (Caschera *et al.*, 2016, Nishimura *et al.*, 2012) and microcapsules (Saeki *et al.*, 2014) and collectively, these efforts in engineering will contribute to development of more advanced, programmable and high-achieving cell-free technologies.

1.3 On-demand biomanufacturing

1.3.1 The need for on-demand biomanufacturing

Science, driven by innovation, has led to discovery of products and compounds that save patients' lives. The approved pharmaceuticals that are released to the patient population are typically manufactured in a large scale-batch format to meet demands. Regardless, drug shortage is a major challenge for the pharmaceutical industry, particularly aggravated by epidemics or pandemics (FDA, 2013). Drug shortage may be attributed to inefficient adaptability of the batch manufacturing system to meet changing demands in the industry (Adamo *et al.*, 2016). Furthermore, access to biopharmaceuticals in remote areas and extreme environments is still a major challenge, to date. To overcome challenges such as the above, scientists have recently begun to investigate on-demand biomanufacturing systems, creating an attractive avenue for personalised medicine and point-of-care applications. In addition, on-demand synthesis aims to eliminate the need for cold storage and 'stockpiling' of medicines. In fact, DARPA (Defense Advanced Research Projects Agency), part of the United States Department of Defense, have selected on-demand biomanufacturing as part of their 'Battlefield Medicine' program. The program aims to employ genetic engineering and cell-free protein synthesis to synthesise biologics on the battlefield and in other austere environments (Jenkins, 2023).

1.3.2 Examples of cell-based biomanufacturing methods

The on-demand biomanufacturing platform is based on either a cell-based or cell-free source. The cell-based biomanufacturing briefly entails cell line development, fermentation, purification and formulation (Cao *et al.*, 2018). Cao and colleagues describe an integrated platform for on-demand production of multiple therapeutics at one time. They demonstrate three strategies – (1) Inducible synthesis with control of drug expression ratios, (2) Consolidated bioprocessing (post-translational

processing) and (3) Co-expression/purification, for flexible and low-cost production of combinatorial therapies where resources are limited. Programmed expression of biologics was attained in portable micro-bioreactors, integrated with genetically engineered *Pichia pastoris* for on-demand applications (Perez-Pinera *et al.*, 2016, Cao *et al.*, 2018).

Based upon a similar ideology, a team of DARPA-funded scientists have described a new cell-based on-demand manufacturing system called 'InSCyT' or 'Integrated Scalable Cyto Technology'. InSCyT is an automated benchtop system that is capable of producing clinical-grade biologics in less than three days. The set-up involves three modules that are responsible for recombinant synthesis, purification, and formulation respectively. Once again, the authors chose to use *P. pastoris* in the protein production module due to its favourable characteristics for protein expression. They also incorporated two to three stage chromatography procedures and ultrafiltration in the purification module, prior to tangential flow filtration in the formulation module. Expression of human growth hormone, granulocyte colony stimulating factor and Interferon α -2b was carried out to exhibit an end-end production system. Purity, potency, biochemical and biophysical traits of final products were tested to ensure similitude to marketed drug (Crowell *et al.*, 2018).

1.3.3 The advantages of cell-free biomanufacturing

The successful deployment of CFPS for on-site and on-demand biomanufacturing of protein-based therapeutics will require integrated systems that are firstly portable for easy transportation and accessibility in extreme environments, and secondly of high efficiency. The latter is veritable for sustainable production of target therapeutics of good-manufacturing-practice (GMP) quality within a reasonable time and at dose relevant amount. As discussed in Section 1.3.5, the open nature of CFPS has allowed it to be performed in various formats such hydrogels, in microfluidics devices, and lyophilised systems. This has previously allowed successful and wide applications of such systems from biosensing and diagnostics in remote environments to generation of artificial cells with unique properties, as discussed in the Section 1.3.6. The open nature of cell-free systems is more useful for on-site and on-demand applications compared to cell-based routes and these are summarised in Table 1.1 below. Although cell-free biomanufacturing also has its limitations, it is younger than cell-based biomanufacturing and ongoing research and technological advancements are addressing these challenges and expanding its scope.

Table 1.1: Comparison of cell-free and cell-based biomanufacturing routes for on-site and on-demand applications

Attributes	Cell-free synthesis	Cell-based synthesis	References
DNA template	Expression from plasmid DNA or linear PCR templates.	Expression from plasmid or genome.	(Carlson <i>et al.</i> , 2012)
Synthesis time	Cellular energy is primarily focused on expression of protein. Downstream purification easier and quicker due to lack of membrane barrier.	Energy is primarily focused on cellular metabolism, hence longer time necessary for expression. Intracellular protein purification requires an additional cell lysis step.	(Levine <i>et al.</i> , 2019, Rosenblum and Cooperman, 2014)
Post-translational modifications (PTMs)	Dependant on choice of cell type/extract. Eukaryotic cells/extracts contain PTM machinery which prokaryotic extracts largely lack. Prokaryotic cells/extract can be engineered/supplemented to perform PTMs.		(Zemella <i>et al.</i> , 2015a, Amann <i>et al.</i> , 2019)
Incorporation of materials	Easy due to open nature of reaction.	Challenging due to compartmental nature of cells.	(Gao <i>et al.</i> , 2019)
Cost of production	Comparatively high. Current and on-going advances in research may improve cost-effectiveness (<i>e.g.</i> energy regeneration).	Comparatively low	(Kim <i>et al.</i> , 2006b, Kim <i>et al.</i> , 2015)
Biomass	Fixed biomass	Capable of self-replication	(Claassens <i>et al.</i> , 2019)

1.3.4 Delivery of pure, functional, and approved products

1.3.4.a Protein purification

An advantage of the cell-based system is ease of purification of proteins secreted from cells into media; this method has been used conventionally since the birth of recombinant protein synthesis. There are significantly less contaminants except for

other metabolites secreted from the cell and media components (Le and Trotta, 1991). For purifying intracellular proteins, affinity tags are universally used. Tags are cloned in the DNA sequence of protein at the design stage. Many tags such as the poly-histidine (His) tag have affinity for metal ions, nickel in this case, and this characteristic can be used to exclusively capture the protein attached to tag. Further considerations like the number of affinity tags (one or more types), location (N/C-terminal) or whether to have a self-cleavage system is decided on a case-by-case basis, dependent on the application of that specific protein. Although residual tags such as the His-tag may not produce a concern, it is required by the FDA that therapeutic proteins for human intake do not have any residual elements (Kimple *et al.*, 2013, Wingfield, 2015).

Let us consider the purification process for His-tagged proteins as an example. The downstream purification techniques for proteins synthesized via CFPS and cell-based expression is similar. To separate proteins secreted from whole cells, the cells are first centrifuged, and the supernatant is used for purification. An immobilised nickel-affinity chromatography column (Ni²⁺-IMAC) or nickel charged affinity resin in binding buffer is added to extract (CFPS)/supernatant (cell-based), where His-tagged proteins interact and bind to metal ions that are later separated from mixture. The proteins are eluted by washing the resin with molecules with higher affinity to nickel (e.g. imidazole). The purity of elutions can be examined through sodium dodecyl sulphate - polyacrylamide gel electrophoresis (SDS-Page)/Western blot analysis, and mass spectrometry (Kimple *et al.*, 2013, Rothchild *et al.*, 2019).

The PUREexpress system (New England Biolabs) is a commercially available CFPS kit that uses a new, different approach called as 'reverse purification'. The protein translation machinery is entirely composed of recombinant proteins that are individually His-tagged, except ribosomes and tRNAs. The protein of interest is synthesized from DNA template without any purification tags. Following synthesis, ribosomes are removed from the mixture by ultracentrifugation. All the tagged translation factors are removed by addition of nickel affinity resin by centrifugation. The remaining synthesized protein is left in the tube devoid of contaminants (NEB, 2020, Shimizu *et al.*, 2001). Humans using an on-site technology in extreme environments may not have the appropriate scientific expertise to carry out complicated processes. Therefore, this approach could be advantageous, especially in spaceflight due to the simplicity of purification.

Post-translational modifications (PTMs) are critical for eukaryotic proteins, especially for human therapeutic proteins. Bacterial extracts may not provide the appropriate PTMs; in which case, a eukaryotic cell line may be better suited for extract preparation (Sachse *et al.*, 2013). However, the aforementioned therapeutic proteins do not require

additional PTMs, thus they are well suited for pilot CFPS experiments using bacterial extracts. It is worth mentioning that *E. coli* platforms have been modified to produce some PTMs due to their otherwise favourable characteristics such as ease of obtaining extract and high protein yields (Gregorio *et al.*, 2019a). Therefore, *E. coli* is an excellent candidate for extract preparation in CFPS systems.

1.3.4.b Quality control

Biopharmaceuticals are subject to rigorous quality control measures and this involves a combination of analytical testing, process monitoring, and adherence to regulatory standards to ensure consistent production of safe and effective medicines (EMA, 1994). Analytical testing verifies the identity, purity, potency, and quality of manufactured and purified product through techniques such as chromatography (like high-performance liquid chromatography; HPLC), electrophoresis, mass spectrometry and immuno/activity assays. The results are analysed in accordance with 'critical quality attributes' and provides data on protein secondary structure, PTMs, structure-function relationships, impurity and sterility profiles (Alt *et al.*, 2016). Enforcing quality control is particularly challenging for on-demand biomanufacturing platforms as it is impractical to carry above systems and equipment to extreme or austere environments. Therefore, innovation is required for developing in-situ quality control measures that allow (near) real-time monitoring and assessment of critical quality attributes during the manufacturing process. Such new technologies offer several advantages including timely interventions and adjustments to respond promptly to deviations or process variations.

1.3.4.c Shelf-life and stability

Perturbations in the stability of a biomolecule is caused by degradation or chemical or physical alteration due to extremal stimuli such as thermal stress. In the case of proteins, this causes alternations in the 3D structure and affects its functionality (Daniel and Cowan, 2000). Hence, the biopharmaceutical industry must follow strict guidelines, such as those instated by the International Council for Harmonisation of Technical Requirements for Pharmaceuticals for Human Use (ICH). This involves performing stability studies to assess factors that may cause degradation/aggregation that affects bioactivity such as temperature, pH, humidity, and oxygen exposure. The results of such studies in turn inform the shelf-life and suitable storage conditions of the product (EMA, 2003). Any platform that is being developed for human use, such as an on-site and on-demand platform, must also comply with these regulations.

The degradation rate of proteins (due to above physical and chemical alterations) can be largely reduced by storing the protein in a solid and/or dry state. This is because

the Brownian motion of molecules is reduced and restricted, which in turn reduces aggregation and hence degradation (Tang and Pikal, 2004). Around 50% of protein therapeutics manufactured via cell-based routes are, therefore, either stored in reduced temperatures (<4°C) and/or lyophilised (or freeze-dried) in powder or pellet form, which are also easier to store and transport (Butreddy *et al.*, 2021). Similarly, cell-free reaction components also require cold-storage to remain active, and lyophilisation has been employed to improve stability of cell-free systems without cold-storage. The stability of lyophilised extracts and energy systems outperforms aqueous extracts and energy systems, and one study demonstrated this up to 60 days by monitoring expression of reporter protein (Smith *et al.*, 2014). Other studies have developed robust methodologies for antimicrobial peptides, vaccines, small molecules, cytotoxic therapeutics and biosensors using 'just-add-water' lyophilized systems (Pardee *et al.*, 2016b, Pardee *et al.*, 2016a, Salehi *et al.*, 2016b, Pardee *et al.*, 2014). Such lyophilised cell-free systems are ideal for on-site and on-demand applications because they offer ease of storage, distribution and use in environments outside a typical scientific laboratory.

Sugars are often incorporated as excipients in biotherapeutic stabilisation for their ability to preserve native protein structure and also as lyoprotectants during lyophilisation (Jovanović *et al.*, 2006). Similar agents have been explored for CFPS stabilisation as well, where the cell extract is the most sensitive component involving complex mixture of biomolecules (proteins and RNA). The most commonly reported candidates for CFPS stabilisation included sugars such as sucrose, trehalose and lactose, and molecular crowding agents such as PEG, trimethylglycine and dextrans (*e.g.* β -cyclodextrin) (Jiang *et al.*, 2021, Gregorio *et al.*, 2020, Warfel *et al.*, 2023, Smith *et al.*, 2014). The sugars protect proteins in the cell-free mix from denaturation and aggregation by forming a protective shell and by exhibiting water replacement properties. This also allows it stabilise proteins under stressful conditions, such as during lyophilisation, freeze-thaw, and heat shock, makes it a valuable additive in CFPS reactions. Osmolytes, such as trimethylglycine, are typically small molecules that aid stress response in cells but are useful in CFPS through counteracting the effects of osmotic stress, preventing protein denaturation, and promoting proper folding. Similar to PEG, dextrans promote molecular crowding and prevents protein aggregation. Through these mechanisms of action, the above agents have shown to increase stability of lyophilised cell-free systems at storage temperatures ranging from 20°C – 37°C.

Agents with different mechanisms of actions (*e.g.* sugars and crowding agents) can be supplemented together for a beneficial combinatorial effect on stability. One study showed no loss in stability when lyophilised CFPS reactions were stored at 23°C for two weeks through the combinatorial effect of three supplements (trehalose,

trimethylglycine and PEG) (Gregorio *et al.*, 2020). Based on the work and findings described in this study, the key message is the importance of optimisation of component/additive concentrations based on the CFPS system, target protein, and desired stability requirements. This may have an effect on the duration of the reaction, which should be well understood based on storage temperature conditions. Additionally, it is crucial to consider the potential impact of these additives on downstream applications, such as protein purification or functional assays.

1.3.4.d Meeting biopharmaceutical regulatory standards

The regulatory requirements and challenges vary depending on the country or region where biomanufacturing will take place. Cell-based biomanufacturing is the conventional route thus far in the biopharmaceutical industry and will heavily inform the development of regulations for cell-free biomanufacturing. In the biopharmaceutical industry, biosafety and efficacy are the two main attributes regulatory agencies focus on (Keiper and Atanassova, 2020). These are critical to ensure the safety of workers, protect the environment, and maintain the integrity of the products being manufactured. Companies are subject to regulations and guidelines set by regulatory authorities specific to a region, *e.g.* the FDA in the US, and the European Medicines Agency (EMA) in Europe. Biosafety measures taken by the facility include containment strategies to prevent the spread of biological agents and regular monitoring and surveillance of facilities/processes ensure compliance. Workers in these facilities must adhere to strict personal protective equipment (PPE) protocol to minimize exposure to hazardous agents. Proper training in topics such as handling of biological agents, emergency response procedures, waste management, and decontamination protocols are essential prior to entering and working in the facility. It should further include the regulatory guidelines for containment and safe disposal of waste (chemical/biological/sharp). Whilst start-ups such as Sutro Biopharma, SwiftScale Biologics and Arbor Biosciences are tapping into the commercial potential of cell-free systems, they will also encounter the first set of regulatory milestones and challenges that will hopefully provide more clarity for other initiatives to learn from. It is believed that these procedures may not be too different to the biopharmaceutical industry standards discussed above but may have additional challenges such as reproducibility and standardisation.

1.3.4.e Biosafety and ethical considerations

In addition to meeting regulatory standards for manufacturing cell-free products, it is important to address biosafety and security risks concerning the misuse of such platforms for harmful applications. Given that defence organisations such as the U.S.

Department of Defense fund projects aiming to develop synthetic biology tools for military use, they recognise the risks associated with biosecurity such as bioterrorism (National Academies of Sciences and Medicine, 2018). On-demand cell-free platforms lower the technological barrier, enabling any user to operate it and obtain products with the correct DNA template. Issues arising from users being able to obtain open access to DNA sequences and print templates using a DNA printer vastly increase the risks associated with the platform (Grinstein, 2023). A global strategy, involving all countries and a joint initiative with governments, industry, and academia, is required to make informed decision and regulate the distribution, training, and best practises for disruptive on-demand biomanufacturing tools.

1.4 Research opportunities

To summarise the topics discussed so far, CFPS is a powerful synthetic biology tool that offers numerous advantages over traditional *in vivo* protein expression systems such rapid protein production, high yields of difficult-to-synthesise proteins and flexibility in protein engineering. CFPS has gained significant attention in recent years and has the potential to revolutionise biomanufacturing (Figure 1.4). These attributes make CFPS a great tool for on-demand and on-site CFPS platforms that are versatile, portable, and customizable for therapeutic applications in extreme and low-resource environments.

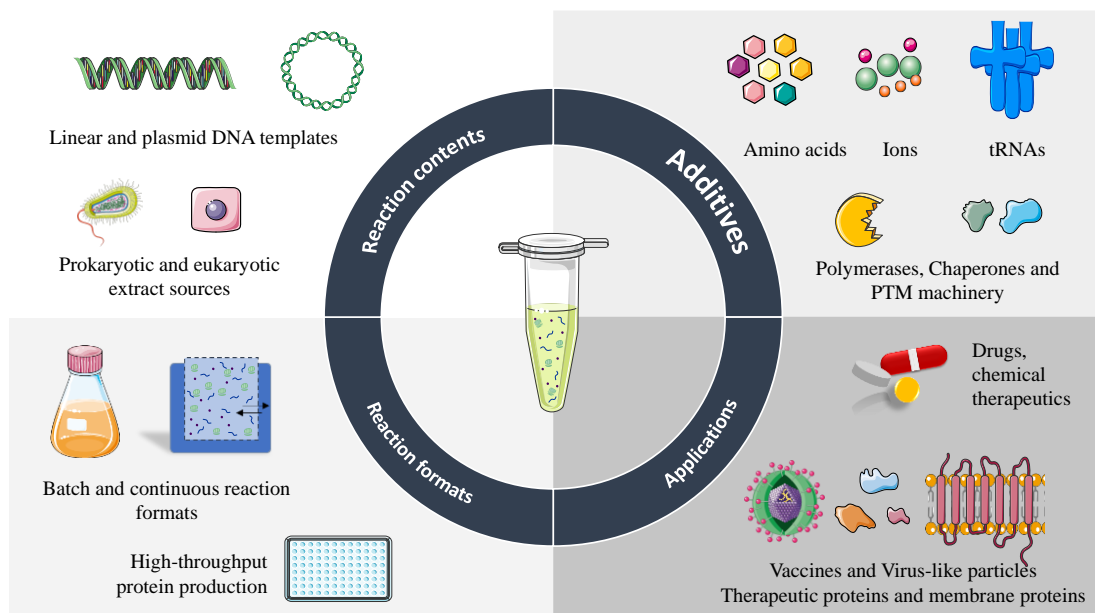


Figure 1.5: Summary of the components, formats and applications of cell-free systems

Since the use of CFPS for on-demand biomanufacturing is a new concept, there are many research opportunities starting with the development and optimisation of a portable CFPS platform. Research should initially focus on miniaturising the CFPS platforms and/or scaling up CFPS reactions with an emphasis on optimising reaction conditions (component concentrations, temperature, shaking, supplements *etc.*), improvement of yields and purification strategies (for obtaining regulatory approval). Research should then shift focus to the development of formats that make them compact, user-friendly and capable of producing dose relevant concentrations of a wide range of proteins without the need for cold-chain storage and transportation. Successful on-site and on-demand biomanufacturing platforms also require integration of synthesis (*i.e.* CFPS) with upstream and downstream processes such as on-demand DNA synthesis (upstream) and purification methods and quality control (downstream) to create a complete on-demand production pipeline.

CFPS offers the ability to customise and personalise therapeutic proteins, allowing tailored treatments for patients at point-of-care. To achieve this, research should aim to first demonstrate the synthesis of therapeutic proteins through a cell-free platform and showcase their activity. To make spaceflight-relevant protein therapeutics (Table 1.2). Five drugs highlighted in Table 1.2 (reteplase*, alfineprase*, teriparatide*, G-CSF* and entolimod*) were chosen as candidate therapeutics for cell-free expression as part of the work described in this thesis. The rationale for this choice are, diversity in terms of size and structural features (*e.g.* number of disulfide bonds; Table 1.3), and their value for spaceborne medical emergencies, as outlined in the ‘Astropharmacy’ proposal, involving a multinational collaboration between NASA Ames Research Centre and the Universities of Minnesota and Nottingham (Rothschild, 2020).

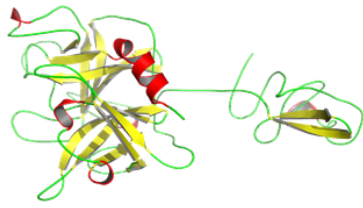
Table 1.2: Examples of biologics with potential use in a space-born emergency; adapted from (Williams et al., 2022)

Drug	Indication	References
Alteplase (t-PA)	Thrombolytic used to treat ischemic stroke, myocardial infarction and pulmonary embolism	(Reed, 2023)
Reteplase*	Similar to alteplase but with sequence modifications to give a longer half-life of 13 to 16 minutes	(Goldhaber, 2001)
Tenecteplase	Similar to alteplase but with sequence modifications to provide higher fibrin specificity and greater resistance to inactivation; glycosylated	(Harvison, 2008)

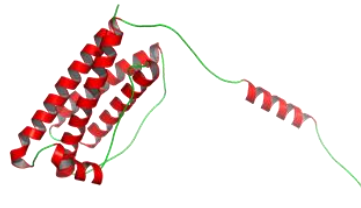
Alfimeprase*	Previously discontinued thrombolytic to treat stroke and catheter occlusion	(NIH, 2008)
Bivalirudin	Anticoagulant (thrombin inhibitor)	(NCBI, 2023)
Lepirudin	Anticoagulant (thrombin inhibitor); sulphated tyrosine residue	(Petros, 2008)
Epoetin alfa	Human erythropoietin used for treating some anaemias	(EMA, 2007)
Salmon calcitonin	Severe hypercalcemia and osteoporosis	(Chesnut <i>et al.</i> , 2008)
Teriparatide*	Form of parathyroid hormone used to promote bone formation and in treatment of osteoporosis	(Brixen <i>et al.</i> , 2004)
Filgrastim (G-CSF)*	Used for neutropenia following chemotherapy or radiation poisoning	(Mehta <i>et al.</i> , 2015)
Entolimod*	Radioprotective agent. Unlike G-CSF entolimod should be given immediately before or after exposure	(Song <i>et al.</i> , 2019)

Below is a brief introduction to the five therapeutic proteins summarising the therapeutic indication, size, structure, and dose. While G-CSF, entolimod and alfimeprase predominantly displayed α -helical secondary structures, β -sheets were also present in reteplase and alfimeprase. Teriparatide does not contain any secondary structural elements (Figure 1.5). While none of the selected drugs require post-translational modifications, this could be considered in futuristic systems especially in cases where modifications may enhance pharmaceutical stability (Solá and Griebenow, 2010). During the construction of an expression system, it is important to consider tags to aid purification and cleavage sites for obtaining scarless proteins (further advantage in cell-free systems is the avoidance of secretion tags which may be necessary in cell-based systems). As tags do not serve a purpose in the final protein product and may increase the risk of modification of biological activity or illicit unwanted immunological response, they need to be removed to obtain regulatory approval. In this work, a histidine tag (6 – 8 histidines; ‘His’) was chosen to be added to expression constructs as they are small and relatively non-immunogenic for initial development of an on-demand cell-free expression system.

(a) Retepase



(b) G-CSF



(c) Entolimod



(d) Alfineprase



(e) Teriparatide

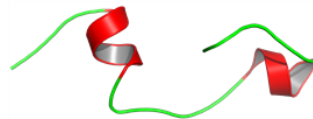


Figure 1.6: Swiss homology models of the five therapeutic proteins, created using SwissModel (Expasy) and images generated using PyMOL 2.5.5 (Schrödinger, Inc.)

Table 1.3: Description of the five chosen therapeutic proteins, their critical features and dosing information, summarised from literature

Drug	Description	Clinical indication in space	Size/ number of amino acids	No. of S-S bonds	Dosing regimen	Total dose per patient	References
Alfimeprase	Recombinant metalloproteinase derived from the venom of the southern copperhead snake	Potentially faster acting therapy for catheter related thrombosis	23 kDa /203 residues	3	Unknown	1 – 3 mg	(Jones <i>et al.</i> , 2001, Adivitiya and Khasa, 2017)
Entolimod	A polypeptide derived from Salmonella flagellin and an agonist for toll-like receptor 5 (TLR5)	Countermeasure to acute radiation syndrome given immediately before or immediately after acute radiation exposure from an un-shielded solar particle event	25 kDa/ 329 residues	Unknown	0.02 mg per day x 5 days	0.1 mg	(Burdelya <i>et al.</i> , 2008)
G-CSF	Naturally occurring glycoprotein that stimulates the production of neutrophils by binding to a transmembraneous receptor	Treatment of radiation-induced neutropenia after acute radiation exposure from an un-shielded solar particle event	18.8 kDa/ 174 residues	2	0.3 mg per day x 7 days	2.1 mg	(Brems, 2002)
Retepase	Thrombolytic agent consisting of Kringle-2 and protease domains of human tissue plasminogen activator	Thrombolytic therapy for acute coronary artery blockage or other vascular blockage, as a result of radiation-induced vascular disease	39 kDa/ 355 residues	9	18.1 mg IV x2, 30 min apart	36.2 mg	(Mandi <i>et al.</i> , 2010)

Teriparatide

Recombinant version (1 -34) of human parathyroid hormone	Role in accelerated fracture healing during spaceflight induced bone demineralization	4.1 kDa/ 34 residues	0	7.5 µg/ kg per day for 30 days	~ 15 mg	(Yari <i>et al.</i> , 2017)
--	---	----------------------	---	--------------------------------	---------	-----------------------------

1.5 Aims and objectives

The main aim of this thesis is to explore the feasibility and effectiveness of cell-free protein synthesis platforms for on-site and on-demand biomanufacturing of therapeutic proteins in extreme and low resource environments. In order to achieve this aim, work packages were created with the following main objectives:

Chapter 3: Development of an in-house CFPS platform based on bacterial cell extract by leveraging advanced biochemical and synthetic biological techniques.

- (a) Identification of optimal growth, induction and harvest conditions to obtain cell-free extract with the highest level of T7 RNA polymerase.
- (b) Cloning of expression constructs for the five therapeutic proteins and a fluorescent reporter protein.

Chapter 4: Optimisation and adaptation of CFPS for on-site and on-demand synthesis

- (c) Optimisation of the system for high synthesis efficiency based on fluorescent reporter production and benchmarking the optimised platform against highly efficient commercially available systems.
- (d) Exploration of formats through which the cell-free platform could be transported and distributed for point-of-care applications in remote locations on Earth and for space-based applications. Build formats based on previously published work related to lyophilisation or drying but also test new methods such as microglassification and the use of other scaffolds that may allow ease of use in a remote setting by any individual.

Chapter 5: Towards testing the developed platform in an extreme environment

- (e) Design, build and test the platform for the VITA mission, a European Space Agency Orbit Your Thesis 3! payload for technology demonstration on the International Space Station.
- (f) Perform stability studies to understand the shelf-life of the on-demand CFPS platform and research ways to enhance sample stability.
- (g) Perform instrumentation tests to ensure the ability to collect real-time data on reaction kinetics.

Chapter 6: Towards obtaining functional and pure therapeutic proteins

- (h) Expression of the five candidate therapeutic proteins and study their structure and functionality.

- (i) Explore new approaches for in-situ purification and quality control for obtaining regulatory approval.

Overall, these aims and objectives allow assessment of the potential of cell-free systems for on-site applications compared to traditional expression methods, and their ability to be employed in resource-constrained settings in a user-friendly manner. Each results chapter begins with a brief introduction and a recap of the above aims along with detailed objectives coordinated with the outlined experiments. Finally, Chapter 7 (Conclusions) summarises the results and evaluates the extent to which the objectives were met.

Chapter 2 Methodology

2.1 Materials

Unless otherwise specified, Table 2.1 details the general items that were procured from the listed suppliers for all methods provided in this chapter below.

Table 2.1: Materials used in this thesis and supplier information

Application	Supplier
Chemicals	Sigma Aldrich
DNA extraction kits	Qiagen
Cloning (assembly/enzymes) kits	New England Biolabs
Custom primers	IDT
Tubes (1.5 mL/50 mL)	Eppendorf/Sarstedt
Water (for media and buffer preparation)	Milli-Q

2.2 Methods in microbiology and molecular biology

2.2.1 Bacterial growth

2.2.1.a LB agar and LB broth starter cultures

LB agar plates were prepared by pouring 20 mL autoclaved LB agar solution (Sigma Aldrich; L3147) supplemented with 100 µg/mL ampicillin, in petri dishes (Thermo Fisher Scientific) which were left to cool at room temperature for at least 30 mins. *E. coli* was streaked onto LB agar plate and incubated at 37°C overnight. A single colony was picked from this plate the next morning and inoculated in 5 mL autoclaved LB broth (Sigma Aldrich; L3522) supplemented with 100 µg/mL ampicillin in a 50 mL falcon tube. The falcon tube was not fully screwed tight in order to maintain air circulation and the lid was taped to the side of the tube. The culture was grown overnight at 37°C, 250 RPM (~ 16 hours).

2.2.1.b Bacterial growth for cell-free extract preparation

1 L YTPG (Yeast Tryptone Phosphate Glucose) media was prepared by combining 750 mL 2x YTP media and 250 mL 0.4 M glucose solution autoclaved separately, as

per Table 2.2. Cells used for cell-free extract preparation were grown in 750 mL YTPG media supplemented with 100 µg/mL ampicillin.

Table 2.2: YTPG media components

1x YTGP	
NaCl	5 g/L
Tryptone	16 g/L
Yeast extract	10 g/L
KH ₂ PO ₄	7 g/L
K ₂ HPO ₄	3 g/L
Glucose	0.4 M

2.2.1.c Optical density measurements

Optical density at 600 nm (OD₆₀₀) was measured to monitor the growth of bacterial cultures over time, using a UV-Vis spectrophotometer (Agilent Multicell Peltier). Where OD₆₀₀ was expected to be greater than 1, 1:10 dilutions were made with the appropriate media.

2.2.2 *E. coli* strains and 32ryostocks preparation

Table 2.3: Bacterial strains used in this thesis and their applications

Strain	Application
<i>E. coli</i> BL21*(DE3)	Growth experiments
<i>E. coli</i> BL21*(DE3)-pAR1219	Cell-free extract preparation
<i>E. coli</i> NEB5α	Plasmid preparation
<i>E. coli</i> NEB5α pET20b(+)	Cloning vector; negative control
<i>E. coli</i> NEB5α pET20b(+)-sfGFP	CFPS DNA template library
<i>E. coli</i> NEB5α pET20b(+)-sfGFP-His	
<i>E. coli</i> NEB5α pET20b(+)-Reteplase-His	
<i>E. coli</i> NEB5α pET20b(+)-Teriparatide-His	
<i>E. coli</i> NEB5α pET20b(+)-Entolimod-His	
<i>E. coli</i> NEB5α pET20b(+)-GCSF-His	
<i>E. coli</i> NEB5α pET20b(+)-Alfimeprase-His	
<i>E. coli</i> NEB5α pET20b(+)-Alfimeprase-His	

Master cryostocks were created for all the above strains (Table 2.3), by combining 300 μ L of culture with 200 μ L 20% glycerol in 1 mL cryovials with internal thread. Cryovials were stored at -80°C . Master cryostocks were created for the BL21 Star (DE3) – p AR1219 strain and working cryostocks were created for fresh starting cultures for cell-free extract preparation.

2.2.3 Plasmid design

2.2.3.a Plasmid designs

The sfGFP gene was obtained from pBAD24-sfGFPx1, which was a gift from Sankar Adhya & Francisco Malagon (Addgene plasmid #51558; <http://n2t.net/addgene:51558>; RRID:Addgene_51558)(Malagon, 2013). DNA sequences for the therapeutic proteins were identified from literature and Drugbank, respectively: reteplase ([DB00015](#)), alfineprase ([DB04919](#)), granulocyte-colony stimulating factor (G-CSF; [DB00099](#)), teriparatide ([DB06285](#)) and entolimod ([DB2304](#)). The Nbs07 sfGFP nanobody gene was obtained from literature, based on the work of [Abbady et al., 2014](#) (Nbs07 was chosen as it exhibited highest affinity for sfGFP). Sequences were codon optimized for *Escherichia coli* expression and custom synthesized by Biomatik with the inclusion of NdeI and XhoI restriction sites and C-terminal histidine tag (CACCACCACCACCACCAC). Full sequences and design strategies have been provided in the supplementary information.

2.2.3.b Polymerase chain reaction (PCR)

Gene templates were amplified by Polymerase Chain Reaction (PCR), using Q5[®] High-Fidelity DNA Polymerase (NEB #M0491) as per Table 2.4.

Table 2.4: PCR reaction set-up

Component	Amount
5X Q5 Reaction Buffer	10 μ L
10 mM dNTPs	1 μ L
10 μ M Forward Primer	2.5 μ L
10 μ M Reverse Primer	2.5 μ L
Template DNA	1 μ g
Q5 High-Fidelity DNA Polymerase	0.5 μ L
Nuclease-Free Water	to 50 μ L

The PCR reactions were carried out in PCR tubes in a PTC-200 thermocycler (MJ Research) with the following setting:

Table 2.5: PCR thermocycler settings

STEP	TEMP	TIME
Initial Denaturation	98°C	30 seconds
	98°C	10 seconds
35 Cycles	*50–72°C	30 seconds
	72°C	20–30 seconds/kb
Final Extension	72°C	2 minutes
Hold	4°C	

*dependent on primer annealing temperature calculated by the [NEB T_m calculator](#)

Forward and reverse primers were custom designed for each construct clones, by Integrated DNA Technologies. Sequences are shown in Table 2.6:

Table 2.6: PCR primer information sheet

Construct	Forward primer	Reverse primer	Cloning method
sfGFP	actttaagaaggagatatacatat gcgtaa aggcgaagagctgttc	ttgtacagttcatcataccatgc gtgatg	Hifi assembly
Reteplase	acgacggccagtgaattcg	catgattacgccaagcttgc	Restriction digest
Alfimeprase	acgacggccagtgaattcg	catgattacgccaagcttgc	Restriction digest
G-CSF	acgacggccagtgaattcg	catgattacgccaagcttgc	Restriction digest
Entolimod	acgacggccagtgaattcg	catgattacgccaagcttgc	Restriction digest
Teriparatide	ccggcgatgggagctcatat gagcgtgagcgaatc	gtggtggtgcgatccctcgagt tattaatggtgatg	Hifi assembly
Nbs07 nanobody	aaggagatatacatatgcaggttc agct	gtggtggtggtggtgctgctcacggt	Hifi assembly

2.2.3.c Restriction digestion

All restriction enzymes were purchased from New England Biolabs and experiments were planned by utilising the [NEBcloner® tool](#). The following reactions were set up for generating vector and insert fragments (separately):

Table 2.7: Restriction enzyme digestion reaction set-up

Component	Amount
DNA (vector or insert)	1 µg
10X cutSmart Buffer	5 µL
EcoRI	1 µL
XhoI	1 µL
Nuclease-free water	to 50 µL

The above reaction was incubated at 37°C in a water bath for 30 minutes. In order to dephosphorylate the 5' ends of the DNA, 2 µL rSAP (shrimp alkaline phosphatase) was added to the reaction. Samples were further incubated for 30 minutes at 37°C in a water bath. Enzymatic activity was stopped by heat inactivation at 65°C for 5 minutes. Ligation was performed using the NEB Quick Ligation Kit (NEB #M2200). Briefly, the following reaction was set up in a microcentrifuge tube with a 1:3 vector: insert ratio as per Table 2.8.

Table 2.8: Ligation reaction set-up

Component	Amount
Reaction Buffer (2X)	10 µL
Vector DNA (3 kb)	50 ng (0.020 pmol)
Insert DNA (1 kb)	37.5 ng (0.060 pmol)
Nuclease-free Water	to 20 µL
Quick Ligase	1 µL

Reaction was incubated at room temperature (on the bench) for 5 minutes. Following this, 2 µL of the ligated mixture was transformed into component cells.

2.2.3.d NEB Hi-Fi assembly

Vector and insert fragments were generated by PCR with an overlap region of < 20 nucleotides. The NEB HIFI DNA assembly kit was used (NEB #E5520S), instructions for the following reaction set up were followed (Table 2.9).

Table 2.9: NEB Hi-Fi DNA assembly reaction set-up

Component	Amount
-----------	--------

Vector and Insert (1:2 ratio)	0.2:0.4 pmol
Assembly Master Mix	10 μ L
Deionized H ₂ O	to 20 μ L

Reactions were incubated in a thermocycler at 50°C for 30 minutes. Following this, 2 μ L of the ligated mixture was transformed into component cells.

2.2.3.e Transformation of DNA into competent cells

Chemically competent cells (NEB5 α NEB #C2987H) were thawed on ice. 2 μ L DNA was added to the cells and mixed by flicking the tube. Tube was placed on ice for 30 minutes. Heat shock was carried out by placing tube in a 42°C water bath for 45 seconds. Tube was placed back on ice for 5 minutes. Following this, 950 μ L SOC (outgrowth media) was added to the tube. The mixture was incubated in a shaker incubator at 37°C, 250 RPM for 1 hour. To freshly prepared LB-Amp agar plated, 100 μ L to 200 μ L of the mixture was spread onto the plate and incubated overnight at 37°C. The following day, individual colonies were picked and subcultured. Picked colonies were grown in LB-Amp broth and subsequently extracted DNA (QIAprep spin mini kit) was sequenced (Eurofins overnight sequencing service). Cryostocks and starter cultures were created as appropriate.

2.2.3.f Plasmid preparation for CFPS

Cells were first prepared for plasmid extraction by inoculating 50 μ L of cells from the working cryostocks in 5 mL LB broth (with 100 μ g/mL ampicillin) in a 50 mL falcon tube. Culture was grown at 37°C and 250 RPM overnight. This culture was then transferred into fresh 250 mL LB broth (with 100 μ g/mL ampicillin) in 1 L baffled shake flasks and grown overnight at 37°C and 250 RPM. Cells were harvested by centrifuging the culture at 7000 RPM for 5 mins. A maxiprep kit (Qiagen) was used to perform plasmid extraction and kit manufacturer's protocol was implemented. DNA was eluted in nuclease free water and the final concentration was measured using a NanodropTM 2000 spectrophotometer (ThermoFisher Scientific).

2.2.3.g Agarose Gel electrophoresis

Agarose gel electrophoresis was employed for detection and size verification of synthesised/cloned DNA. 1 % agarose gels were prepared by dissolving 1 g of agarose in 100 mL TAE buffer. The mixture was heated for 2 minutes in a microwave oven to make a molten gel solution. Following a 10-minute cooling period, ethidium bromide was added to the gel (0.5 μ g/mL) and the gel was poured into a casting tray

with a comb placed on one end. The DNA samples were mixed with 6x gel loading buffer and loaded into the wells, alongside a 1 kb plus DNA ladder (Invitrogen #10787026). The gel was run with a constant voltage of 100 V in TAE buffer for 1 hour, following which it was imaged under UV transilluminator.

2.2.3.h Quantification of nucleic acids

DNA was quantified using a Nanodrop™ 1000 spectrophotometer (Thermo Fisher Scientific) at a 260 nm wavelength. Water was used as a blank (as DNA was always eluted with nuclease-free water).

2.3 CFPS reactions

2.3.1 Commercial kits

Two commercial cell-free systems were used to benchmark in-house reaction compositions. The *E. coli* T7 S30 Extract System for Circular DNA kit (Promega #L1130) and PURExpress® *In Vitro* Protein Synthesis Kit (New England Biolabs #E6800L) were purchased and stored at -80°C. Unless otherwise specified, commercial reactions were set up accordingly to manufacturer's instructions, in 50 µL reaction volumes.

2.3.2 Extract preparation

Cell-free extract was prepared as described previously (Au - Levine et al., 2019). Briefly, BL21-pAR1219 cells were grown overnight in LB broth supplemented with 100 µg/mL ampicillin. This overnight culture was used to inoculate 750 mL 1x YTPG media supplemented with 100 µg/mL ampicillin in 2 L baffled shake flasks, at a starting optical density (OD_{600nm}) of 0.1. Cell growth was conducted at 37°C, 250 RPM, and T7 polymerase expression was induced with 1 mM IPTG (isopropyl β-D-1-thiogalactopyranoside) at OD_{600nm} 0.8. Thereafter, cells were allowed to grow up to OD_{600nm} 4.0 and harvested by centrifugation at 7000 RPM and 4°C for 5 minutes. Cell pellet was washed three times and lastly resuspended in S30A buffer (**1 mL per gram of wet cell mass**; as per recipe in Table 2.10 below).

Table 2.10: S30A buffer components

S30A buffer (autoclaved and stored at 4°C)	
Tris	50 mM

Magnesium Glutamate	14 mM
Potassium Glutamate	60 mM
Acetic acid	to pH 7.8

Cell suspension was supplemented with RNAse inhibitor (Roche), protease inhibitor (Roche) and 2 mM dithiothreitol. Extract was prepared by sonication of harvested cell suspension for 3 minutes (four cycles of 45 seconds with one-minute rest intervals) on ice using a Bandelin Sonopuls HD 2070 ultraprobe Digital Sonicator (Bandelin Electronics, Berlin, Germany) at 70% amplitude. Lysate was supplemented with an additional 2 mM dithiothreitol followed by clarified by centrifugation for 10 minutes at 4°C. A run-off reaction was then carried out for one hour at 37°C and 250 RPM. The final extract was prepared by centrifuging the run-off reaction for 10 minutes at 4°C, which was flash frozen in liquid nitrogen and stored at -80°C until use. Protein concentration was quantified using a Micro BCA™ Protein Assay Kit (Thermo Fisher Scientific).

2.3.3 CFPS buffer components preparation

2.3.3.a Amino acids

A 4x amino acid mixture was prepared for use in CFPS: each amino acid (Sigma Aldrich BioUltra) was weighed separately to make a 3 mL solution at a 300 mM concentration (as per Table 2.11 below). Appropriate amount of each amino acid was dissolved first in 1 mL of 2 M KOH at room temperature by vortexing until completely dissolved. Then 2 mL distilled water was added to bring the total volume to 3 mL. 2 mL of each prepared amino acid was pipetted into a bigger flask and DI water was added to adjust the final concentration to 10 mM (4x working concentration). The flask was vortexed at regular intervals and placed on ice. 1 mL aliquots were created, flash frozen in liquid nitrogen and stored at -80°C until further use.

Table 2.11: List of amino acid components

Amino acid	Amount (mg)	Molecular Weight (g/mol)
Alanine	80	89.1
Arginine	157	174.2
Asparagine	119	132.1
Aspartic Acid	120	133.1
Cysteine	109	121.2
Glutamic acid	132	147.1
Glutamine	132	146.2

Glycine	68	75.1
Histidine	140	155.2
Isoleucine	118	131.2
Leucine	118	131.2
Lysine	132	146.2
Lysine monohydrochloride	164	182.65
Methionine	134	149.2
Phenylalanine	149	165.2
Proline	104	115.1
Serine	95	105.1
Threonine	107	119.1
Tryptophan	184	204.2
Tyrosine	163	181.2
Valine	105	117.1

2.3.3.b Energy solutions

Individual components for preparation of energy solutions were purchased from Sigma Aldrich (Bio Ultra) and stored at -20°C. A 20x master mix was prepared by weighing individual components (as per Table 2.12 below) and mixing them in 5 mL nuclease-free water. After addition of each component, the solution was vortexed to ensure even mixing while otherwise being kept on ice. The final mixture was divided into 200 µL aliquots, flash frozen in liquid nitrogen, and stored at -80°C until further use.

Table 2.12: List of energy components

Component	Final concentration in CFPS	Amount (mg)	Mol. (g/mol)	Weight
HEPES	50 mM	1192	238.3	
ATP.Na ₂ .2H ₂ O	1.2 mM	83	551.14	
ATP.K ₂ .2H ₂ O	1.2 mM	88	583.4	
GTP	1.2 mM	68	523.18	
UTP	1 mM	55	484.14	
CTP	1 mM	53	483.15	
Coenzyme A	0.3 mM	23	76753	
NAD	0.4 mM	27	663.43	
cAMP	0.8 mM	26	329.2	
Folinic acid	0.07 mM	4	473.44	
Spermidine	1 mM	15	145.25	
3-PGA	30 mM	690	186.06	
PEP*	33 mM	554.5	168.04	

* PEP was only added to the energy mixtures where specified

2.3.3.c Other components for optimisation

- Magnesium glutamate (molecular weight 388.62 g/mol) and potassium glutamate (molecular weight 185.22 g/mol) were individually weighed and reconstituted to a final concentration of 1 M in nuclease free water. The mixtures were sterile filtered (Millex-GP 0.22 μm filter) and stored at 4°C until further use.
- Polyethylene glycol (PEG; molecular weight 600 g/mol, 6000 g/mol, and 8000 g/mol) was diluted in nuclease-free water to produce a 50% w/v stock, stored at room temperature (in the case where PEG had solidified, heat was applied to obtain a solution first).
- RNase inhibitor was purchased from Roche (#3335399001) and stored at -20°C. For each 50 μL cell-free reaction, 8 units of RNase inhibitor was added.
- Master stocks (1 M, in nuclease free water) of the following stabilising agents were created and stored at 4°C:
 - Sucrose (molecular weight: 342.3 g/mol)
 - Trehalose (molecular weight: 342.3 g/mol)
 - α/β -lactose (molecular weight: 342.3 g/mol)
 - B-cyclodextrin (molecular weight: 1134.98 g/mol)
 - Trimethylglycine (molecular weight: 117.148 g/mol)
 - Maltodextrin (molecular weight: 504.5 g/mol)

2.3.4 Setting up a cell-free protein synthesis reaction

For implementing in-house CFPS, reactions were set up in 50 μL volumes in Eppendorf tubes and were incubated at 37°C and 180 RPM with compositions as outlined in Table 2.13. For kinetic sfGFP fluorescence assays, reactions were set up in 50 μL volumes in black, flat bottom 96-well assay plates (Thermo Fisher Scientific). Reactions were supplemented with PEG 600 (Merck #25322-68-3) where specified.

Table 2.13: CFPS set-up for standard in-house reactions

Reagent (<i>final concentration</i>)	Reaction (<i>n</i> = 3)	Control (<i>n</i> = 3)
<i>E. coli</i> cell-free extract (40% v/v)	20 μL	20 μL
Energy components master mix (1x)	8 μL	8 μL
Amino acid mixture (2.5 mM)	12.5 μL	12.5 μL
Plasmid DNA	250 ng – 500 ng protein construct	250 ng – 500 ng pET20b vector
Magnesium glutamate (20 mM)	1 μL	1 μL
Potassium glutamate (50 mM)	2.5 μL	2.5 μL
RNase Inhibitor (4 units)	0.2 μL	0.2 μL
Nuclease free water	to 50 μL	to 50 μL

2.3.5 Freeze-dried CFPS on cellulose stacks

For investigating freeze-dried CFPS on paper format, three types of paper were used: Toilet paper; hand towel (Boots Science Building); blue roll (laboratory). Paper circles were cut using a 5 mm diameter hole puncher and one paper was deposited in each Eppendorf tube. Each tube was supplemented with one type of solution as outlined in Table 2.14. Tubes were flash frozen using liquid nitrogen and freeze-dried overnight under vacuum (<120 mTorr) and condenser (-60°C) settings (VirTis Benchtop Lyophiliser Sentry 2.0). In order to test air-dried paper, samples were left inside biological safety cabinet with tubes open overnight. In the following morning, tubes were retrieved from freeze-drier and safety cabinet and the three papers (lysate, S.1 and S.2) were combined in one tube, followed by rehydration with 50 μ L nuclease-free water. Reactions were incubated at 37°C and 180 RPM overnight, unless otherwise specified. Fluorescence recordings were recorded, and protein samples were retrieved for analysis.

Table 2.14: Cell-free reaction set-up for paper and microglassification reaction formats

Components	Contents
Lysate	30 μ L cell-free extract supplemented with 4 units of RNase Inhibitor
Solution S.1	23 μ L amino acid mixture + 250 ng to 500 ng DNA
Solution S.2	23 μ L energy components, 20 mM magnesium glutamate, 50 mM potassium glutamate

2.3.6 Microglassification of CFPS components

Microglassification was conducted in 1.5 mL tubes containing 1 mL solvent (pentanol) and cell-free extract or complete cell-free reactions amounting to 50 μ L was pipetted. The mixture was vortexed in short bursts (3x, 10 seconds each) and briefly centrifuged (10 seconds at 4000 RPM) to collect the beads in the bottom of the tube. Excess solvent was removed by pipetting and the rest was allowed to evaporate from the samples, which were placed inside a vacuum desiccator overnight. The microglassified beads were rehydrated with either nuclease-free water or S30A buffer to 80% original reaction volume (~ 40 μ L). Viability of microglassified reactions or extract (all other reaction components fresh) was assessed by utilisation in cell-free reactions and synthesis of sfGFP, which was recorded using a Nanodrop™ 3300 Fluorospectrometer. Variations in mixing methods were carried out by tilting (tube was tilted on each side three times), injection (using a 30G 0.5 inch UniSharp needle) and no mixing (solution was slowly pipetted into solvent).

RNA extraction was carried out from BL21 Star (DE3) – pAR1219 cells grown in LB broth, similar to cell-free extract preparation. RNeasy kit (Qiagen) was used to isolate total RNA based on manufacturer's instructions and concentration was determined using a Nanodrop™ 2000 instrument. Samples were loaded on a TBE-Urea gel (BioRad) in 2x NOVEX loading dye (Invitrogen) after being heated at 70°C for 5 minutes. The gel ran for 35 minutes at 200V in 1x TBE running buffer (BioRad) and was further washed two times in TBE buffer. Then, the gel was incubated in 25 mL TBE buffer containing 25 mg/mL ethidium bromide. The gel was visualised under UV light after two further washes with TBE buffer to remove any excess ethidium bromide stain.

2.4 Analytical methods

2.4.1 Protein concentration

The Micro BCA™ Protein Assay Kit (Thermo Fisher Scientific) was used to determine total protein concentration. Dilutions and replicates of protein samples and BSA (bovine serum albumin) standards were created in 20 µL volumes. 500 µL of working reagent A and 250 µL working reagent B were added to each sample/standard. After a 30-minute incubation period at room temperature, absorbance readings were taken at 562 nm using a UV-Vis spectrophotometer (Agilent Multicell Peltier). Lastly, quantities of unknown protein concentrations were interpolated from a standard curve generated from the BSA standards. GraphPad Prism software 9.0 was used for statistical analyses like linear regression.

2.4.2 Quantification of fluorescence and protein yield

For kinetic sfGFP fluorescence assays, continuous fluorescence readings were taken for 12 hours to 24 hours in a plate reader (TECAN Spark® Multimode Microplate reader) for every 10 minutes. For four-hour timepoint analysis, fluorescence recordings and protein samples were retrieved after incubation of cell-free reactions for four hours in a shaker incubator revolving at 180 RPM. Recordings were taken using a NanoDrop™ 3300 Fluorospectrometer (Thermo Fisher Scientific). The excitation and emission wavelength for detection of sfGFP were 485 nm and 510 nm, respectively. For both kinetic and timepoint cell-free analysis, sfGFP protein yield was determined by interpolating fluorescence recordings (RFU) in a standard curve generated from known sfGFP concentrations. To achieve this, pure sfGFP stock concentration was determined using a Micro BCA™ Protein Assay Kit (Thermo Fisher Scientific) and appropriate dilutions were made. It was assumed that all sfGFP proteins in a sample were correctly folded.

2.4.3 SDS-Page and western blotting

Protein samples were combined with 2x protein loading buffer containing 5% β -mercaptoethanol and heated at 95°C for 5 minutes for SDS-PAGE and western blot analysis. Samples were run on a 12% TGX gel (BioRad) alongside a Precision Plus protein ladder (BioRad) and submerged in 1x TGX running buffer (BioRad) for 45 minutes at constant 200 V. For SDS-Page analysis, the gel was retrieved and incubated in 10 mL coomassie stain (Protein Ark) for 1 hour to 3 hours (for crude cell-free reactions) or overnight (for low yield purified proteins) with gentle shaking on a shaking platform. The stain was discarded, and the gel was washed with water three times for 10 minutes each and further incubated for 1 hour. The gel was then imaged using the Invitrogen white light transilluminator and an image was captured with the user's iPhone.

For western blot analysis, a Thermo Scientific™ SuperSignal™ West HisProbe kit was used and the gel was first transferred onto a nitrocellulose membrane (BioRad) using a BioRad Trans-Blot Turbo Transfer system. This membrane was blocked with BSA for one hour and washed with TBS-tween (Tris Buffered Saline with 0.1 % Tween-20). Then, the membrane was incubated with HisProbe™-HRP conjugated antibody (Thermo Fisher Scientific) for one hour. Five more washes with TBS-tween were performed for 10 minutes each and membrane was incubated with 4 mL ECL substrate (Thermo Fisher Scientific) and finally visualized using a GelDoc system to image the blot.

The following variations in the above protocol were opted for non-reducing, native gel and fluorescent gel analysis. The protein samples for non-reducing gels were prepared with 2x protein loading buffer without 5% β -mercaptoethanol or heat. For Native-Page analysis, samples were prepared in native protein loading buffer (BioRad) and loaded on a 12% TGX gel. The pI of the protein to be separated was calculated based on its amino acid compositions. Only proteins with a net negative charge (typically pI 3 to 8) are able to migrate through the gel or the polarity of the electrodes was inversed to allow basic proteins to migrate. A native running buffer (1x) was used to run the gel at 200 V for 1 hour. The absence of SDS and β -mercaptoethanol in the native-page analysis provided a non-reducing and non-denaturing environment that in turn allowed protein separation in its native state. Lastly, fluorescent gels were simply imaged by placing the gel of interest on a blue light transilluminator and the resulting signal was captured using the user's iPhone.

2.4.4 RT-qPCR analysis

Cell-free reactions amounting to 100 μ L were prepared with the following templates each: pET20b(+), sfGFP-His, reteplase-His, teriparatide-His, alfineprase-His, entolimod-His and G-CSF-His. The reactions were prepared without the amino acid mixture to prevent translation (S30A buffer was added in place of 4x amino acids) and incubated at 37°C for 4 hours. The RNA was extracted from each reaction using a Qiagen RNeasy kit; manufacturer's instructions were followed. The yield of the extracted RNA was quantified using a Nanodrop™ 2000 instrument with the RNA quantification setting (absorbance at 260 nm). Yields around 200 ng/ μ L with a purity (260 nm / 280 nm) ratio of \sim 1.8 - 2 was considered satisfactory. Next, reverse transcription of the RNA was carried out using the Qiagen Quantitech reverse transcription kit. Briefly, 1 μ g RNA pertaining to each template was added and a DNA wipeout reaction was performed. Next, reverse transcription (along with a no reverse transcription control) reactions were performed using primers provided with the kit to obtain cDNA.

2x QuantiFast SYBR Green PCR Master Mix, the template cDNA, primers and RNase free water were thawed on ice and combined according to Tables 2.15 and 2.16. Reactions were set up in triplicate for each construct and controls (pET20b and no reverse transcription controls), were thoroughly mixed and aliquoted in qPCR strip tubes (cDNA was added in last).

Table 2.15: Primer information sheet for RT-qPCR

Construct	Forward primer	Reverse primer	Size	% GC
sfGFP	ATGCGCAAGGGCGAG	GGTGGTGCAGATGAACTTCAG	15/21	67/2
Reteplase	AACCTGCATGACGCCTG	CAGTCCAGGTAGTTGGTCAC	17/20	59/56
Alfineprase	ATGAGCTTCCCGCAGC	GGATATTCAGCGGGCGATAG	16/20	63/55
G-CSF	CGCAGAGCTTCTGCTG	ACGGAATGCCCAGGC	15/17	65/67
Entolimod	TAGCCTGAGCCTGCTGAC	GGTGAAGCGATTGGCAATG	18/19	61/53
Teriparatide	ATGAGCGTGAGCGAAATCC	GAAGTTATGCACATCCTGCAG	19/21	53/48

Table 2.16: RT-qPCR reaction set up

Component	Amount
Quantifast mastermix (2X)	10 μ l
Forward primer (10 μ M)	2 μ L

Reverse primer (10 μ M)	2 μ L
cDNA (< 100 ng/reaction)	2 μ L
RNase free water	4 μ L

The following cycle settings were used for the qPCR in the Rotor-Gene Q instrument (Qiagen):

Table 2.17: qPCR thermocycler settings

Step	Temp.	Time
Heat activation	95°C	5 minutes
40 Cycles	95°C	10 seconds
	60°C	30 seconds
Hold	4°C	

The real-time fluorescence recordings were taken during all cycles, and the cycle threshold values were exported as a .csv file and cycle threshold values were plotted for analysis.

2.4.5 FTIR spectra collection and data analysis

Purified proteins in need of FTIR investigation were first lyophilised (protocol detailed in Section 2.5.1) and the subsequent pellet was rehydrated in D₂O to achieve a concentration of > 1 mg/mL. An Agilent Cary 630 FTIR spectrophotometer was used to take IR absorbance readings from 4000 cm⁻¹ – 500 cm⁻¹ with 16 scans at a 4 cm⁻¹ resolution. The instrument was cleaned thoroughly with isopropyl alcohol, and the pedestal was purged with dry air for 10 seconds before loading a protein sample (~ 5 μ L). Background subtraction was carried out with D₂O and three spectra were collected per sample. The spectra were then subject to mathematical analysis using the Origin Lab software. A user-defined baseline correction was performed, and the second derivative method was used to deconvolute the peak in the 1700 cm⁻¹ – 1600 cm⁻¹ amide I region. The derivative curve was smoothed using the Savitsky-Golay function and gaussian curves were fitted for each identified peak. Curve fitting was judged by the goodness-of-fit to the original baseline subtracted data. Peak assignments were made based on previously assigned wavenumbers and the percentage secondary structure was determined by the area integral of each individual peak in the 1700 cm⁻¹ – 1600 cm⁻¹ region.

2.4.6 CD spectra collection

Far-UV CD spectra were obtained using a ChiraScan™ spectrophotometer (Applied Photophysics) at ~ 25°C. An average of three scans were obtained for all spectra, which were recorded in a 10 mm path length cell from 260 nm to 190 nm. A water background recording was first taken and subtracted from all subsequent spectra. All spectra were collected in water, protein samples and dilutions were made in water as well. The HT (photo multiplier) voltage and the absorbance values were recorded for each sample. Absorbance readings that recorded HT values above 600 were discarded due to high noise. The cell was cleaned thoroughly with water and then purged with nitrogen gas for 30 seconds between each reading and sample type. The exported absorbance recordings for the dilutions that reported HT < 600 were plotted on GraphPad Prism to obtain the raw spectra.

2.4.7 Statistical analysis and software

Statistical parameters such as the *n* value and standard deviations are detailed in the figures and legends. For CFPS time point analysis, each data point represents a mean of biological triplicates measured at 10-minute intervals, where the error bars represent the standard deviation. GraphPad Prism (version 9) software was used to calculate the means and standard deviations. One-way ANOVA was performed to determine significant differences in optimized reaction compositions. Other software such as SnapGene was used for cloning of reporter/therapeutic constructs and ImageJ was used for imaging and editing western blots.

2.5 Other methods

2.5.1 Lyophilisation

Tubes were flash frozen using liquid nitrogen and placed in a freeze-drier overnight under the following vacuum (<120 mTorr) and condenser (-60°C) settings (VirTis Benchtop Lyophiliser Sentry 2.0). Unless otherwise specified, each reaction (~50 µL) was lyophilised in 1.5 mL Eppendorf tubes, lid open and sealed with parafilm. A hole was made in each parafilm seal to allow for water to leave the tubes during lyophilisation. After lyophilisation, the seals were removed, the Eppendorf lids were closed and tubes stored until later use. Note that freeze-drying/freeze-drier may be used interchangeably with lyophilisation and Lyophiliser.

2.5.2 Stability studies

The accelerated stability studies were planned according to temperature, humidity and time requirements in lyophilised pellets and cellulose stacks format. Appropriate time points for sampling and the number of samples required at each time point (taking biological triplicates into account) were calculated beforehand. The adequate number of stability samples were prepared and lyophilised in 1.5 mL Eppendorf tubes to a volume of 50 μ L in the case of lyophilised pellets or three individual cellulose stacks as described in Section 2.3.5. Each stability sample was labelled with a batch number, temperature, date of preparation, and sampling time point. Samples were placed in a stability oven or cold room for 40°C and 4°C temperatures respectively. For room temperature experiments, samples were placed on the lab bench and a temperature monitor was placed directly beside the samples. Sample stability was analysed by first rehydrating the sample with S30A to 80% original reaction volume (40 μ L unless otherwise specified). Reactions were incubated at 37°C for at least 16 hours at 180 RPM and fluorescence recordings were taken with a Nanodrop™ 3300 Fluorospectrometer (ThermoFisher Scientific).

2.5.3 Bead-based protein purification

HisPur™ Ni-NTA Magnetic Beads (ThermoFisher Scientific) were used for the bead based purification approach. The beads composed of Nickel (Ni^{2+}) - nitrilotriacetic acid, have high affinity to proteins with a histidine tag (6x) and other substances such as imidazole and can be pulled down using a magnetic holder. First, the binding buffer (50 mM NaH_2PO_4 , 300 mM NaCl and 20 mM Imidazole) and elution buffers (50 mM NaH_2PO_4 , 300 mM NaCl and 400 mM Imidazole) were prepared from the appropriate stock solutions in water and adjusted to pH 8.0. The buffers were then sterile filtered and stored under refrigerated conditions until use. The protein mixtures (500 μ l for each protein) were added to the magnetic beads (125 μ L) after the beads were washed thoroughly in binding buffer. For mixing, slurries were vortexed briefly and for collection of beads, a magnetic Eppendorf stand (Invitrogen) was utilised. The protein-bead slurry was incubated at 4°C for 1 hour on a rolling platform with gentle rotation. The beads were then collected, and supernatant was removed. The beads were washed with binding buffer 3 times and the supernatant was discarded after taking fractions each time. The pure protein was eluted by adding 25 μ L elution buffer and two supernatant fractions were collected, combined and examined by SDS-Page or western blot analysis. A Vivaspin® 20 centrifugal column was used to concentrate and exchange the protein sample from elution buffer to DNase and RNase free water (Invitrogen).

2.5.4 ÄKTA start column-based protein purification

Similar in principle to the bead-based purification method, the column -based method utilised a HisTrap™ affinity chromatography column (Cytiva Life Sciences) containing the Ni-NTA resin and an ÄKTA start fluidic system to automate the purification process. The system was first washed with water to remove the storage buffer (ethanol) and the column was connected to a liquid chromatography system (10x column volume). The system was thoroughly washed with binding buffer and then the protein sample (~ 1 mL) was loaded. The column selectively bound the histidine-tagged proteins, while other non-specific proteins passed through, and this was observed through the real-time UV absorbance readings at 280 nm. (10x column volume at a flow rate of 1 mL/minute). Then, the bound proteins were eluted using elution buffer containing imidazole (6x column volume at a flow rate of 1 mL/minute; six fractions collected). UV absorbance recordings informed which fractions were combined (in the case of sfGFP, the fractions that contained pure sfGFP was readily visible due to the bright green signal). A Vivaspin® 20 centrifugal column was used to concentrate and exchange the protein sample from elution buffer to DNase and RNase free water (Invitrogen), carried out three times.

Chapter 3 Generation of in-house bacterial cell-free extract and DNA templates

3.1 Introduction and aims

CFPS is a method that utilises components extracted from living cells to produce various proteins of interest, when supplemented with the appropriate building blocks (DNA template, energy, amino acids *etc.*). Of these starting materials, cell-free extract and the DNA templates are particularly susceptible to batch-batch variation (*i.e.* small changes in the preparation process can lead to large variations in the cell-free reactions yields). Therefore, this project began with the aim to establish a reliable in-house CFPS system, founded on *E. coli* cell-free extract, with expression driven by T7 polymerase.

BL21 (DE3) (and its variants BL21 Star, Rosetta, and ClearColi® BL21) and the Shuffle T7 strain are among the most commonly used bacterial strains in literature, for steady, endotoxin-free synthesis in the former category, and inducing disulfide bonds in the later (Krinsky et al., 2016, Wilding et al., 2019, Kwon and Jewett, 2015, Kim et al., 2006b, Dopp and Reuel, 2019).

BL21 Star (DE3) was chosen as the lead candidate for cell-free extract preparation owing to its high protein expression capabilities, quick growth/reaction times, and an already well-established history with CFPS (Au - Levine et al., 2019). It is a genetically engineered strain offering higher mRNA and protein stability (low endogenous RNAses and proteases) and has been optimized for protein expression from low-copy number T7-promoter based plasmids. However, a high level of soluble and active T7 polymerase is required for cell-free synthesis in such extracts. Hence, the enzyme is often added as a supplement to BL21 Star (DE3) cell-free extracts, making it a more expensive and time-consuming procedure. To address this challenge, a plasmid (pAR1219) coding for T7 polymerase was transformed, in addition to the basal T7 polymerase already expressed in the BL21 Star (DE3) strain. Impact of this transformation was studied through turbidimetric analysis. Furthermore, solubility of T7 polymerase was studied at various timepoints to identify most soluble T7 polymerase levels for cell-extract preparation.

DNA template design is another critical step for successful CFPS. Codon optimisation significantly enhances expression when tailored to the strain of choice for cell-free extract preparation (Zhang et al., 2021). Many types of nucleic acid templates have been utilised for CFPS: Plasmid DNA (Levine et al., 2019) and linear DNA (PCR

products)(Wu et al., 2007, Nomoto and Tada, 2018, Sato et al., 2022), with very limited work on understanding mRNA, perhaps owing to its instability (Hansen et al., 2016). Plasmid DNA was the main source of genetic material for this work, primarily for ease of production (*e.g.* large-scale DNA isolation using midi-preps) and ease of generating linear templates through PCR using existing primers, if needed.

The broad aims for this chapter are -

- (a) Identify the optimal growth, induction and harvest conditions to obtain cell-free extract with the highest level of T7 RNA polymerase
- (b) Clone the expression constructs for the five therapeutic proteins and a fluorescent reporter protein.

3.2 Results and discussion

3.2.1 Development of the BL21 Star (DE3) – pAR1219 strain

3.2.1.a Effect of pAR1219 transformation on expression host BL21 Star (DE3) growth kinetics

The T7 bacteriophage RNA polymerase has been widely reported for efficient expression of recombinant proteins in both cell-based and cell-free systems (Angius et al., 2018, Failmezger et al., 2017, Tabor, 2001). pAR1219, a commercially available plasmid traditionally used for gene knockout experiments, has more recently become a tool for T7 polymerase overexpression in cell-free synthetic biology (Krinsky et al., 2016, Krinsky et al., 2018). pAR1219 can be transformed in bacterial strains to enhance the endogenous levels of T7 polymerase in strains already expressing the polymerase (such as BL21 Star (DE3)). Similar to endogenous expression, pAR1219 expresses T7 RNA polymerase under the control of inducible *lac* promoter.

Firstly, *E. coli* BL21 Star (DE3) was transformed with pAR1219 to create recombinant strain *E. coli* BL21 Star (DE3)-pAR1219 (Figure 3.1, a). Then, the growth of *E. coli* BL21 Star (DE3)-pAR1219 was monitored to study the impact of the transformation. Detailed protocols for this experiment are provided in Section 2.2.1. Briefly, the experimental set up consisted of two strains, BL21 Star (DE3) and BL21 Star (DE3)-pAR1219 studied with and without IPTG induction (0.2 mM) when cultures reached $OD_{600} = 1.0$.

The results indicate a clear exponential growth pattern in all batches, shifting to a stationary trend after nine hours of incubation. The recombinant strain, *E. coli* BL21

(DE3)-pAR1219, grew slower (growth rates 0.1838 hr^{-1} for induced and 0.1809 hr^{-1} for un-induced) in comparison to *E. coli* BL21 Star (DE3) (growth rates 0.2605 hr^{-1} for induced and 0.2825 hr^{-1} for un-induced; Figure 3.1, b). Although linear regression analysis confirmed that the difference between slopes is not significant, the recombinant strain is expected to have a lower growth rate due to additional protein expression from transformed plasmid.

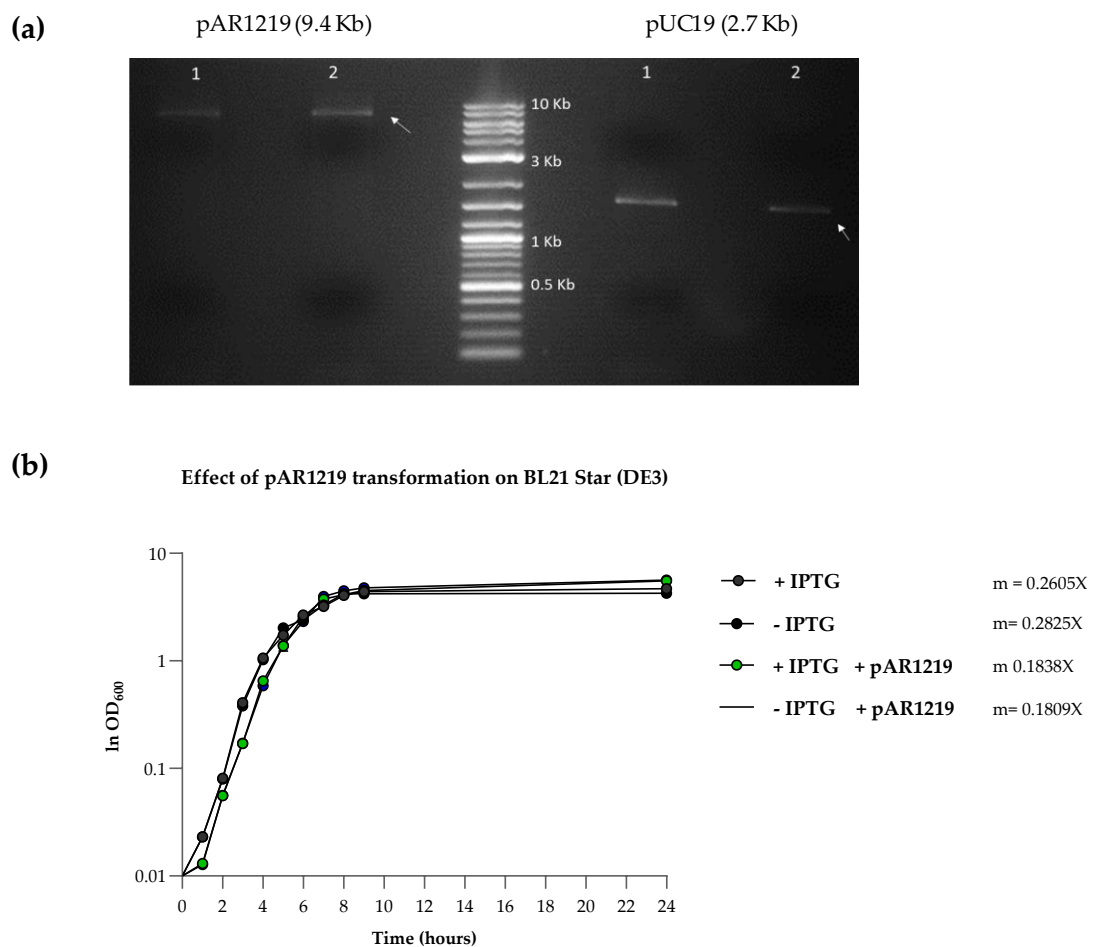


Figure 3.1: (a) A stained agarose gel showing DNA corresponding to plasmid purified from BL21 Star (DE3) – pAR1219 cells. Samples were run alongside 1 kb Plus DNA ladder for comparison of size. Arrow shows bands corresponding to plasmid pAR1219 (left; 9.4 kb) and control plasmid pUC19 (right; 2.7 kb); (b) Growth curve of BL21 Star (DE3) – pAR1219 compared with BL21 Star (DE3) shown with and without IPTG induction. Growth rates calculated from linear regression analysis are shown in the legend ($n = 6$)

3.2.1.b pAR1219 transformation enhances the levels of T7 polymerase in BL21 Star (DE3) cells

The T7 RNA polymerase expression profiles of both strains were studied by SDS-Page analysis, in an effort to enhance T7 polymerase levels. Proteins were stained

using coomassie dye and the T7 polymerase bands (99 kDa) were identified adjoining the 100 kDa band of molecular ladder.

T7 polymerase expression was detected in both conditions with and without pAR1219 within two hours after induction (Figure 3.2; '2 hr'). However, strongest expression was seen in BL21 Star (DE3)-pAR1219 induced with IPTG (Figure 3.2, b; '2 hr'). A similar pattern was observed five hours after induction (Figure 3.2; '5hr'), from which T7 polymerase was present predominantly in the insoluble fraction.

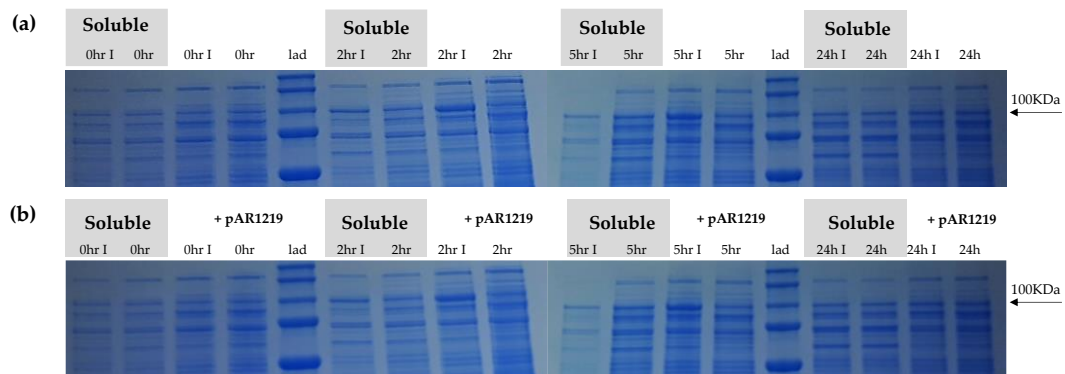


Figure 3.2: SDS-Page analysis of (a) BL21 Star (DE3) and (b) BL21 Star (DE3)-pAR1219. Both soluble and insoluble fractions were collected in the following times: 0 hr sample taken before induction; 2 hr, 5 hr and 24 hr samples taken after those hours of induction respectively. 'Lad' indicates molecular ladder. Arrow indicates expected size of T7 RNA polymerase. Induced samples are labelled 'I' and soluble sample are highlighted within a grey box.

3.2.1.c Time course analysis of BL21 Star (DE3) – pAR1219 under various growth temperatures

In order to improve solubility of T7 polymerase, a number of culture conditions were tested. Firstly, two lower incubation temperatures, 25°C and 30°C, were tested in addition to previously used 37°C. Next, the concentration of IPTG used to induce expression was expanded to 0.2 mM, 0.5 mM and 1 mM (with 0 mM as the un-induced control). Collectively, 12 different temperature-IPTG combinations were tested and OD₆₀₀ measurements were plotted over time to obtain growth curves. It was evident that cells had slower growth rates as incubation temperatures decreased (Figure 3.3 b, c, d).

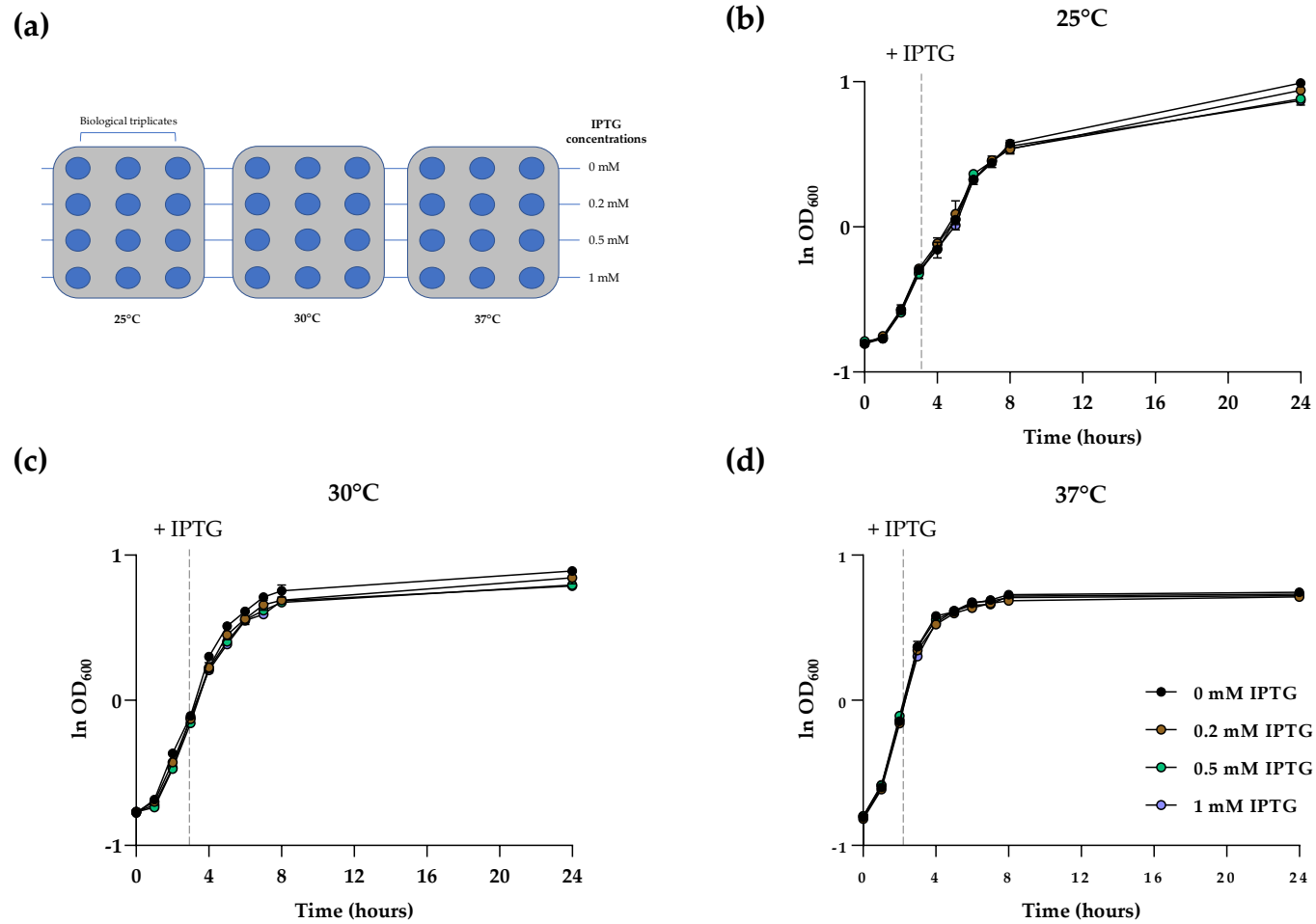


Figure 3.3: (a) Experimental set up for time course analysis of BL21 Star (DE3) – pAR1219. Each circle indicates 1 flask. BL21 Star (DE3)_pAR1219 growth curves at (a) 25°C, (b) 30°C and (c) 37°C respectively. Grey dotted line indicates time of induction and error bars are smaller than data points, where they are not visible ($n = 9$).

3.2.1.d SDS-Page analysis reveals best temperature and IPTG concentrations for most soluble levels of T7 polymerase

SDS-Page analysis was carried out to determine solubility of T7 polymerase, similar to Section 3.2.1.b. At 25°C, little expression was detected two hours post-induction at 0.5 mM and 1 mM IPTG concentrations (Figure 3.4; soluble fraction). Stronger expression was detected at 0.5 mM, five hours post-induction in comparison to 1 mM, suggesting that 0.5 mM is perhaps adequate (Figure 3.4; soluble fraction). Most T7 RNA polymerase was insoluble at 24 hours (Figure 3.4; insoluble fraction).

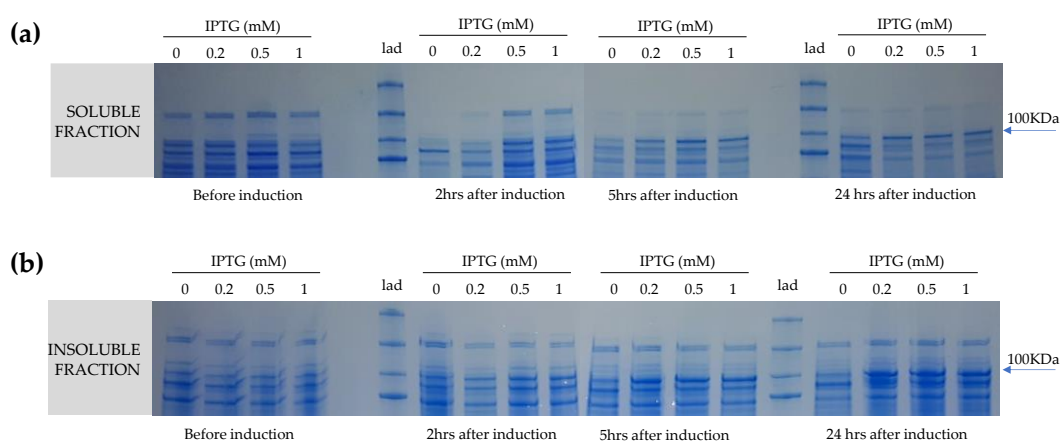


Figure 3.4: SDS-Page analysis of (a) soluble and (b) insoluble BL21 Star (DE3)-pAR1219 cell extract obtained from cells grown at 25°C and induced using varied concentrations of IPTG (0 – 1 mM IPTG). ‘Lad’ indicates molecular ladder.

At 30°C, the enzyme was produced two hours post-induction at all IPTG concentrations (Figure 3.5; soluble fraction). Strong bands around 100 kDa were observed at 0.5 mM and 1 mM five hours post-induction (Figure 3.5; soluble fraction). However, strong bands in the insoluble fraction were also observed (Figure 3.5; soluble fraction). Very little soluble T7 polymerase was detected at 24 hours (Figure 3.5; 24 hrs soluble and insoluble fractions).

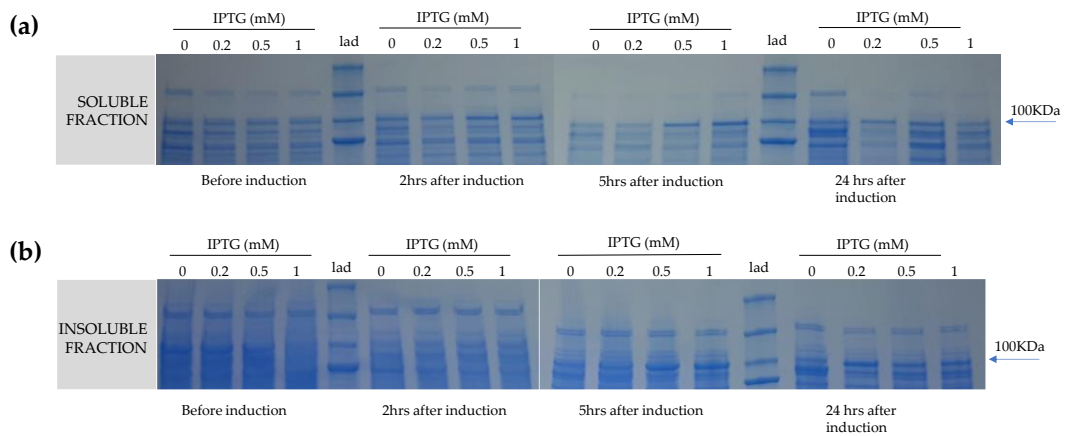


Figure 3.5: SDS-Page analysis of (a) soluble and (b) insoluble BL21 Star (DE3)-pAR1219 cell extract obtained from cells grown at 30°C and induced using varied concentrations of IPTG (0 – 1 mM IPTG). Lad' indicates molecular ladder.

Unlike what was observed at 25°C and 30°C, a majority of soluble T7 polymerase was found expressed two hours post-induction at 37°C, with maximum production at 0.5 mM IPTG concentration (Figure 3.6; soluble fraction). By five hours after induction, majority of T7 RNA polymerase had shifted to the insoluble fraction and few traces of T7 polymerase were found by 24 hours.

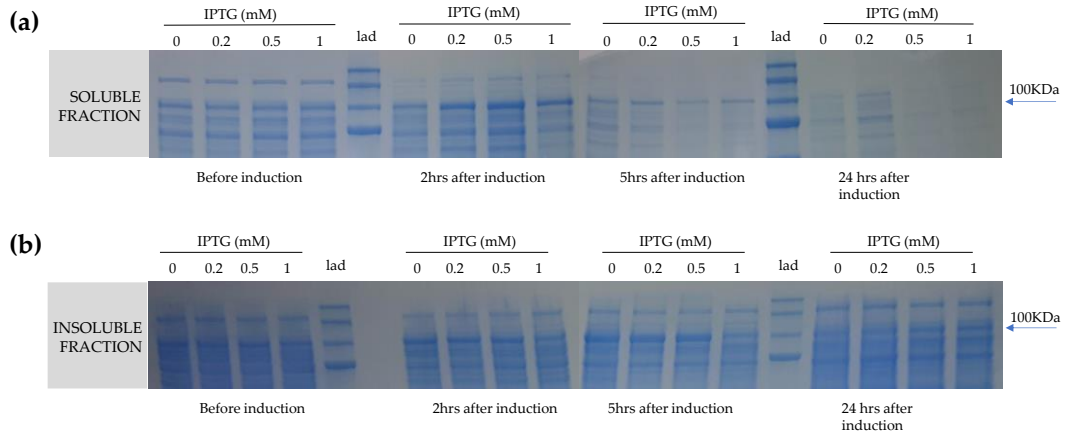


Figure 3.6: SDS-Page analysis of (a) soluble and (b) insoluble BL21 Star (DE3)-pAR1219 cell extract obtained from cells grown at 37°C and induced using varied concentrations of IPTG (0 mM – 1 mM IPTG). Lad' indicates molecular ladder.

Collectively from all conditions tested, production of T7 RNA polymerase was strongest at five hours post-induction and 24 hours post-induction at 25°C, two hours and five hours post-induction at 30°C and two hours post-induction at 37°C. Strongest production in the soluble fraction was seen at 37°C, two hours after induction with 0.5 mM IPTG; this was also observed to be the fastest method of obtaining soluble T7 polymease expression.

3.2.2 Development of fluorescence reporter templates: sfGFP and sfGFP-His

Superfolder green fluorescent protein (sfGFP) is revolutionising the field of protein biochemistry since its first appearance in 2006, due to several enhancements from its parent protein, GFP (Pédelacq et al., 2006). Derived from folding reporter GFP, sfGFP contains six mutations (S30R/Y39N/N105T/Y145F/I171V/A206V), conferring exceptional stability and fast folding kinetics. It is a 26.8 kDa protein with an excitation and emission wavelength of 485 nm and 510 nm, respectively (Cranfill et al., 2016). sfGFP comprises eleven β -strands, enveloping an α -helix containing the chromophore responsible for fluorescence (amino acids Gly-Tyr-Gly; PubChem ID 49866829). The β -barrel structure (formed as a result of hydrogen bonding between the eleven β -strands) surrounding the central pore is thought to contribute to the remarkable stability of fluorescent proteins in general (Figure 3.7, a). This property has allowed sfGFP to be used, for example: as a fusion protein to enhance solubility of binding partners; in cellular localisation experiments; and as fluorescence reporters in synthetic biology. Therefore, it is no surprise that sfGFP was often chosen as the fluorescent protein of choice for many cell-free studies.

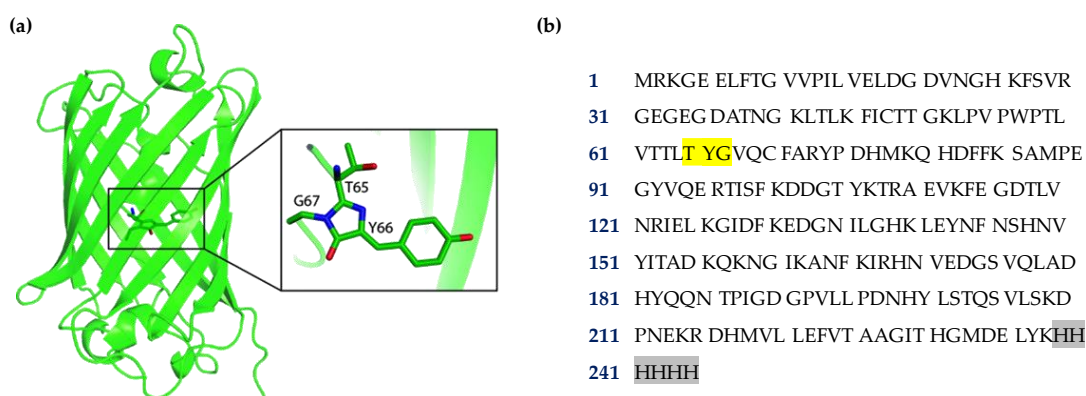


Figure 3.7: **Structure of sfGFP** (a) Wild-type sfGFP showing the β -barrel structure enveloping the α -helix and three amino acids forming the chromophore (b) Amino acid sequence of sfGFP used for cloning experiments, with the chromophore (TYG) and C-terminal histidine tag (HHHHHH), used in pET20b-sfGFP-His. Adapted from (Oleingski et al., 2021).

Two plasmids harbouring the sfGFP gene were created for cell-free applications outlined in this thesis: pET20b(+)-sfGFP and pET20b(+)-sfGFP-His (Figure 3.7, b). pET20b(+)-sfGFP was first cloned and a C-terminal Histidine tag was later added to create pET20b(+)-sfGFP-His. As described in Section 3.2.1, a T7 polymerase-driven cell-free expression system was envisioned. On that account, the pET plasmid system was selected for T7 promoter-driven production of downstream protein(s). The pET20b(+) vector carries a T7 promoter, T7 transcription terminator and an ampicillin resistance gene to allow selection of bacteria harbouring the plasmid.

3.2.2.a Assembly of pET20b(+) and sfGFP to generate pET20b(+) - sfGFP

The plasmid pBAD24 – sfGFPx1 (5228 bp) was used as a source of sfGFP gene and cloned into the pET20b(+) vector using NEB HiFi DNA assembly (Figure 3.8, a). This was achieved by first amplifying the sfGFP and the vector backbone fragments (Figure 3.8, b). The sfGFP fragment was subsequently assembled into the multiple cloning site of pET20b(+) using assembly cloning and the assembled DNA was transformed in NEB 5 α competent cells. Seven single colonies were sub-cultured, and an agarose gel was run to verify the presence and sizes of the extracted DNA (Figure 3.8, c).

Four different sized colonies were chosen (Colonies 1 – 4; Figure 3.9, a) based on size for further confirmation. DNA was extracted and re-amplified using previously designed primers to scan for the presence of two (sfGFP and pET20b) assembled fragments. Amplified products were visualised on a 1% agarose gel. The vector (pET20b+ backbone) and insert (sfGFP) fragments were found to be present in Colonies 2, 3 and 4, but vector was absent in Colony 1 (Figure 3.9, a). DNA sequencing results indicated mutations and truncations in colonies 1, 3 & 4 when aligned with known *in silico* sequences. DNA from Colony 2 and Colony 3 were individually transformed in BL21 Star (DE3) cells for expression of sfGFP. It was immediately evident that Colony 3 contained the correct sequence as it produced a bright green colour, distinctive of sfGFP, whereas Colony 2 culture did not (Figure 3.9, b & c). The cells were in fact not induced to start expression, however, cells still expressed the sfGFP gene due to the leaky nature of T7 promoter. Meanwhile, samples were sequenced (Eurofins Genomics) and aligned against known pET20b(+) – sfGFP sequence. Sequence from Colony 3 aligned devoid of any mutations, confirming a successful cloning.

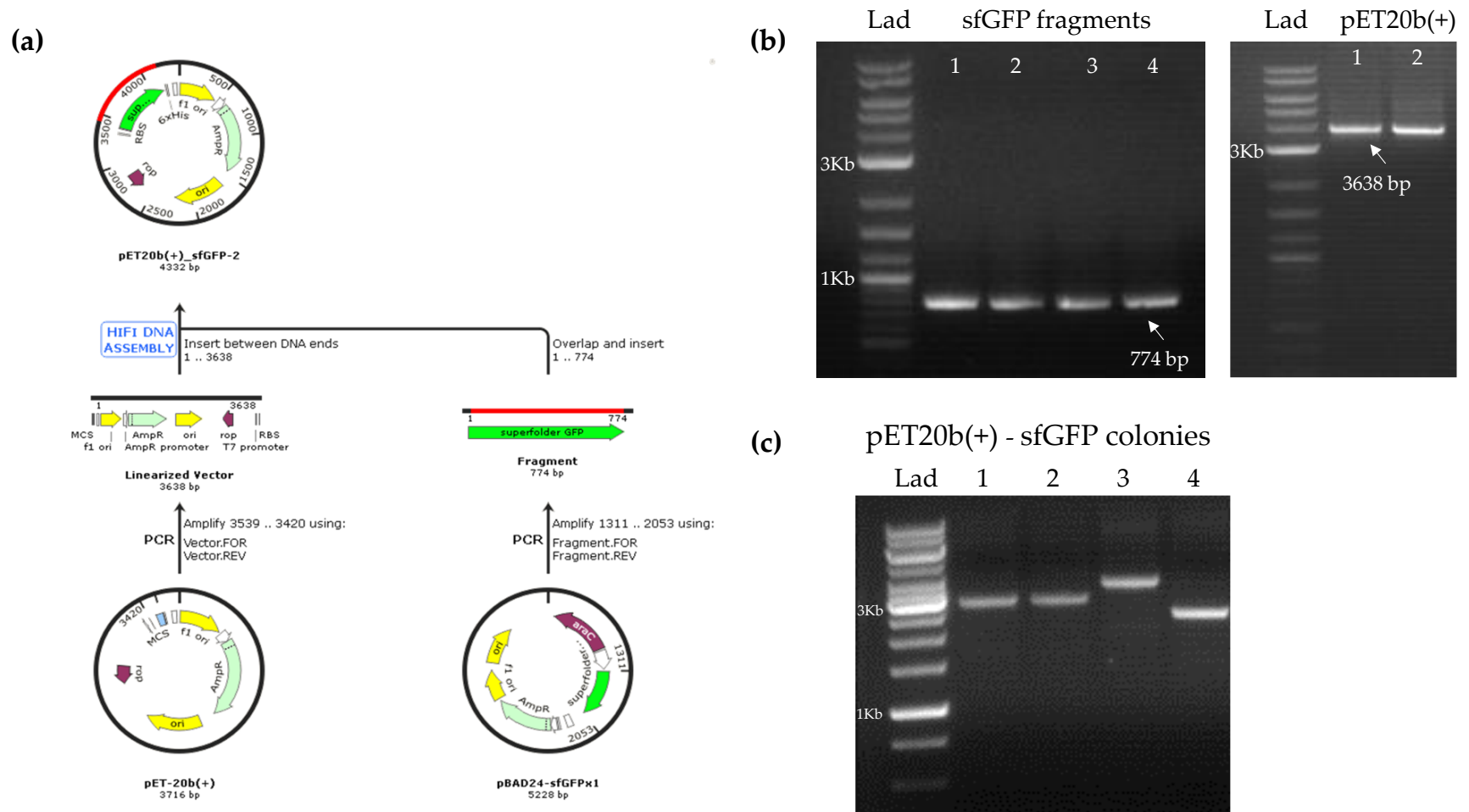


Figure 3.8: Cloning of pET20b(+) – sfGFP (a) Summary of the cloning procedure (obtained from SnapGene) (b) Stained 1% agarose gels showing PCR-amplified vector (right) and insert (left) fragments (c) Stained 1% agarose gel showing DNA extracted from 7 different NEB5α colonies transformed with assembled pET20b(+) – sfGFP. Lad' indicates molecular ladder.

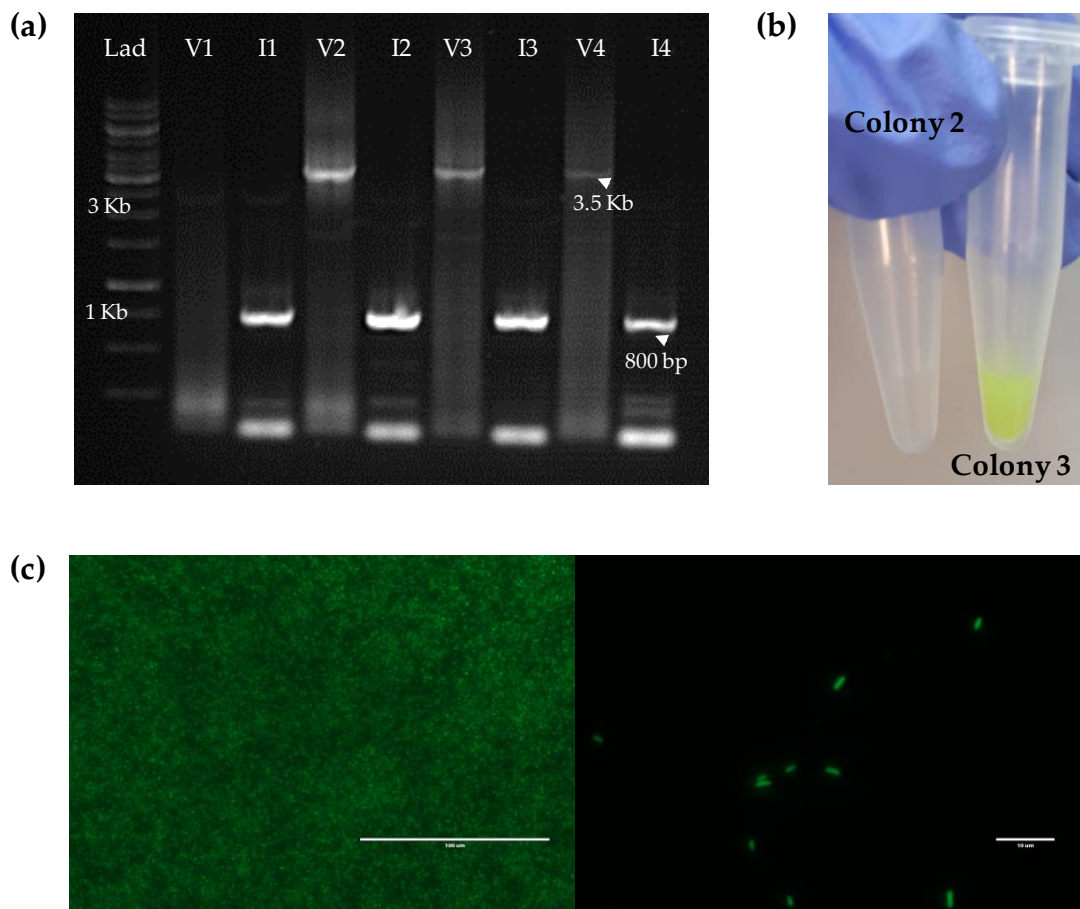


Figure 3.9: Verification of pET20b(+) – sfGFP (a) Stained 1% agarose gel showing re-amplified vector (V) and insert (I) fragments from pET20b(+) – sfGFP. The expected sizes and bands are marked with white arrows. Lad' indicates molecular ladder. (b) Picture of BL21 Star (DE3) cells transformed with colony 2 and colony 3 DNA. Cells transformed with colony 3 DNA were yellow/green in colour, an indication of sfGFP expression. Cells cultivated with colony 2 DNA were translucent. (c) **Images of BL21 Star (DE3) cells transformed with colony 3 DNA**, captured using the EVOS M5000 imaging system (Thermo Fisher Scientific) with the GFP Light cube. A 10x (left) and 100x (right) magnification of cells in suspension is shown.

3.2.2.b Cloning a C-terminal histidine tag to enable purification of pET20b(+) – sfGFP

The NEB HiFi DNA assembly was, once again, used to add a C-terminal histidine (His) tag to sfGFP, leading to the creation of pET20b(+)-sfGFP-His. Primers were designed such that 6x histidine were inserted to amplified sfGFP fragments when the samples were subject to PCR amplification (Figure 3.10; 'sfGFP-His;'). The sfGFP-His fragments were then combined with pET20b fragments and the overlapping region was assembled to obtain final plasmid (Figure 3.10; lanes 1 & 2). Sequence of assembled DNA was confirmed (Eurofins Genomics) and aligned with known pET20b(+) – sfGFP-His sequence.

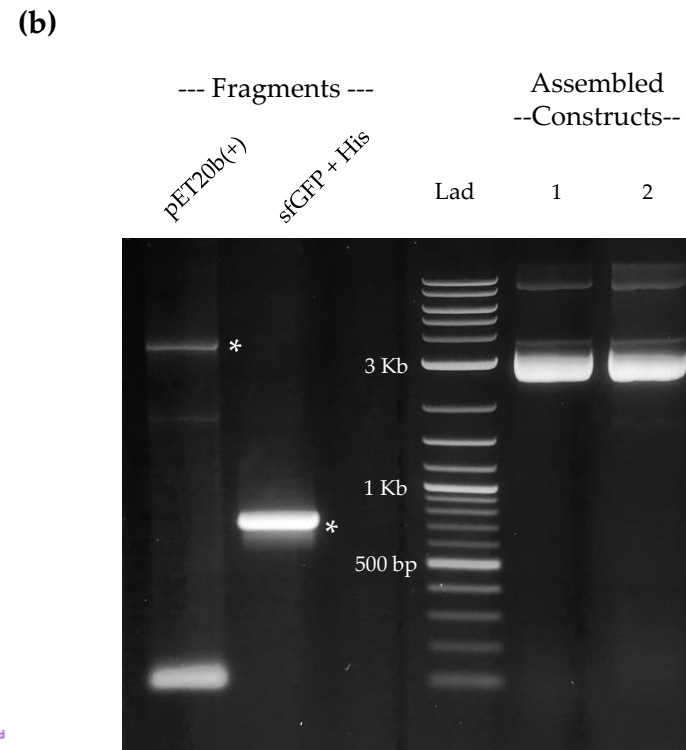
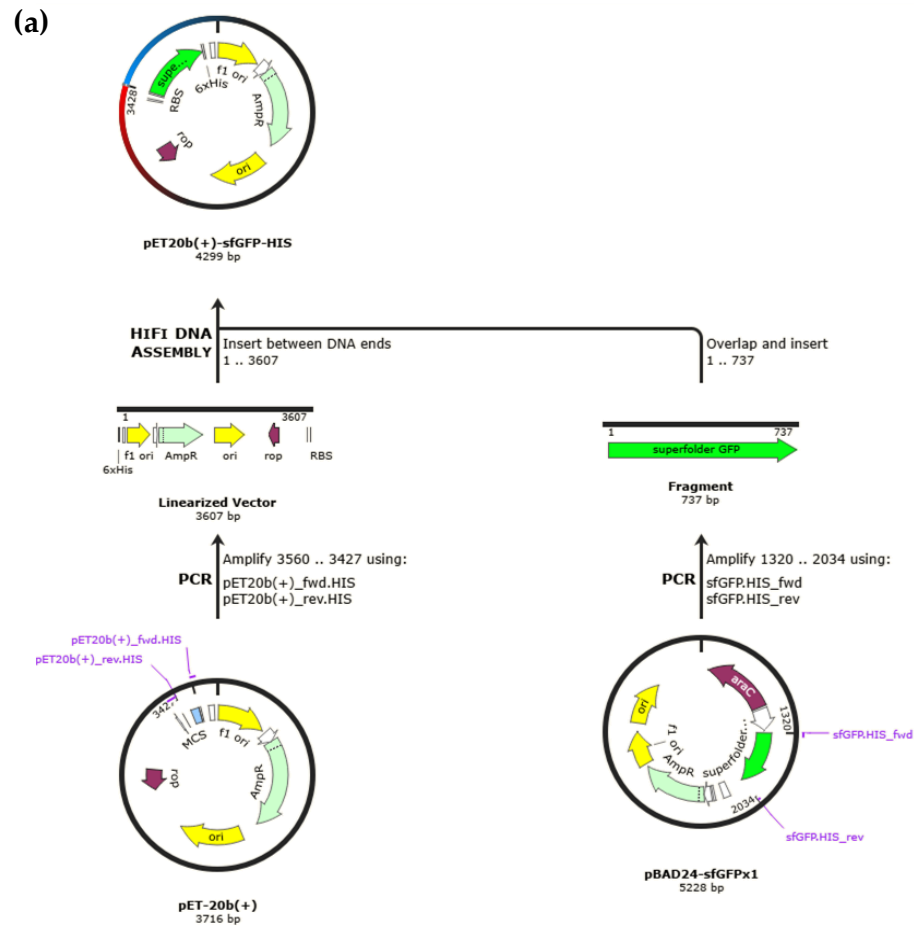


Figure 3.10: Cloning of pET20b(+)-sfGFP-His (a) Summary of the cloning procedure (obtained from SnapGene) (b) Stained 1% agarose gel showing PCR-amplified vector (pET20b+) fragment, insert (sfGFP-His) fragment and assembled pET20b(+)-sfGFP-His fragments (1 & 2). Lad' indicates molecular ladder.

3.2.3 Generation of therapeutic protein constructs

3.2.3.a Restriction enzyme cloning of reteplase, alfineprase, entolimod, and G-CSF

Codon optimized DNA corresponding to therapeutic proteins reteplase, alfineprase, entolimod, and G-CSF (including C-terminal 6x His) each arrived in a pUC57 carrier plasmid. The DNA was first transformed and amplified in cloning host NEB5 α (Figure 3.11). Then, these plasmids and pET20b(+) vector were digested using EcoRI and XhoI restriction enzymes to generate fragments with sticky ends (Figure 3.12). Fragments coding for the therapeutic proteins were ligated with the pET20b(+) vector fragment and transformed into NEB5 α cloning host. Several colonies were screened, and plasmids were sequenced to obtain therapeutic protein templates (Figure 3.13).

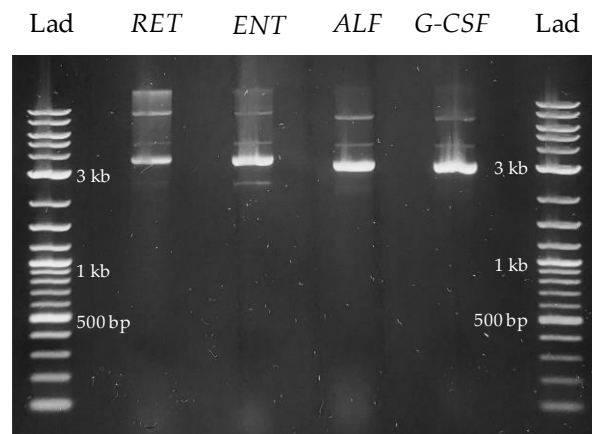


Figure 3.11: Stained 1% agarose gel showing amplified pUC57 DNA containing reteplase (RET), entolimod (ENT), alfineprase (ALF) and granulocyte-colony stimulating factor (G-CSF) coding sequences. Lad' indicates molecular ladder.

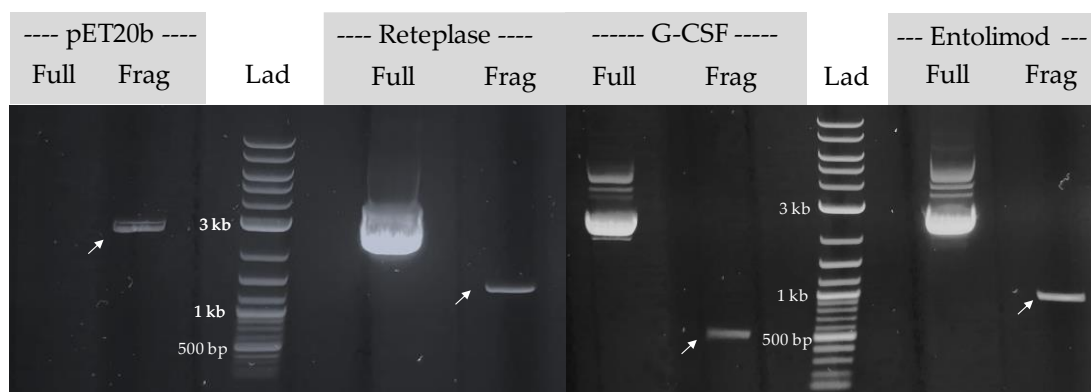


Figure 3.12: Stained 1% agarose gel showing restriction digested fragments ('frag') using EcoRI and XhoI enzymes, alongside each coding sequences' carrier plasmid pUC57 ('full'). Arrows indicate identified fragment for each coding sequence. Lad' indicates molecular ladder.

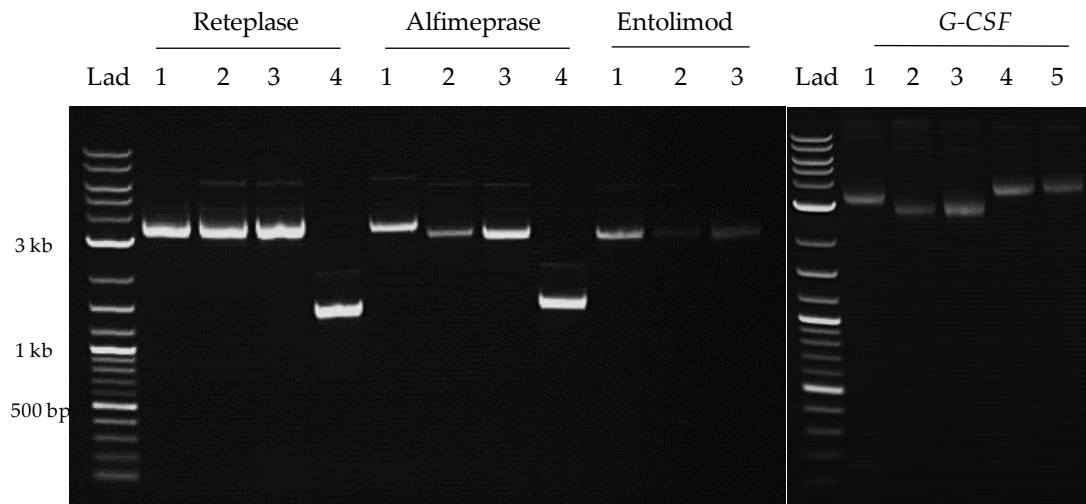


Figure 3.13: Stained 1% agarose gel showing plasmids extracted from various NEB5 α colonies transformed with ligated DNA. At least three colonies were screened for each cloned plasmid; Lad' indicates molecular ladder.

3.2.3.b NEB Hi-Fi assembly cloning of teriparatide

Codon optimized DNA encoding teriparatide (with a C-terminal 6x His tag) arrived in a pUC57 carrier plasmid. The DNA was first transformed and amplified in cloning host NEB5 α . In a similar fashion to the other proteins shown above (Figure 3.12), restriction digestion was attempted with EcoRI and XhoI. However, fragments could not be generated, even when reaction was allowed to proceed for a longer time period (2 hours and 5 hours; Figure 3.14, a). This could be attributed to the small size of teriparatide's coding sequence (~160 base pairs). Therefore, an alternative cloning strategy was opted, namely NEB HiFi DNA assembly. Teriparatide gene fragment was detected on an agarose gel when DNA was amplified by PCR using specific primers (Figure 3.14, b). This fragment was assembled with the pET20b(+) vector fragment and transformed into NEB5 α cloning host. Colonies were screened and plasmids were sequenced to obtain final DNA template pET20b-Ter-His. The 1% agarose gel with prepared plasmids (Figure 3.14, c) summarises all therapeutic DNA templates generated in this chapter.

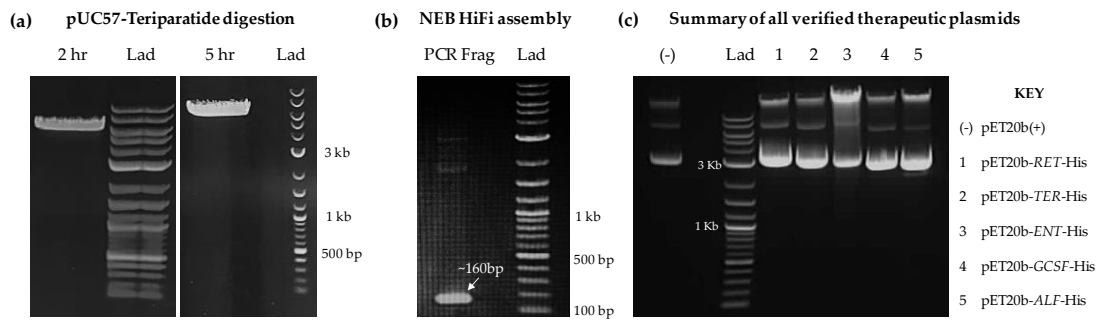


Figure 3.14: Stained 1% agarose gels showing (a) restriction digestion of pUC57-Teriparatide using *EcoRI* and *XhoI* enzymes for 2 hrs and 5 hrs, (b) PCR amplification of the teriparatide DNA fragment assembled in the pET20b vector; identified with an arrow at approximately 160 base pairs, (c) All cloned plasmids detailed in this chapter: pET20b (empty vector), pET20b-RET-His (reteplase), pET20b-TER-His (teriparatide), pET20b-ENT-His (entolimod), pET20b-GCSF-His (G-CSF) and pET20b-ALF-His (alfimeprase). Lad' indicates molecular ladder.

3.3 Summary

This chapter described the generation of two critical elements for in-house cell-free protein expression: cell-free extracts and DNA templates for expression of protein-of-choice. BL21 Star (DE3) was chosen as the foundational bacterial strain for cell-free extract preparation. By supplementing pAR1219 to BL21 Star (DE3), T7 polymerase production levels were enhanced. Further optimisation of cell growth and induction parameters led to identification of two hours post-induction with 0.5 mM IPTG at 37°C as the best conditions for cell growth and target for harvesting of cells. Hence, all cell-free experiments described in this thesis are derived from BL21 Star (DE3)-pAR1219 cell extract, grown at 37°C, and induced using 0.5 mM IPTG, where cells are harvested at approximately two hours post-induction ($\sim OD_{600} = 3 - 4$).

Next, sfGFP was chosen as the fluorescent reporter for studying CFPS, owing to its extraordinary stability and ease-of-detection. *In silico* designs were made for sfGFP and its His-tagged version 'sfGFP-His' in the pET20b vector, flanked by the T7 promoter and T7 terminator. Both templates were generated successfully using NEB HiFi DNA assembly.

Five more DNA templates were cloned for demonstrating expression of therapeutic proteins, for on-demand applications in extreme and low-resource environments. Four plasmids containing the coding sequences for reteplase, entolimod, alfimeprase and granulocyte colony stimulating factor, each were cloned using the restriction digestion method. One plasmid, containing the coding sequence for teriparatide, was cloned using the NEB HiFi DNA assembly method, following little success with the restriction digest method. Collectively, a preliminary DNA library of two fluorescent

reporter templates and five therapeutic templates were created for cell-free applications that are compatible with most T7 polymerase-containing bacterial extracts.

Chapter 4 Development and optimisation of CFPS and experimenting with formats for on-demand manufacturing

4.1 Introduction

An attribute of a good cell-free system is high efficiency, with sufficient to high levels of output (protein yield) for a given input (cell-free components). Although the cost of CFPS is higher than cell-based biomanufacturing (mainly due to energy supplementation), advances in the former is lowering the price at a rapid pace. Some inputs in particular, such as energy components, are particularly expensive to procure. This, in part, is contributing to efforts in energy regeneration and adaptation of cheaper energy substrates, often leading to the creation of in-house cell-free systems for each research group. Taken together with large batch-to-batch variation, each cell-free system is highly unique, and any comparison must be performed with care. This chapter builds on previous work (Chapter 3) by utilising the cell-free extracts and DNA templates to develop a fully in-house CFPS system unique to the School of Pharmacy at the University of Nottingham (owing to pAR1219 driven T7 polymerase overexpression).

Following the establishment of cell-free systems, considerations on storage and transportation are important to preserve these materials for long-term use. Most protocols from groups that have established their own in-house cell-free systems report storage of raw materials at temperature ranging from -20°C to -80°C, and cell-free components are typically flash frozen and stored at -80°C after preparation, until further use (Pardee, 2018). This is because, CFPS components also require cold storage to remain active, similar to conventional pharmaceutical storage solutions. Liquids aside, lyophilisation is the most studied format for improving stability of cell-free systems without cold-storage – a concept that was inspired from biopharmaceuticals manufactured in a cell-based route.

The performance of lyophilised extracts and energy systems improved drastically in comparison to aqueous extracts from 30 days to up to a year (Pardee, 2018). Studies have also demonstrated cell-free synthesis of antimicrobial peptides, vaccines, small molecules, cytotoxic therapeutics, and biosensors using ‘just-add-water’ lyophilised systems (Pardee et al., 2014, Pardee et al., 2016a, Pardee et al., 2016b, Salehi et al., 2016a). However, to implement lyophilised cell-free reactions on-site, further considerations, such as the ease of storage, distribution, and use in environments

outside the laboratory and biosafety, need to be addressed. This chapter also explores various methods and formats for implementation of CFPS in a simplistic manner – for use by scientists and others without a STEM background. Finally, some considerations for the formulation and delivery of protein products are discussed.

The broad aim for this chapter is to produce a flexible CFPS system with the following objectives -

- (a) Optimisation of the system for high synthesis efficiency based on fluorescent reporter production and benchmarking the optimised platform against highly efficient commercially available systems.

- (b) Exploration of formats through which the cell-free platform could be transported and distributed for point-of-care applications in remote locations on Earth and for space-based applications. Build formats based on previously published work related to lyophilisation or drying but also test new methods such as microglassification and the use of other scaffolds that may allow ease of use in a remote setting by any individual.

4.2 Results and discussion

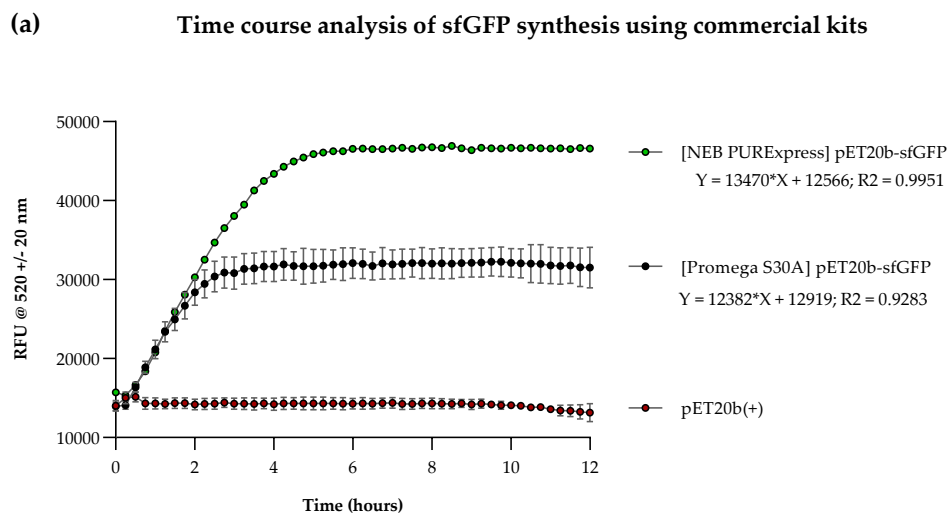
4.2.1 Commercial kits provide a good understanding of highly efficient CFPS

4.2.1.a PURExpress (NEB) and *E. coli* S30A Extract System for Circular DNA (Promega)

The use of CFPS for difficult-to-synthesise proteins (*e.g.* membrane proteins) has gained traction in the recent years, as labs working with complex proteins realised cell-free synthesis offered an easier route. This increase in interest has led to commercial development of CFPS kits – two such kits are the PURExpress (manufactured by NEB) and the *E. coli* S30A Extract System for Circular DNA (manufactured by Promega). PURExpress consists of the purified enzymes necessary for transcription and translation, derived from *E. coli* BL21 cells. The Promega system consists of crude bacterial cell extract (from an *OmpT* endoproteinase and *Ion* protease knockout strain). Both kits were commercialised from previously published work (Shimizu et al., 2001, Zubay, 1973, Zubay, 1980) and are some of the most popular CFPS kits in the market.

The PURExpress and Promega systems were initially used to set up baseline cell-free experiments to understand CFPS and to compare performances with a fully developed in-house CFPS system. The two commercial systems were studied through monitoring of sfGFP production over time using the in-house generated

templates described in Chapter 3 (Figure 4.1, a). The rate of synthesis of sfGFP (transcription + translation) was similar in both kits (13470 hr⁻¹ for PURExpress, and 12382 hr⁻¹ for Promega), with expression starting in the first 15 minutes. It was, however, observed that the S30A reaction reached saturation earlier (~ 3 hours) compared to PURExpress (~ 4 hours), with the latter recording 1.5 times more fluorescence, suggesting a higher protein yield. This may be attributed to the purified nature of components in PURExpress, allowing it to be devoid of DNases, RNases, and Proteases, whereas the S30 kit reaction may be more susceptible to degradation of DNA, RNA and proteins. The components and protein product(s) from PURExpress were visualised on an SDS-Page gel (Figure 4.1, b), where a protein band corresponding to sfGFP was identified, further validating its expression.



(b) SDS-Page analysis of PURExpress products

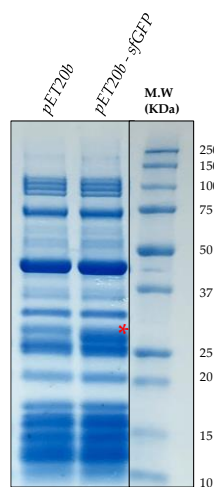


Figure 4.1: CFPS using commercial kits (a) Time course analysis of sfGFP production using PURExpress and Promega systems, showing fluorescence over time alongside a negative control (pET20b empty vector); Experiments were performed in triplicates ($n = 3$); data are shown as mean \pm SD. Equation and goodness of fit for

*the linear regression analysis shown aside key, (b) SDS-Page analysis of PURExpress reaction, where '**' indicates the presence of sfGFP alongside a negative control (pET20b empty vector) and molecular ladder ('M.W.');* Molecular weight of sfGFP is 26.8 kDa.

4.2.1.b Commercial components were used to test in-house cell-free extract and DNA templates

Chapter 3 described the design and preparation of an in-house cell-free extract using BL21 Star (DE3) - pAR1219 cells. The total protein concentration of the cell-free extract was first measured by means of a BCA (bicinchoninic acid; Pierce™ ThermoFisher Scientific) colourimetric assay. Results are shown for three independent cell-free extract preparation procedures with technical repeats (n = 3) for each assay (Figure 4.2, a). The assay was calibrated using known concentrations of bovine serum albumin, and the resulting linear regression was used to determine unknown protein concentrations. Goodness of fit (R^2) was consistently > 0.95. The average protein concentration was ~ 55 mg/mL. This was found to be slightly higher than a well-cited protocol (where this extract preparation method was inspired from), which reported a concentration between 30 mg/mL and 50 mg/mL (Au - Levine et al., 2019). This could be partly due to overexpression of the T7 polymerase from pAR1219; a method modification in this project.

In order to test the integrity of the in-house cell-free extract, a cell-free reaction was executed with this extract and DNA templates described in Chapter 3, and commercial energy buffers and amino acids provided in the *E.coli* S30A Extract System for Circular DNA (Promega). Time course analysis revealed sfGFP production over time, indicating successful CFPS, as compared to no increase in the negative control 'pET20b' reaction (Figure 4.2, b). The exponential increase in fluorescence, although small, was observed for ~ 2 hours, after which the reaction reached a saturation phase. The small increase in fluorescence and the short exponential phase both indicate that this set-up requires substantial optimisation to provide good protein yield and compete with the commercial systems described previously.

(a) Cell-free extract protein concentration assays

Assay no.	Concentration obtained (mg/mL)	Final concentration (mg/mL)	R ²
1	1.539	53.8 ± 5.5	0.999
	1.265		
	1.232		
2	1.522	56.6 ± 6.8	0.993
	1.175		
	1.551		
3	1.441	54.8 ± 7.8	0.985
	1.106		
	1.567		

(b) CFPS time course with in-house extract

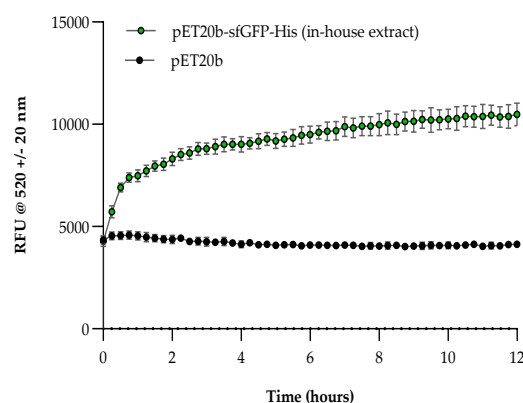


Figure 4.2: In-house extract preparation (a) Protein concentration (BCA) assay results of three independent extract preparation procedures with three technical repeats each (total N = 9) using a 1 in 40 dilution. Final concentrations are shown as a mean of three technical repeats \pm SD; R² value indicates the goodness of fit for the regression performed to calculate unknown protein concentrations (R² = 1 indicates that regression fitted data perfectly); (b) Time course analysis of cell-free synthesis of sfGFP using all in-house components, showing increase in sfGFP fluorescence ('pET20b-sfGFP-His in-house extract') compared against a stagnant negative control ('pET20b'); Experiments were performed in triplicates (n = 3); data are shown as mean \pm SD.

4.2.2 Development and optimisation of a fully functional in-house CFPS system

4.2.2.a Higher concentration of energy components contributed to yield improvement

Having shown that the in-house cell-free extract was adequately concentrated and functional, the next step was to develop and test a fully in-house CFPS system, where all components are procured and produced in UoN labs. Energy components, amino acids and other buffers were prepared as detailed in Methods (Chapter 2). Series of experiments were conducted in a one-factor-at-a-time method to identify large trends in improving the yield of the in-house system. The first in-house cell-free reaction was performed with a preliminary energy mix, which led to a CFPS trend as seen previously (Figure 4.2, b). Similarly, a small increase in fluorescence with a short exponential phase was observed. Next, the impact of supplementing the reaction with more energy mix was studied, as energy depletion is a well-known bottleneck in CFPS reaction progression (Calhoun and Swartz, 2007, Dondapati et al., 2020). Figure 4.3 shows a time course of sfGFP production under two conditions: 'in-house initial' corresponding to the initial energy mix and 'in-house improved' corresponding to 2x (doubled) energy mix. As suspected, a significantly higher fluorescence output was obtained with the new reaction mix containing 2x energy components, with fluorescence rising exponentially to 4 hours, followed by a saturation phase. This concentration of energy mix was maintained for all further CFPS reactions for higher yields.

Higher energy mix concentration contributes to higher protein yield

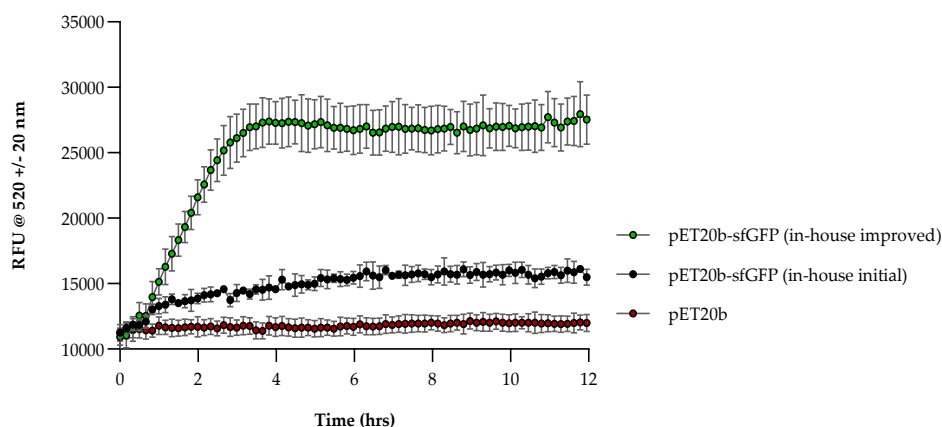


Figure 4.3: Higher energy mix concentration contributes to higher protein yield. Time course of sfGFP production is shown under two conditions: ‘in-house initial’ (1x energy mix) and ‘in-house improved’ (2x energy mix), where pET20b is a negative control showing no change in fluorescence over time. Experiments were performed in triplicates ($n = 3$); data are shown as mean \pm SD.

4.2.2.b Identifying the optimal magnesium glutamate and DNA concentrations

Successful CFPS relies on optimal concentrations of multiple components in the reaction mix. Magnesium glutamate was the next component explored for optimisation. Magnesium ions (Mg^{2+}) play a critical role in protein synthesis inside living cells; therefore, there is no doubt that the ion plays a critical role in cell-free synthesis of proteins as well - in addition to being a cofactor for the many enzymes involved in translation, it is involved in ribosome assembly (also critical for translation), and even appears to play a protective role during lyophilisation of proteins (Jewett et al., 2009a, Petrov et al., 2012, Guo et al., 2020).

Magnesium Glutamate (Mg-Glu) concentrations have been thoroughly optimised in previous studies, nevertheless, Mg-Glu optimisation is highly recommended for each unique cell-free extract preparation (Kim et al., 2006a, Jewett et al., 2009b, Silverman et al., 2019). A range of Mg-Glu concentrations (from 0 mM to 50 mM) was chosen and time course analysis was performed in 5 mM increments, in an effort to optimise the in-house CFPS system (Figure 4.4, a). It was clear that an absence of Mg-Glu inhibited protein synthesis (Figure 4.4, a; ‘0 mM’). Of the concentrations tested, 20 mM Mg-Glu produced the highest fluorescence, when compared with other concentrations and the negative control (Figure 4.4, a; ‘20 mM’). Concentrations higher than 20 mM also seemed to repress protein synthesis; similar observations for Mg-Glu concentrations beyond 15 mM – 20 mM have been made in literature, although it is not clear why (Nagaraj et al., 2017, Cai et al., 2015). Collectively, 20 mM Mg-Glu was determined to be the best concentration of this in-house CFPS system.

The effects of DNA concentration on CFPS was next explored. There is some evidence to suggest that a saturation point is reached with specific DNA concentrations (where transcription machinery is fully utilised) (Zhang et al., 2021, Li et al., 2017). Therefore, a range of DNA concentrations were tested in the Mg-Glu optimised in-house CFPS system, with the aim to identify the concentration that produced highest fluorescence (and hence indicating higher protein yield). As expected, an increase in protein yield was observed with increasing DNA concentrations until 350 ng. Then, the yield decreased as a function of DNA concentration (350 ng – 3000 µg). This may be due to dilution of other components in the cell-free reaction mix (ions in particular) as the DNA was eluted and stored in water, rather than S30A buffer.

It was further noted that two reaction conditions namely 10 mM Mg-Glu (Figure 4.4, a) and 450 ng DNA (Figure 4.4, b) represent similar reaction set-ups and yet produce significantly different fluorescent signals. This discrepancy may be due to batch-batch variation as the two experiments were conducted on different lysate batches. Furthermore, the experimental data shows that 350 ng DNA is a suitable concentration for effective CFPS. It is worth noting that this concentration is suitable for plasmid DNA only and may differ for linear DNA templates - a similar experiment with linear DNA templates could be considered for future work.

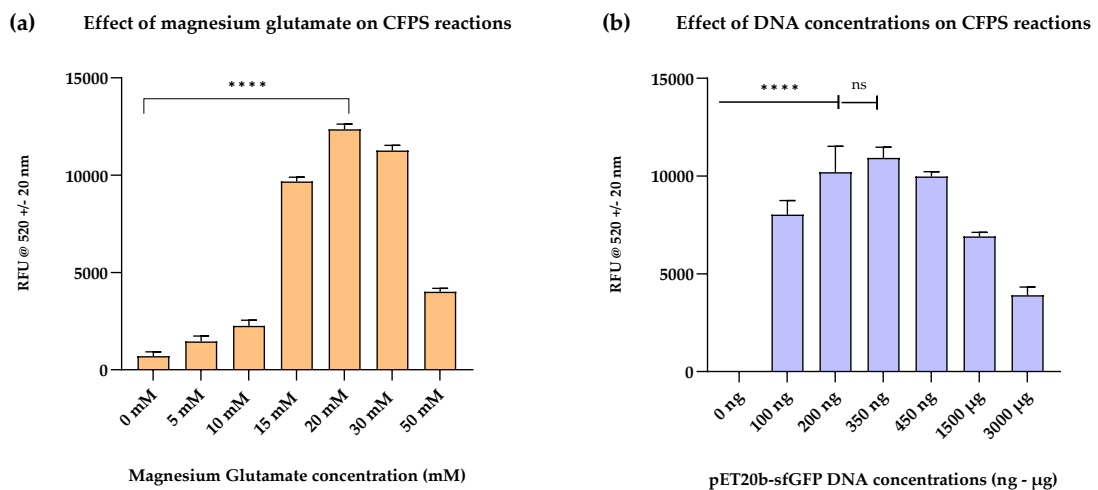


Figure 4.4: Optimisation of magnesium glutamate (Mg-Glu) and DNA concentrations for CFPS (a) Graph showing sfGFP fluorescence from cell-free reactions at varying concentrations of Mg-Glu after 4 hours of incubation; (b) Graph showing sfGFP fluorescence from cell-free reactions at varying concentrations of DNA after 4 hours of incubation. Initial reaction conditions before optimisation were: 30% (v/v) extract, 10 mM Mg-Glu and 500 ng DNAs. Experiments were performed in triplicates (n = 3); data are shown as mean ± SD and fluorescence was normalised with negative control reactions (pET20b), P value > 0.05 = ns, P < 0.0001 = ****.

4.2.2.c PEG supplementation enhances CFPS efficiency

The initial optimisation experiments revealed best concentrations of components like DNA and Mg-Glu, without which CFPS would not function. This was followed by an experiment to study the effects of supplementary agent, PEG (Polyethylene Glycol). PEG is a well-known macromolecular crowding agent, aiding protein stability and flexibility in less crowded cell-free environments. For this reason, PEG is often included as a supplement even in minimal cell-free buffers (less complex mixtures for highly efficient CFPS), particularly for artificial cell development (Foley and Shuler, 2010, Ge et al., 2011). It is, however, well documented that excess PEG has negative implications, with typically optimised concentrations ranging between 1% and 2% (Whitfield et al., 2020, Borkowski et al., 2020, Banks et al., 2022).

Impact of PEG on CFPS yield and kinetics was studied at two concentrations: 1.5% and 3% and compared with an unsupplemented control. A significant difference in sfGFP fluorescence and thereby protein yield was observed with the unsupplemented reaction and the 3% PEG-supplemented reaction, confirming previously observed benefits of PEG; cell-free kinetics remained unchanged (Figure 4.5). Interestingly, no significant difference was observed with the unsupplemented reaction and the 1.5% PEG-supplemented reaction - indicating that a higher concentration is beneficial for this cell-free system – nevertheless, an extensive range of PEG concentrations and molecular weights could be tested for better optimisation (Chapter 5 discusses a Design-of-Experiment (DoE) approach that lead to the identification of better PEG concentrations and molecular weights for better stability of cell-free systems at room temperature).

PEG supplementation enhances CFPS efficiency

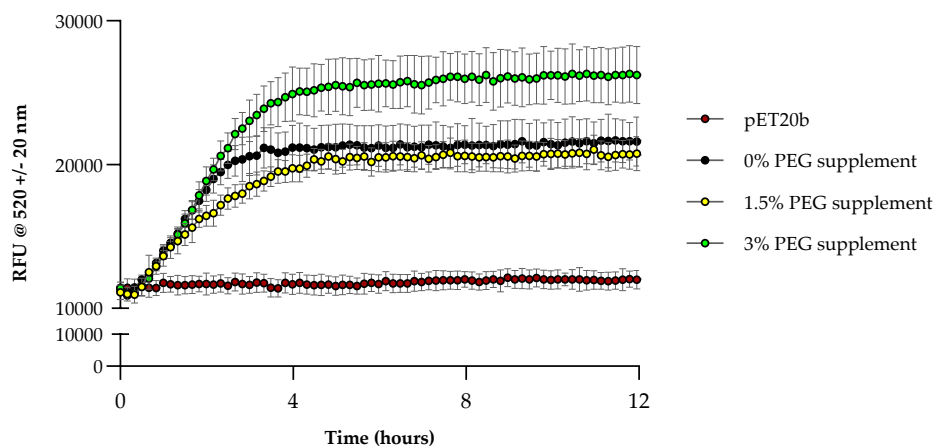


Figure 4.5: Effects of supplementation of PEG on CFPS. Time course of sfGFP production is shown under three conditions: 0% PEG supplement (unsupplemented reaction); 1.5% and 3% supplement indicating the final PEG concentrations in the reaction; pET20b is a negative control showing no change in fluorescence over time. Experiments were conducted using optimised parameters (2x energy mix, Mg-Glu 10 mM and 350 ng DNA). Experiments were performed in triplicates ($n = 3$); data are shown as mean \pm SD.

4.2.2.d Summary and comparison of all optimised in-house components

Four main aspects of CFPS were studied and optimised: Energy components, magnesium glutamate levels, DNA concentrations and PEG concentrations, results for which were discussed in this chapter so far. A consolidation experiment was carried out to finalise the optimised conditions for this in-house system. One last variable was also tested in combination with optimised conditions, namely, cell-free extract protein concentration. This was tested last as optimal concentrations of all other components are required to maximize the performance of the transcriptional and translational machinery present in the extract. It is well-known from literature that the optimal bacterial extract concentration in the final cell-free reaction is approximately 30 mg/mL (Levine et al., 2019) and that higher concentrations can be inhibitory due to occupation of volume that is critical for other components like energy, DNA, amino acids *etc.* (Takahashi et al., 2021, Nagaraj et al., 2017). Hence, three feasible concentrations between 20 mg/mL and 30 mg/mL were identified for testing with volume held constant.

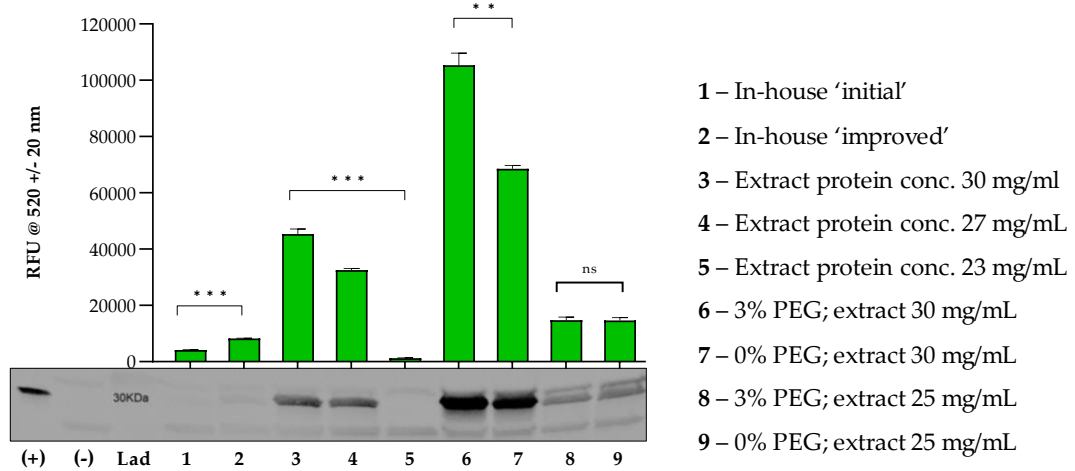
The summary graph provided in Figure 4.6 shows the consolidation of all optimised conditions and results were further confirmed through a western blot, shown below the graph. First, the 'in-house initial and in-house improved' conditions discussed in Section 4.2.2.a were plotted (Figure 4.6, a; lanes 1 & 2). When doubling the concentration of the energy components, a significantly higher fluorescence output

was detected, indicating higher yield. Next, three extract concentrations were tested using the optimised Mg-Glu (20 mM) and DNA concentrations (300 ng) discussed in section 4.2.2.b. When comparing 30 mg/mL, 27 mg/mL and 23 mg/mL final extract concentrations, the detected fluorescence signal was directly proportional to extract protein concentration – these concentrations attributed to ~ 40% v/v, 35% v/v and 30% v/v in the final reaction composition, respectively (Figure 4.6, a; lanes 3, 4 & 5).

In accordance to previous observations, 30 mg/mL extract concentration produced the highest protein. When the optimised conditions (40% v/v extract, double energy, 20 mM Mg-Glu and 300 ng DNA) were tested in the presence and absence of 3% PEG (supplementation studies discussed in 4.2.2.c), a significantly higher fluorescence output was observed, in comparison to the unsupplemented reaction (Figure 4.6, a; lanes 6 vs. 7). However, there was no significant difference in fluorescence in supplemented and unsupplemented reactions when the extract concentration was lowered to 25 mg/mL (Figure 4.6, a; lanes 8 vs. 9). This behaviour hints that the molecular crowding property of PEG and its benefits to CFPS as a result may be obtained only above certain concentrations of proteins in a cell-free environment. Any other differences in fluorescence outputs would be explained by batch-batch variation arising from manual preparation of cell-free mixes, as previously discussed in Section 4.2.2.b.

In summary, the best parameters for this newly developed cell-free system was found to be 40% v/v extract, double energy, 20 mM Mg-Glu, 300 ng DNA and 3% PEG. This optimised reaction composition was compared with the commercial CFPS systems tested previously (Figure 4.1, a). It is clear from the time course analysis that the in-house CFPS system closely mimicked the PURExpress trend and exceeded the yield from Promega system (Figure 4.6, b). Rates of protein synthesis (slope 'm') were identical among the three experimental samples and fluorescence outputs were similar between the in-house and PURExpress reactions. This result indicates that the performance of the in-house cell-free system is comparable to commercially available systems and this reaction composition was opted for all cell-free reactions and positive control reactions described in all further results, unless otherwise specified.

(a) Summary of in-house CFPS optimisation



(b) In-house CFPS vs. commercial CFPS

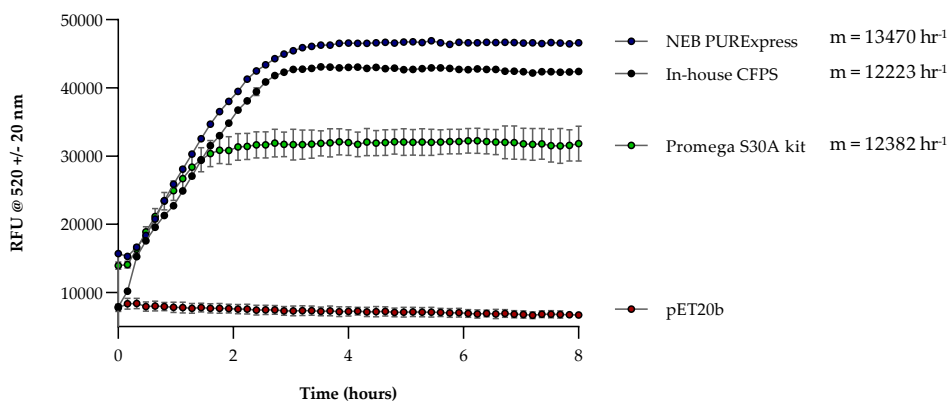


Figure 4.6: Development of an in-house cell-free system. (a) Summary of all optimised cell-free components. Expression of super sfGFP was quantified as relative fluorescence units normalised to pET20b negative control (-); protein product was visualized through anti-His western blot, shown below the graph. Expression of sfGFP under nine compositions were tested (see key provided). P value $> 0.05 = ns$, $P < 0.05 = *$, $P < 0.01 = **$, $P < 0.001 = ***$ and $P < 0.0001 = ****$. (b) Time course analysis showing expression of sfGFP from commercial PURExpress and Promega commercial kits and optimised in-house reaction composition ('in-house CFPS') as compared with negative control ('pET20b'). Experiments were performed in triplicates ($n = 3$); data are shown as mean \pm SD.

4.2.3 CFPS formats that enable on-site, on-demand synthesis

Successful application of CFPS for on-site and on-demand biomanufacturing requires the system to firstly, be highly efficient and secondly, formulated in a portable (accessible/transportable) and user-friendly fashion. The development and optimisation of the in-house cell-free system described in Section 4.2.2 has enabled it to be highly efficient for protein synthesis (comparable to commercial systems). This

section addresses the next challenge of portability and user-friendliness of such a system.

As discussed in Chapter 1 (Introduction), CFPS is highly unstable and unportable in its standard liquid format. One solution for improving both stability and portability is drying cell-free components into a solid state (freezing the molecular dynamics in time), that can be rehydrated to obtain the standard liquid format later. Four methods were identified for investigating this idea:

- (a) **Microglassification:** dehydration of proteins, typically in alcohol solvents, to form solid amorphous microspheres (Aniket et al., 2014)
- (b) **Air-drying (on paper):** The process of removing water from the cell-free components to the surrounding atmosphere; this was carried out inside a microbial safety cabinet (sterile environment) and upon paper discs.
- (c) **Freeze-drying (on paper):** The process of removing water from the cell-free components by freezing at low temperatures and removing the ice by sublimation under vacuum; this was carried out inside a freeze-drier, whereby components are freeze-dried upon paper discs. Each cell-free component is freeze-dried on an individual paper disc, where a disc for each component is layered into a stack to create a complete cell-free reaction.
- (d) **Freeze-drying (pellets):** Same as (c) but all components are freeze-dried into pellets, forming a 'one-pot' reaction where all components are in one tube.

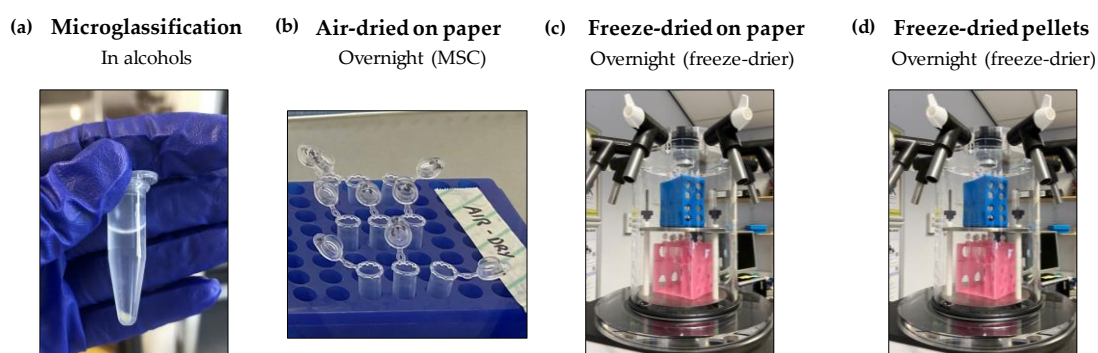


Figure 4.7: Overview of the four formats explored for on-site and on-demand applications of CFPS. (a) Microglassification, (b) Air-drying, (c) Freeze-drying on paper and (d) Freeze-drying into pellets. Images briefly show the methodology used for each format.

The many successes and challenges encountered during the experimentation of these formats are discussed in the remaining sections below.

4.2.3.a Microclassification

Dehydration of protein-based therapeutics are typically carried out by (spray-/freeze-) drying. In 2014, a new procedure, Microclassification™, was introduced by Aniket and colleagues, showing successful preservation of BSA following suspension in pentanol and decanol (Aniket et al., 2014). This success has been expanded to homogenous enzyme solutions, and the technology is being developed commercially by Lindy Biosciences. This procedure has, however, never been shown with complex mixtures of proteins and other biomolecules, which is the case in cell-free extracts and CFPS. This section presents and discusses a series of experiments conducted on the microclassification of cell-free systems. Briefly, the process entails suspension of aqueous cell-free solution in a large excess by volume of dry pentanol. The water from the aqueous suspended droplets diffuses into the pentanol, leaving the CFPS material behind to form a solidified bead. Excess pentanol is removed and the solidified bead is allowed to fully dry in a vacuum desiccator (Figure 4.8).

Overview of the microclassification procedure

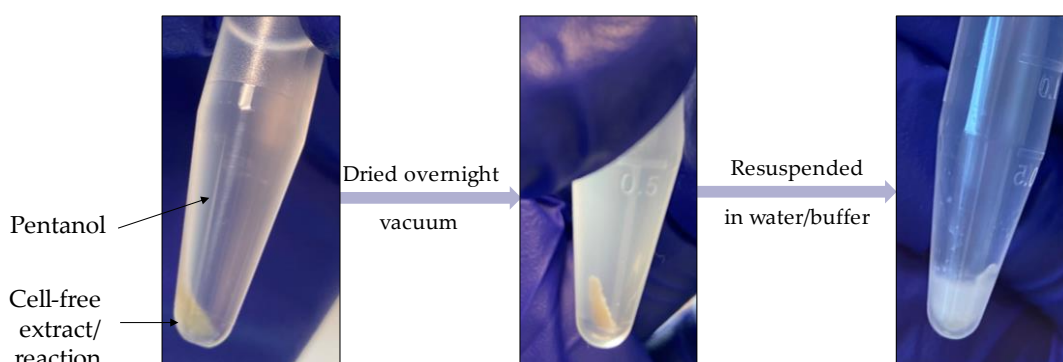


Figure 4.8: Overview of the microclassification procedure. The aqueous cell-free extract or the full cell-free reaction is suspended in a solution of pentanol to form 'glass beads' and the solvent is subsequently allowed to evaporate under vacuum, leaving a solid pellet of cell-free components behind. The pellet is rehydrated with water/buffer at a later time to obtain a liquid solution.

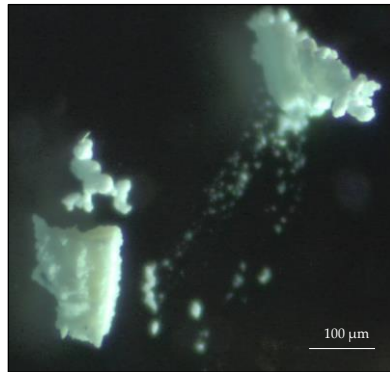
i Cell-free extract forms 'microspheres' or 'glass beads' upon microclassification and lose viability upon resuspension

The cell-free extract forms the predominant protein content in CFPS. The remaining components comprise of other biomolecules (DNA, RNA and amino acids) and chemicals. Initially, microclassification was tested for two types of solutions: Cell-free extract; full cell-free reactions (containing all components in the final reaction composition).

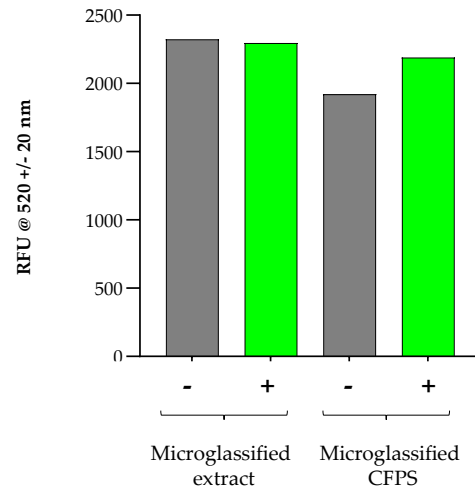
To better understand the physical features of the microclassified product, the pellet obtained from the cell-free extract was viewed under a microscope. Microspheres were visible in the sample (Figure 4.9, a). The individual beads were also found clustered into bigger structures that eventually formed the pellet following solvent evaporation. To test whether the beads could release viable protein, the pellets from the cell-free extracts and the full cell-free reactions were rehydrated with S30A buffer, and further used to set up cell-free reactions (other components were added fresh in the case of microclassified cell-free extract). The experimental cell-free reactions would produce sfGFP (green fluorescence) if the cell-free components were well-preserved during microclassification. When fluorescence was recorded for the experimental and control samples, no significant difference was observed in neither extract-only nor fully-microclassified reactions (Figure 4.9, b). The fact that no significant increase in fluorescence was detected from the microclassified extract samples imply that the proteins did not survive the microclassification procedure, hence, it is no surprise that the fully microclassified cell-free reaction did not yield any more fluorescence.

The protocol published by Aniket and colleagues involved rehydration of microclassified BSA with water. In the procedure described here, S30A was used as the rehydration buffer to prevent dilution of Mg-Glu concentrations in the final cell-free reaction (Section 4.2.2.b emphasised the importance of Mg-Glu for CFPS). A test was performed whereby microclassified cell-free extract was rehydrated in S30A or water, in an effort to mitigate challenges seen with viability previously. Fluorescence readings were taken for each cell-free reaction with the rehydrated extract (all other components were added fresh). No significant difference was observed in the samples rehydrated with S30A buffer, however, an increase in fluorescence was seen in the experimental samples rehydrated with water (Figure 4.9, c). However, no band(s) were detected from this sample on a western blot, indicating that the expression is insignificant when compared to the positive control (sfGFP band from a completely fresh cell-free reaction). In conclusion, either the proteins or some other component in the cell-free extract fails to retain functionality during the process of microclassification.

(a) Glass bead formation following the microglassification procedure



(b) CFPS using rehydrated microglassified components



(c) Effect of rehydration of microglassified components with water or buffer

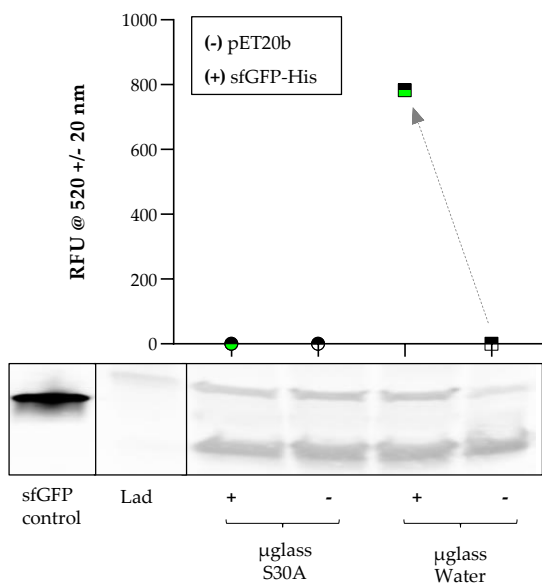


Figure 4.9: Effect of microglassification on CFPS (a) Microscopic image of the microglassified cell-free extract taken at 40x magnification with a white light source, showing formation of spheres, (b) Fluorescence readings of CFPS reactions performed with rehydrated microglassified extract and whole cell-free reaction, (c) Fluorescence readings of CFPS reactions performed with rehydrated microglassified extract, rehydrated with either S30A buffer or water. This is shown together with a western blot of the samples, aside a positive control ('sfGFP control') and protein ladder at 25 kDa. (-) indicates the pET20b negative control and (+) indicates the experimental samples with sfGFP-His DNA. Experiments were performed in triplicates ($n = 3$); data are shown as mean \pm SD (error bars are small where they are not visible).

ii RNA supplementation does not aid CFPS post-microglassification

In addition to proteins, there is one more biomolecule in the cell-free extract that is critical for CFPS, RNA. The three main types of RNA, namely, messenger RNA

(mRNA), transfer RNA (tRNA), and ribosomal RNA (rRNA), are indispensable for transcription and translation, and hence for CFPS. mRNA is generated in the cell-free environment following addition of DNA. On the other hand, tRNA is often supplemented in cell-free extracts for translational efficiency (Des Soye et al., 2019, Levine et al., 2019, Kwon and Jewett, 2015). BL21 Star (DE3) – pAR1219 cells contain good levels of endogenous tRNA and rRNA and therefore, the cell-free extract for the in-house system is sufficiently pre-loaded. During microglassification, however, biomolecules not soluble in pentanol such as tRNAs and rRNAs may not take part in bead formation, especially considering their low stability. If this were true, supplementation of RNA should enhance the viability of the microglassified and reconstituted cell-free extract.

A test was devised with total RNA extracted from BL21 Star (DE3) – pAR1219 using an RNA extraction kit (containing mRNA, tRNA, and rRNA from the same strain as the cell-free extract; Figure 4.10, a). The extraction was performed in biological triplicates (from three different bacterial colonies), compositions were identical in the RNA gel and concentrations of 200 ng/μl were obtained. This mixture was then supplemented to cell-free reactions containing microglassified extract reconstituted with water. When compared to unsupplemented reactions, the reactions containing supplemented RNA and sfGFP DNA had a considerably higher fluorescence endpoint (Figure 4.10, b). However, this difference was not significant when compared with positive control reactions (fresh CFPS with and without supplemented RNA), which was further confirmed from absence of bands corresponding to sfGFP on a western blot. On a different note, there was no significant difference in fluorescence output between the two positive control reactions confirming that tRNA supplementation is indeed not a requirement for highly efficient CFPS with minimal buffers (Figure 4.10, b).

In summary, RNA supplementation does not improve the viability of microglassified cell-free extracts. This indicates that the proteins may be the limiting factor in the exploitation of microglassification for cell-free applications.

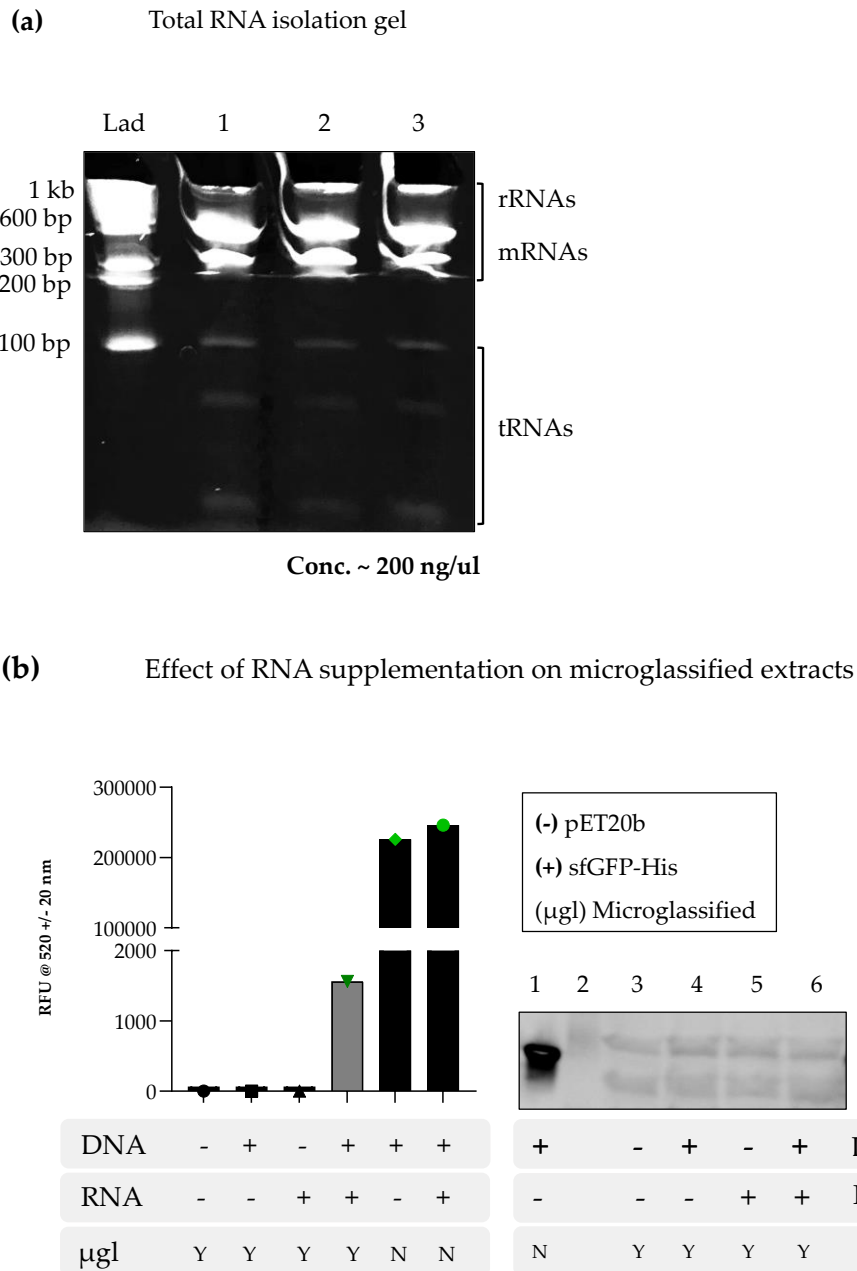


Figure 4.10: Effect of RNA supplementation on CFPS using microclassified cell-free extract. (a) 10% TBE-Urea gel showing resolved RNA fragments from a total RNA extraction from BL21 Star (DE3) – pAR1219 cells. Each lane corresponds to a biological triplicate at concentrations approximating to 200 ng/μl. The type of RNA corresponding to the size is labelled alongside a molecular ladder ('Lad'), (b) End-point fluorescent readings and western blot of cell-free reactions under various conditions: with and without microclassified extract ('Y/N μglass'; where labelled 'N', fresh extract was used as positive control), with and without sfGFP DNA ('+/-'; where labelled '-' negative control pET20b DNA was used), with and without RNA supplementation ('+/-' RNA). Experiments were performed in triplicates (n = 3); data are shown as mean ± SD (error bars are small where they are not visible). Note the axis break between 2000 and 100,000 RFUs.

iii Gentler mixing methods may improve activity, although not significantly

In a final attempt to improve viability of microclassified cell-free extracts, various methods of suspension of the protein solution in alcohol were sought out. Aniket and

colleagues had described a method for single bead formation (by micro pipetting) and bulk bead formation for microclassification of BSA. They demonstrated that the bulk scale method (involving mixing of 50 μ L protein solution in 1.1 mL pentanol by vortexing and later centrifugation) produced smooth, homogenous beads of protein in reconstitutable state. This was the chosen method of mixing for all microclassification experiments detailed in this chapter so far.

Following little success with viability of microclassified extracts, less vigorous mixing techniques were studied such as gently tilting the tube, injecting the solution into solvent through a narrow channel (simulates micro pipetting) and no mixing whatsoever (Figure 4.11, a). In each case, the viability of the microclassified cell-free extract was tested by rehydration with water and utilised for CFPS. Interestingly, end-point fluorescence increased with less vigorous mixing methods, indicating some viability. Vortexing produced the lowest levels of sfGFP and microclassified extract that was not mixed yielded the highest fluorescence, when compared with negative controls (Figure 4.11, b). Unfortunately, even the fluorescence recorded from the less mixed sample was significantly lower than the freshly made positive control reaction.

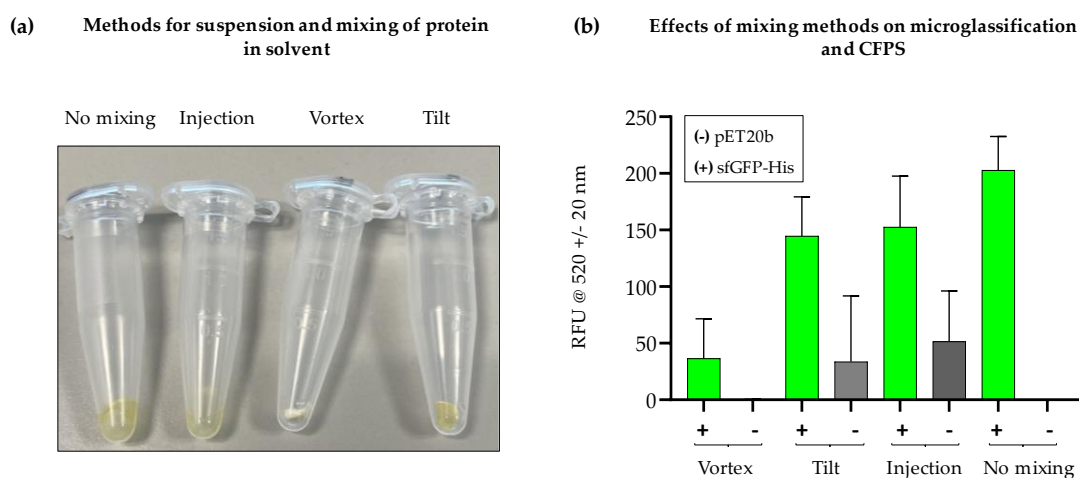


Figure 4.11: Effect of gentler mixing methods of the viability of microclassified cell-free extract. (a) Four methods were tried: no mixing (just pipetted protein solution in solvent), injection (syringe and needle used for injection of solution through a narrow channel), vortex (standard mixing method used in all previous studies) and tilt (tube was tilted 4 – 6 times to aid gentle motion of protein in solvent), (b) End-point fluorescent readings of cell-free reactions using rehydrated microclassified cell-free extract mixed with the four methods. Negative control pET20b DNA is labelled ‘-’ and experimental sfGFP DNA is labelled ‘+’, Experiments were performed in triplicates ($n = 3$); data are shown as mean \pm SD (error bars/data points are small where they are not visible)

For the purpose of ratification, a BCA assay was performed to note any difference in cell-free extract before and after microclassification. Protein concentration of reconstituted microclassified extract was no different to the crude cell-free extract (in liquid format before microclassification; Figure 4.12, a). This confirms that no

proteins were lost during the microglassification process, however, this does not shed any light on the activity of the present proteins. Suspiciously, the microglassified extract had a different physical appearance to the crude extract before microglassification, indicating a change in nature. Opaque and cloudy samples are often a sign of denaturation and aggregation, which may be the case in Figure 4.12, c, as compared to Figure 4.12, b.

(a) BCA assay reveals no significant difference

Extract type	Protein concentration
Crude	1.36 ± 0.26 mg/mL
Microglassified	1.30 ± 0.11 mg/mL

(b) Crude extract



(c) Microglassified extract

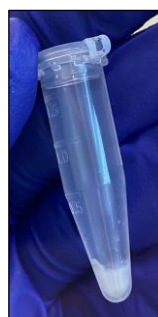


Figure 4.12: Effect of microglassification on the proteins that make up the cell-free extract. (a) BCA assay results showing protein concentration before ('crude') and after microglassification ('microglassified'). Both fractions were present in S30A buffer and concentrations were extrapolated from absorbance of known BSA concentrations. Good of fit for the linear regression ($R^2 = 0.992$). Experiments were performed in triplicates ($n = 3$); data are shown as mean ± SD. (b) Image showing crude cell-free extract in liquid, translucent format, (c) Image showing microglassified cell-free extract reconstituted in S30A buffer (coloured white and visibly opaque).

In summary, microglassification of cell-free reactions or cell-free extract alone proved to be challenging. Although the format (solid micro beads for later rehydration) was highly appropriate for on-site and on-demand applications, the viability of the proteins in the cell-free extract was extremely poor. When compared to < 95% preservation of BSA reported in literature, the unsuccessful microglassification of cell-free extract could be due to a number of reasons. The loss of non-protein components in the extract may be a reason, however supplementation of RNA (the next most valuable component in the extract) did not increase viability. The complex mixture of proteins may be preventing formation of homogenous beads like in the case of purified BSA. Although this was not further studied in this project, future work involving imaging of the micro beads could provide more insights.

4.2.3.b Lyophilisation preserves CFPS components

Lyophilisation or freeze-drying is one of the most commonly employed methods for the development of solid formulations of proteins and thereby enhancing stability, typically compared to that observed in liquid states. This method offers many benefits and presents many challenges, which are mostly well-understood and thoroughly reviewed in the past few decades (Wang, 2000, Kasper et al., 2013, Wang et al., 2022). Lyophilisation methods were also, unsurprisingly, employed for cell-free systems, with both extracts and whole cell-free reactions preserved. Such preservation contributed to enhanced stability, as compared to standard liquid formats, but also enabled easy transportation and revival after rehydration, attributes that are highly desirable for on-site and on-demand applications (Smith et al., 2014, Wilding et al., 2019, Des Soye et al., 2019, Salehi et al., 2016a).

To evaluate the ability of the in-house cell-free reactions to be preserved in this manner, whole cell-free reactions were lyophilised. The impact of the procedure was studied by rehydration with S30A buffer and measuring cell-free synthesis of sfGFP. There was approximately 2.5 times reduction in sfGFP fluorescence in samples that underwent lyophilisation, in comparison to freshly made samples without lyophilisation (Figure 4.13). Nevertheless, a significant difference was seen in the experimental samples (containing sfGFP) over the control samples (with pET20b; Figure 4.13).

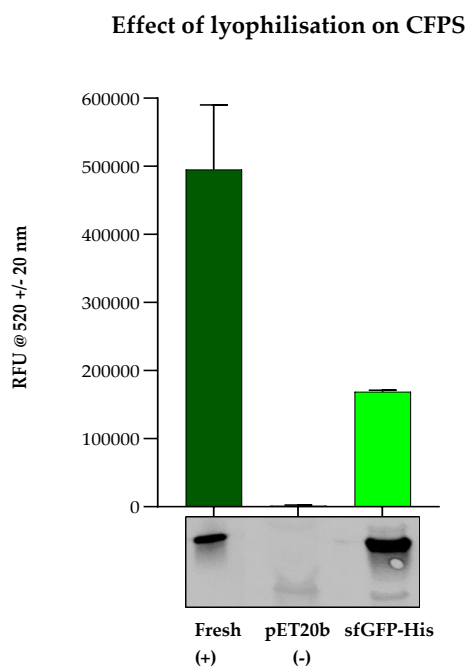


Figure 4.13: Effect of lyophilisation on CFPS. End-point fluorescence readings from cell-free reactions under various conditions: 'Fresh (+)' corresponds to a positive control reaction where all reagents were prepared fresh,

without lyophilisation; 'pET20b (-)' corresponds to a negative control reaction without sfGFP DNA where the cell-free reaction was lyophilised and reconstituted in S30A buffer; 'sfGFP-His' corresponds to the experimental sample with sfGFP DNA where the cell-free reaction was lyophilised and reconstituted in S30A buffer. Experiments were performed in triplicates (n = 3); data are shown as mean \pm SD (error bars/data points are small where they are not visible).

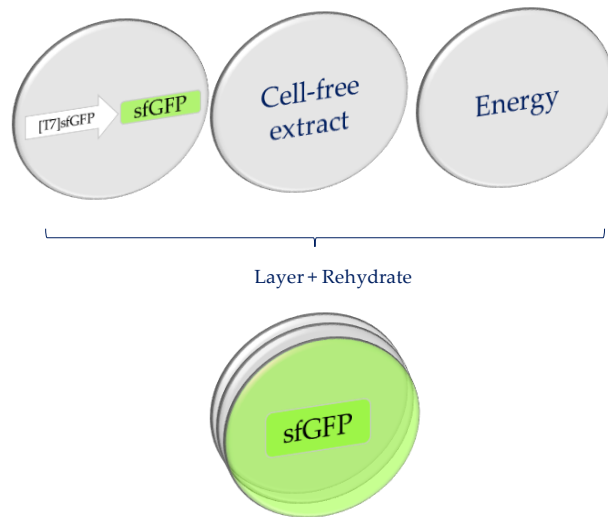
The above result still indicates that lyophilisation is a suitable method for preservation of whole cell-free reactions in a solid, light weight format for on-site, on-demand applications. This is because no lyoprotectants or cryoprotectants were added to the reactions prior to lyophilisation. Lyoprotectants are often supplemented in protein solutions to reduce the temperature and pressure related stress during the lyophilisation process (Merivaara et al., 2021). The fact that lyophilised cell-free reactions produce a significant fluorescence signal without these protectants is a promising start. It should be noted that PEG, the molecular crowding agent that was found to enhance CFPS efficiency, has been reported to have unknown to even detrimental effects during lyophilisation (Frank et al., 2018, Manohar and Ramesh, 2019). These properties of PEG may have had a role to play during the lyophilisation process for cell-free reactions. The stability of lyophilised samples and the role of protectants and stabilisers are further explored in Chapter 5.

4.2.3.c A paper-based platform for drying CFPS components to yield protein upon resuspension

A paper-based CFPS platform was developed to synthesize protein products for on-site, on-demand applications. Paper discs or cellulose discs are a popular choice of support for many biosensor projects that have successfully used CFPS for portable, on-site applications (Pardee et al., 2014, Gräwe et al., 2019, Lin et al., 2020). Their popularity can be attributed to compactness (ease of use, storage and transportation) and robustness.

The primary aim of the paper-based platform for this in-house system was to create an interchangeable and flexible approach where the DNA can be modified to produce any therapeutic at point-of-care. The key components of this platform were three cellulose discs individually dried with the different CFPS components of: cell extract; ions and energy; DNA and amino acids. The components were designed according to previously identified optimal concentrations (Figure 4.14, a). Moreover, three types of cellulose (toilet tissue; hand towel; and laboratory blue roll, procured from Boots Science Building, University of Nottingham) were tested to study any differences in cellulose composition and identify the best scaffold for this system (Figure 4.14, b).

(a) Concept of lyophilisation on cellulose



(b) Types of cellulose tested

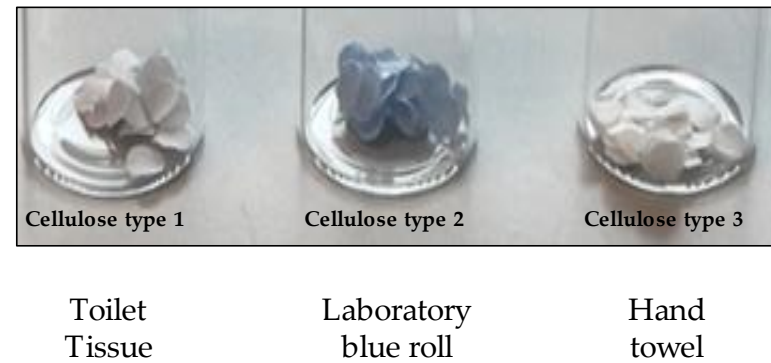
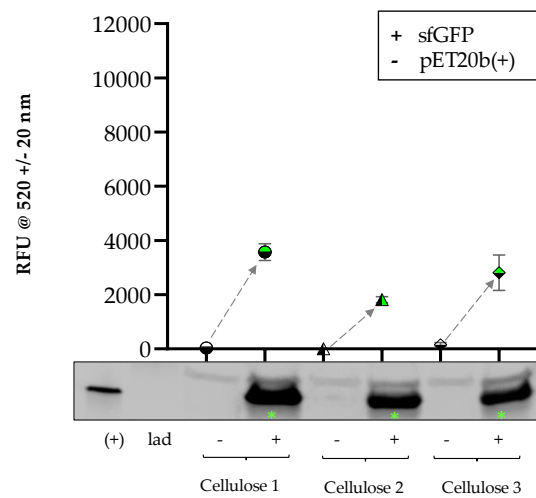


Figure 4.14: Overview of the paper-based platform. (a) Diagram showing the concept behind the platform, where different cell-free components are dried on an individual cellulose disc. The individual discs are layered and rehydrated with S30A buffer to kickstart CFPS. The DNA layer can be easily interchanged to produce any proteins, be it a fluorescent protein or a biologic. (b) Image showing the three types of cellulose tested (1) toilet tissue, (2) laboratory blue roll (dye blue) and (3) hand towel.

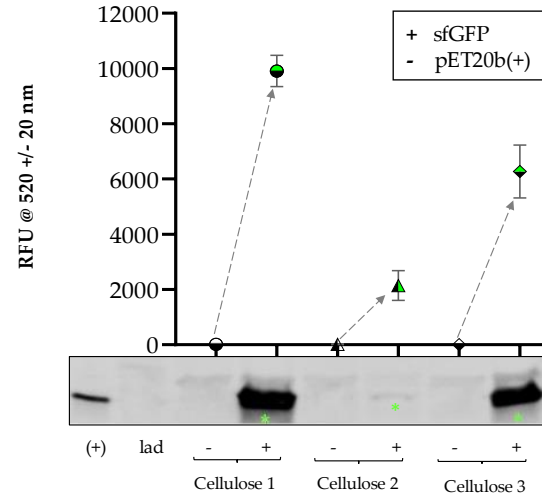
Two types of drying methods were employed to test this platform, namely air-drying and freeze-drying (lyophilisation shown previously). In each case, the freshly prepared liquid CFPS components were added to individual autoclaved cellulose discs and allowed to dry overnight. sfGFP expression was monitored upon stacking, rehydration with S30A buffer and incubation.

sfGFP was detected and quantified for both air-dried and freeze-dried paper CFPS reactions (Figure 4.15, a & b). All three types of paper aided sfGFP expression upon rehydration, when compared to the pET20b negative control reaction. The proteins were found in the aqueous phase, and this was confirmed by imaging and western blot analysis, where the sfGFP band is present in samples only with sfGFP DNA (Figure 4.15, a, b & c). Furthermore, compared with the air-dried setup, reactions that were freeze-dried showed a greater level of sfGFP fluorescence (Figure 4.15, c). This could be attributed to better preservation of protein structure and activity when lyophilised, which is in agreement with work reported in literature (Hunt et al., 2017, Pardee, 2018, Tonooka, 2020a, Tonooka, 2020b). It was also noted that the reactions on toilet tissue (cellulose type 1) yielded the highest fluorescence in both air-dried and freeze-dried samples, indicating that this scaffold is perhaps more suitable for on-cellulose synthesis. Details on the type of cellulose(s) and the structural arrangements of fibres could not be obtained due to lack of information from the suppliers and the University. Future work involving paper characterisation and SEM image analysis could shed more light into the properties of this paper and why it is superior for CFPS.

(a) Air-dried CFPS on cellulose stacks



(b) Freeze-dried CFPS on cellulose stacks



(c) Fluorescence from rehydrated stacks

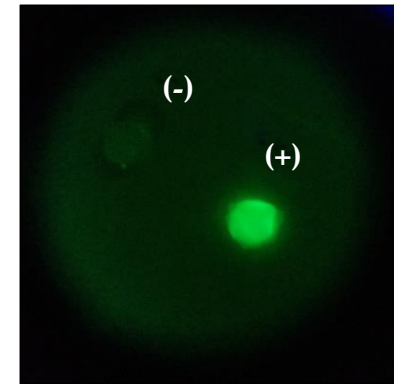


Figure 4.15: CFPS on paper enables protein expression upon rehydration. (a) sfGFP fluorescence recorded after rehydration of air-dried CFPS components on cellulose stacks, (b) sfGFP fluorescence recorded after rehydration of freeze-dried CFPS components on cellulose stacks. '+' indicates the experimental sfGFP samples and '-' indicates the pET20b negative control. '(+)' indicates the sfGFP positive control for western blot size verification alongside protein ladder ('lad'). Experiments were performed in triplicates ($n = 3$) and fluorescence data are shown as mean \pm SD. * indicates sfGFP band. (c) Image showing green fluorescence of the rehydrated end-point experimental sample '(+)' alongside the negative control '(-)' after freeze-drying, as seen over a blue light transilluminator.

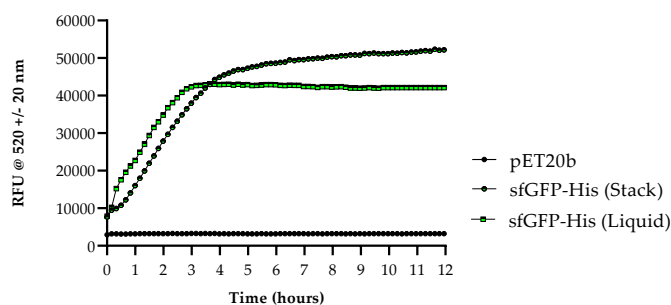
The main advantage of this platform is that the produced proteins can be varied by easily changing the DNA component, allowing for on-site flexibility. This versatility enables applications where therapeutic proteins can be synthesized in a patch containing layers of cellulose with extract and energy components, whereby different proteins can be synthesized by changing only the DNA layer. Another advantage of this platform is that expressed protein is found in the aqueous solution that is not attached to the paper support, aiding subsequent purification and application of the protein.

ii Kinetics of CFPS on paper support is identical to liquid CFPS

In order to ensure that the rate of CFPS on paper was similar to the liquid format that has been thoroughly studied in this thesis, a time course experiment was devised. Fluorescence from sfGFP-expressing liquid CFPS reactions and rehydrated cellulose stacks (Type 1) containing freeze-dried components were monitored over time. The initial observation was that CFPS trend on cellulose stacks closely overlapped the liquid reactions (Figure 4.16, a). This was further confirmed through linear regression analysis of the exponential phase; the rates of reactions between the two formats were found to be 11018 hr^{-1} in stack and 10267 hr^{-1} in liquid formats, with exponential phases lastly ~ 4 hours and 3 hours, respectively.

In conclusion, changing the format of CFPS had little impact on its kinetics. In fact, there was even a significantly higher fluorescence at 12 hours (and hence yield) in cellulose stacks than in liquid format four hours post-synthesis due to a longer exponential phase in stack format. However, four, rather than twelve hours holds more significance as, the shorter the time to obtain protein, the better for an on-site, on-demand platform as this allows for quick availability during high-demand periods and emergencies.

(a) CFPS kinetics in liquid and on cellulose stacks



(b) Linear regression analysis (exponential phase)

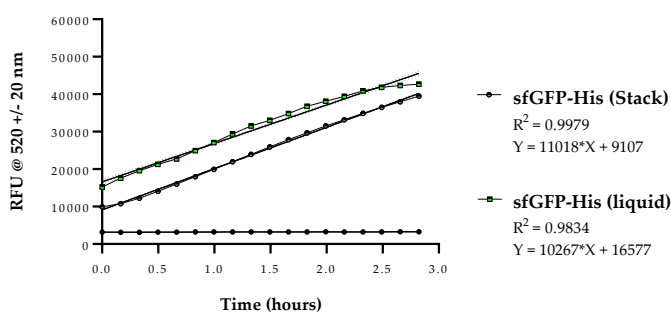


Figure 4.16: CFPS kinetics on cellulose is similar to that in liquid format. (a) Time course analysis of CFPS on cellulose ('sfGFP-His stack') and in liquid format ('sfGFP-His Liquid') in comparison to negative control ('pET20b'), (b) Linear regression analysis of the two formats showing the slope (rate of reaction), line equation and goodness of fit (R^2). Experiments were performed in triplicates ($n = 3$); data are shown as mean \pm SD.

4.2.3.d sfGFP expressing-cellulose stacks release sfGFP when loaded onto microneedles

This section audaciously explores and attempts to predict what CFPS on paper may look like for therapeutic applications. Firstly, the interchangeable DNA characteristic would be the primary advantage of choosing CFPS on paper over any other cell-free platform (e.g. lyophilised pellets) or cell-based platforms (e.g. *B. subtilis* spores). Figure 4.17 illustrates the various inputs (cellulose discs) and outputs (protein) that form the platform. The fundamental concept remains the same, whereby, the layered cell-free components freeze-dried on paper are rehydrated in a top-down fashion to kickstart CFPS. The produced protein is determined by the coding layer in the nucleic acid disc (top layer, Figure 4.17). Moreover, two coding DNAs could be affixed, enabling co-expression of proteins – such co-expression could, one day, even enable synthesis of chemical therapeutics by making use of enzyme synthesis and metabolic pathways in the extract source.

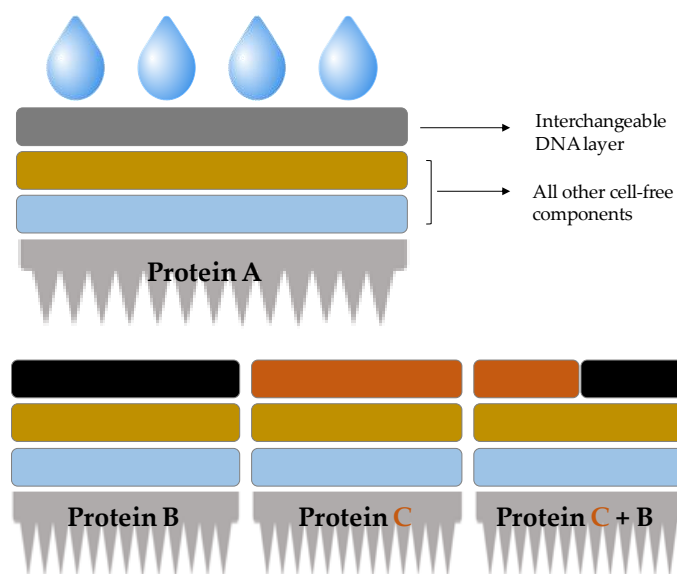


Figure 4.17: Concept of on-site and on-demand CFPS in a patch format. The cell-free components are freeze-dried on cellulose discs that are typically layered and rehydrated top-down, as proteins could be programmed to attach to the scaffold or release after synthesis. The top DNA layer can be interchanged to code for any protein (A, B, or C, or even co-express C and B). The layers are shown mounted above a microneedle patch (grey spikes).

The next advantage of CFPS on paper is its scaffold – cellulose - a commonly used material for protein purification, owing to its cheap availability. Recombinant proteins with cellulose binding domains could be programmed to attach to the cellulose discs themselves. Protein purification is an important consideration as the aim of the platform involves biomanufacturing intended for human use. Other methods of purification (*e.g.* affinity or size-based methods) could be combined with cellulose based methods to obtain highly pure products.

Lastly, the pure product requires a suitable formulation for delivery to targeted regions of the human body. Although biologics delivery for cell-free synthesised proteins have never been shown before, ideas that exist for cell-based methods mostly involve a syringe-injection (Rothschild, 2020). This format can be equally applied for cell-free synthesis; however, a patch may be better suited owing to the layered in-stack nature of CFPS in this platform. As part of a preliminary feasibility study, cell-free cellulose stacks expressing sfGFP were loaded onto dissolving microneedles that were kindly provided by Fiona Smith (School of Pharmacy, University of Nottingham). The microneedles were imaged before loading, shortly after loading and during dissolution under the microscope and illuminated by a blue light source to capture sfGFP fluorescence (Figure 4.18).

Cellulose stacks release protein when loaded onto microneedles

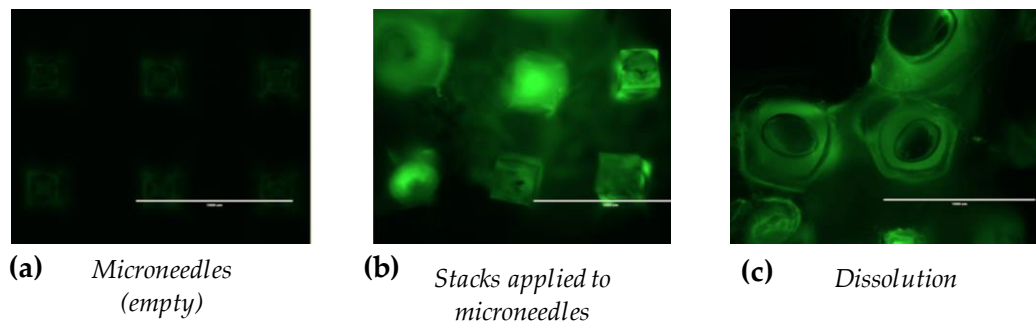


Figure 4.18: Cellulose stacks release sfGFP when loaded onto dissolving microneedles. (a) Before loading (empty microneedles have some background fluorescence), (b) sfGFP-expressing cellulose stacks applied to microneedles (although some dissolution already visible, most sfGFP seen on microneedles) and, (c) Dissolution (sfGFP fluorescence seen in the liquid compartment surrounding the dissolving microneedle). Six microneedles are shown with each stack made separately; scale bar indicates 1 millimetre (1000 μm).

The dissolving microneedles are fabricated with biocompatible polymers capable of releasing proteins upon application (data not included in this thesis). Some background fluorescence was detected from empty microneedles prior to loading (Figure 4.18, a). Cellulose stacks expressing sfGFP (rehydrated and incubated at 37°C, 4 hours) were readily trackable owing to strong fluorescence signals immediately after loading (Figure 4.18, b). Dissolution of the microneedles took place instantly after loading (< 1 min) and most sfGFP was found in the liquid fraction surrounding the microneedles (Figure 4.18, c). Biocompatible dissolving microneedles allow quick and easy delivery to the skin tissue which is ideal for on-demand applications when combined with in-stack CFPS. Other drug delivery methods should also be explored for on-demand CFPS as delivery targets are highly dependent on the product, disease and the environment.

4.3 Summary

This chapter initially described the development of an in-house CFPS system based on understanding from commercial systems such as the NEB PURExpress and Promega *E.coli* S30A Extract System for Circular DNA. The in-house system was optimised thoroughly after experimentation with energy component, magnesium glutamate and DNA concentrations. Supplementing the system with PEG, a molecular crowding agent, significantly enhanced expression, taken together with a higher fraction of cell-free extract in the reaction mix. Based on these findings, the optimised reaction composition consisted of 40% v/v cell-extract (30 mg/mL protein concentration), 2x energy mix, 20 mM Mg-Glu, 300 ng DNA and 3% PEG.

Next, various formats were explored for on-site and on-demand applications of the in-house system. Microclassification, the first format tested, failed to preserve the cell-free extract in a reconstitutable format. This was most likely due to protein denaturation and aggregation, as RNA supplementation did not revive the extract, but gentler mixing methods had a small yet significant difference. On the other hand, lyophilisation preserved all components in 'one-pot', enabling a 'just-rehydrate' format for CFPS. This format was further expanded to lyophilisation of cell-free components on individual cellulose discs, capable of kickstarting CFPS upon layering and rehydration. Cellulose Type 1 (toilet tissue) was found to be most efficient for this purpose and cell-free kinetics on this scaffold was identical to that of liquid reactions.

Lastly, the advantages of cellulose stacks and ideas for their application were discussed. In a feasibility study, stacks applied to dissolving microneedles successfully released sfGFP. Although the work discussed towards the end of this chapter set the scene for synthesis of life-saving and life-enhancing therapeutics, many challenges arise, and a significant amount of work is required to lay concrete foundations for the described platform(s). The biggest challenges revolve around meeting regulatory standards and gaining approval from drug administration agencies. Smaller challenges include the purification process itself and scale up of the system according to the required dose. On a positive note, this platform provides a convenient solution for obtaining therapeutic proteins on-site and on-demand. It benefits from lightweight and convenient distribution, in addition to being easy-to-use in low-resource and extreme environments. In the developed world, this platform may offer a sustainable solution to break cold-chain supply, end overproduction and wastage of pharmaceuticals.

Chapter 5 Improving stability of CFPS for VITA (Visualising In-Situ Tx-TL Astropharmaceuticals)

5.1 Introduction

Given that CFPS is a very active field of research, it is only recently being studied in microgravity. Therefore, a proposal was sent to the European Space Agency's Orbit Your Thesis!3 programme (ESA OYT), to study any similarities and differences in CFPS in a true space environment (microgravity and radiation on the International Space Station; ISS). During the proposal submission, a United States student-led project composed of freeze-dried cell-free pellets was flown to the ISS (2022; in collaboration with MiniPCR BioBits and NEB). Information on the details, success and findings of this mission could not be obtained as they were not shared online so it is difficult to discuss if this experiment was based on the NEB PURExpress system that was discussed in Chapter 4. Although the technology is similar, it should be noted that the experiment utilised cell-free systems requiring long term storage at -20°C, with short term storage (up to three months) requiring refrigeration, whereas Nottingham's proposed system aimed to demonstrate utility with storage at room temperature. This proposal was also intended for a different application and is a fully automated demonstration that does not require astronaut research and analysis time. The NEB system uses a visual signal to detect the presence of pathogens in the water supply (biosensing), whereas this platform is intended for producing various therapeutic proteins by simply changing the DNA variable, as described in Chapter 4.

The proposal titled 'VITA' (Visualising In-situ Tx-Tl Astropharmaceuticals) was selected by ESA Academy in May 2022 following a round of panel discussions. The team comprises of students (UG, MEng, and PhD) from the Faculties of Science and Engineering, mentored by endorsing professors Phil Williams (Science) and Chantal Cappelletti (Engineering). Aiming to launch to the ISS in mid-2024, reviews and tests by the student team are currently underway. Aside from the exciting science that this project will study, VITA is an educational project designed to further collaboration and learning across UoN Departments, Schools, and Faculties, while providing project-based training to students in space sector operations and engineering. Participating students are exposed to ECSS (European Cooperation for Space Standardization) and the professional environment of the European Space Agency, giving valuable experience towards pursuing their own careers in the UK's growing space sector.

This chapter focuses on the scientific goals of VITA and narrates the development of the scientific the payload itself. Where necessary, information and work carried out on other engineering sub-systems have been provided. It borrows heavily from cell-free work already discussed in Chapters 3 and 4, with the overarching aim to test the on-site, on-demand platform in a truly extreme environment – the ISS.

In order to achieve overall aim, the following sub-aims were addressed -

- (a) Design, build and test the platform for the VITA mission, a European Space Agency Orbit Your Thesis 3! payload for technology demonstration on the International Space Station.
- (b) Perform stability studies to understand the shelf-life of the on-demand CFPS platform and research ways to enhance sample stability.
- (c) Perform instrumentation tests to ensure the ability to collect real-time data on reaction kinetics.

Results and discussion

5.1.1 Introduction to VITA (Visualising In-situ Tx-TL Astropharmaceuticals)

VITA aims to demonstrate on-site and on-demand production of model therapeutic proteins for long-duration human spaceflight, *e.g.* during a crewed mission to Mars where stockpiled medications are consumed, expired or damaged. Therefore, the ideal proof-of-concept should be generated in an environment that is inhabited by humans, with characterises of a real space mission such as constant microgravity, radiation, launch loads and long-duration isolation. Therefore, the ISS environment is highly suitable for performing the experiment, and this will greatly accelerate the development of an “astropharmacy” in space.

Having said that, there are also numerous Earth-based applications and benefits for this Astropharmacy. The distribution and use of biopharmaceuticals are severely limited in low-resource and extreme environments due to the products typically requiring cold-chain storage. In these environments, the on-site and on-demand format of VITA will be of great benefit due to the lightweight, easy-to-use nature and convenient ambient temperature distribution. Moreover, in the developed world, this platform also offers a sustainable solution by reducing the need for cold-chain supply

and overproduction of pharmaceuticals (which is unsustainable due to stockpiling and wastage).

Besides intending to demonstrate on-demand CFPS technology, VITA also strives to test other technologies such as telecommand-controlled microfluidic rehydration of freeze-dried cellulose stacks, active thermal control to maintain a temperature of $30^{\circ}\text{C} \pm 1.5^{\circ}\text{C}$ for CFPS and near real-time, in-situ detection and downlink of data to earth. A simple overview of the science and engineering units is provided below in Section 5.1.1.a for the reader's understanding; however, this thesis only discusses the work on scientific payload and does not include data from the engineering sub-systems.

5.1.1.a Operations of the VITA mission

VITA will be launched by ESA to the ICE Cubes Facility (ICF) onboard the ISS and will be teleoperated by the team on the ground until return of the cube for post-flight sample analysis on Earth. Environmental conditions within the cube and the ISS will be logged and this will in turn inform the ground control experiment(s). As summarised in Figure 5.1, the Concept of Operations (ConOps) for the VITA mission is divided into three broad stages: *Upload* (from sample integration until cube integration in the ICF); *Experiment* (teleoperation of the cube in the ICF to perform the experiments); and *Download* (transfer of the cube into on-orbit refrigerated stowage and return to Earth for post-flight analyses). Furthermore, the cube will undergo five 'modes' namely *Safe*, *Standby*, *Rehydrate*, *Science*, and *Decommission* modes (Figure 5.1). This chapter narrates the development of the science unit and the operations during the mission's science mode in the experiment stage of the mission.

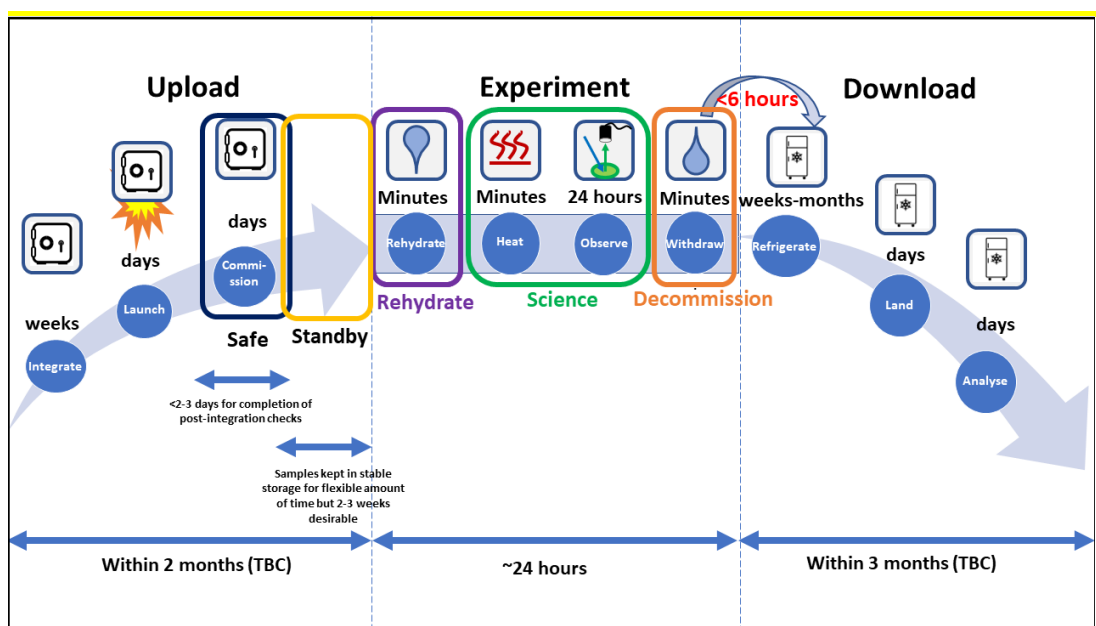


Figure 5.1: VITA Concept of Operations. The mission has three phases (top) and five modes (below highlighted icons; colour coded). Actions and estimated timeframes are indicated where known, marked 'TBC' (To Be Confirmed) for timeframes pending confirmation. Adapted from the VITA Activities Requirements Document submitted to ESA.

5.1.1.b Design of the VITA cube and scientific payload

The VITA cube will remain hermetically sealed (internal atmospheric pressure = 1 atmosphere) for its entire flight encapsulating four principle hardware stacks or 'science units' consisting of fluidics, thermal control and instrumentation (cameras and spectrophotometer) subsystems. Each of these units are then connected to the electronics and Printed Circuit boards (PCB) of the On-Board Data Handling (OBDH) system containing the on-board computer (Figure 5.2). Distributed throughout the cube are environmental sensors (for recording air temperature, humidity, pressure, and quality) and two miniature viewing cameras for outreach photos and verification of specific hardware functions (liquid containment in reservoirs over launch, filling of wells upon telecommand *etc.*).

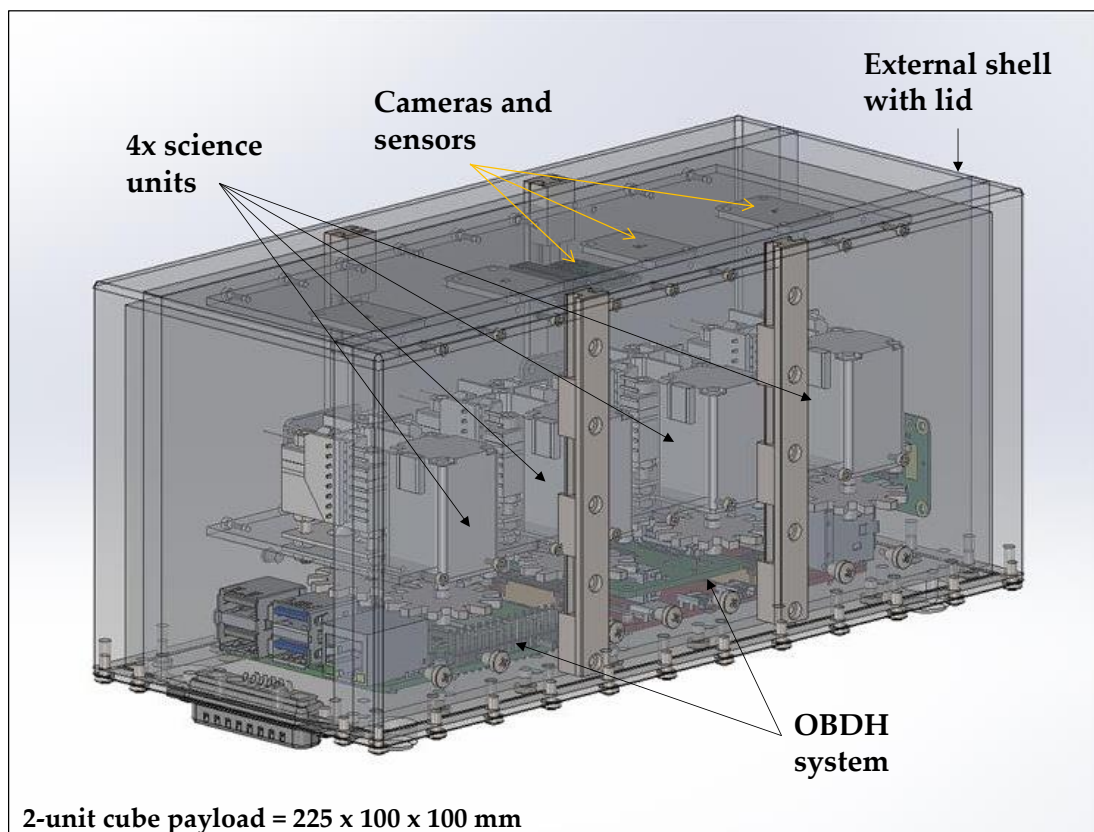


Figure 5.2: Computer Aided Diagram (CAD) of the VITA experiment cube. The assembly shows the four science units connected to the OBDH system, with sensors and cameras from instrumentation subsystem above. Adapted from the VITA Design Report submitted to ESA.

Each science unit will contain four cellulose stacks with four different DNA disks. The layers of the cellulose stacks are designed as follows (Figure 5.3):

- (a) **DNA layer:** pET20b vector with a T7 promoter, C-terminally His-tagged insert, T7 terminator, with the insert being either:
- sfGFP gene
 - sfGFP nanobody gene
 - sfGFP gene and sfGFP nanobody gene (two DNA layers for co-expression; as illustrated in 4.2.3.d)
 - No insert (negative control)
- (b) **Cell-free extract layer** (derived from BL21 Star DE3 – pAR1219)
- (c) **Biochemical layer** (Energy components, glutamates, sugars etc.)

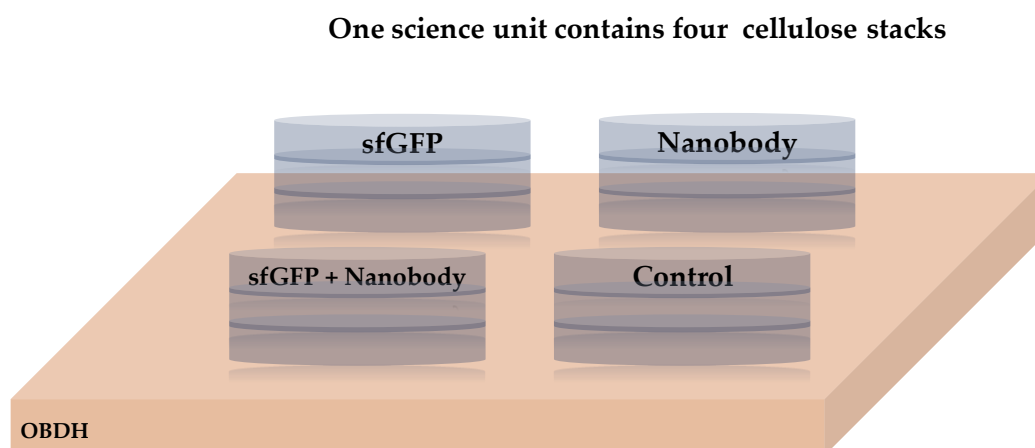


Figure 5.3: Image showing contents of one science unit. Four types of cellulose stacks with four different DNA layers coding for sfGFP, Nanobody for sfGFP, a negative control with no protein expression and a co-expression stack with both the sfGFP and Nanobody DNA are contained in wells that are connected to the OBDH system.

The chosen nanobody is a fragment of an antibody generated against sfGFP and is termed 'NBS07-sfGFP'. The properties of the nanobody and co-expression studies are further discussed in Chapter 6. Briefly, it is made up of 122 amino acids (13.1 kDa) and contains two disulfide bonds, when folded correctly. A fluorophore tag will be cloned to the nanobody enabling production of recombinant nanobodies in the 'Nanobody' and 'sfGFP + Nanobody' wells (Figure 5.3). Although the fluorophore itself has not been determined for the mission, choices will be made based on properties such as quantum yield, size, stability, and contrast to sfGFP signal (excitation, emission and Stoke's shift; for best signal over noise with sfGFP fluorescence). It is noted that black walls will be built in between each sample in all science units to prevent unwanted noise in the spectrophotometer data and images taken by the camera.

The fluidics subsystem is designed such that each sample well will be rehydrated with 40 μL of liquid S30A buffer (this comprises 80% initial reaction volume of the 50 μL reaction before lyophilisation). The total volume of rehydration including all 16 wells split in four science units is approximately 0.8 mL. This ensures that there are enough biological repeats ($N = 4$ for each protein produced) and also mitigates the risk of a rehydration/data collection failure in one science unit.

5.1.1.c Detection of fluorescent proteins in VITA

i Instrumentation

Each well in the 2 x 2 grid in the science unit is designed to have its own excitation source that will be activated sequentially and therefore each well's fluorescence will be monitored individually and precisely. The excitation sources comprise of commercial-off-the-shelf (COTS) LEDs aimed at the centre of each well to provide the highest intensity in a narrow beam angle (reducing the noise recorded from the above sensor). Blue light and UV LEDs were tested in feasibility studies and it was found that UV LEDs generated a better signal:noise when compared to blue, however, presented an increased risk of sample beaching from prolonged UV exposure (data not shown in this thesis). The nanobody fluorophore may similarly be excited by blue or other RGB (Red-Green-Blue) COTS LEDs.

The spectrophotometer will capture fluorescence emissions from each well and is placed 30 mm above each well grid. The spectrophotometer sensor module functions by recording received light intensity across various bands of wavelength without any spatial resolution, *i.e.*, the sensor measures the received intensity within a Field of View (FOV) and produces an output number for each colour channels intensity in Arbitrary Light Units (ALU), for each time point (Figure 5.4). In the case of detecting sfGFP, the ALUs in the green region is plotted, when the samples are excited by a blue light source (corelating to the excitation [485 nm] and emission parameters [510 nm] of sfGFP) (Pédélecq et al., 2006).

ii Preliminary Image analysis

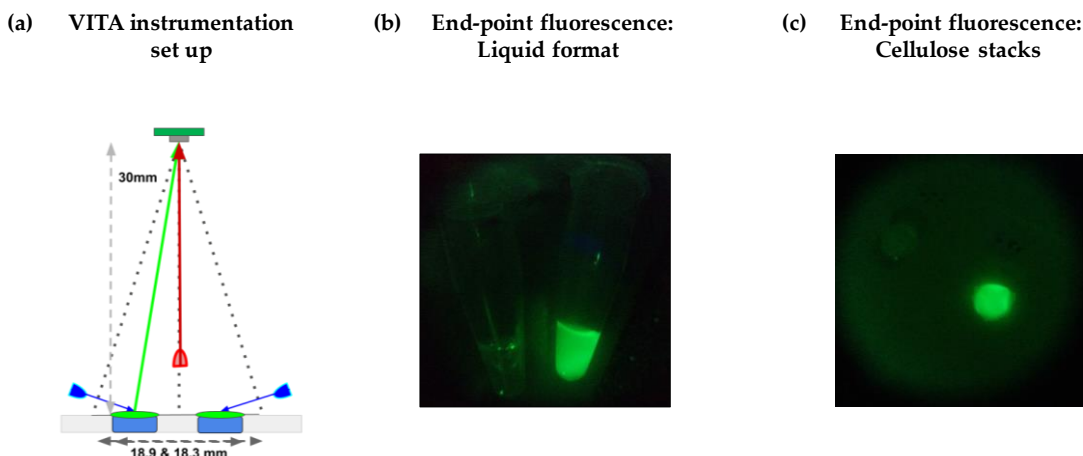


Figure 5.4: Preliminary VITA instrumentation tests. (a) Diagram showing the main components of the instrumentation system: Excitation of sfGFP inside wells by LED blue icon and arrows), emission recorded (spectrophotometer) and captured (camera) by the above sensors (green arrow). Green ALUs are normalised to Red ALUs (for noise correction; red arrow); adapted from the VITA Design Report submitted to ESA, (b) Image of an aqueous end-point CFPS reaction expressing sfGFP (green; right) compared with a negative control (no colour; left), (c) Image of an end-point CFPS reaction on cellulose stacks expressing sfGFP (green; right) compared with a negative control (no colour; left).

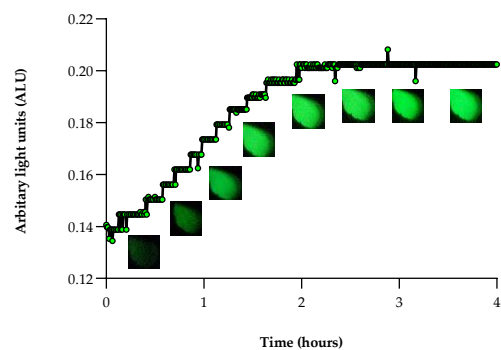
The VITA instrumentation was able to image end-point CFPS reactions with good precision and resolution. Figure 5.4 (b & c) shows two images from end-point reactions on cellulose and in aqueous format, where the green fluorescence from samples that produced sfGFP is readily visible with the naked eye (both images are raw and unprocessed). This both validates the capabilities of the camera for use during the mission, and provides instant and visual confirmation that the CFPS reaction was a success. In addition to the primary time course data that will be obtained from the VITA spectrophotometer, further image analysis could be performed to obtain secondary quantitative information from such images (e.g. integrated pixel density on Image).

iii Preliminary time course analysis

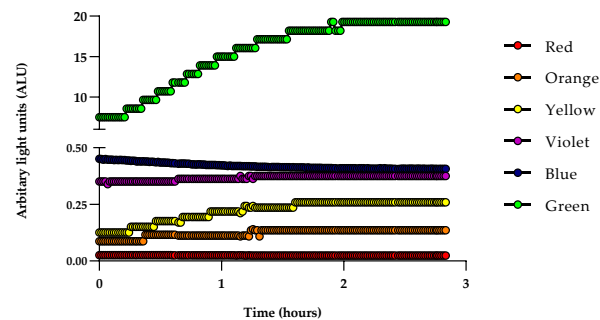
A good level of confidence was obtained from successful imaging analysis, thus far. Next, the VITA spectrophotometer was tested for its ability to take multiple, programmed ALU measurements over a prolonged course of a cell-free reaction. A series of commands were created in Python to enable flashing on of the blue LED, execution of the sensor reading (or image the reaction) and flashing off of the LED every minute (or 30 minutes for imaging) for a total time period of four hours (script development and tests not included as part of this thesis). This set-up was placed inside an incubator to maintain a constant temperature of 37°C for the initial cell-free

studies, in aqueous format. This VITA prototype set-up was successfully able to detect sfGFP from cell-free reactions over the four-hour time period (Figure 5.5, a). Kinetics of the cell-free reaction closely resembled that of the in-house reactions observed in Chapter 4. Additionally, the green signal captured from sfGFP was significantly distinct to the noise from all other colour channels except yellow, which had a similar increasing trend to green (Figure 5.5, b). This could perhaps be attributed to the proximity of the yellow wavelength to green on the visible spectrum. The CFPS trendlines obtained after two other experiments also closely resembled that of the in-house reactions, after normalisation to negative control reactions (Figure 5.5, c). The high standard deviation could be attributed to either or combinations of batch-batch variation, noise, or instrument variation/positioning as this was carried out manually. Collectively, these results suggest that the VITA instrumentation system is suitable for following the kinetics of the scientific payload and with optimisation, has the potential to become highly suited for automated detection in extreme environments.

(a) Time course of sfGFP synthesis (spec and images)



(b) Other colour channels show insignificant changes over time



(c) VITA time course of sfGFP synthesis (three independent samples)

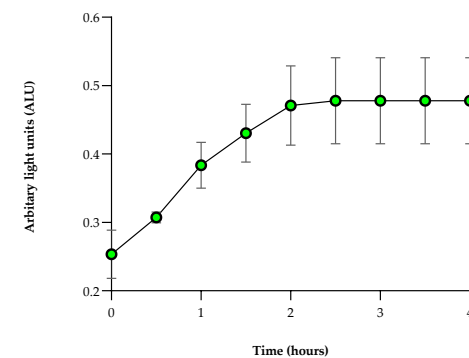


Figure 5.5: CFPS time course analysis of sfGFP using VITA instrumentation. (a) Graph showing Arbitrary Light Units (ALUs) from the green channel of the spectrophotometer readings plotted over time, alongside images taken every 30 minutes with the VITA camera; results for one CFPS reaction expressing sfGFP in liquid format at 37°C shown (N = 1), (b) Graph showing Arbitrary Light Units (ALUs) from all colour channels of the spectrophotometer readings plotted over time; violet and blue units were reduced by a factor of 100 to be accommodated in this graph (N= 1), (c) Graph showing Arbitrary Light Units (ALUs) from the green channel of the spectrophotometer readings plotted over time, results represent three independent CFPS reactions normalised to negative control (n = 3); data are shown as mean \pm SD.

5.1.1.d Effect of VITA temperature on CFPS kinetics 30°C

A temperature of 30°C ($\pm 1.5^\circ\text{C}$ margin) was chosen for the VITA mission as a compromise between feasibility of the thermal control system, safety (prevent overheating of electronics) and time required for a complete reaction to occur. CFPS can be performed at a wide range of temperatures (25°C to 50°C for bacterial extracts), however, 37°C is the most common bacterial growth temperature reported in literature and also the temperature at which the system was studied in this thesis so far (Krinsky et al., 2016). Therefore, time course analyses were conducted to understand the effects of lowering reaction temperature to 30°C.

Positively, reaction yield was not compromised, in fact, a higher yield was observed 16 hours after reaction progression (Figure 5.6). However, kinetics slowed down significantly at 30°C, allowing experiment to progress longer. Rather than a single exponential and plateau phase as seen at 37°C, the reaction at 30°C had a tri-phasic trend that did not quite reach saturation by 16 hours. This is not necessarily a challenge, as the mission timeline provided by ESA enables the team to conduct the mission for up to 4 months. Nevertheless, the concept of Astropharmacy involves production of therapeutics at a rapid time scale (~ 4 hours as seen at 37°C), therefore, the reaction temperature of 30°C only remains as a preliminary temperature for this technology demonstration mission. Further missions and work with VITA could consider improving the engineering heat tolerance levels and/or bring innovative solutions for managing risks associated with overheating of electrical components.

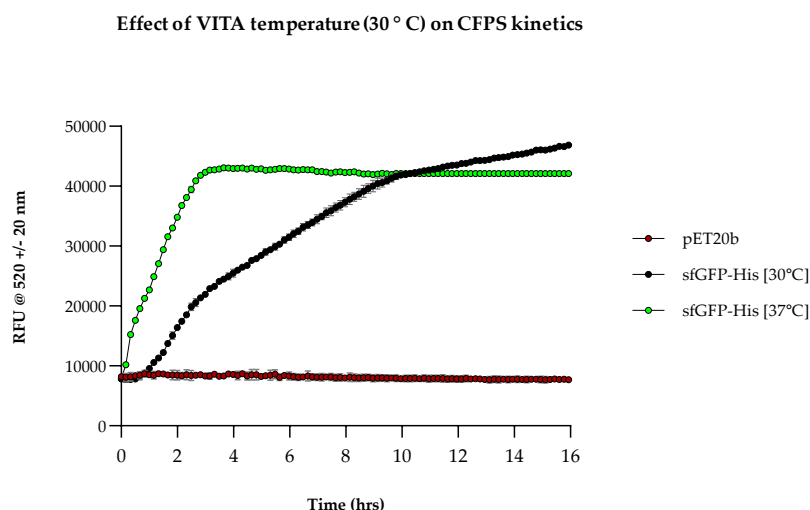


Figure 5.6: Effect of VITA temperature (30 ° C) on CFPS kinetics. Time course analysis showing expression of sfGFP from in-house reactions in aqueous format at 30°C and 37°C, compared with negative control ('pET20b') at 37°C. Experiments were performed in triplicates ($n = 3$); data are shown as mean \pm SD.

5.1.1.e Scaling up reaction volumes does not impact CFPS

The VITA prototype contains sample wells that were sized to accommodate up to 50 μL of liquid solution. This was because smaller volumes were a more cost-effective solution for both the science and engineering sub-systems for a 1U cube. Since the development of the prototype, the cube size has been increased to 2U, offering the possibility to increase the number of samples. Since this may involve complications for the microfluidics subsystem, the possibility of increasing sample well size was next explored. The impact of increasing reaction size (from 50 μL to 75 μL , 100 μL , 150 μL , 200 μL , and 250 μL) was studied through end-point fluorescence analysis.

sfGFP fluorescence was compared in these sample volumes (all performed in a 1.5 mL eppendorf tubes, in S30A buffer) in both aqueous format and lyophilised pellets (80% rehydration volume was used in the case of lyophilisation). The cell-free reactions expressing sfGFP from the reconstituted lyophilised system did not have significantly different fluorescence outputs between the sample volumes tested (Figure 5.7). However, the cell-free reactions in aqueous format produced significantly lower fluorescence in reaction volumes over 100 μL (Figure 5.7). Regardless, the fluorescence output is still well within the VITA detection range (see Section 5.1.4.b), enabling all reaction formats and volumes studied here to be implemented for the mission.

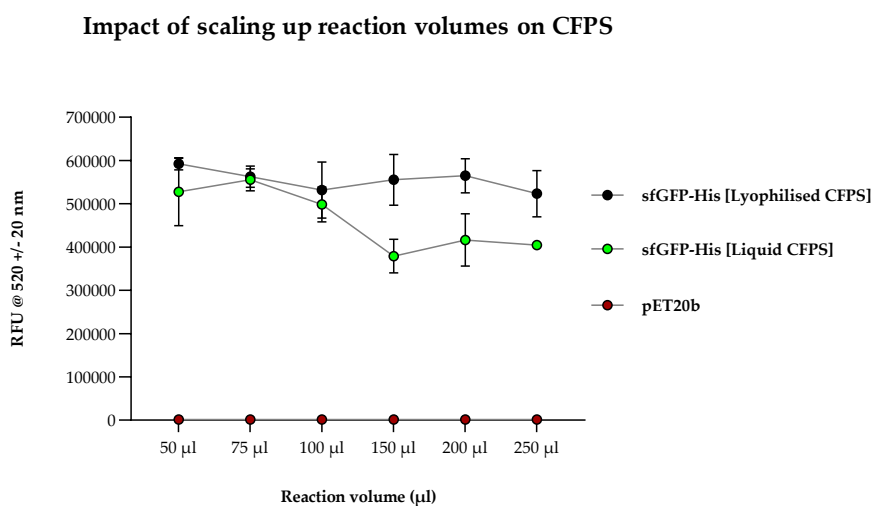


Figure 5.7: Impact of Scaling up reaction volumes on CFPS. Graph showing end-point fluorescence recordings for six reaction volumes (50 μL , 75 μL , 100 μL , 150 μL , 200 μL and 250 μL) tested in two reaction formats (standard aqueous format; [sfGFP-His Liquid CFPS] and lyophilised pellets representative of flight samples; sfGFP-His [Lyophilised CFPS]), alongside a pET20b negative control. Experiments were performed in triplicates ($n = 3$); data are shown as mean \pm SD.

As discussed in Chapter 1, continuous exchange formats enable highly efficient CFPS, however, are not suited for on-demand, on-site applications. Batch formats offer a

convenient solution, in that programmable quantities of input allow reception of predictable quantities of output. It is important that the required dose of proteins is manufactured for therapeutic applications, hence cell-free systems should be scaled up or down appropriately. One particular scale up study has shown preservation of protein yield in reaction volumes from 15 μL to 500 μL , allowing for dose appropriate syntheses of a vaccine candidate (Voloshin and Swartz, 2005). In a further advancement, another study reported linear scalability of cell-free systems for volumes up to 100 L (in a bioreactor). Also based upon a bacterial cell-free extract, high yields were obtained for a disulfide bonded cytokine (Zawada et al., 2011). Hence, the results shown in Figure 5.7 broadly align with other reported results and suggests that scaling up to higher reaction volumes may be a possibility that can be further examined in the future.

5.1.2 Stability studies for CFPS shelf life determination

Similar to the food and drink industry, biopharmaceuticals also expire and require a shelf-life, and their stability is no new challenge (FDA, 2003). Stability testing is a protocol that involves data collection of the characteristics of a product in order to determine its shelf life. A product is no longer considered stable when the storage time has exceeded its shelf life or if its characteristics do not match those provided in the manufacturer's specification.

For the purposes of this project, stability (extended shelf-life) of CFPS systems are important for two broad reasons: (1) One aim of Astropharmacy involves providing on-site and on-demand access to therapeutics and hence, the required raw materials need to endure environmental stress in those extreme environments, and (2) The VITA mission operations entails a period of approximately 2 months between cube integration and launch to the ISS. The scientific payload must remain viable until telecommanded rehydration and this involves cell-free components to show long-term stability (initially 1 to 2 months; at temperatures between 5°C and 45°C; based on temperature data provided by ESA). A series of stability tests were first conducted on the in-house cell-free system, in order to determine its shelf life. The pass/fail criteria for the tests were based on the ability of the cell-free platform to produce sfGFP fluorescence, following rehydration after a set storage time at a set temperature.

It is well known that cell-free components in aqueous format are commonly stored at -80°C and degrade at elevated temperatures, where degradation is directly proportional to increase in temperature. A similar trend for lyophilised cell-free systems has been reported in literature, however, rate of degradation is slower in these systems than aqueous systems. This is attributed to the solid state, wherein,

motionless molecular dynamics contribute to increased stability (Smith et al., 2014). To test if this result is representative of the VITA's cellulose stack-CFPS system (composed of lyophilised cell-free components), the cellulose stacks were subject to a range of storage times and temperatures, and later rehydrated to compute their shelf-life.

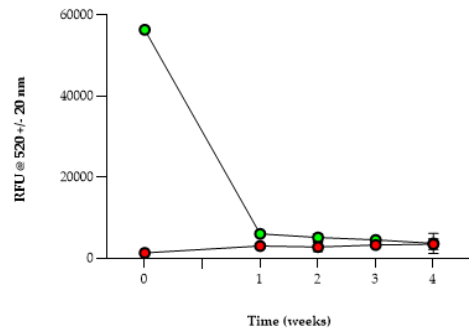
Primarily, three storage temperatures were tested: 40°C, room temperature (RT; 16°C - 22°C; average 19°C) and 4°C. These temperatures were chosen for a number of reasons. Firstly, they are the most studied temperatures for stability testing. And secondly, they are the most representative for storage and transport (*e.g.* RT is typically maintained in households or on the ISS, 4°C is a common refrigerator temperature *etc.*). Furthermore, two humidity conditions were tested for RT samples – nominal (40 %) and high humidity (60 %), as the normal internal humidity at RT is 30% to 50% RH (average of 40%); however, the internal environment of the ISS is typically maintained at ~ 60 % RH. And finally, stability of lyophilised pellets was also tested at RT to study any differences in stability when components are lyophilised on cellulose.

In all temperatures and formats tested, stability dropped significantly over the first week of storage (Figure 5.8; all). Even at RT, which is considered a nominal environment, no significant difference in fluorescence was detected between sfGFP and negative control samples, after 4 days of storage in both medium and high humidity environments (Figure 5.8 b & c). The samples stored at 4°C exhibited a significantly higher fluorescence in the sfGFP-expressing stacks compared to the negative control, however there was still a 75% reduction in stability after 4 days of storage (Figure 5.8, d). Additionally, there was no significant difference in stability between the cellulose stack and lyophilised pellet formats, as both formats reported no stability after one week of storage (Figure 5.8 c & e; left). In fact, stability recordings taken from lyophilised pellets every day for one week shed more light on this diminishing trend (Figure 5.8, e; right). A 50% drop in stability is seen after 1 day of storage at room temperature, which increased to 75% by day 4 and day 5. By day 7 (1 week), all stability was lost, which was the observed result for all succeeding data points then on.

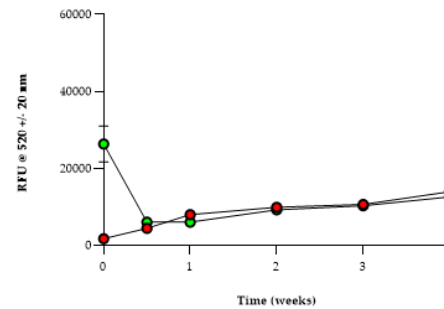
The shelf-life of in-house CFPS was found to be < 1 week and this needs improvement to > 1 month. Collectively, these results suggest that the stability of lyophilised in-house cell-free components is extremely poor and need drastic improvement for on-site, on-demand applications, and also for the success of the VITA mission. This is, however, not an uncommon result, as similar diminishing trends in stability have been reported previously (Karig et al., 2017). This published study in fact observed no stability after a single day of storage of unpreserved CFPS mix at 37°C. It was

further discovered that the cell-free extract degraded faster than the other buffer components, indicating that the proteins lose stability at room temperature within a day. Therefore, innovative solutions for enhancing protein stability may aid any efforts in improving the long-term stability of lyophilised in-house CFPS systems.

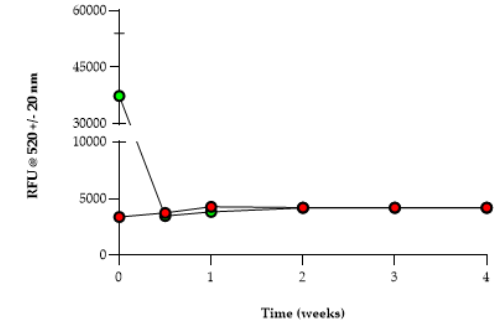
(a) Stability of cellulose stacks over time at 40°C



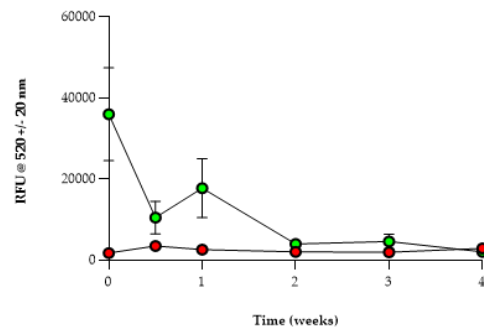
(b) Stability of cellulose stacks over time at room temperature (high humidity ~ 60% RH)



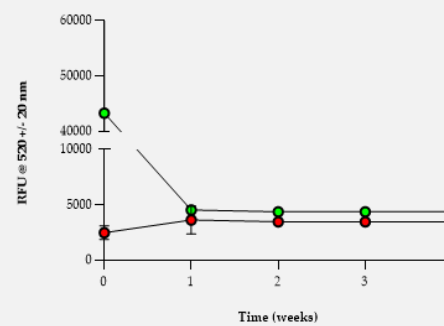
(c) Stability of cellulose stacks over time at room temperature



(d) Stability of cellulose stacks over time at 4°C



(e) Stability of lyophilised pellets over time at room temperature



Stability of lyophilised pellets over time at room temperature

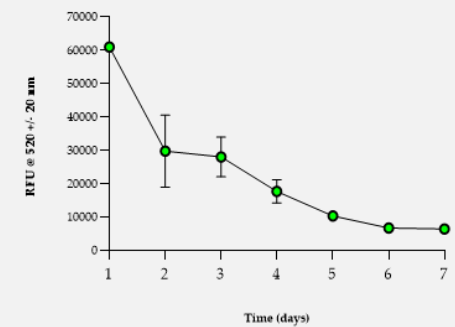


Figure 5.8: Stability tests of in-house CFPS in cellulose stack format and lyophilised pellets. Graph showing sfGFP fluorescence following rehydration of CFPS on cellulose stacks after storage over 1 month at (a) 40°C, (b) Room temperature (~ 22°C; 60% RH), (c) Room temperature (~ 22°C; 40% RH), (d) 4°C, and (e) CFPS in lyophilised pellets format after storage over 1 month at room temperature (left) with data points shown for the first seven days (right). All CFPS reactions were rehydrated with S30A buffer; green data points correspond to reactions expressing sfGFP and red data points indicate the pET20b negative control. Experiments were performed in triplicates ($n = 3$); data are shown as mean \pm SD.

5.1.3 Impact of various supplements on CFPS kinetics

As discussed in Chapter 1 (1.4.4.c), a thorough literature search led to the identification of certain types of carbohydrates (sugars) as excellent candidates for stabilisation of cell-free systems. This was no surprise as sugars are often incorporated as excipients in biotherapeutic stabilisation for their ability to preserve native protein structure (during lyophilisation, this is preserved in amorphous state) (Jovanović et al., 2006). The most commonly reported candidates for CFPS stabilisation included sugars such as sucrose, trehalose and lactose, and molecular crowding agents such as trimethylglycine and dextrin (*e.g.* β -cyclodextrin) (Jiang et al., 2021, Gregorio et al., 2020, Warfel et al., 2023, Smith et al., 2014).

These candidates were studied for their potential role in improving stability of the in-house CFPS platform. Prior to studying the stability of CFPS itself, the impact of these candidates on cell-free kinetics was first studied. A time course analysis was performed to monitor sfGFP synthesis upon supplementation with the following candidates: sucrose, trehalose, trimethylglycine, β -cyclodextrin, and lactose. Supplementation concentrations were chosen based on previously published work, serving as an initial starting point; ranges of concentrations were tested for some candidates where advised (Jiang et al., 2021, Gregorio et al., 2020, Warfel et al., 2023, Smith et al., 2014).

The first observation was that cell-free kinetics were notably different in all supplemented reactions, when compared to unsupplemented reactions (Figure 5.9; all). All supplemented reactions, except for lactose, displayed significantly lower reaction rates, where synthesis saturated ~ 8 hours after commencement; unsupplemented reactions saturated $\sim 3 - 4$ hours after commencement, which was the observed result for all in-house reactions seen so far in Chapters 4 and 5 (Figure 5.9; a, b, c & d). Reactions supplemented with α/β -lactose had a similar exponential phase that reached saturation $\sim 3 - 4$ hours after commencement, however protein yield was compromised (Figure 5.9; e). In fact, most supplemented reactions had significantly lower protein yield, with sucrose displaying the worst (30% yield of unsupplemented reaction; Figure 5.9, a) and trehalose and β -cyclodextrin displaying the best (90 – 95% yield of unsupplemented reaction; Figure 5.9, b & d).

The low rates of reaction and subsequent yields could be attributed to molar ratios of the supplement and proteins in the cell-free extract – high affinity of supplements to water reduces molecules available for protein interaction (Guzman-Chavez et al., 2022). This may explain why a concentration-dependent decrease in yield was observed in reactions supplemented with trehalose and sucrose (*e.g.* 100 mM trehalose supplement reduced yield compared to a 20 mM supplement; Figure 5.9, a

& b). Nevertheless, this study led to the identification of the properties of some candidates for stability testing that will be further discussed in Section 5.1.3.b.

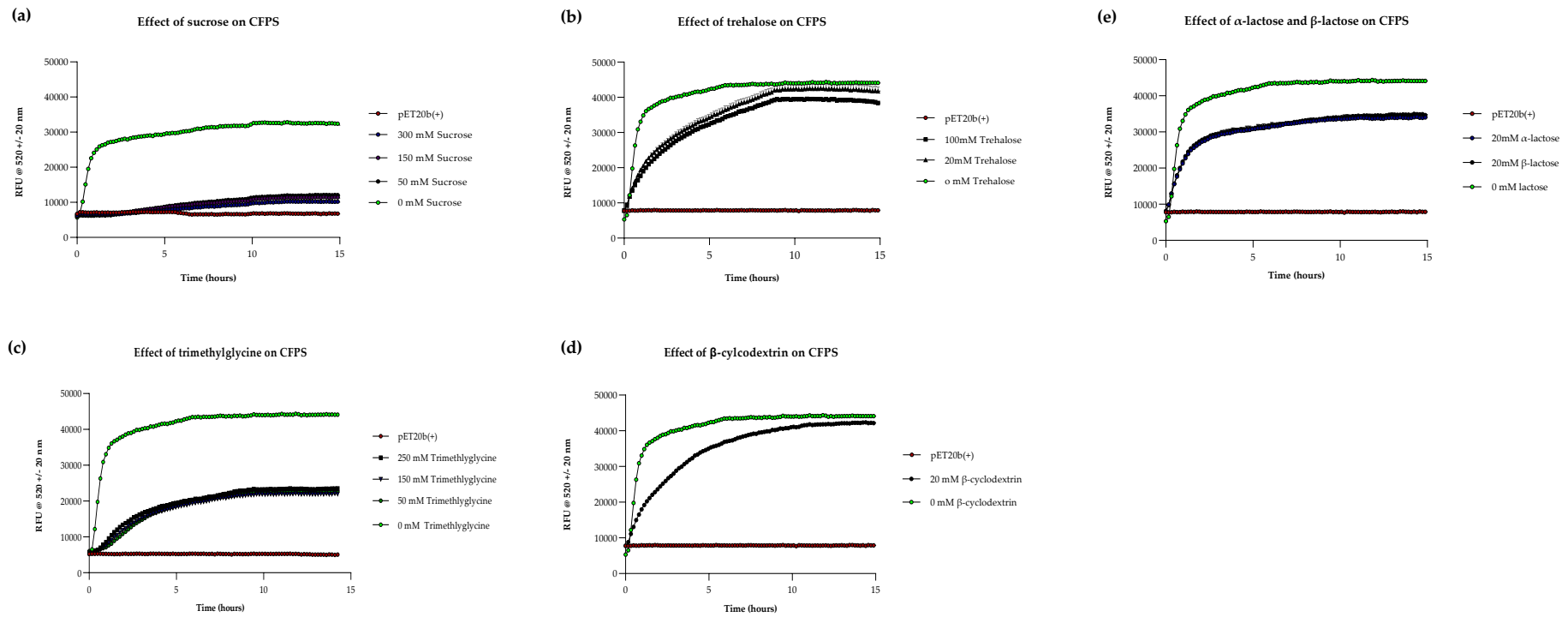


Figure 5.9: Impact of various supplements on CFPS. Time course analysis showing expression of sfGFP from in-house cell reactions in aqueous format supplemented with (a) sucrose, (b) trehalose, (c) trimethylglycine, (d) β -cyclodextrin and (e) α/β -lactose, compared with unsupplemented reactions (0 mM) and negative control ('pET20b+') at 37°C. Experiments were performed in triplicates ($n = 3$); data are shown as mean \pm SD.

5.1.3.a Impact of secondary energy substrates on CFPS (PEP and Maltodextrin)

This section describes the tests performed to study the impact of secondary energy substrates phosphoenol pyruvate (PEP) and maltodextrin (MDX) on the in-house cell-free platform, which was traditionally based on nucleoside triphosphates. It does not wish to establish any new energy mixes as appreciable amounts of progress has already been made in literature (Chapter 1; 1.3.4.c) (Guzman-Chavez et al., 2022, Warfel et al., 2023). Therefore, concentrations of PEP and MDX reported in literature (33 mM PEP; 25 -100 mM MDX) were initially tested for its impact on the in-house cell-free platform, in addition to the nucleoside triphosphates.

Briefly, time course analysis revealed that addition of PEP lowered protein yield by ~ 50% although kinetics remained the same (Figure 5.10, a). On the other hand, MDX improved reaction yield by ~ 50%, whereby the initial reaction rate match that of the unsupplemented reaction, but it was followed by another slower exponential phase in all concentrations tested (Figure 5.10, b). By 16 hours, there was no significant difference between 25 mM – 100 mM MDX supplemented reactions, indicating 25 mM is a sufficient concentration – this was a particularly exciting finding as a doubled yield was obtained for a low cost as MDX is a relatively cheap energy source.

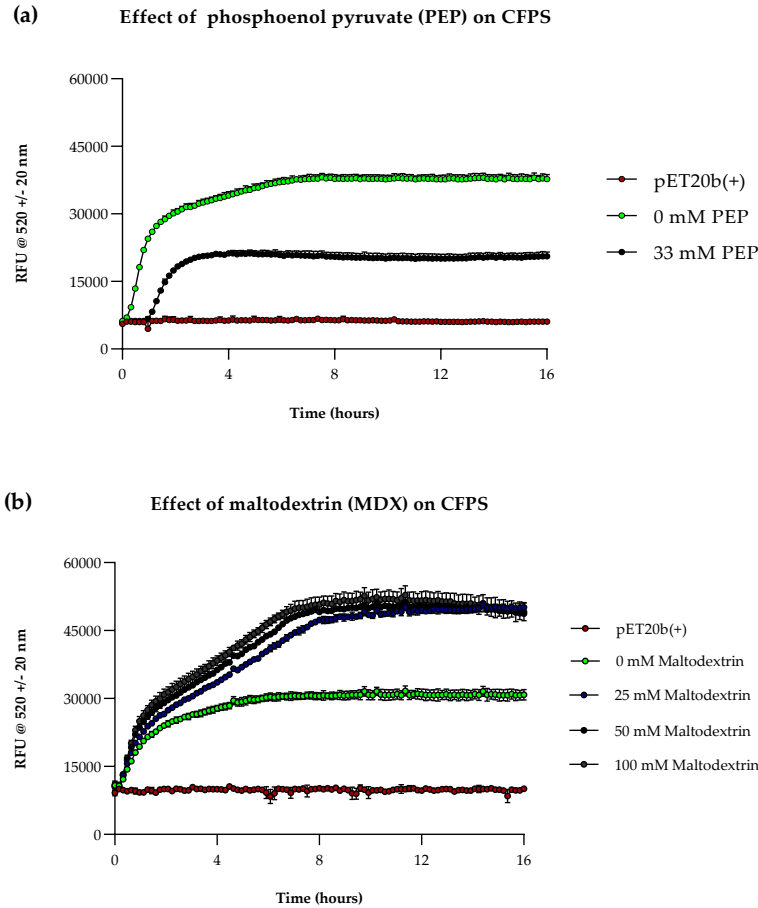


Figure 5.10: Impact of secondary energy sources on CFPS. Time course analysis showing expression of sfGFP from in-house cell-free reactions in aqueous format supplemented with (a) Phosphoenol pyruvate (PEP) and (b) Maltodextrin (MDX) compared with unsupplemented reactions (0 mM) negative control ('pET20b +') at 37°C. Experiments were performed in triplicates ($n = 3$); data are shown as mean \pm SD.

The reduction in yield with PEP supplementation remains a mystery. One theory from Wang and Zhang is that PEP, containing a high energy phosphate bond, results in the generation of inorganic phosphates which lowers the availability of Mg^{2+} ions that are critical for translation (utilisation of ATP also contributes to this)(Wang and Zhang, 2009). This theory is plausible because the opposite (increase in yield) was observed with MDX, which has a slower rate of metabolism and further utilises the inorganic phosphates generated from the primary energy source (nucleoside triphosphates). This explains the two phases seen in the MDX time courses – first exponential phase during consumption of nucleoside triphosphates and second pertaining to the metabolism of MDX. Although this not further studied in this thesis, one future work suggestion would be to further explore optimisation and combinatorial work on PEP to improve reaction yields.

5.1.3.b Maltodextrin alone does not confer stability

After the positive findings that revolved around MDX as a secondary energy source, new interest on the role of MDX in CFPS stability developed. Recently published work showed that MDX enhanced the thermostability of CFPS for 4 weeks, playing roles as both a lyoprotectant and energy source (Warfel et al., 2023). To test whether this applies to the in-house cell-free platform, a short-term stability study was devised (lyophilised pellets were used for this experiment as they are quicker to make and no significant difference was observed between this format and cellulose stacks; Figure 5.8, c & e).

Lyophilised cell-free reactions supplemented with 25 mM MDX were stored at RT for five days and later rehydrated with S30A buffer. Fluorescence readings were compared to a negative control and a positive control, which was a fresh cell-free reaction with no storage time. No significant difference in fluorescence was detected between the MDX supplemented reaction and the negative control (Figure 5.11). Regrettably, this implies that MDX did not confer any stabilising effects on lyophilised CFPS despite the yield enhancing effects seen by Warfel *et al.*, (Figure 5.10, b). Although there was a significant protective effect, the referred study did indeed see a decrease in stability in reactions with MDX compared to PEP-based reactions. In addition, all lyophilised pellets in the study were stored in vacuum sealed bags, which was reported to have additional positive effects (Warfel et al., 2023). This is simply not possible for the VITA mission as the cube requires a hermetic sealed with an internal atmospheric pressure of 1 unit. Therefore, another solution is required to mitigate challenges with room-temperature stability.

Impact of maltodextrin (MDX) on short-term CFPS stability

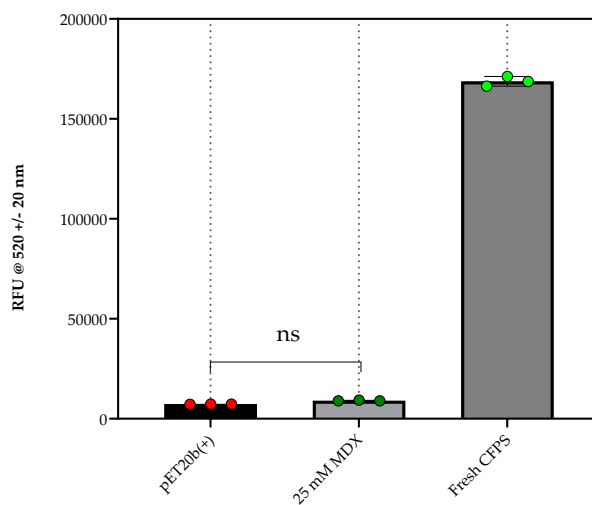


Figure 5.11: Impact of maltodextrin on short-term CFPS stability. Graph showing sfGFP fluorescence following rehydration of lyophilised cell-free pellets with S30A buffer after storage at RT for five days. Experimental sample supplemented with maltodextrin (25 mM MDX) shown alongside negative control ('pET20b+') and positive control (fresh CFPS without storage). Experiments were performed in triplicates ($n = 3$); data are shown as mean \pm SD; P value $> 0.05 = ns$.

5.1.4 From short-term to long-term stability: An iterative process

Long-term stability studies are required under standard guidelines for pharmaceutical stability testing. These are highly intensive and long studies, which will eventually need to be performed for the in-house cell-free platform. However, short-term stability experiments allow researchers to test many candidates/supplements and compare alternative formulations. This was the rationale for many experiments described in the last comprehensive section of this chapter. It narrates an iterative process of candidate identification and using process of elimination to progress these candidates from demonstrating short-term to long-term stability.

Note: Experiments discussed in this section were performed partly based on guidelines and instructions from ESA for the VITA mission's Preliminary Design Review – the approach to these preliminary experiments may appear disjointed but were critical for passing the PDR. It has been included in this thesis as the results were aligned to the on-site and on-demand platform. Thank you to Dr Nigel Savage, ESA Academy programme coordinator, for his help and guidance.

5.1.4.a Effect of sugar supplementation on short-term stability

The shelf life was found to be less than 1 week and the priority for the VITA mission remains 1 to 2 month RT stability (Section 5.1.2). Candidates for stabilisation were chosen and their impacts on cell-free kinetics were studied in Section 5.1.3. The sugars were now supplemented and their effects on stability of lyophilised pellets were studied. The experimental set up briefly entailed lyophilisation of all cell-free components (supplemented with sugars and unsupplemented reactions) and storage of the pellets at RT for 5 days (short-term), following which they were rehydrated with S30A buffer, and end-point fluorescence recordings were taken.

Four types of sugars, namely sucrose, trehalose, β -cyclodextrin, and lactose (two anomeric forms α - and β -lactose), were tested alongside a negative control, unsupplemented control and a fresh cell-free reaction (with no storage). Sucrose was chosen for testing despite significant reduction in yield (as seen in Figure 5.9, a) because some stability conferring properties were still reported in literature (Warfel et al., 2023). Interestingly, sucrose, trehalose and β -cyclodextrin supplementation did not produce a significantly higher fluorescence compared to unsupplemented reactions, although lactose had significantly higher stabilising properties (Figure 5.12; top). In fact, reactions supplemented with 100 mM β -lactose preserved 70% sfGFP fluorescence when compared to a fresh cell-free reaction without storage, indicating that it is an excellent candidate for long-term stability studies.

These results and the integrity of the produced proteins were further confirmed through western blot analysis. A band corresponding to sfGFP was detected in all supplemented reactions and this was found in the same size and position as a positive control, where no sfGFP bands were seen in the negative control (Figure 5.12, bottom). Reactions supplemented with 100 mM β -lactose produced the highest band intensity, matching the fluorescence data in the graph above. Indeed, all band intensities for other supplemented reactions also correlated to the fluorescence output, validating β -lactose as the front-running sugar supplement.

Another interesting finding was that the stabilising effect of α -lactose was significantly lower than β -lactose (Figure 5.12; top). This may be due to the fact that β -lactose is more soluble than α -lactose. Another reason could be lower reactivity of the secondary hydroxyl group in α -lactose, where there is spatial repulsion of proteins and α -lactose due to steric hindrance. Furthermore, β -lactose has been shown to demonstrate better compaction than α -lactose due to the presence of more spherical particles, rougher surfaces and a higher degree of fragmentation, which may have also played a role (Gamble et al., 2010).

Effect of sugar supplementation on short-term stability

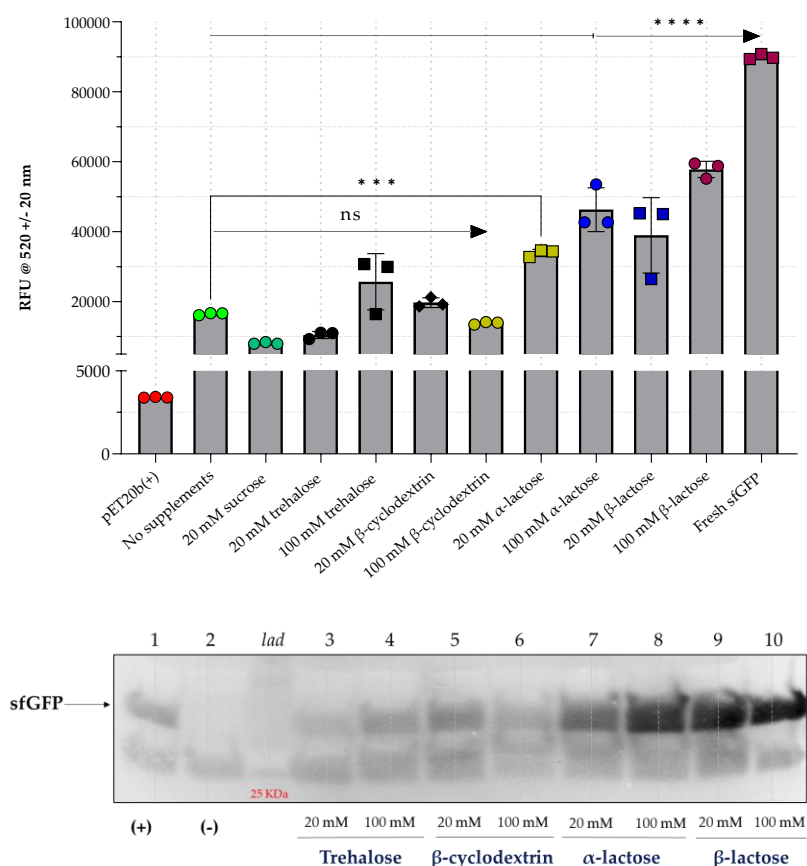


Figure 5.12: Effect of sugar supplementation on short-term stability. (Top) Graph showing sfGFP fluorescence following rehydration of lyophilised cell-free pellets with S30A buffer after storage at RT for five days. Experimental samples supplemented with various sugars shown alongside negative control ('pET20b+'), unsupplemented control ('No supplements') and a positive control (fresh CFPS without storage). Experiments were performed in triplicates ($n = 3$); data are shown as mean \pm SD; P value $> 0.05 = ns$, $P < 0.05 = *$, $P < 0.01 = **$, $P < 0.001 = ***$ and $P < 0.0001 = ****$. (Bottom) Anti-His western blot showing sfGFP bands from supplemented reactions with four sugars: trehalose, β -cyclodextrin, α / β -lactose in two concentrations: 20mM and 100 mM alongside a positive control ('+'), negative control ('-') and molecular ladder ('lad'; marked 25 kDa band). Sucrose not shown as only 20 mM concentration was tested. Protein samples had an equal fraction of each triplicate in the above graph; sfGFP band indicated by a black arrow.

5.1.4.b Visualisation and detection with VITA instrumentation

One consideration aligned with stability is whether the VITA cube can detect fluorescence proteins after storage and rehydration. So far, VITA instrumentation tests have only been performed with freshly prepared samples, hence, ESA were keen to study any changes with stored samples. There was also some interest in uncovering the margins for detection (high and low thresholds). Therefore, a few post-short-term stability samples (described in Section 5.1.4.a) were chosen for imaging and analysis through the VITA instrumentation platform.

The VITA camera was used to take images of five samples: a negative and positive control (pET20b and pure sfGFP protein), the 20 mM trehalose, 20 mM β -lactose, and 100 mM β -lactose supplemented samples from the short-term stability studies discussed above. These samples were chosen to study if the instrumentation could identify intricate changes in fluorescence as trehalose did not yield a significantly high fluorescence, but the β -lactose samples did in previous studies (Figure 5.12; top). The VITA images were analysed using ImageJ, where the intensity of the integrated area was plotted after correction with a background reading (image with no sample). The same samples were also analysed using a Nanodrop™ 3300 fluorescence spectrophotometer, serving as a tool for comparison with the newly developed VITA instrumentation platform.

Figure 5.13 shows a plot of the VITA and Nanodrop™ 3300 readings for the five samples tested (note: the VITA trend was overlaid on the Nanodrop trend to offset the differences in the light units). Firstly, the trends between the two instruments were similar and matched the images shown on the graph. Secondly, the Nanodrop was clearly more sensitive as it was able to differentiate between two samples where VITA reported no significant difference (20 mM trehalose and 20 mM β -lactose; Figure 5.13). This could partly be attributed to the ad-hoc positioning of the VITA camera over the samples as this was carried out manually. Thirdly, the Nanodrop reported more variation in the triplicates tested, whereas VITA did not (20 mM β -lactose; Figure 5.13). Overall, the VITA instrumentation and analysis fares well compared to the state-of-the-art Nanodrop™ 3300, however, the more stable the samples are, the better the VITA sensitivity. Bearing in mind that the readings were based on samples stored for five days, there needs to be a significant increase in RT stability for samples requiring storage for 1 – 2 months. It is believed that the sensitivity and resolution has further potential for improvement when the sub-system is fixed, and recordings are taken in an automated fashion.

Comparison of VITA instrumentation with the Nanodrop™ 3300

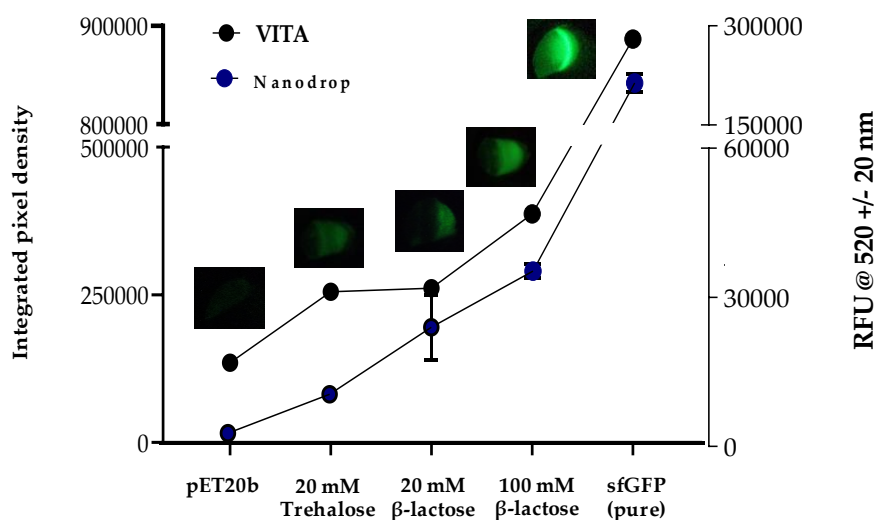


Figure 5.13: Comparison of the VITA instrumentation with the Nanodrop™ 3300 spectrophotometer. Graph showing the light/fluorescence units (integrated pixel density) from five samples analysed using two instruments: the VITA instrumentation (black data points) and the Nanodrop™ 3300 (blue data points). The five samples included a negative control (pET20b), a positive control (sfGFP; pure) and samples supplemented with 20 mM trehalose, 20 mM β -lactose and 100 mM β -lactose after five days of RT storage. The recordings are shown alongside images taken with the VITA camera; each tube contained $\sim 40 \mu\text{L}$ samples except the positive control which contained $\sim 5 \mu\text{L}$ to prevent oversaturation of signal due to high sfGFP concentration. Experiments were performed in triplicates ($n = 3$); data are shown as mean \pm SD (error bars too small if invisible); only one image shown.

5.1.4.c Design-of-Experiments approach enables identification of new formulations for short-term stability

Sugars clearly play an important role in stabilising cell-free components at room temperature and improving CFPS yields, based on observations so far. However, the role of PEG (molecular crowding agent) and the impact of altering the molecular weights of PEG is unknown. Since there are multiple input variables whose combinatorial effects are sought for study, a design-of-experiments (DoE) style-approach was undertaken for a more structured experimental design requiring fewer trials. A trial-and-error approach was undertaken thus far, and the obtained data formed the baseline data used to inform the DoE-screening plan. The experimental plan was carried out by PhD student Joshua Clark using the statistical computing software R and the Design of Experiments package (RcmdrPlugin.DoE). Relationships between, and the additive effects of, β -lactose, maltodextrin, and PEG were investigated in a two-factorial method (*e.g.* present/absent) to minimise sample size. This allowed for investigation of each additive's effects on CFPS productivity, as well as giving preliminary insight into the interactions between each factor (centre

points were not included, and randomization was done with a seed randomly generated by the program).

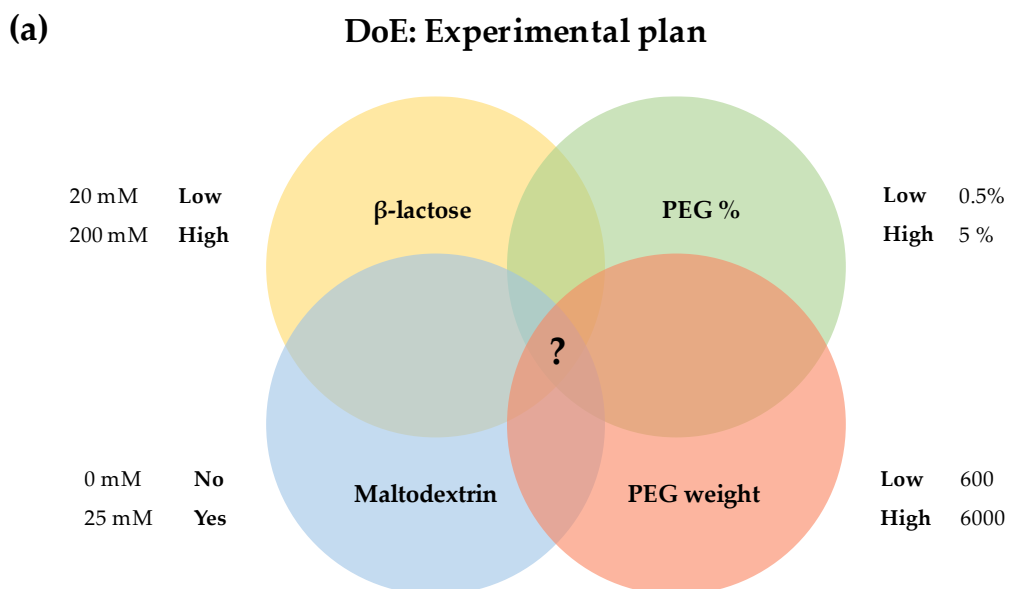
Two factors of four variables were tested, as summarised in Figure 5.14, a. Previously observed yield enhancing effects of maltodextrin (MDX; Figure 5.10, b), stability enhancing effects of β -lactose (Figure 5.12), levels of PEG (%; studied briefly in Chapter 4) and molecular weights of PEG (not studied thus far) were the four variables of interest. The two factors for these variables were low concentrations/molecular weights and high concentrations/molecular weights for β -lactose, PEG % and PEG molecular weight, and presence (25 mM) and absence (0 mM) of MDX. A ten-fold difference was chosen between the low and high concentrations/molecular weights; although this may seem quite high, it offers a broad window for initial studies following which further refinements can be carried out if a significant trend is observed.

The reason for choosing a presence-absence setting of MDX rather than low/high concentrations is because there was already evidence to suggest that MDX alone does not enhance stability (Figure 5.11). Furthermore, one main research question (also raised by ESA) was whether the stabilising effect of lactose could be combined with the yield increasing effects of MDX to produce highly fluorescent reactions that could be readily detected using the VITA platform. The short-term stability studies indeed confirmed that lactose and MDX have favourable combinatorial effects (Figure 5.14, b). In fact, two formulations even exceeded the fluorescence generated from a fresh aqueous CFPS reactions (grey line, Figure 5.14, b). A common pattern in these two formulations were the presence of both β -lactose and MDX, however, this effect was reversed in reactions in the presence of MDX and higher concentrations of β -lactose. This indicates that 25 mM MDX and 20 mM β -lactose greatly enhances yield and stability of lyophilised CFPS.

The impact of PEG levels and their molecular weights was less clear – the two best formulations had differing concentrations and molecular weights of PEG (Figure 5.14, b). There was no significant difference observed with changes to PEG MW and PEG concentration. Based on this initial observation, it may appear that these variables do not play a critical role in improving stability, however, a more detailed experimental plan based on these initial observations could reveal insights that may currently be hidden. Having said that, it is apparent that PEG alone does not offer protective effects, as reactions in the presence of PEG but absence of MDX did not yield adequate fluorescence, regardless of high/low concentrations of β -lactose.

Overall, this has been a fruitful venture, as two new formulations were identified whereby fluorescence after storage at RT for five days was higher than a fresh CFPS reaction in aqueous format. The main characteristics of the newly identified

formulations were the presence of MDX at 25 mM, presence of β -lactose at 20 mM and variable levels and molecular weights of PEG. The highest mean fluorescence was obtained from reactions containing 25 mM MDX, 20 mM β -lactose and 5% 6000 kDa PEG.



(b) **DoE: Short-term stability studies**

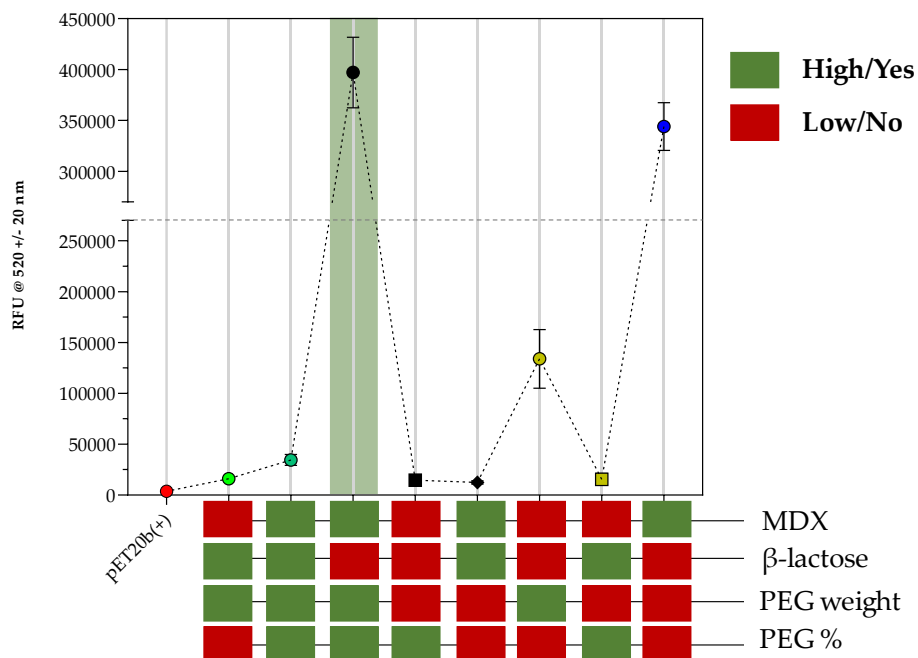


Figure 5.14: Design of experiments approach for improving stability of lyophilised CFPS. (a) Image summarising the four variables: β -lactose, maltodextrin, PEG concentration (%) and PEG molecular weight (kDa), and two factors: High/Low or Yes/No (presence/absence). Question mark ('?') indicates an unknown formulation to be

identified for stability enhancement. (b) Graph showing sfGFP fluorescence following rehydration of lyophilised cell-free pellets with S30A buffer after storage at RT for five days. Experimental samples were supplemented with the variables shown below the data points marked in green blocks (high concentrations or presence of MDX) and red blocks (low concentrations and absence of MDX). 'pET20b+' corresponds to the negative control, and the positive control (fresh CFPS in aqueous format without storage) is indicated by the grey dotted line (at RFU 27,5000). Green bar on the graph highlights the highest mean fluorescence obtained, in comparison to the positive control. Experiments were performed in triplicates ($n = 3$); data are shown as mean \pm SD.

The formulation with the highest mean fluorescence was chosen for longer-term studies, for submission to ESA as part of the preliminary design review data pack, but also to study if the promising results observed in the short-term studies could be prolonged. It should be noted that although 'long-term stability studies' are typically conducted for 6 months to 1 year in the pharmaceutical industry, long-term studies refer to studies conducted > 1 month in this thesis, for purposes of distinction to the short-term studies that were conducted for 5 days. Furthermore, the VITA mission refers 1 to 2 month stability as long-term stability, as detailed in the concept of operations.

The experimental set-up for the long-term stability study was quite similar to the short-term studies, with the exception of several samples prepared for timed data points up to 2 months. The experimental samples contained 25 mM MDX, 20 mM β -lactose and 5% 6000 kDa PEG and this was tested alongside an unsupplemented sample and a negative control. Positively, a highly fluorescent signal was observed in the supplemented reactions, and this was sustained from day 0 to day 28 (~ 1 month; Figure 5.15). This result indicates that 100% stability was achieved for 1 month. A contrasting observation in the unsupplemented reactions agreed with previously discussed sharp drop in signal (Figure 5.8, e). Unfortunately, a 50% decrease in fluorescence was observed in supplemented reactions between days 28 and 42. However, the signal at day 42 was not dissimilar to that of the unsupplemented reaction on day 0 (no significant difference according to Šídák's multiple comparisons statistical test). This confirms that this signal is still above the VITA detection threshold (Figure 5.13). Although there was a significant sfGFP signal on day 56 (\sim month 2) over the negative control, there was a 90% reduction in signal from month 1 which was too low for VITA detection.

Long-term stability studies (lyophilised pellets at RT)

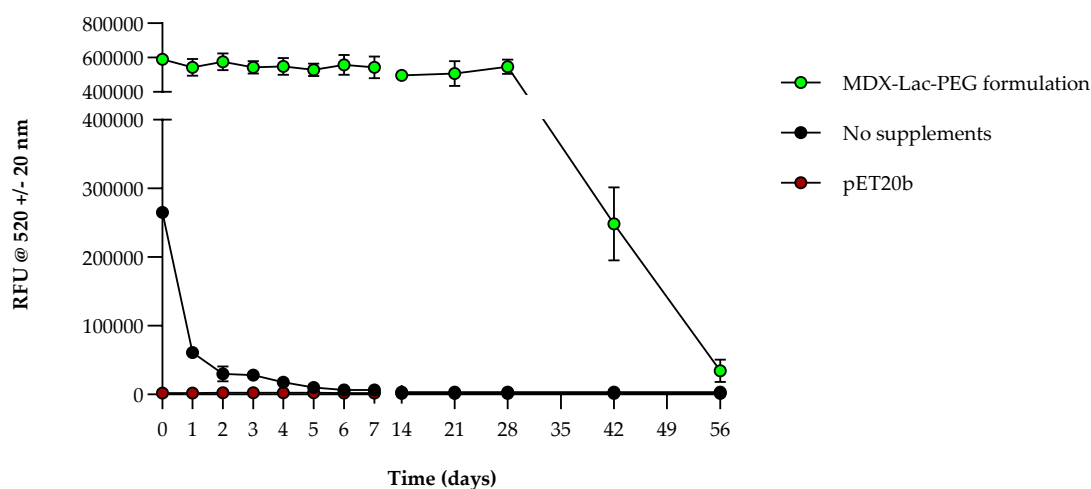


Figure 5.15: Long term stability studies using newly identified supplements. Graph showing sfGFP fluorescence following rehydration of cell-free components in lyophilised pellets format after storage for upto 2 months at room temperature with data points shown for the first 7 days and every week or bi-weekly from then on. All CFPS reactions were rehydrated with S30A buffer; green data points correspond to reactions supplemented with 25 mM MDX, 20 mM β -lactose and 5% 6000 kDa PEG, black data points correspond to unsupplemented reactions and red data points indicate the pET20b negative control. Experiments were performed in triplicates ($n = 3$); data are shown as mean \pm SD.

The above results have dramatically increased the stability of in-house cell-free components from < 1 week to 1+ months, which offers a promising solution for the VITA payload and mission. Without storage under vacuum conditions, this formulation has been shown to remain fully stable for at least a month at room temperature, offering an ideal cold-storage free solution to the on-site, on-demand platform. There is, however, still much room for improvement as components have previously been shown to be stable up to a year using the commercial PURExpress system composed of purified proteins and up to 3 months for crude extract (typically bacterial) sources such as the in-house system (Smith et al., 2014, Pardee et al., 2014, Karig et al., 2017).

Further improvements in stability could be made by executing a more detailed DoE with the above results as a baseline. Given a generous sample size, a multi-factorial approach could be undertaken to cover a better range of concentrations, especially for MDX since only 'presence or absence' was tested. Secondly, more sugars could be tested in combination with MDX. Lastly, the role of PEG and its sizes need to be unravelled. Alternatively, other molecular crowding agents such as trimethylglycine could be incorporated in the new, extensive DoEs. Given that there is some baseline data already available for trimethylglycine (Figure 5.9, c), it was not considered in this work due to lack of time, but certainly would make an ideal candidate for future studies.

5.2 Summary

This chapter first introduced the VITA mission, its timeline for operations and the basic hardware for the science units that house the cellulose stacks. The first aim was to demonstrate the ability to detect fluorescent proteins through fluorescent spectroscopy and imaging, following rehydration of the cell-free components inside the cube in an automated manner. This was successfully shown by using cameras to image end-point cell-free reactions expressing sfGFP in both aqueous formats and on cellulose stacks. Furthermore, time course analysis was successfully able to capture the CFPS trend for four hours using a teleoperated set-up. Lastly, the effect of lowering the reaction temperature to 30°C and the reaction volumes to up to 250 μ L were studied with no significant impact on CFPS and on the mission.

The focus next shifted to the scientific payload and its integrity over time, in order to ensure viability from payload integration to arrival on the ISS. The shelf-life of the in-house cell-free system was found to be less than one week, through accelerated stability studies, in both lyophilised pellets and cellulose stack formats. In an effort to increase this to at least 1 to 2 months, supplements were chosen and their effects on CFPS kinetics were first studied. Then, short-term stability studies were performed, where some candidates such as β -lactose enhanced stability after storage for five days. Next, the role of secondary energy sources such as PEP and maltodextrin was studied. Maltodextrin significantly enhanced CFPS yields but failed to aid short-term stability. Based on these findings, a design-of-experiments style approach was pursued, where combinations of maltodextrin, β -lactose, and PEG (various concentrations and molecular weights) were tested for short-term stability. Two formulations outperformed even an unsupplemented fresh CFPS reaction in aqueous phase. The best identified formulation for supplemented CFPS was found to contain: 25 mM MDX, 20 mM β -lactose and 5% 6000 kDa PEG. This formulation demonstrated 100% RT stability for up to 28 days in a longer-term stability study. Although the stability plummeted to 50% by Day 42, this still provided a high fluorescence signal (same signal as unsupplemented CFPS) for detection in the VITA mission; most stability was lost by Day 56. In conclusion, the shelf-life of the in-house formulated system currently stands at 1 month. The system can still be utilised until 1.5 months with 50% activity remaining.

Collectively these results enhanced the shelf-life of the VITA cell-free components to enable preservation at room temperature (1.5 months from integration, launch and transit to the ISS). Ideally, the stability should be further enhanced for an additional month or two to account for any rocket launch delays. By doing so, a platform with 3-month stability would also be available for any earth-based applications for the on-site and on-demand platform. In this case, further stability studies should be

conducted at a wider range of temperatures (0°C – 50°C) to cover the temperatures that are commonly experienced on earth. Furthermore, temperature exposure studies could be performed to understand how the system behaves during temperature fluctuations.

Chapter 6 Towards obtaining functional and pure therapeutics from cell-free systems

6.1 Introduction

Chromogenic proteins are ideal for sensing applications, which is why they are often chosen for synthetic biology projects involving biosensing. sfGFP detection has been instrumental in understanding the science behind CFPS and has been the protein product-of-choice for many cell-free biosensors in the past (Pardee et al., 2014, Gräwe et al., 2019, Voyvodic et al., 2019). In this project so far, sfGFP was not only used for the development and optimisation of the in-house system, but also for calculating and extending its shelf-life. It mainly served as a model protein for other protein therapeutics that have applications in low resource/extreme environments. For the first time in this work, therapeutic protein expression was explored and reported in this chapter.

Given that these protein-based products are intended for human administration, several considerations need to be made, starting from purity. Affinity chromatography and size exclusion chromatography are perhaps the most commonly utilised methods for purification of biopharmaceuticals, but not much work has been published on purification of cell-free products. The challenges of protein purification for point-of-care applications are many and are well reviewed elsewhere (Thole et al., 2022). Therefore, innovative cell-free expression and purification methods are starting to be published only recently (DeWinter et al., 2023). This chapter initially discusses some mainstream purification experiments for analysing the structure and function of cell-free products (one chromogenic control and one therapeutic) and further explores tertiary and secondary structure analysis.

On a different note, there was significant interest in two-in-one protein purification principles due to the mass, energy and storage constraints on the on-site and on-demand system. Hence, an idea to exploit 'Nanobodies' as a purification and quality control tool was conceived. Nanobodies are single domain antibodies that are small, recognise and bind to target antigens (*i.e.* therapeutic proteins in this case) (Dmitriev et al., 2016). Therefore, co-expression of the therapeutic protein and the corresponding nanobody was investigated – co-expression has been performed in cell-based systems, but is interesting in cell-free reactions for many reasons. First, it allows synthesis of more than one product at a time for therapeutic applications (*e.g.* personalised medications). Secondly, it allows for production of complexes, thereby increasing the portfolio of biomolecules that can be synthesised in a cell-free manner.

Lastly, it introduces the possibility of expressing proteins that may interact with one another, which could be exploited for many more applications such as protein pulldown/purification. Due to its potential to serve as a versatile tool for cell-free applications, this was a final idea that was explored in this chapter.

This chapter details multiple experiments that were pursued from various ideas which could, in their own right, be an independent project. Even though they might not all link together, each subject contains immense potential that is further discussed in the future work section in the next chapter and due to restrictions in time, some ideas could not be pursued until completion.

The broad aims for this chapter are –

- (a) Demonstrate the expression of model therapeutic proteins in the in-house cell-free system based on constructs that were developed in Chapter 3, and troubleshoot if and when necessary.

- (b) Experiment with ideas for *in situ* purification and quality control for on-site and on-demand applications of the cell-free system for obtaining regulatory approval.
 - a. Test co-expression of proteins in the cell-free system, enabling a Nanobody-driven approach as a dual purification and quality control operation.

6.2 Results and discussion

6.2.1 Cell-free expression of therapeutic proteins

As discussed in Chapter 1 (Introduction), five therapeutic proteins were chosen for on-site, on-demand applications based on their importance for human health and their need in low resource/extreme environments. The five proteins were reteplase, entolimod, granulocyte-colony stimulating factor (G-CSF), alfimeprase, and teriparatide. They form a diverse cohort of therapeutic proteins varying broadly in size and number of disulfide bonds, but do not require any other complex post-translational modifications (Table 1.3, Chapter 1)

6.2.1.a Successful detection of therapeutic protein expression in the PURExpress system

In Chapter 4, the NEB PURExpress system was first used to monitor cell-free sfGFP expression prior to the development of the in-house system. Similarly, it was used once again to detect the expression of the five therapeutic protein constructs prior to in-house tests. Since the therapeutic proteins are not chromogenic, detection was carried out through SDS-Page analysis of end-point cell-free reactions.

Four out of the five proteins were easily visible on the SDS-Page gel, with teriparatide, the exception, detected with some uncertainty due to its low size (Figure 6.1). This is perhaps the first reported synthesis of some of the five protein therapeutics in a cell-free system. Cell-free synthesis of tissue plasminogen activator (of which reteplase is a truncated form) has been shown previously (Yang et al., 2019). Unfortunately, further western blot (anti-His) analysis could not be performed because all proteins in the PURExpress are also His-tagged.

Cell-free expression of therapeutic proteins in the PURExpress system

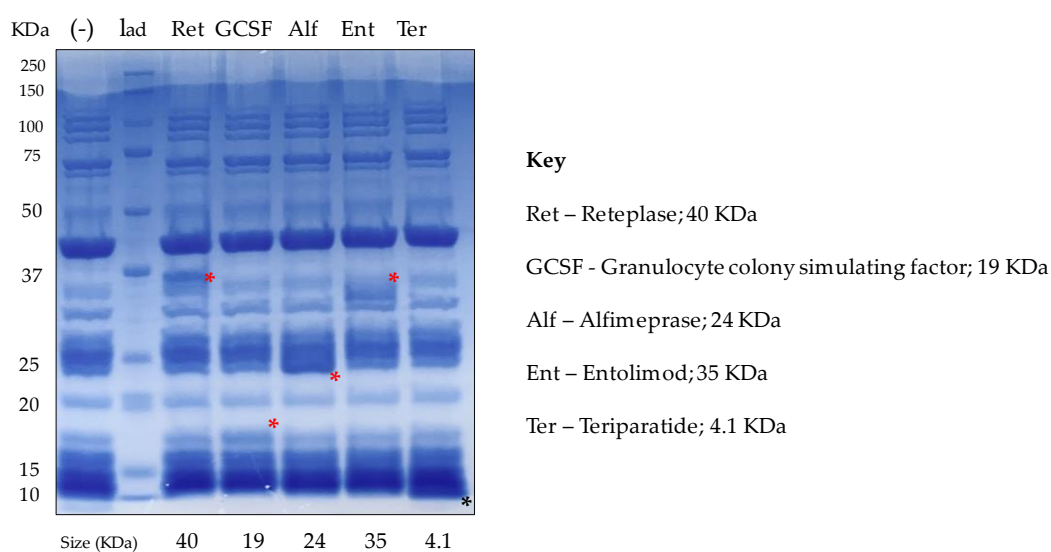


Figure 6.1: Cell-free expression of therapeutic proteins using the NEB PURExpress system. SDS-Page showing proteins separated based on size in five samples expressing reteplase, G-CSF, alfimeprase, entolimod, and teriparatide alongside a negative control ('-') and protein ladder ('lad'). The expected sizes of the five proteins are provided below and bands are marked with a red asterisk where known; teriparatide band marked with black asterisk due to uncertainty and low size.

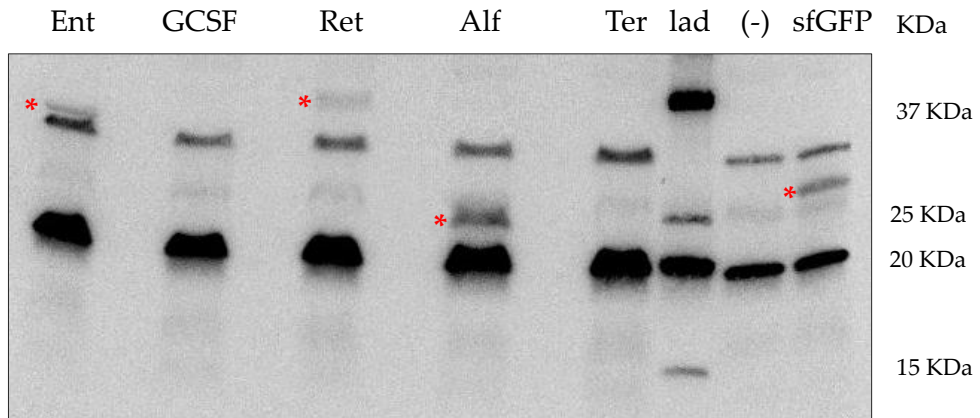
6.2.1.b Successful detection of most therapeutic proteins in the in-house cell-free system

The ability of the in-house cell-free system to express proteins other than sfGFP was tested for the first time in this section. All five therapeutic constructs were added to in-house cell-free mix (all experiments were performed in aqueous format). This time,

a western blot was chosen for detection of cell-free produced His-tagged proteins since all other proteins in the cell-free extract were derived from crude bacterial lysate, unlike PURExpress. Anti-His western blot revealed expression of three therapeutic proteins, namely entolimod, reteplase, and alfineprase, but no bands were detected in the samples that contained DNA coding for G-CSF and teriparatide (full gel not shown below, however, no bands were detected lower than 15 kDa; Figure 6.2, a). Considering that expression was detected for these proteins in the PURExpress system (Figure 6.1), the in-house cell-free extract may be preventing production of these proteins.

The NEB PURExpress kit contains disulfide bond enhancing supplements that can be added to PURExpress reactions targeted to express proteins with multiple disulfide bonds. The kit instructions specify that the supplement contributes to higher level expression of soluble disulfide bonded proteins; to test this, in-house cell-free reactions were supplemented and compared to previously tested unsupplemented reactions. Western blot analysis confirmed that supplementation of disulfide bond enhancers did not enable production of G-CSF nor teriparatide (full gel not shown below, however, no bands were detected lower than 15 kDa; Figure 6.2, b). Furthermore, similar bands for entolimod, reteplase and alfineprase were detected as seen in the unsupplemented reactions, with no notable increase in band intensities (Figure 6.2). Therefore, the disulfide bond enhancers did not improve production in the in-house system. It is difficult to form any hypotheses or theories in this case as the enhancers are a proprietary formulation of proteins in buffer (based on an additional band observed on the supplemented blot; Figure 6.2 b). The cell-free extract is derived from the reducing environment in the bacterial cytoplasm and it is currently unknown whether the enhancers change this environment in the cell-free reactions. Although no other firm conclusions can be drawn based on this information and results, production of entolimod, reteplase and alfineprase was successfully shown.

(a) In-house cell-free synthesis of therapeutics



(b) Disulphide bond enhancers do not aid expression

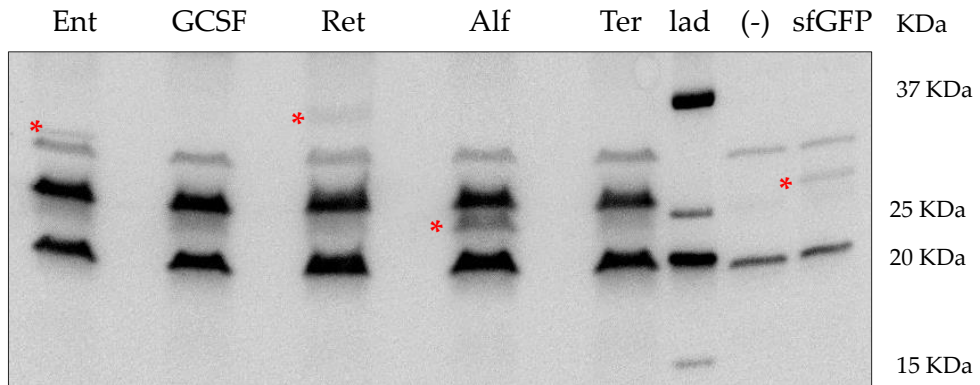


Figure 6.2: In-house cell-free expression of therapeutic proteins. (a) Anti-His western blot showing five protein samples expressing entolimod (Ent), granulocyte-colony stimulating factor (G-CSF), reteplase (Ret), alfineprase (Alf), and teriparatide (Ter) alongside a negative control ('-'), known sample (sfGFP) and protein ladder ('lad'). 10 μ L protein loaded in each lane. Where present, proteins of interest were marked with a red asterisk (*); ladder sizes have been provided on the right. (b) Same as (a), but samples were supplemented with disulfide bond enhancers (provided in the PURExpress NEB kit), which are also His-tagged (bands seen in all samples around 25 kDa).

6.2.1.c RT-qPCR analysis: mRNA levels provide insights into lack of G-CSF and Teriparatide expression

The absence of G-CSF and teriparatide bands in the western blot (Figure 6.2, a) could be explained in two ways: degradation took place soon after expression, or, no expression took place. Western blots and SDS-Page gels typically allow signs of degradation such as smearing of samples or fragmented, low-migrating bands to be seen, which was not the case in Figure 6.2. For the latter suspicion, one method to obtain insight into the absence of expression would be to study mRNA levels. CFPS is driven by transcription of DNA template into mRNA which is subsequently translated into protein-of-interest, so mRNA translation is a prerequisite for protein

production. Hence, the hypothesis was that the absence of protein production is a result of absence of mRNA expression.

In order to test this hypothesis, a qualitative RT-qPCR experiment was planned with the following set-up: cell-free reactions were first performed with the therapeutic DNA templates alongside a negative control (pET20b; no expression) and a positive control (sfGFP; known expression). After reaction completion, mRNA was isolated from the reactions and reverse transcribed to obtain cDNA (complementary DNA). Here, samples without reverse transcriptase were also prepared as additional controls, which are instrumental to account for any background qPCR amplification from the DNA templates or any non-specific primer binding. Using specifically designed primers and DNA-binding dyes, the amplification of the cDNA copies was quantified to obtain indirect information about starting mRNA levels.

The traditional metric used for analysing real-time PCR data is the cycle threshold value, which is the cycle number at which the fluorescent signal (from double stranded DNA) exceeds a certain background signal. Cycle threshold values are inversely proportional to the amount of starting material (in this case, mRNA derived cDNA). Typically, values ≤ 20 indicate abundance and values > 30 indicate a weak presence of starting material (Notarangelo et al., 2021, Waudby-West et al., 2021). When cycle threshold values were compared for the various therapeutic templates, significantly low values were found for all five therapeutics (Figure 6.1, a). This indicates the presence of good levels of mRNA in all cell-free reactions with therapeutic templates. Surprisingly, high values were recorded for sfGFP templates which was unexpected as high-level expression of sfGFP was found in all previous studies (Chapters 4 and 5). However, a high cycle threshold for pET20b was found, as expected, as the template does not contribute to any expression.

Additionally, it was important to study any differences between samples that underwent reverse transcription versus those that did not, to account for amplification from any background templates such as the plasmid DNA itself. The experimental set-up included a DNA wipeout step that in theory should eliminate all genetic material except RNA, however this is inefficient. As a result, amplification was still reported in samples without reverse transcriptase (Figure 6.3, a; red data points). Nevertheless, therapeutic samples that were reverse transcribed had a significantly lower cycle threshold, indicating higher amounts of starting material in the form of mRNA. All observations were also visually confirmed through agarose gel electrophoresis, where all five therapeutic samples treated with reverse transcriptase produced brighter bands (Figure 6.3, b). The sfGFP cycle threshold values remain a mystery; high cycle threshold values were seen despite protein production and no significant difference was reported between the two sample

conditions, due to unknown reasons. No predominant bands pertaining to sfGFP were detected on the agarose gel either, hence, the only possibility that remains is a failure of RNA isolation and further experimentation is required to draw firm conclusions.

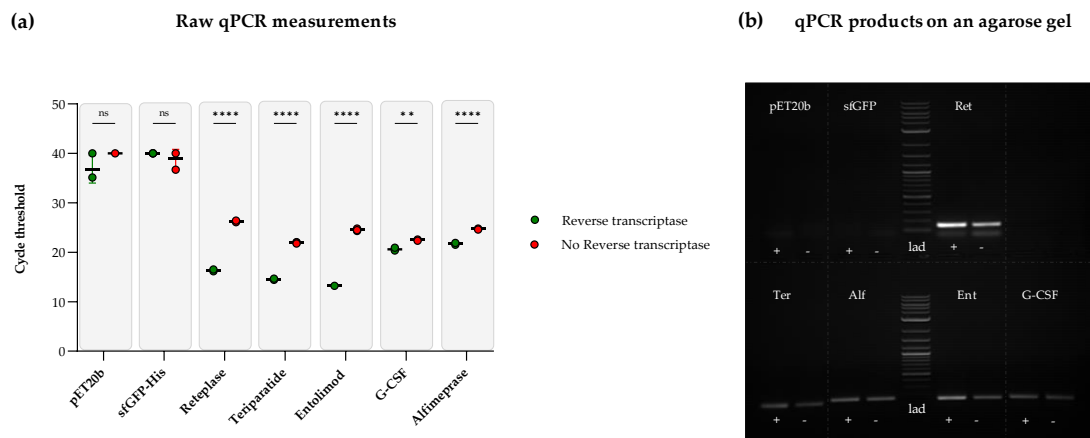


Figure 6.3: Qualitative RT-qPCR analyses provides insights into cell-free mRNA levels. (a) A plot of cycle threshold values obtained by amplifying cDNA from reverse transcribed (green data points) and non-reverse transcribed mRNA (red data points) from end-point cell-free reactions. Experiments were performed in triplicates ($n = 3$); data are shown as mean \pm SD; Unpaired t -test was performed to compare means; P value $> 0.05 = ns$, $P < 0.05 = *$, $P < 0.01 = **$, $P < 0.001 = ***$ and $P < 0.0001 = ****$. (b) 1% agarose gel loaded with amplified qPCR reactions shown in (a), alongside molecular ladder ('lad'); samples with highest cycle threshold values for reverse transcribed ('+') and non-reverse transcribed ('-') conditions were loaded onto the gel.

Despite the positive control not behaving as expected, good levels of all five therapeutic mRNAs were found in the cell-free samples. Hence, the fact that production of G-CSF and teriparatide was not detected (in Section 6.2.1.b) is perhaps not due to a failure of transcription, rather mRNA translation. Degradation of mRNA is not an uncommon problem in CFPS; however, it is unlikely to be the reason for lack of production, as production of other proteins have been successfully shown. G-CSF and teriparatide are the smallest in size out of the five (19 kDa and 4.1 kDa, respectively), hence, this could be a contributing factor for no/low production in bacterial extracts. In fact, this kind of behaviour has been reported for cell-free systems in literature before. A change in strain or addition of a fusion tag has been reported to solve this issue, *e.g.* 'SUMO fusion tag' which was shown to improve production and solubility of target proteins (DeWinter et al., 2023, Meng et al., 2023).. In conclusion, more strategies need to be considered for production of more protein therapeutics. Although the fusion tag strategy was not progressed in this work, it would be an excellent starting point for expression of G-CSF and teriparatide.

6.2.2 Purification of cell-free products

This section describes the purification of two main proteins: sfGFP (fluorescent protein) and reteplase (therapeutic protein) for structural and functional experiments later discussed in this chapter. Both proteins contained a C-terminal histidine tag that was utilised for either bead-based (Ni^{2+} charged beads) or Ni-NTA column-based purification following cell-free synthesis. The histidine tag was also utilised for detecting the two proteins on a western blot by probing with anti-His antibody.

6.2.2.a Purification of cell-free expressed sfGFP and reteplase at 37°C and 32°C

Reteplase is a fairly complex and large protein, and it is well-known that lowering the cell culture temperature aids higher levels of more soluble protein, in cell-based batch cultures (Schein, 1989, Sadeghi et al., 2011). Hence, one aim that was addressed here was the effect of lowering cell-free reaction temperature to 32°C from 37°C. Another aim was to purify reteplase and sfGFP for future studies, hence cell-free reactions (totalling a volume of 400 μL) coding for sfGFP and reteplase each were prepared for expression at both 32°C and 37°C and subsequently purified using a histidine tag pulldown method facilitated by magnetic Ni-NTA beads.

Reteplase and sfGFP were successfully purified and this was confirmed through SDS-Page and western blot analysis (Figure 6.4). The bands for sfGFP in cell-free reactions and hence total concentration after purification was significantly higher than that of reteplase (Figure 6.4, b vs. d), perhaps owing to reteplase's higher size and complexity. Most interestingly, reteplase expression was significantly higher at 32°C than 37°C which was clear on the western blot, but not on SDS-Page due to low yields (Figure 6.4, d). No such difference was observed for sfGFP (Figure 6.4, b).

The results indicate that lowering the temperature of cell-free reactions may contribute to better expression of soluble proteins, which is particularly important for proteins intended for therapeutic applications. Lowering reaction temperature (for bacterial cell extracts) is not a parameter that has been investigated thoroughly in literature, and this suggests that optimisation of cell-free reaction conditions will be necessary for efficient synthesis of a wide range of proteins, similar to the optimisation that is typically carried out in cell-based methods.

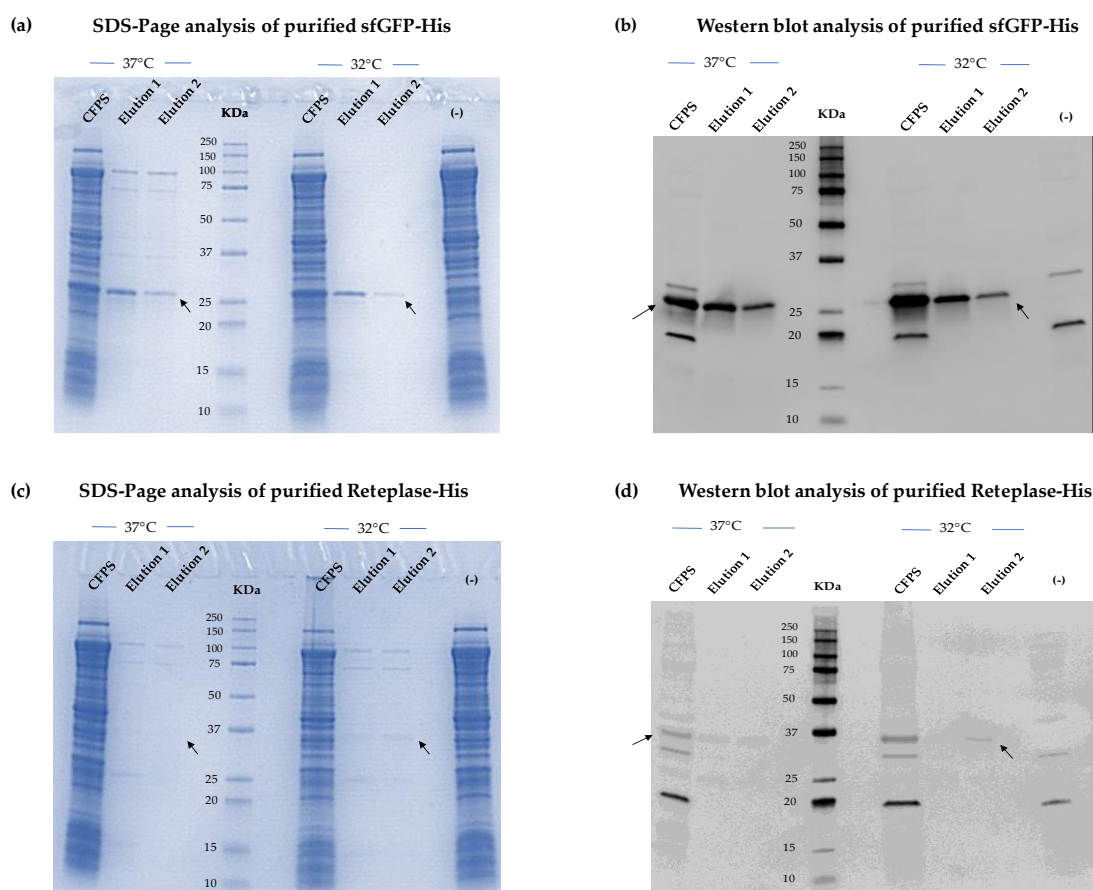


Figure 6.4: Purification of cell-free expressed sfGFP and Reteplase-His. (a) SDS-Page of various fractions collected during the purification of sfGFP-His following cell-free synthesis at 37°C and 32°C, alongside negative control ('-') and protein ladder, (b) Anti-His western blot of various fractions collected during the purification of sfGFP-His following cell-free synthesis at 37°C and 32°C, alongside negative control ('-') and protein ladder, (c) SDS-Page of various fractions collected during the purification of reteplase-His following cell-free synthesis at 37°C and 32°C, alongside negative control ('-') and protein ladder, (d) Anti-His western blot of various fractions collected during the purification of reteplase-His following cell-free synthesis at 37°C and 32°C, alongside negative control ('-') and protein ladder.

6.2.2.b Fluorescence standard curve

The chromogenic nature of sfGFP was exploited yet again, to enable estimations of protein yields from CFPS. Purified sfGFP described in the previous section was utilised to produce a standard curve (fluorescence against protein concentration) that allows extrapolation of protein yields from fluorescence signals. Dilutions of purified sfGFP (Section 6.2.2.a) were made, fluorescence intensities were measured using a Nanodrop™ 3300 and protein concentration was determined through a DC assay for the same samples. Thus, obtained values were plotted to obtain a concentration versus fluorescence standard curve (Figure 6.5, a & b). The Nanodrop detection threshold was reached at 2.5 mg/mL sfGFP concentration, beyond which dilution will need to be made (Figure 6.5, b). The concentration of the purified sfGFP protein was found to be ~ 3.7 mg/mL (Table 6.1).

Table 6.1: Extrapolation of pure sfGFP protein concentration from DC assay standard curve

Absorbance (750 nm)	Dilution factor	Total concentration (mg/mL)
0.1346 0.135 0.1351	5	3.678 ± 0.007

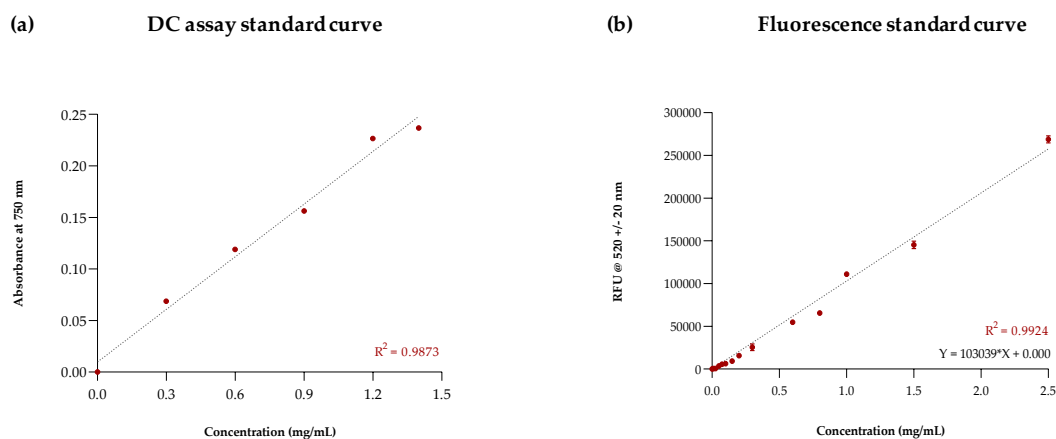


Figure 6.5: Cell-free protein yield determination. (a) Standard curve of bovine serum albumin protein concentrations and absorbance at 750 nm from which pure sfGFP concentrations were extrapolated. R^2 value indicates the goodness of fit for the linear regression performed to extrapolate unknown sfGFP protein concentrations ($R^2 = 1$ indicates that regression fitted data perfectly); (b) Standard curve of pure sfGFP protein concentrations [extrapolated from standard curve shown in (a)] and corresponding fluorescence signals. Line equation and goodness of fit (R^2) provided on the graph; Experiments were performed in triplicates ($n = 3$); data are shown as mean \pm SD.

Standard curves serve as a tool for estimating protein concentrations and are typically based on BCA assay data. Their usefulness and relative accuracy have been expanded for yield analyses in cell-free studies for fluorescent proteins like sfGFP (Wiegand et al., 2018, Au - Levine et al., 2019). In a similar initiative, protein yields were estimated for selected in-house cell-free experiments, as summarised in Table 6.2. Obvious differences were observed due to supplementation with maltodextrin or lactose in some samples, for example or due to samples being lyophilised or stored in a different format. Evidently, other large variations in yield were primarily thought to be due to batch-batch variation, which is a well-known disadvantage in CFPS (Hunter et al., 2018, Cole et al., 2019). Moreover, some discrepancy may arise from estimating sfGFP concentrations in crude cell-free reactions based on standard curves obtained from purified protein, although fluorescence intensities were normalised to a negative control to account for any background fluorescence. Although batch-batch variation was not further studied in this thesis, some methods and studies could be referred to for future work (Banks et al., 2022).

Table 6.2: Example estimates of yields from previous experiments. Concentrations were extrapolated from standard curve shown in Figure 6.5, b and yield was calculated based on reaction volume. Examples from commercial systems and other research groups are provided for comparison.

Experiment reference	Mean sfGFP fluorescence	Reaction volume (μL)	Protein yield (mg/mL)
Figure 4.13 Fresh CFPS	492928.6 ± 95367.17 RFUs	50	0.84
Figure 4.13 Lyophilised CFPS	166630.7 ± 2132.66 RFUs	40	1.617
Figure 5.14 Highest DoE formulation	393717.1 ± 34610.59 RFUs	50	3.821
Figure 5.15 Month 1 stability sample	544487.6 ± 42703.17 RFUs	40	5.285
Commercial: PURExpress	Reported by manufacturer		≥ 0.5
(Des Soye et al., 2019) Michael Jewett group	Reported on a Cell Chemical Biology paper		2.67

6.2.3 Structural and functional studies of cell-free synthesised proteins

So far, expression of therapeutic proteins reteplase, entolimod and alfineprase was successfully shown, and reteplase was further purified by leveraging the C-terminal His-tag. The next step was to assess the structure and function of cell-free produced proteins to further assess their suitability for therapeutic applications. Reteplase was chosen as an ideal primary candidate for such studies for several reasons: in-house expression, and purification was shown previously. Additionally, it is one of the more complex proteins, composed of nine disulfide bonds, and also the highest in size making it a fairly ambitious target. Lastly, provided functionality is shown, relatively simple activity assays could be performed to validate thrombolytic action. Hence, reteplase, along with sfGFP (a known functional protein) were the two main proteins studied in this section.

6.2.3.a Tertiary and quaternary structure analysis

Disulfide bond formation is important for the function of reteplase (Zhuo et al., 2014). Although sfGFP does not contain any native disulfide bridges, there is a small possibility for two cysteine residues in the protein background to interact with one another, leading to unknown/new structure formation (Aronson et al., 2011). The state of disulfide bond formation in cell-free synthesised and purified reteplase and sfGFP (cell-free and cell-based sources) was studied through non-reducing SDS-Page and native-Page analysis.

It was hypothesized that cell-free-synthesised reteplase formed some/all disulfide bonds and hence would produce a band shift on a protein gel when compared under reducing and non-reducing/native conditions. The native-Page gel first revealed many bands for both reteplase and sfGFP, which indicates the presence of protein in many sizes, or the presence of contaminants (Figure 6.6, a). Three faint bands were observed for reteplase, which indicates a fragmented protein fraction; this may correspond to a complete protein (highest band) and two fragmented domains (kringle 2 and serine protease domains further below); this pattern has been documented previously (Ma et al., 2019, Izadi et al., 2021). Interestingly, two bands were seen for sfGFP from both cell-based and cell-free sources on the native-Page gel. Both bands produced fluorescence when the gel was exposed to blue light, indicating that both bands correspond to sfGFP, perhaps a result of dimerization.

Both reducing and non-reducing fractions of reteplase were identical with no shift observed, which indicates that no disulfide bonds were formed whatsoever (Figure 6.6, b). Multiple bands were observed further confirming the protein fragmentation intuition. Many other high and low migrating bands indicate protein aggregation and/or degradation or low sample purity. Interestingly, reduced and non-reduced sfGFP samples produced a different gel pattern (Figure 6.6, b). The reduced samples only produced one predominant band at ~ 25 kDa whereas the non-reduced samples also produced other high-migrating bands; similar to the native and fluorescent gel, this may correspond to dimers or trimers. Collectively, functionality of sfGFP was confirmed on the protein gels, because structurally and functionally active protein is a prerequisite for fluorescence. However, there is low confidence of the same for reteplase. The results reported here are not sufficient to proceed with activity assays for functionality tests, however, secondary structure analysis was pursued for more insight.

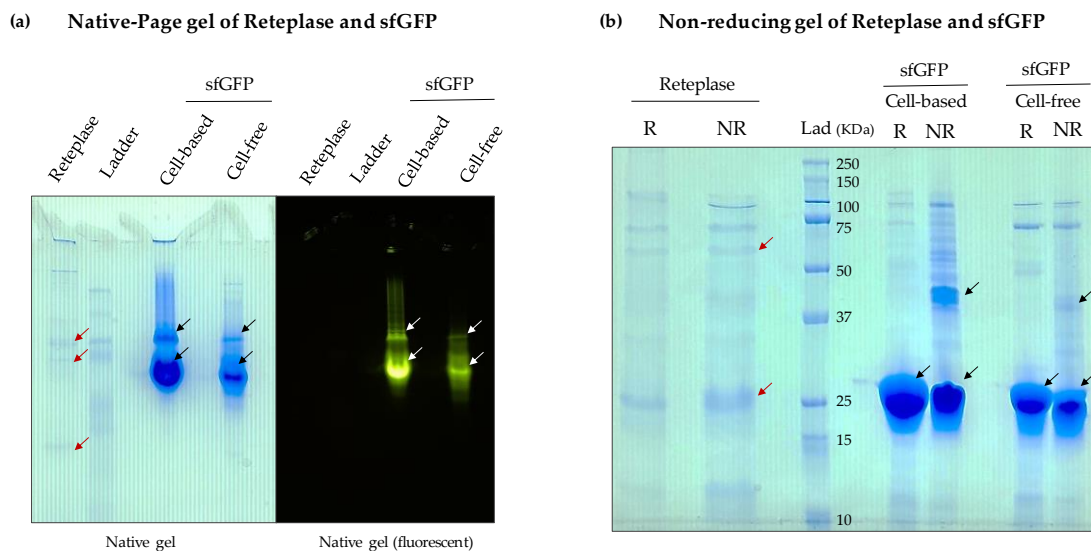


Figure 6.6: Tertiary and quaternary structure analysis. (a) Native gel (No β -mercaptoethanol or SDS or heat) loaded with reteplase, sfGFP (purified from cell-based or cell-free manufacturing routes) alongside molecular ladder. An image of the same gel on a blue light transilluminator also shown for visualising the fluorescent signal from sfGFP. (b) An SDS-Page gel loaded with reteplase, sfGFP (purified from cell-based or cell-free manufacturing routes) alongside molecular ladder shown under reducing ('R') and non-reducing conditions ('NR'; no β -mercaptoethanol or heat). Bands thought to correspond to reteplase marked with red arrows and known bands corresponding to sfGFP are marked with a black or white arrow.

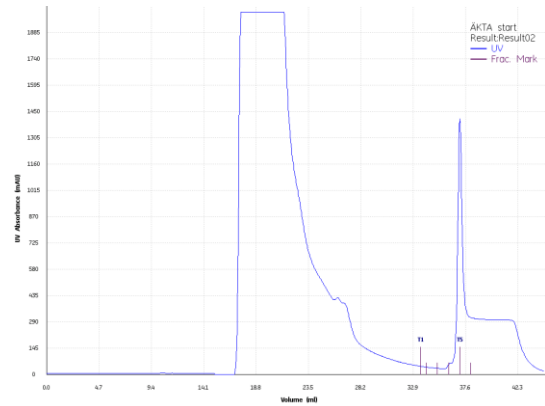
6.2.3.b Secondary structure analysis

Secondary structure is the regular, local structure of the protein backbone, and is a 3D intermediate before proteins fold into their tertiary structures and is characterised by the hydrogen bonding pattern in the peptide backbone (Stollar and Smith, 2020). The two broad types and most commonly found secondary structural elements are α -helices and β -sheets; determining such compositions can provide more information about the integrity of expressed and purified proteins. Therefore, secondary structure information can shed light on the previously discussed discrepancies in tertiary structure analysis. Circular Dichroism and Fourier Transform Infrared (FTIR) spectroscopies are two predominant techniques used to analyse protein secondary structure (Greenfield, 2006, Barth, 2007). Both techniques are complimentary and are often used hand-in-hand to obtain definitive information about purified recombinant proteins (Calero and Gasset, 2005, Goormaghtigh et al., 2009). Hence, both techniques were employed for the analysis of the following purified proteins: Reteplase (following cell-free synthesis); sfGFP (following cell-free synthesis and cell-based synthesis routes), with the hypothesis that the cell-free system produces correctly folded proteins, as seen in cell-based manufacturing routes

Contrary to the previous bead-based approach, the proteins were first synthesised through a cell-free or cell-based route and then purified using a His-Trap column

(nickel affinity chromatography) inside an AKTA start protein purification system. The wash fractions were discarded, and the eluted fractions were collected and concentrated to obtain the final purified protein sample (Figure 6.7). Unlike Section 6.2.2.a, the proteins were exchanged in D₂O instead of H₂O to reduce background signal arising from H₂O in the FTIR amide I region, as suggested in literature (Yang et al., 2015). The final concentration of purified reteplase was approximately eight times lower than that of sfGFP (cell-free and cell-based), and this was also visible in the UV absorbance recordings taken during elution (Figure 6.7, c). This could be attributed to the low yield of reteplase in cell-free reactions, as observed in Section 6.2.2.a. Nevertheless, this concentration met the threshold for secondary structure analysis and hence was subject to FTIR and CD spectroscopy.

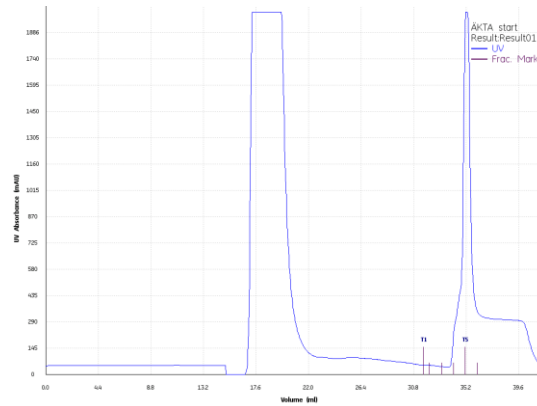
(a) sfGFP (cell-free)



Absorbance @ 280 nm = 7.469

Protein concentration = 11.83 mg/ml

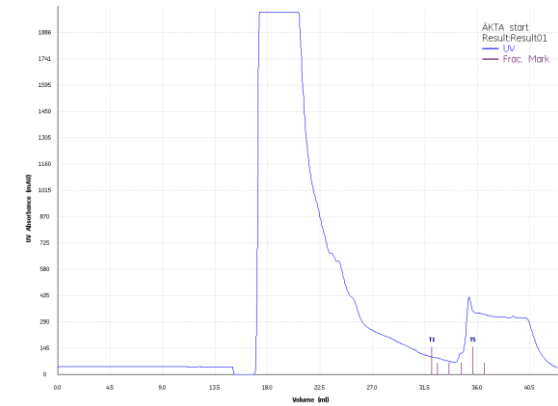
(b) sfGFP (cell-based)



Absorbance @ 280 nm = 8.376

Protein concentration = 13.26 mg/ml

(c) Reteplase



Absorbance @ 280 nm = 2.586

Protein concentration = 1.57 mg/ml

Figure 6.7: Purification of proteins for secondary structure analysis. UV absorbance recordings taken during affinity column chromatography shows the wash steps (first peak), elution steps (subsequent peaks) and elution fractions ('Frac Mark') for three proteins (a) sfGFP (cell-free), (b) sfGFP (cell-based) and (c) reteplase.

i Fourier transform infrared spectroscopy (FTIR)

FTIR has long been used to derive protein compositions based on absorption of infrared light. The FTIR spectrum has many amide bands due to vibrations in the protein sample. Most notably, the amide I and amide II bands correspond to the C=O and N-H stretching and bending, which in turn are involved in the hydrogen bonding pattern of a protein's secondary structure. The amide I band is regarded as the most useful predictor for assessing protein structure, due to higher sensitivity (Yang et al., 2015). The raw spectra of the above three purified proteins was first obtained using an Agilent Cary 630 Spectrometer (Figure 6.8). Non-amide regions such as the functional group and fingerprint region are useful for chemical identification. On the other hand, regions such as amide A, I, II and III are analysed for proteins, hence, the labelled amide I region was selected for further analysis.

Raw FTIR Spectra

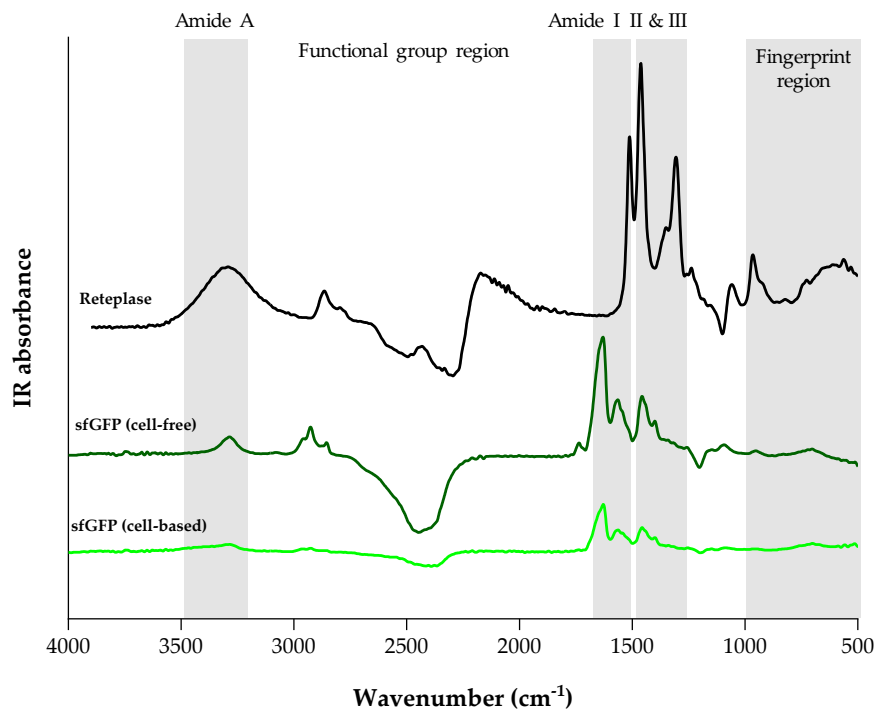
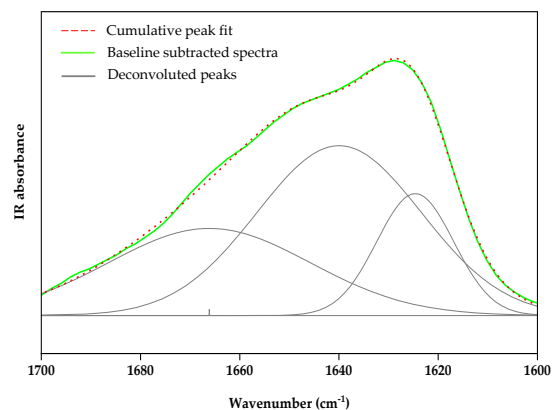


Figure 6.8: Unprocessed infrared spectra of purified proteins reteplase (black trendline), (b) sfGFP (cell-free; dark green trendline) and (c) sfGFP (cell-based; fluorescent green trendline). The main amide bands (A, I, II & III) are highlighted alongside other characteristic regions such as the functional group and fingerprint regions. The three spectra are shown on an offset Y-axis (IR absorbance) across wavenumbers 4000 to 500 cm⁻¹.

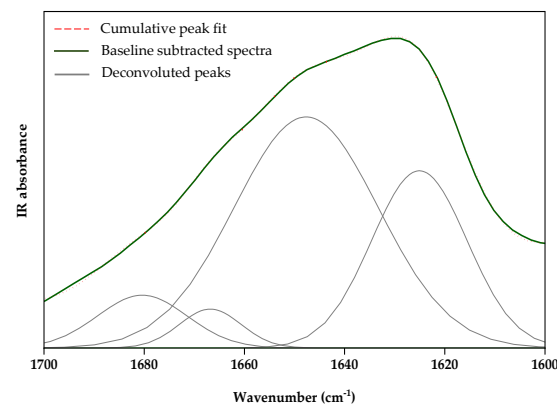
The amide I band often manifests as one peak and resolved peaks corresponding to each secondary structure are invisible compared to band width. Hence, the peaks are deconvoluted from the raw spectra by employing mathematical tools such as Fourier self-deconvolution and second derivative analysis. For deconvoluting the amide I peak from Figure 6.8, the second derivate of the spectra was first obtained for the identification of individual peaks, which were then fitted and assigned a secondary structure based on previously published assignments (Jackson and Mantsch, 1995, Yang et al., 2015, Sadat and Joye, 2020). Second derivate analysis performed in OriginLab revealed hidden peaks in all three protein samples (Figure 6.9). Three peaks were identified for reteplase and sfGFP (cell-based), and four peaks for sfGFP (cell-free). The assigned secondary structures and their percentage in the protein composition were calculated based on peak wavenumber and area integral. Although the peak positions were largely invariable, the intensities differed among the three different samples. The following peak assignments were made based on previously published work: 1625 = β -sheet, 1639 = β -sheet, 1647 = random coils, 1666 = β -turn, 1667 = β -turn, 1690 = β -turn (Jackson and Mantsch, 1995, Yang et al., 2015, Sadat and Joye, 2020).

The secondary structure assignments were similar in sfGFP from cell-free and cell-based synthesis, which predominantly had α -helices and β -sheets configurations (Figure 6.9, a & b). This was expected as the protein populations contain the same protein manufactured in a different route; the two baseline subtracted data were also observed to be similar in trend, as were the raw spectra in Figure 6.8. The peak assignments and secondary structure compositions reported in one published study significantly matched that of wild type GFP studied using FTIR and that of previously known sfGFP secondary structure as discussed in Chapter 3 (3.2.2) (Herberhold et al., 2003). Moreover, sfGFP was present in its native, functional form (due to fluorescence observed during characterisation) in these two routes.

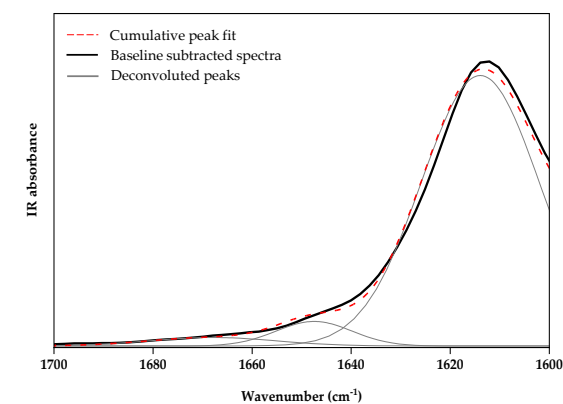
The same conclusion could not be drawn for reteplase. Firstly, the amide I region had shifted to the right, with a notable peak at 1613 cm^{-1} (Figure 6.9, c). The peak assignment was side chains, which formed 91.7% of the reteplase's secondary structure. Although α -helices and β -sheets were found in a lower percentage, this does not match published spectra for reteplase in either the correctly folded or improperly folded format in inclusion bodies, or structural predictions carried out by other groups (Ghaheh et al., 2019, Naeimipour et al., 2020). Although there is good confidence in these peak-fitted spectra as the cumulative peak fit overlaid the baseline subtracted data well, there is low to no confidence in the secondary structure of reteplase synthesised from the in-house cell-free system.

(a) sfGFP (cell-based synthesis)

Vibrational frequency (cm ⁻¹)	Area (integral)	Secondary structure assignment	% secondary structure
1625	0.155	Side chains/ β -sheets	17.3 %
1639	0.462	Random coils/short chains connecting α -helical segment	51.3 %
1666	0.282	β -sheets	31.4 %

(b) sfGFP (cell-free synthesis)

Vibrational frequency (cm ⁻¹)	Area (integral)	Secondary structure assignment	% secondary structure
1625	0.755	Side chains/ β -sheets	29.4 %
1647	1.489	Random coils/ α -helix	58.1 %
1666	0.107	β -sheet	12.4 %
1690	0.211	β -sheets	

(c) Reteplase

Vibrational frequency (cm ⁻¹)	Area (integral)	Secondary structure assignment	% secondary structure
1613	2.17	Side chains	91.7%
1647	0.127	Random coils/ α -helix	5.4%
1667	0.07	β -sheets	2.9%

Figure 6.9: Infrared spectrum in the amide I region of (a) sfGFP (cell-based), (b) sfGFP (cell-free) and (c) reteplase. The figures show the curve fitted and baseline subtracted data along with the individual peaks for each spectrum. The table summarises peak wavenumbers, the secondary structure assignment and percentage secondary structure. The percentage secondary structure was calculated from the area under each hidden peak and indicates the relative amount of each structure. Spectrum shown for one purified sample only.

ii Circular Dichroism (CD) spectroscopy

Circular Dichroism (CD) spectroscopy studies the differential absorbance of right and left circular polarised light in chiral sample (biomolecules such as proteins are largely chiral). The CD spectra of proteins that predominantly contain α -helices, β -sheets, or random coils appear different, and this property can be used to find out secondary structural information for unknown or purified proteins (Woody, 1995). Hence, the three purified samples that underwent FTIR analysis was also subject to CD spectroscopy. It should be noted that only a qualitative analysis was performed for confirmation, hence the raw spectra for each protein were plotted without peak analysis (Figure 6.10).

Three raw CD spectra were collected for each of the three proteins along with the HT (photo multiplier) voltage readings. Appropriate dilutions of the proteins were made if and when HT values exceeded 600. Three spectral measurements are shown for dilutions with low noise ($HT < 600$) for each purified protein sample (Figure 6.10). In the case of sfGFP, both cell-free and cell-based samples produced a distinct negative absorption band in the 210 nm – 220 nm region which is a well-known characteristic of β -sheet rich proteins. Moreover, the spectral pattern was largely similar to that reported in literature for other variants of GFP, all of which contained the conserved β -barrel formed from β -sheets (Visser et al., 2002).

The spectra obtained from sfGFP cell-free and cell-based samples produced a very similar trend and β -sheet composition, which aids the argument that these two samples contain the same protein population. These spectra are however starkly different to that of reteplase, which was expected as reteplase composition is different to that of sfGFP. For reteplase, a positive absorption band was detected in the 200 nm - 210 nm region of the spectrum, which is a characteristic of proteins with a α -helical content (Figure 6.10). In fact, this spectrum closely matched the only CD spectra that was found in literature for the closely related protein - alteplase (Lu et al., 2019). The paper reports CD spectra for biologically active alteplase, a second generation tissue plasminogen activator from which reteplase was derived from – reteplase is a single-chain deletion mutant and is ~20 kDa smaller than alteplase (Mandi et al., 2010). Although the spectra for alteplase may not be appropriate for quantitative analysis due to these structural differences, it still serves as a model for predicting some structural and functional aspects of reteplase. Collectively, the reteplase CD spectra suggests that the in-house, cell-free synthesised protein may have intact secondary structure. Deconvolution of the bands may provide further insight. In addition, spectral recordings taken at lower wavelengths (with a new lamp

and less noise for higher protein concentration) may provide a better basis for comparison with previously published spectra.

Far UV Circular Dichroism spectra

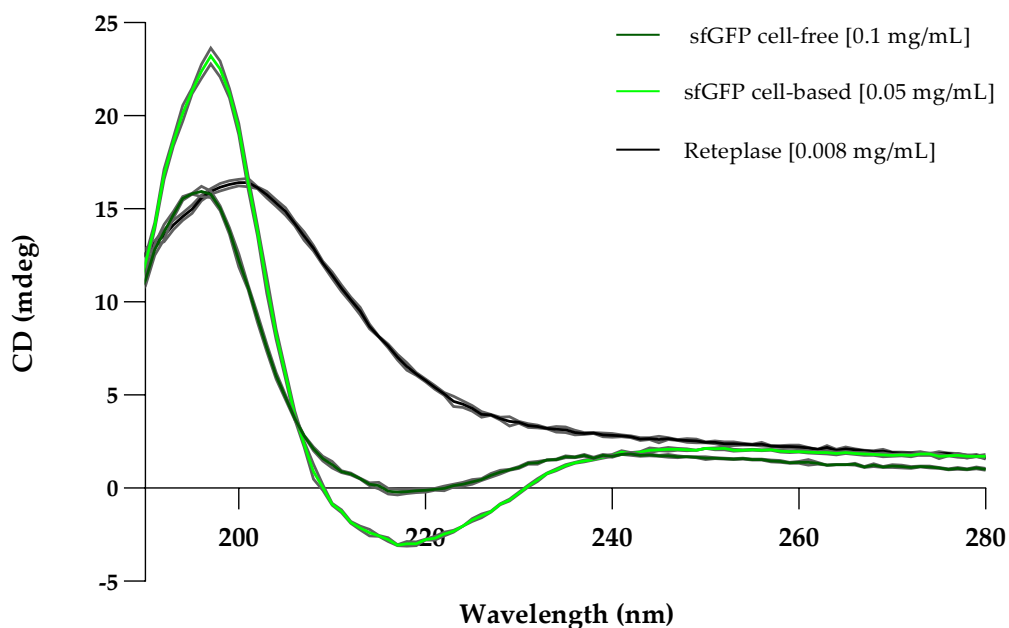


Figure 6.10: Raw Circular Dichroism (CD) spectra for purified sfGFP (cell-free and cell-based) and reteplase in D₂O shown at optimised concentrations. The concentrations indicate the final concentration in the CD sample which was optimised based on HT (photo multiplier) voltage recordings (< 600); spectra taken when HT values exceeded 600 were considered too noisy and were discarded. Trends shown for three samples prepared independently (the grey trendlines indicate error). X-axis covers wavelengths from 190 nm to 280 nm (< 190 nm values could not be taken due to overused lamp hours) and Y-Axis indicates ellipticity, which is related to observance (reported in millidegrees or 'mdeg').

6.2.3.c Conclusions from tertiary and secondary structure analyses

Overall, sfGFP was a good candidate for functional analyses as fluorescence is easily visualised (simply through the naked eye) and detected (using spectroscopy) only in correctly folded proteins. sfGFP was found to form dimers and potentially trimers in the non-reducing gels, and this was further confirmed in fluorescent gels (Figure 6.6, a & b). FTIR and CD spectroscopy resulted in the identification of β -sheets as the main secondary structure component, with good agreement to other studies reported in literature (Figures 6.9 & 6.10). Lastly, a good level of confidence was obtained to conclude that both cell-free and cell-based manufacturing routes led to the synthesis of structurally and functionally active sfGFP.

Tertiary and secondary structure analysis for reteplase resulted in some puzzling findings. No shifts in reteplase bands were observed in reducing and non-reducing gels (Figure 6.6, b). FTIR analysis led to the identification of some α -helical and β -sheet components, but the vast majority of the composition was designated to random coils. On the other hand, CD analysis suggested α -helix to be the richest secondary structural component in reteplase. The CD spectra largely agreed with spectra of a similar protein reported in literature whereas FTIR findings did not. These conflicting results did not allow progression of reteplase for further *in vitro* activity assays at this time. One cause for these conflicting findings could be protein aggregation and/or fragmentation. This was somewhat visible in the form of multiple bands detected in the gels (Figure 6.6). Hence, significant optimisation of cell-free expression and purification procedures should be undertaken to mitigate this. Then, tertiary and secondary structure analysis should be repeated before proceeding to test activity.

The use of secondary structure analysis has informed the understanding of the integrity of the purified proteins and confirm the similarities between cell-based and cell-free expression routes. This is perhaps the first collection of studies that tapped into FTIR and CD spectroscopy to unravel information on post-cell-free synthesised proteins. Owing to its usefulness, it is hoped that they could be further exploited for studying stability, integrity and quality control of cell-free products.

6.2.4 Co-expression studies

This section introduces one final experimental idea – co-expression of proteins in cell-free systems for capture and quality control of target protein - and to the best of our knowledge, is the first demonstration of production of more than one type of protein in cell-free systems for this purpose. The vision of the on-site and on-demand platform would require delivery of purified and functional therapeutics at point-of-care, with in-built quality control features. To achieve this, a nanobody driven in-situ purification process was envisioned. ‘Nanobodies’ are target recognition fragments of an antibody and can be generated for virtually any therapeutic protein-of-interest and can be engineered to bind to target protein(s) only when it is found in a structurally and functionally active state (Dmitriev et al., 2016). This is a highly desirable property, as nanobodies can be used to capture only functional protein, which allows it to function as a quality control applicant. For example, sfGFP and its nanobody (sfGP-Nbs) will only bind when both proteins are synthesised and present in their structurally active states (Figure 6.11, a). Moreover, tags can be introduced in the nanobody construct to enable pulldown/purification of the active complex and any change or failure to form the correct structure will not allow retention during the pulldown process (*e.g.* during affinity chromatography). Although histidine or

cellulose binding domain based tags could be considered, scarless tags such as the SNAC-tag or SUMO-tag are better candidates for obtaining protein products that meet regulatory standards (Dang et al., 2019, DeWinter et al., 2023) (supplementary information). Collectively, the envisioned strategy involved co-expression of target protein and its nanobody to serve as a quality control measure, to test the integrity of target proteins for on-site, on-demand CFPS.

To test this strategy, a feasibility study was first conducted to test co-expression of sfGFP and the sfGFP-Nbs07 in the in-house cell-free system. The sfGFP-Nbs07 is one of the sfGFP nanobodies (or NBS in short) and is made up of 122 amino acids (13.1 kDa in length) and contains two disulfide bonds, when folded correctly. This was chosen from previously published work, and due to its low size and high binding efficiency (sfGFP capture EC_{50} of 24.1 ± 8.1 nM) (Twair et al., 2014). Both the sfGFP and NBS constructs contained a C-terminal histidine tag and cell-free products were detected on western blots by means of an anti-His antibody. Cell-free reactions were performed with no DNA, sfGFP only and NBS only DNA, and both sfGFP and NBS DNA (Figure 6.11, b). Bands corresponding to sfGFP and NBS were detected on the western blot in individual reactions and bands for both were seen in the co-expression reactions (Figure 6.11, b, lanes 6 & 7). This provides support for the concept that more than one protein can be produced via CFPS.

The co-expression reactions were subject to reducing and non-reducing ('native-like') environment similar to previous analysis in Figure 6.6. Since successful co-expression of both protein and nanobody was achieved, the hypothesis was that the resultant protein-nanobody complex would manifest together as a higher sized band in a western blot in native-like conditions when compared to reduced samples detected as two separate bands. There was indeed a shift in individual bands for NBS in native samples and faint bands were spotted around 37 kDa, which may indicate either a higher band migration pattern for GFP or this may correspond to the GFP-NBS complex (Figure 6.11, b, lanes 8 & 9). No other bands were detected on the western blot apart from the ones visible on the cropped portion.

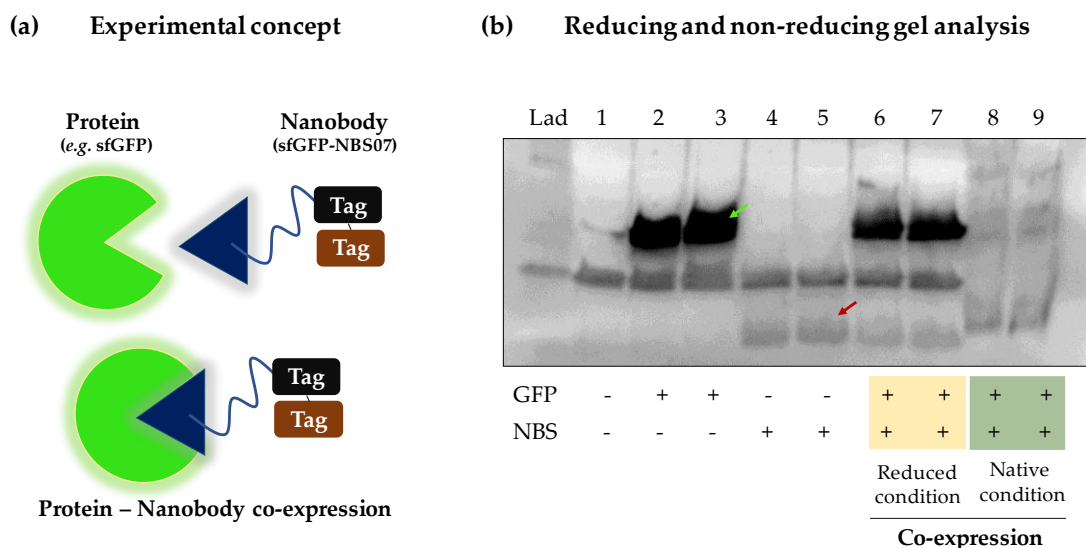


Figure 6.11: Co-expression studies. (a) *Illustration of the experimental concept.* Proteins and Nanobodies can be expressed together and binding will be achieved only when both parties are in structurally and functionally active states. The Nanobody can be engineered to contain tags that could be exploited for purification of the target protein. (b) *Western blot* of the reactions with (+) and without (-) DNA coding for sfGFP ('GFP') and sfGFP-Nbs07 ('NBS') in reduced and 'native-like' conditions. The term 'native-like' refers to samples that were prepared with Native-Page sample loading buffer which does not contain SDS, however, were exposed to SDS in the gel running buffer. Green arrow indicates sfGFP, and red arrow indicates sfGFP-Nbs07. Two reactions were performed and shown for each condition tested.

To further confirm if the faint bands at ~ 37 kDa were in fact the NBS-GFP complex, another SDS-Page analysis was performed, without western blotting however, to enable fluorescence imaging of the gel. The stained SDS-Page gel did not provide any distinct bands, understandably due to overloaded protein content, which was why western blots were performed previously (Figure 6.12, a). However, more insight was obtained when the same gel was captured under a blue light transilluminator. Fluorescence from sfGFP was readily visible in reactions containing sfGFP DNA in both reduced and native-like environments; an upward band migration was also detected in native conditions (Figure 6.12, b, lane 1). As expected, no fluorescence was detected in NBS only or negative control samples (Figure 6.12, b, lanes 2 and '-'). Although fluorescence was detected in co-expressed reactions, two main differences were observed. Firstly, the fluorescence signal was much lower than the sfGFP only sample (Figure 6.12, lane 1 vs. 3). This perhaps indicates that the yield of proteins differs during co-expression. Secondly, the fluorescent bands in the sfGFP only and co-expression reactions were in the same position in both reduced and native-like conditions (Figure 6.12, lane 1 vs. 3). This result leads to the conclusion that sfGFP was not found bound to NBS after CFPS reaction completion (this analysis was conducted immediately after CFPS).

(a) Coexpression studies: SDS-Page

(b) Fluorescent gel

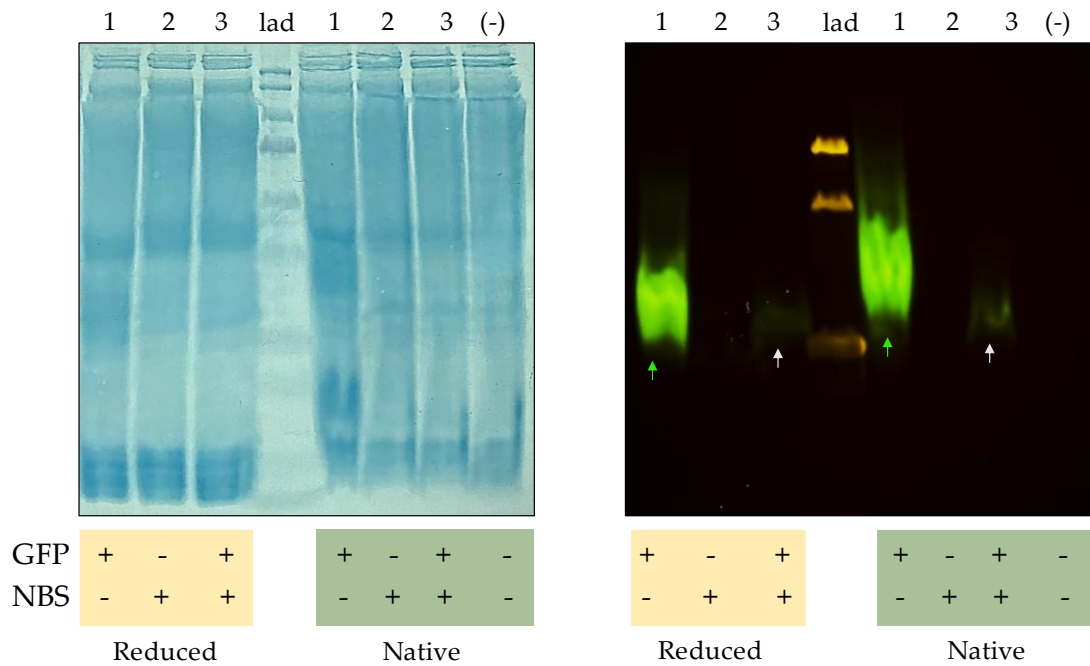


Figure 6.12: SDS-Page and native PAGE analysis. (a) SDS-Page, and (b) Fluorescent gel of the reactions with (+) and without (-) DNA coding for sfGFP ('GFP') and sfGFP-Nbs07 ('NBS') in reduced and 'native-like' conditions. The term 'native-like' refers to samples that were prepared with Native PAGE sample loading buffer which does not contain SDS, however, were exposed to SDS in the gel running buffer.

There is enough evidence for sfGFP and NBS expression, individually and during co-expression but no evidence for their interaction in the latter condition. One explanation for this could be the improper formation of the two disulfide bonds in sfGFP-Nbs07, or lack thereof. Disulfide bonds are critical for the structural stability of nanobodies and several studies reported reduced thermal denaturation temperatures when mutations were introduced (Rudikoff and Pumphrey, 1986, Hagihara et al., 2007, Akazawa-Ogawa et al., 2015, Liu et al., 2019). Disulfide bonds improve antigen binding in general, but the second disulfide bond is thought to reduce aggregation-induced irreversible denaturation and increase the conformational stability of the nanobody (Govaert et al., 2012, Kunz et al., 2018). Therefore, creating a cell-free environment that promotes disulfide bond formation and further qualitative and/or secondary structure analysis of co-expressed proteins are the next calls-to-action prior to testing purification strategies for the protein complex.

6.3 Summary

The first set of experiments outlined in this chapter involved the production of five therapeutic proteins for on-site and on-demand applications. Four of five proteins were successfully produced using the PURExpress system, where teriparatide expression was detected with uncertainty. Production of three of five proteins was successfully shown using the in-house method. Teriparatide and G-CSF synthesis was perhaps unsuccessful due to low protein size. Supplementation of disulfide bond enhancers neither caused production of the two proteins nor increased the levels of the other three proteins. RT-qPCR analysis was sought for understanding reasons for lack of G-CSF and teriparatide synthesis. Although the positive control did not behave as expected, mRNA pertaining to all five therapeutic constructs was detected - such analyses must be repeated for more concrete understanding and better confidence in control samples. Overall, some suggestions for improving production were made and in summary, this included fusion-tag approaches (such as SUMO tag) and altering CFPS extract strains.

The next set of experiments focused on cell-free synthesis of reteplase and sfGFP at 37°C and 32°C and their subsequent purification. CFPS reaction temperature of 32°C showed higher yields for reteplase but no significant difference in sfGFP - this signified that reaction parameters must be optimised for each protein product. Moreover, a standard curve was generated for estimating CFPS yields based on sfGFP protein concentration and fluorescence. This proved to be a great tool for predicting yields in previous reactions' fluorescence and will certainly be useful to estimate protein yield when the VITA platform is tested on the ISS (Chapter 5). Tertiary and secondary structure analysis confirmed the presence of structurally and functionally active sfGFP, however, conflicting results for reteplase did not allow *in vitro* activity assays to be carried out at this time. Since neither method is fully successful in determining protein secondary structure, CD spectra is often presented aside FTIR spectra for confirmation purposes, which was also the rationale in this work. One cause for conflicting findings from these two methods could be protein aggregation and/or fragmentation. As already recognised, significant optimisation of cell-free expression and purification procedures should be undertaken.

The final set of experiments described the idea of co-expression of proteins such as nanobodies to capture and purify target protein. Feasibility studies showed the expression of sfGFP and the sfGFP nanobody in a single reaction, however, interaction could not be established which was likely due to limitations in disulfide bond formation. Further work is required to understand CFPS kinetics (if and how it differs) during co-expression and also any extract strain modifications or supplements to aid disulfide bond formation. The purity of cell-free produced

therapeutics must meet regulatory standards for approval for human administration, therefore, the nanobody-protein strategy is a reassuring quality control feature for the manufacturers and the regulators, in the context of an on-site and on-demand platform in austere environments.

Chapter 7 Conclusions

7.1 Recap of project objectives

The motivation behind this research was to establish an on-site and on-demand biomanufacturing platform based on cell-free protein synthesis for the production of protein therapeutics. The objective was to explore innovative approaches and new ideas that could enable applications of this system in extreme and low-resources environments. The project started with the following research aims to address this main objective:

- a) Develop an in-house cell-free protein synthesis platform based on bacterial cell extract by leveraging advanced biochemical and synthetic biological techniques and optimise the system for high synthesis efficiency.
- b) Explore formats through which the cell-free platform could be transported and distributed for point-of-care applications in remote locations on Earth or for space-based applications. Build on previously published work related to lyophilisation or drying, but also test new methods such as microglassification and the use of other scaffolds that may allow ease of use in a remote setting by any individual.
- c) Design, build and test the platform for the VITA mission, a European Space Agency Orbit Your Thesis 3! payload for technology demonstration on the International Space Station. Perform sample stability and instrumentation tests to ensure the integrity of the cell-free payload and the ability to collect real-time data on reaction kinetics.
- d) Expand the repertoire of synthesised proteins to include five therapeutic proteins, involving studying the structure and functionality of the expressed protein(s) and employing new approaches to overcome challenges associated with in-situ purification.

In summary, the first three objectives were successfully achieved from results shown in Chapters 3, 4 and 5. Chapter 6 was partially successful in the fulfilling the final objective, however, further work is required for a full picture. The main conclusions from each of the chapters are first laid out, the recommended further work is then detailed in the following section. Finally, some regulatory challenges, which are seen as long-term future work, are discussed in the final section of this chapter. There are certainly more improvements that can be made, but this project has constructed a good foundation for a bacterial cell-free system for on-demand production of proteins of value in extreme and low-resource environments.

7.2 Overall conclusions and achievement of research objectives

The key findings reported in this thesis, their relevance to the research objectives and their contribution to the CFPS field is summarised below.

The third chapter described the generation of two critical elements for in-house cell-free protein expression: cell-free extract preparation and DNA templates for expression of proteins-of-choice. To achieve the first goal, a bacterial strain, BL21 Star (DE3) was chosen for cell-free extract preparation. This strain was successfully modified through transformation of pAR1219, which enhanced T7 polymerase levels. Further optimisation led to identification of optimal IPTG concentration (0.5 mM), cell growth temperature (37°C) and time of harvest (2 hours post induction or ~ OD₆₀₀ = 3 to 4) for obtaining the most soluble T7 polymerase levels, which is a prerequisite for transcription of DNA template in CFPS. As for the DNA templates, six main cloning projects were undertaken for generating constructs for expression of sfGFP (fluorescent reporter), retE, entolimod, alfineprase, and G-CSF (model therapeutic proteins for on-demand applications in extreme and low-resource environments). Hence, the work detailed in this chapter successfully led to the generation of two key components that make up a tailored cell-free system.

The fourth chapter focused heavily on the development of the in-house CFPS system following experimentation with commercial NEB PURExpress and Promega S30A platforms. Then, a series of experimental trials led to the identification of optimal concentrations of energy components (double the concentration typically reported in literature), magnesium glutamate (20 mM), and DNA template (300 ng). Molecular crowding agent PEG, also significantly enhanced expression, taken together with a higher fraction of cell-free extract in the reaction mix. The distinct differences of the optimised CFPS developed here to those reported in literature are the higher energy component and DNA template concentrations, which was thought to be due to the omission of phosphoenol pyruvate (an energy compound containing more high energy phosphate bonds) and a slightly higher protein concentration in the cell-free extract. Thus, a highly efficient in-house cell-free system was developed, meeting the first thesis objective. This is a particularly novel set of findings as T7 polymerase is often supplemented into reactions widely discussed in literature, adding an extra step and making reactions costlier. The BL21 Star (DE3) – pAR1219 strain circumvents these issues. When combined with the optimised conditions, the in-house cell-free system performed on par with the highly efficient commercial NEB PURExpress system.

The fourth chapter also met the second thesis objective – formats for on-site and on-demand application. Two main methods were thoroughly assessed for fulfilling this

aim, namely, microclassification, and drying (air drying and freeze-drying; freeze-drying on paper for the 'cellulose stacks approach' and as lyophilised pellets were the methods tested). Although microclassification offers great potential (discussed in the future work section), it failed to preserve the cell-free extract in a reconstitutable format, likely due to protein denaturation and aggregation. Lyophilisation, however, preserved all components in 'one-pot', enabling a 'just-rehydrate' format for CFPS. This was further expanded to lyophilisation on cellulose stacks capable of kickstarting CFPS upon layering and rehydration. One type of cellulose was found to have superior retention capabilities and a further feasibility study was performed where lyophilised stacks of the superior cellulose type were rehydrated and applied to dissolving microneedles, which successfully dissolved with the cell-free synthesised sfGFP. In conclusion, the work discussed in this chapter sets the scene for synthesis of life-saving and life-enhancing therapeutics, but a significant amount of work is required to meet challenges that emerge from batch-batch variation, purification, and meeting regulatory standards.

The fifth chapter aimed to demonstrate the cell-free technology developed in the previous chapters in a truly extreme environment – the International Space Station. The mission, VITA (Visualising In-situ Tx-TI Astropharmaceuticals), was introduced and the ability to detect sfGFP through fluorescent spectroscopy and imaging following rehydration of the cell-free components was shown in an automated manner. The mission instrumentation sub-system was successfully able to capture CFPS time course for four hours using a teleoperated set-up. To address other mission objectives, reaction temperature was lowered to 30°C and the reaction volumes were increased to up to 250 μ L, with no significant impact on CFPS yield.

The next challenge that was tackled in this chapter was CFPS component shelf-life, which was found to be less than one week through stability studies. A series of exploratory investigations led to the identification of sugars such as β -lactose to enhance room temperature stability, and maltodextrin to enhance the yield in fresh reactions. A subsequent design of experiments approach allowed combinations of these sugars, in addition to molecular crowding agent PEG, to be tested through short-term stability studies. The best identified formulation (25 mM MDX, 20 mM β -lactose, and 5% 6000 kDa PEG) was progressed to long-term stability studies, where findings showed full stability until 1 month, but only 50% retention by 1.5 months. In conclusion, the shelf-life of the in-house formulated system was improved from 1 week to 1.5 months, enabling good preservation of cell-free components for the VITA mission. Although the stability should be furthered for at least an additional month or two to account for any rocket launch delays, these results were reasonably successful in accomplishing the third thesis objective.

The sixth chapter partially achieved the final thesis aim by demonstrating in-house cell-free synthesis of all target therapeutic proteins except for teriparatide and G-CSF. As disulfide bond enhancers did not aid expression and RT-qPCR analysis showed the presence of their mRNA, it is thought the teriparatide and G-CSF were not seen due to their low size. sfGFP was purified from cell-free and cell-based routes, the former serving as a positive control and the latter for comparison with the cell-free sample. Purified cell-free sfGFP was utilised for producing a fluorescence standard curve, which allowed yield predictions based on fluorescence signals. Next, reteplase, a complex target, was chosen for further purification and functional analysis. It was found that lowering cell-free reaction temperature to 32°C improved the yield. FTIR and CD analysis confirmed that both cell-free and cell-based sfGFP samples had secondary structures composed mainly of β -sheets. FTIR analysis of reteplase suggested a high probability of random coils, but CD showed a high propensity to α -helices. Due to these conflicting findings, no functional assays were carried out and it was concluded that protein aggregation or degradation may be the cause of this result and further optimisation of reaction conditions would be required. Lastly, nanobodies were successfully co-expressed with the target protein in a single reaction, however, non-reducing and fluorescent gels failed to show their interaction, likely due to lack of formation of appropriate disulfide bonds, which are essential for nanobody stability. In conclusion, this chapter met some aims and explored some new ideas, which were not fully executed but contain great potential to revolutionise CFPS in the future.

7.3 Recommendations for Future Research

This thesis has aimed to establish an on-site and on-demand manufacturing platform based on cell-free protein synthesis. Whilst several formats, targets and tests were attempted, there are certainly some areas that require further investigation or refinement, as detailed below.

Chapter 4 showed the development and optimisation of a bacterial strain that formed the basis of cell-free extract preparation. Although the bacterial extract was chosen because they tend to be easier and faster to prepare and contribute to higher yields, they are not ideal for synthesising proteins that require low to high number of post-translational modifications. This was evident in Chapter 6, where small proteins such as G-CSF and teriparatide could not be expressed, and disulfide bonds could also not be formed in reteplase. In order to tackle the former, some suggestions for improving expression were made and in summary, this included fusion-tag approaches to improve both expression and solubility. For example, SUMO tag, which stands for small ubiquitin-like modifier, can be fused to the N-terminal of the protein of interest

and later be cleaved using the ubiquitin-like protease-1 to leave behind a scarless, soluble product (Guerrero et al., 2015).

Many therapeutic proteins belong in the category of antibodies and hormones, which typically contain disulfide bonds. Hence, an on-site and on-demand system should allow such critical features to be formed during protein synthesis. Although BL21 Star (DE3) - pAR1219 allows some disulfide bonds to form, the stability of the bond is very low due to the net reducing environment. Thus, a change of strain with an oxidising environment could be worth considering. Overexpression of thioredoxin, chaperones and disulfide bond isomerases may aid the formation of disulfide bonds, however, strains such as SHuffle (New England BioLab), Origami (Novagen) and Rosetta-gami 2 (DE3) (Novagen) are commercially available (de Marco, 2009). Furthermore, their existing compatibility with T7 expression offers an easy workflow and good adaptability to the already developed and optimised in-house cell-free system. Future work could focus on optimizing CFPS conditions to enhance protein folding, incorporation of chaperones/folding catalysts, and development of other eukaryotic systems that support specific post-translational modifications (glycosylation and phosphorylation being the most common types). This would enable the production of functional and biologically relevant proteins in on-site CFPS platforms.

The stability of cell-free components is a subject that requires more time and resource investment. Although a good improvement was made from one week to 1.5 months in Chapter 5, the target of 2 months stability at room temperature could not be achieved. Further DoE studies with more intricate concentrations of the β -lactose, maltodextrin and PEG supplements could lead to the identification of a better formulation (concentrations were scaled by a factor of 10 in this study and could be decreased to 2). Furthermore, new candidates and energy sources could also be tested; stability tests for the cell-free components on cellulose stacks are necessary as the described studies were conducted in lyophilised pellet format.

Specifically to ensure the success of the VITA mission, short temperature exposure studies should be conducted to understand how the system behaves during temperature fluctuations. This is in case the payload experiences a higher temperature during launch to the ISS, depending on the rocket that is selected (a window of 10°C - 35°C for SpaceX dragon and 10°C - 46.1°C for the Orbital Science Cygnus launch vehicle). The initial studies should test exposure to temperatures of 22°C as this is thought to accelerate degradation than the lower temperatures based on results shared in Chapter 5. For Earth-based applications of the on-demand platform, further stability studies should be conducted at a wider range of temperatures (0°C – 50°C) to cover the temperatures that are commonly experienced

on Earth. Furthermore, temperature exposure studies (intervals of exposure to high temperatures such as 50°C for Earth-based applications and 46.1°C for the Cygnus launch vehicle) could be performed.

In relation to the co-expression studies in Chapter 6, further work is required to understand CFPS kinetics (if and how it differs) during co-expression, and any extract strain modifications or supplements to aid disulfide bond formation in nanobodies, as above. Co-expression kinetics could be monitored in real-time by expression of two fluorescent proteins, for example, and the VITA mission aims to study how this would alter in microgravity. Hence, a good understanding from ground studies is first required. It is also important to balance target protein and nanobody expression levels, as bottlenecks should be avoided during both expression and purification.

7.4 Future work for addressing challenges of on-demand biomanufacturing

An on-demand biomanufacturing system must be flexible, portable, and user-friendly. This thesis has set the scene, but further work is required for enhancing the efficiency, automation and multiplexing with other technologies such as purification and quality control.

A compact and lightweight CFPS platform would allow for better distribution and deployment in resource-limited settings. The systems could further be made easy to use by incorporating automatic processes through a robotic platform or a microfluidic device, similar to 'lab-on-a-chip' platforms. For end-to-end automation, various steps will need to be streamlined and built in, for example: sample preparation (*i.e.* rehydration of cellulose stacks or lyophilised pellets in the case of this in-house system) and addition of DNA template depending of the required target protein and purification strategy (*i.e.* nanobodies); mixing of these reagents; an environmental control and monitoring system (temperature, mixing rates and time limit for reaction progression).

Another challenge for on-demand manufacturing of therapeutics is the on-demand synthesis of the required DNA template. Rapid synthesis and assembly of the DNA template is required for protein synthesis, and this could be facilitated by methods such as high throughput DNA assembly, or by using inkjet printing to obtain customised oligonucleotides through orderly deposition of the nucleotide building blocks (Li et al., 2019). The technology readiness levels of these platforms are still low for adoption in automated biomonitoring platform; however, they contain promising attributes that could be exploited in the near to distant future. The regulatory milestones associated with DNA assembly are provided in the next section.

Another area where further innovation is required is the integration of on-site CFPS platforms with downstream applications for administration of the synthesised protein. An example is coupling the platform with a purification system, like an affinity or size exclusion column, to achieve the nanobody driven purification strategy discussed in Chapter 6. This may not be required for diagnostic applications like biosensing. Further protein engineering tools and technologies will be required for quality control and varying the drug delivery method. From the end user's point of view, developing usable interfaces, instructions, and providing initial training will enable widespread adoption of this CFPS platform. This will also ensure that users from a diverse background (non-STEM users) and levels of expertise are able to access and take advantage of the versatility of this technology.

7.5 Meeting regulatory standards

Meeting regulatory standards for cell-free products is perhaps the most challenging of all. It involves rigorous procedures to ensure products are pure, safe, and efficacious. It is first important to understand the regulatory guidelines that are in place for applications in a specific target market. For example, regulations are instated by the Food and Drug Administration (FDA) in the US, European Medicines Agency (EMA) for the European Union and the Medicines and Healthcare Products Regulatory Agency (MHRA) for the UK following Brexit, for approval of medicines and medical devices (MHRA, 2021). Next, preclinical assessments must be made via *in vitro* and toxicological studies to evaluate the safety and efficacy of the product. Since the on-demand biomanufacturing platform aims to synthesise market-available and well understood biologics, the regulatory process may be different and more focussed on purity and quality assurance.

During the design phase, additional considerations should be made to obtain 'scarless' protein product, meaning no additional tags incorporated for purification should remain intact in the final product. Self-cleaving tags (those that cleave without additional protease or chemical treatments) such as Intein are good candidates for further work. Intein remove themselves via self-splicing, and this can be induced commonly through a pH or temperature change or by addition of a ligand (Aranko and Iwai, 2021). In relation to the DNA synthesis and assembly methods described previously, it is crucial to account for ethical and legal implications, especially when involving sensitive or regulated DNA sequences for the proteins, nanobodies, and tags. Guidelines and safety precautions should be well understood before carrying out any genetic modification.

Good Manufacturing Practices (GMP) must next be implemented to ensure consistent production and quality control. Although the work conducted as part of thesis did

not aim to reduce batch-batch CFPS variation, it addressed the issue of quality control through implementation of the nanobody strategy. Although successful binding could not be shown at this time, further work is required to fully validate this proposition. By allying with analytical methods to characterise the synthesised biologics, these methods will help identify and quantify critical attributes such as purity, stability and impurities. Product-specific data could be acquired for the first set of cell-free produced biologics in the form of activity assays, animal studies and subsequent clinical trials that are designed to evaluate dosing, pharmacokinetics and immunogenicity.

Based on the success and fulfilment of the above, applications with relevant data should be sent to the relevant regulatory bodies for market authorisation. It is important to engage promptly with the agencies during the review process and address any further concerns they may have. Although this process may be straightforward for applications of the platform on Earth, the laws and regulations remain blurry for space-based applications. For example, there is a lack of clinical evidence on the use and effects of medicines on the ISS, which is formed of many cooperating agencies with their own regulatory bodies (The Department of State, 1998, Blue et al., 2019). This type of 'Intergovernmental Agreement' allows each partner to enforce their national jurisdiction in outer space, and the elements and equipment they bring such as laboratories are territories of that partner's State. The reason as to why there are no specific regulations so far is because space related activities are still primarily government-led, and it is thought that new regulations (e.g. utilising space resources) are starting to be laid as more commercial interest is arising. The possibility of a new regulatory body ('Space Medicines Agency') and their role in ensuring post-process regulatory/quality control procedures, dosage and administration has been suggested (Sawyers et al., 2022, Seoane-Viaño et al., 2022). Telemedicine and Telepharmacy will no doubt play a big role in the future of space travel, but the legal framework will follow slowly but surely.

Finally, it is essential to develop a surveillance plan to keep track of the performance and safety of the biologics that were synthesised and administered from the on-demand platform after gaining approval for distribution. The collected data could be used to analyse risks and adverse effects but could also be useful feedback for future improvement of the system. Although the regulatory challenges are many, they ensure safe and useful access to valuable therapeutics. It is still early days to address the many regulatory challenges for extreme environments, but it is important to consider these during the design, build and test cycles for on-demand biomanufacturing platforms.

References

- ADAMO, A., BEINGESSNER, R. L., BEHNAM, M., CHEN, J., JAMISON, T. F., JENSEN, K. F., MONBALIU, J.-C. M., MYERSON, A. S., REVALOR, E. M., SNEAD, D. R., STELZER, T., WEERANOPPANANT, N., WONG, S. Y. & ZHANG, P. 2016. On-demand continuous-flow production of pharmaceuticals in a compact, reconfigurable system. *Science*, 352, 61-67.
- ADIVITIYA & KHASA, Y. P. 2017. The evolution of recombinant thrombolytics: Current status and future directions. *Bioengineered*, 8, 331-358.
- AKAZAWA-OGAWA, Y., UEGAKI, K. & HAGIHARA, Y. 2015. The role of intra-domain disulfide bonds in heat-induced irreversible denaturation of camelid single domain VHH antibodies. *The Journal of Biochemistry*, 159, 111-121.
- ALT, N., ZHANG, T. Y., MOTCHNIK, P., TATICEK, R., QUARMBY, V., SCHLOTHAUER, T., BECK, H., EMRICH, T. & HARRIS, R. J. 2016. Determination of critical quality attributes for monoclonal antibodies using quality by design principles. *Biologicals*, 44, 291-305.
- AMANN, T., SCHMIEDER, V., FAUSTRUP KILDEGAARD, H., BORTH, N. & ANDERSEN, M. R. 2019. Genetic engineering approaches to improve posttranslational modification of biopharmaceuticals in different production platforms. *Biotechnology and Bioengineering*, 116, 2778-2796.
- ANGIUS, F., ILIOAIA, O., AMRANI, A., SUISSE, A., ROSSET, L., LEGRAND, A., ABOU-HAMDAN, A., UZAN, M., ZITO, F. & MIROUX, B. 2018. A novel regulation mechanism of the T7 RNA polymerase based expression system improves overproduction and folding of membrane proteins. *Scientific Reports*, 8, 8572.
- ANIKET, GAUL, D. A., RICKARD, D. L. & NEEDHAM, D. 2014. Microglassification™: A Novel Technique for Protein Dehydration. *Journal of Pharmaceutical Sciences*, 103, 810-820.
- ARANKO, A. S. & IWAÏ, H. 2021. The Inducible Intein-Mediated Self-Cleaving Tag (IIST) System: A Novel Purification and Amidation System for Peptides and Proteins. *Molecules*, 26.
- ARNSTEIN, H. R. V. 1965. MECHANISM OF PROTEIN BIOSYNTHESIS. *British Medical Bulletin*, 21, 217-222.
- ARONSON, D. E., COSTANTINI, L. M. & SNAPP, E. L. 2011. Superfolder GFP is fluorescent in oxidizing environments when targeted via the Sec translocon. *Traffic*, 12, 543-8.
- AU - LEVINE, M. Z., AU - GREGORIO, N. E., AU - JEWETT, M. C., AU - WATTS, K. R. & AU - OZA, J. P. 2019. Escherichia coli-Based Cell-Free Protein Synthesis: Protocols for a robust, flexible, and accessible platform technology. *JoVE*, e58882.
- BAI, H., SUN, F., YANG, G., WANG, L., ZHANG, Q., ZHANG, Q., ZHAN, Y., CHEN, J., YU, M., LI, C., YIN, R., YANG, X. & GE, C. 2018. CBLB502, a Toll-like receptor 5 agonist, offers protection against radiation-induced male reproductive system damage in mice†. *Biology of Reproduction*, 100, 281-291.
- BANKS, A. M., WHITFIELD, C. J., BROWN, S. R., FULTON, D. A., GOODCHILD, S. A., GRANT, C., LOVE, J., LENDREM, D. W., FIELDSSEND, J. E. & HOWARD,

- T. P. 2022. Key reaction components affect the kinetics and performance robustness of cell-free protein synthesis reactions. *Computational and Structural Biotechnology Journal*, 20, 218-229.
- BARTH, A. 2007. Infrared spectroscopy of proteins. *Biochimica et Biophysica Acta (BBA) - Bioenergetics*, 1767, 1073-1101.
- BENÍTEZ-MATEOS, A. I., ZEBALLOS, N., COMINO, N., MORENO DE REDROJO, L., RANDELOVIC, T. & LÓPEZ-GALLEGO, F. 2020. Microcompartmentalized Cell-Free Protein Synthesis in Hydrogel μ -Channels. *ACS Synthetic Biology*, 9, 2971-2978.
- BERG JM, T. J., STRYER L 2002a. Protein Structure and Function. *Biochemistry*. New York: W.H. Freeman.
- BERG JM, T. J., STRYER L. 2002b. Eukaryotic Protein Synthesis Differs from Prokaryotic Protein Synthesis Primarily in Translation Initiation. *Biochemistry*. New York: W H Freeman.
- BLUE, R. S., BAYUSE, T. M., DANIELS, V. R., WOTRING, V. E., SURESH, R., MULCAHY, R. A. & ANTONSEN, E. L. 2019. Supplying a pharmacy for NASA exploration spaceflight: challenges and current understanding. *npj Microgravity*, 5, 14.
- BORKOWSKI, O., KOCH, M., ZETTOR, A., PANDI, A., BATISTA, A. C., SOUDIER, P. & FAULON, J.-L. 2020. Large scale active-learning-guided exploration for in vitro protein production optimization. *Nature Communications*, 11, 1872.
- BREMS, D. N. 2002. The kinetics of G-CSF folding. *Protein Sci*, 11, 2504-11.
- BRIXEN, K., CHRISTENSEN, P., EJERSTED, C. & LANGDAHL, B. 2004. Teriparatide (Biosynthetic Human Parathyroid Hormone 1–34): A New Paradigm in the Treatment of Osteoporosis. *Basic & clinical pharmacology & toxicology*, 94, 260-70.
- BRONDYK, W. H. 2009. Chapter 11 Selecting an Appropriate Method for Expressing a Recombinant Protein. *In: BURGESS, R. R. & DEUTSCHER, M. P. (eds.) Methods in Enzymology*. Academic Press.
- BUNTRU, M., VOGEL, S., SPIEGEL, H. & SCHILLBERG, S. 2014. Tobacco BY-2 cell-free lysate: an alternative and highly-productive plant-based in vitro translation system. *BMC Biotechnology*, 14, 37.
- BURDELYA, L. G., KRIVOKRYSENKO, V. I., TALLANT, T. C., STROM, E., GLEIBERMAN, A. S., GUPTA, D., KURNASOV, O. V., FORT, F. L., OSTERMAN, A. L., DIDONATO, J. A., FEINSTEIN, E. & GUDKOV, A. V. 2008. An agonist of toll-like receptor 5 has radioprotective activity in mouse and primate models. *Science*, 320, 226-30.
- BUTREDDY, A., JANGA, K. Y., AJJARAPU, S., SARABU, S. & DUDHIPALA, N. 2021. Instability of therapeutic proteins – An overview of stresses, stabilization mechanisms and analytical techniques involved in lyophilized proteins. *International Journal of Biological Macromolecules*, 167, 309-325.
- BUTTGEREIT, F. & BRAND, M. D. 1995. A hierarchy of ATP-consuming processes in mammalian cells. *Biochem J*, 312 (Pt 1), 163-7.
- CAI, Q., HANSON, J. A., STEINER, A. R., TRAN, C., MASIKAT, M. R., CHEN, R., ZAWADA, J. F., SATO, A. K., HALLAM, T. J. & YIN, G. 2015. A simplified and robust protocol for immunoglobulin expression in Escherichia coli cell-free protein synthesis systems. *Biotechnol Prog*, 31, 823-31.

- CALERO, M. & GASSET, M. 2005. Fourier Transform Infrared and Circular Dichroism Spectroscopies for Amyloid Studies. *In: SIGURDSSON, E. M. (ed.) Amyloid Proteins: Methods and Protocols*. Totowa, NJ: Humana Press.
- CALHOUN, K. A. & SWARTZ, J. R. 2005. Energizing cell-free protein synthesis with glucose metabolism. *Biotechnology and Bioengineering*, 90, 606-613.
- CALHOUN, K. A. & SWARTZ, J. R. 2007. Energy Systems for ATP Regeneration in Cell-Free Protein Synthesis Reactions. *In: GRANDI, G. (ed.) In Vitro Transcription and Translation Protocols*. Totowa, NJ: Humana Press.
- CAO, J., PEREZ-PINERA, P., LOWENHAUPT, K., WU, M.-R., PURCELL, O., DE LA FUENTE-NUNEZ, C. & LU, T. K. 2018. Versatile and on-demand biologics co-production in yeast. *Nature Communications*, 9, 77.
- CARLSON, E. D., GAN, R., HODGMAN, C. E. & JEWETT, M. C. 2012. Cell-free protein synthesis: Applications come of age. *Biotechnology Advances*, 30, 1185-1194.
- CASCHERA, F., LEE, J. W., HO, K. K. Y., LIU, A. P. & JEWETT, M. C. 2016. Cell-free compartmentalized protein synthesis inside double emulsion templated liposomes with in vitro synthesized and assembled ribosomes. *Chemical communications (Cambridge, England)*, 52, 5467-5469.
- CHESNUT, C. H., AZRIA, M., SILVERMAN, S., ENGELHARDT, M., OLSON, M. & MINDEHOLM, L. 2008. Salmon calcitonin: a review of current and future therapeutic indications. *Osteoporosis International*, 19, 479-491.
- CLAASSENS, N. J., BURGNER, S., VÖGELI, B., ERB, T. J. & BAR-EVEN, A. 2019. A critical comparison of cellular and cell-free bioproduction systems. *Current Opinion in Biotechnology*, 60, 221-229.
- COLE, S. D., BEABOUT, K., TURNER, K. B., SMITH, Z. K., FUNK, V. L., HARBAUGH, S. V., LIEM, A. T., ROTH, P. A., GEIER, B. A., EMANUEL, P. A., WALPER, S. A., CHÁVEZ, J. L. & LUX, M. W. 2019. Quantification of Interlaboratory Cell-Free Protein Synthesis Variability. *ACS Synthetic Biology*, 8, 2080-2091.
- CRANFILL, P. J., SELL, B. R., BAIRD, M. A., ALLEN, J. R., LAVAGNINO, Z., DE GRUITER, H. M., KREMERS, G.-J., DAVIDSON, M. W., USTIONE, A. & PISTON, D. W. 2016. Quantitative assessment of fluorescent proteins. *Nature Methods*, 13, 557-562.
- CRICK, F. 1970a. Central dogma of molecular biology. *Nature*, 227, 561-3.
- CRICK, F. 1970b. Central Dogma of Molecular Biology. *Nature*, 227, 561-563.
- CROWELL, L. E., LU, A. E., LOVE, K. R., STOCKDALE, A., TIMMICK, S. M., WU, D., WANG, Y., DOHERTY, W., BONNYMAN, A., VECCHIARELLO, N., GOODWINE, C., BRADBURY, L., BRADY, J. R., CLARK, J. J., COLANT, N. A., CVETKOVIC, A., DALVIE, N. C., LIU, D., LIU, Y., MASCARENHAS, C. A., MATTHEWS, C. B., MOZDZIERZ, N. J., SHAH, K. A., WU, S.-L., HANCOCK, W. S., BRAATZ, R. D., CRAMER, S. M. & LOVE, J. C. 2018. On-demand manufacturing of clinical-quality biopharmaceuticals. *Nature Biotechnology*, 36, 988-995.
- CUI, J., WU, D., SUN, Q., YANG, X., WANG, D., ZHUANG, M., ZHANG, Y., GAN, M. & LUO, D. 2020. A PEGDA/DNA Hybrid Hydrogel for Cell-Free Protein Synthesis. *Frontiers in Chemistry*, 8.

- DAI, D., HORVATH, N. & VARNER, J. 2018. Dynamic Sequence Specific Constraint-Based Modeling of Cell-Free Protein Synthesis. *Processes*, 6, 132.
- DANG, B., MRAVIC, M., HU, H., SCHMIDT, N., MENSA, B. & DEGRADO, W. F. 2019. SNAC-tag for sequence-specific chemical protein cleavage. *Nat Methods*, 16, 319-322.
- DANIEL, R. M. & COWAN, D. A. 2000. Biomolecular stability and life at high temperatures. *Cellular and Molecular Life Sciences CMLS*, 57, 250-264.
- DE MARCO, A. 2009. Strategies for successful recombinant expression of disulfide bond-dependent proteins in Escherichia coli. *Microbial Cell Factories*, 8, 26.
- DES SOYE, B. J., GERBASI, V. R., THOMAS, P. M., KELLEHER, N. L. & JEWETT, M. C. 2019. A Highly Productive, One-Pot Cell-Free Protein Synthesis Platform Based on Genomically Recoded Escherichia coli. *Cell Chemical Biology*, 26, 1743-1754.e9.
- DESOUKY, O., DING, N. & ZHOU, G. 2015. Targeted and non-targeted effects of ionizing radiation. *Journal of Radiation Research and Applied Sciences*, 8, 247-254.
- DEWINTER, M. A., THAMES, A. H., GUERRERO, L., KIGHTLINGER, W., KARIM, A. S. & JEWETT, M. C. 2023. Point-of-Care Peptide Hormone Production Enabled by Cell-Free Protein Synthesis. *ACS Synthetic Biology*, 12, 1216-1226.
- DIDOVYK, A., TONOOKA, T., TSIMRING, L. & HASTY, J. 2017. Rapid and Scalable Preparation of Bacterial Lysates for Cell-Free Gene Expression. *ACS Synthetic Biology*, 6, 2198-2208.
- DMITRIEV, O. Y., LUTSENKO, S. & MUYLDERMANS, S. 2016. Nanobodies as Probes for Protein Dynamics in Vitro and in Cells. *J Biol Chem*, 291, 3767-75.
- DONDAPATI, S. K., PIETRUSCHKA, G., THORING, L., WÜSTENHAGEN, D. A. & KUBICK, S. 2019. Cell-free synthesis of human toll-like receptor 9 (TLR9): Optimization of synthesis conditions and functional analysis. *PLOS ONE*, 14, e0215897.
- DONDAPATI, S. K., STECH, M., ZEMELLA, A. & KUBICK, S. 2020. Cell-Free Protein Synthesis: A Promising Option for Future Drug Development. *BioDrugs*, 34, 327-348.
- DOPP, J. L. & REUEL, N. F. 2019. One-Pot *E. coli* Cell-Free Extract for *in vitro* Expression of Disulfide Bonded Proteins. *bioRxiv*, 2019.12.19.883413.
- EMA 1994. PRODUCTION AND QUALITY CONTROL OF MEDICINAL PRODUCTS DERIVED BY RECOMBINANT DNA TECHNOLOGY. *In*: AGENCY, E. M. (ed.).
- EMA 2003. NOTE FOR GUIDANCE ON STABILITY TESTING: STABILITY TESTING OF NEW DRUG SUBSTANCES AND PRODUCTS. *In*: AGENCY, E. M. (ed.) CPMP/ICH/2736/99. London.
- EMA 2007. Epoetin Alfa Hexal. Holzkirchen, Germany: European Medicines Agency.
- EYAL, S. & DERENDORF, H. 2019. Medications in Space: In Search of a Pharmacologist's Guide to the Galaxy. *Pharmaceutical Research*, 36, 148.
- EZURE, T., SUZUKI, T., SHIKATA, M., ITO, M. & ANDO, E. 2010. A cell-free protein synthesis system from insect cells. *Methods Mol Biol*, 607, 31-42.
- FAILMEZGER, J., RAUTER, M., NITSCHHEL, R., KRAML, M. & SIEMANN-HERZBERG, M. 2017. Cell-free protein synthesis from non-growing, stressed Escherichia coli. *Scientific Reports*, 7, 16524.

- FAILMEZGER, J., SCHOLZ, S., BLOMBACH, B. & SIEMANN-HERZBERG, M. 2018. Cell-Free Protein Synthesis From Fast-Growing *Vibrio natriegens*. *Frontiers in Microbiology*, 9.
- FALLAH-ARAGHI, A., BARET, J.-C., RYCKELYNCK, M. & GRIFFITHS, A. D. 2012. A completely in vitro ultrahigh-throughput droplet-based microfluidic screening system for protein engineering and directed evolution. *Lab on a Chip*, 12, 882-891.
- FDA 2003. Guidance for Industry Q1A(R2) Stability Testing of New Drug Substances and Products. In: SERVICES, U. S. D. O. H. A. H. (ed.). Rockville, MD.
- FDA 2013. Strategic Plan for Preventing and Mitigating Drug Shortages In: ADMINISTRATION, F. A. D. (ed.). online: FDA.
- FOLEY, P. L. & SHULER, M. L. 2010. Considerations for the design and construction of a synthetic platform cell for biotechnological applications. *Biotechnology and Bioengineering*, 105, 26-36.
- FOTHERGILL-GILMORE, L. A. 1993. Recombinant Protein Technology. In: FRANKS, F. (ed.) *Protein Biotechnology: Isolation, Characterization, and Stabilization*. Totowa, NJ: Humana Press.
- FRANK, J., RICHTER, M., DE ROSSI, C., LEHR, C.-M., FUHRMANN, K. & FUHRMANN, G. 2018. Extracellular vesicles protect glucuronidase model enzymes during freeze-drying. *Scientific Reports*, 8, 12377.
- GAMBLE, J. F., CHIU, W. S., GRAY, V., TOALE, H., TOBYN, M. & WU, Y. 2010. Investigation into the degree of variability in the solid-state properties of common pharmaceutical excipients-anhydrous lactose. *AAPS PharmSciTech*, 11, 1552-7.
- GAO, W., CHO, E., LIU, Y. & LU, Y. 2019. Advances and Challenges in Cell-Free Incorporation of Unnatural Amino Acids Into Proteins. *Frontiers in Pharmacology*, 10.
- GE, X., LUO, D. & XU, J. 2011. Cell-Free Protein Expression under Macromolecular Crowding Conditions. *PLOS ONE*, 6, e28707.
- GHAHEH, H. S., GANJALIKHANY, M. R., YAGHMAEI, P., POURFARZAM, M. & MIR MOHAMMAD SADEGHI, H. 2019. Improving the solubility, activity, and stability of reteplase using in silico design of new variants. *Res Pharm Sci*, 14, 359-368.
- GOLDHABER, S. Z. 2001. Thrombolysis in pulmonary embolism: a debatable indication. *Thromb Haemost*, 86, 444-51.
- GOORMAGHTIGH, E., GASPER, R., BÉNARD, A., GOLDSZTEIN, A. & RAUSSENS, V. 2009. Protein secondary structure content in solution, films and tissues: Redundancy and complementarity of the information content in circular dichroism, transmission and ATR FTIR spectra. *Biochimica et Biophysica Acta (BBA) - Proteins and Proteomics*, 1794, 1332-1343.
- GOVAERT, J., PELLIS, M., DESCHACHT, N., VINCKE, C., CONRATH, K., MUYLDERMANS, S. & SAERENS, D. 2012. Dual Beneficial Effect of Interloop Disulfide Bond for Single Domain Antibody Fragments*. *Journal of Biological Chemistry*, 287, 1970-1979.
- GRÄWE, A., DREYER, A., VORNHOLT, T., BARTECZKO, U., BUCHHOLZ, L., DREWS, G., HO, U. L., JACKOWSKI, M. E., KRACHT, M., LÜDERS, J., BLECKWEHL, T., ROSITZKA, L., RUWE, M., WITTCHEM, M., LUTTER, P.,

- MÜLLER, K. & KALINOWSKI, J. 2019. A paper-based, cell-free biosensor system for the detection of heavy metals and date rape drugs. *PLOS ONE*, 14, e0210940.
- GREENFIELD, N. J. 2006. Using circular dichroism spectra to estimate protein secondary structure. *Nature Protocols*, 1, 2876-2890.
- GREGORIO, N. E., KAO, W. Y., WILLIAMS, L. C., HIGHT, C. M., PATEL, P., WATTS, K. R. & OZA, J. P. 2020. Unlocking Applications of Cell-Free Biotechnology through Enhanced Shelf Life and Productivity of *E. coli* Extracts. *ACS Synthetic Biology*, 9, 766-778.
- GREGORIO, N. E., LEVINE, M. Z. & OZA, J. P. 2019a. A User's Guide to Cell-Free Protein Synthesis. *Methods and protocols*, 2, 24.
- GREGORIO, N. E., LEVINE, M. Z. & OZA, J. P. 2019b. A User's Guide to Cell-Free Protein Synthesis. *Methods and Protocols*, 2, 24.
- GRINSTEIN, J. D. 2023. The Long and Winding Road: On-Demand DNA Synthesis in High Demand. *GEN Biotechnology*, 2, 63-68.
- GUERRERO, F., CIRAGAN, A. & IWAÏ, H. 2015. Tandem SUMO fusion vectors for improving soluble protein expression and purification. *Protein Expr Purif*, 116, 42-9.
- GUO, X., ZHU, Y., BAI, L. & YANG, D. 2020. The Protection Role of Magnesium Ions on Coupled Transcription and Translation in Lyophilized Cell-Free System. *ACS Synthetic Biology*, 9, 856-863.
- GUZMAN-CHAVEZ, F., ARCE, A., ADHIKARI, A., VADHIN, S., PEDROZA-GARCIA, J. A., GANDINI, C., AJIOKA, J. W., MOLLOY, J., SANCHEZ-NIETO, S., VARNER, J. D., FEDERICI, F. & HASELOFF, J. 2022. Constructing Cell-Free Expression Systems for Low-Cost Access. *ACS Synthetic Biology*, 11, 1114-1128.
- HAGIHARA, Y., MINE, S. & UEGAKI, K. 2007. Stabilization of an immunoglobulin fold domain by an engineered disulfide bond at the buried hydrophobic region. *J Biol Chem*, 282, 36489-95.
- HANSEN, M. M., VENTOSA ROSQUELLES, M., YELLESWARAPU, M., MAAS, R. J., VAN VUGT-JONKER, A. J., HEUS, H. A. & HUCK, W. T. 2016. Protein Synthesis in Coupled and Uncoupled Cell-Free Prokaryotic Gene Expression Systems. *ACS Synth Biol*, 5, 1433-1440.
- HARVISON, P. J. 2008. Tenecteplase. In: ENNA, S. J. & BYLUND, D. B. (eds.) *xPharm: The Comprehensive Pharmacology Reference*. New York: Elsevier.
- HERBERHOLD, H., MARCHAL, S., LANGE, R., SCHEYHING, C. H., VOGEL, R. F. & WINTER, R. 2003. Characterization of the Pressure-induced Intermediate and Unfolded State of Red-shifted Green Fluorescent Protein—A Static and Kinetic FTIR, UV/VIS and Fluorescence Spectroscopy Study. *Journal of Molecular Biology*, 330, 1153-1164.
- HODGMAN, C. E. & JEWETT, M. C. 2013. Optimized extract preparation methods and reaction conditions for improved yeast cell-free protein synthesis. *Biotechnology and Bioengineering*, 110, 2643-2654.
- HODKINSON, P. D., ANDERTON, R. A., POSSELT, B. N. & FONG, K. J. 2017. An overview of space medicine. *BJA: British Journal of Anaesthesia*, 119, i143-i153.
- HUNT, J. P., GALIARDI, J., FREE, T. J., YANG, S. O., POOLE, D., ZHAO, E. L., ANDERSEN, J. L., WOOD, D. W. & BUNDY, B. C. 2022. Mechanistic

- discoveries and simulation-guided assay optimization of portable hormone biosensors with cell-free protein synthesis. *Biotechnology Journal*, 17, 2100152.
- HUNT, J. P., YANG, S. O., WILDING, K. M. & BUNDY, B. C. 2017. The growing impact of lyophilized cell-free protein expression systems. *Bioengineered*, 8, 325-330.
- HUNTER, D. J. B., BHUMKAR, A., GILES, N., SIERECKI, E. & GAMBIN, Y. 2018. Unexpected instabilities explain batch-to-batch variability in cell-free protein expression systems. *Biotechnol Bioeng*, 115, 1904-1914.
- ISECG 2018. Global Exploration Roadmap. International Space Exploration Coordination Group.
- IZADI, S., JALALI JAVARAN, M., RASHIDI MONFARED, S. & CASTILHO, A. 2021. Reteplase Fc-fusions produced in *N. benthamiana* are able to dissolve blood clots ex vivo. *PLoS One*, 16, e0260796.
- JACKSON, K., KHNOUF, R. & FAN, Z. H. 2014. Cell-free protein synthesis in microfluidic 96-well plates. *Methods Mol Biol*, 1118, 157-68.
- JACKSON, M. & MANTSCH, H. H. 1995. The use and misuse of FTIR spectroscopy in the determination of protein structure. *Crit Rev Biochem Mol Biol*, 30, 95-120.
- JAROENTOMEECHAI, T., STARK, J. C., NATARAJAN, A., GLASSCOCK, C. J., YATES, L. E., HSU, K. J., MRKSICH, M., JEWETT, M. C. & DELISA, M. P. 2018. Single-pot glycoprotein biosynthesis using a cell-free transcription-translation system enriched with glycosylation machinery. *Nature Communications*, 9, 2686.
- JENKINS, D. A. 2023. Battlefield Medicine. In: DOD (ed.). Department of defense.
- JEWETT, M. C., MILLER, M. L., CHEN, Y. & SWARTZ, J. R. 2009a. Continued protein synthesis at low [ATP] and [GTP] enables cell adaptation during energy limitation. *Journal of Bacteriology*, 191, 1083-1091.
- JEWETT, M. C., MILLER, M. L., CHEN, Y. & SWARTZ, J. R. 2009b. Continued protein synthesis at low [ATP] and [GTP] enables cell adaptation during energy limitation. *J Bacteriol*, 191, 1083-91.
- JIANG, N., DING, X. & LU, Y. 2021. Development of a robust *Escherichia coli*-based cell-free protein synthesis application platform. *Biochem Eng J*, 165, 107830.
- JIN, X., KIGHTLINGER, W. & HONG, S. H. 2019. Optimizing Cell-Free Protein Synthesis for Increased Yield and Activity of Colicins. *Methods and Protocols*, 2, 28.
- JOHNSTON, S. L., BLUE, R. S., JENNINGS, R. T., TARVER, W. J. & GRAY, G. W. 2014. Astronaut Medical Selection During the Shuttle Era: 1981-2011. *Aviation, Space, and Environmental Medicine*, 85, 823-827.
- JONES, G., RONK, M., MORI, F. & ZHANG, Z. 2001. Disulfide structure of alfimeprase: A recombinant analog of fibrolase. *Protein Science*, 10, 1264-1267.
- JOVANOVIĆ, N., BOUCHARD, A., HOFLAND, G. W., WITKAMP, G. J., CROMMELIN, D. J. & JISKOOT, W. 2006. Distinct effects of sucrose and trehalose on protein stability during supercritical fluid drying and freeze-drying. *Eur J Pharm Sci*, 27, 336-45.
- JUNG, J. K., ALAM, K. K., VEROSLOFF, M. S., CAPDEVILA, D. A., DESMAU, M., CLAUER, P. R., LEE, J. W., NGUYEN, P. Q., PASTÉN, P. A., MATIASEK, S. J., GAILLARD, J. F., GIEDROC, D. P., COLLINS, J. J. & LUCKS, J. B. 2020.

- Cell-free biosensors for rapid detection of water contaminants. *Nat Biotechnol*, 38, 1451-1459.
- KARIG, D. K., BESSLING, S., THIELEN, P., ZHANG, S. & WOLFE, J. 2017. Preservation of protein expression systems at elevated temperatures for portable therapeutic production. *Journal of The Royal Society Interface*, 14, 20161039.
- KARLIKOW, M., DA SILVA, S. J. R., GUO, Y., CICEK, S., KROKOVSKY, L., HOMME, P., XIONG, Y., XU, T., CALDERÓN-PELÁEZ, M. A., CAMACHO-ORTEGA, S., MA, D., DE MAGALHÃES, J. J. F., SOUZA, B., DE ALBUQUERQUE CABRAL, D. G., JAENES, K., SUTYRINA, P., FERRANTE, T., BENITEZ, A. D., NIPAZ, V., PONCE, P., RACKUS, D. G., COLLINS, J. J., PAIVA, M., CASTELLANOS, J. E., CEVALLOS, V., GREEN, A. A., AYRES, C., PENA, L. & PARDEE, K. 2022. Field validation of the performance of paper-based tests for the detection of the Zika and chikungunya viruses in serum samples. *Nat Biomed Eng*, 6, 246-256.
- KARZBRUN, E., SHIN, J., BAR-ZIV, R. H. & NOIREAUX, V. 2011. Coarse-grained dynamics of protein synthesis in a cell-free system. *Phys Rev Lett*, 106, 048104.
- KASPER, J. C., WINTER, G. & FRIESS, W. 2013. Recent advances and further challenges in lyophilization. *European Journal of Pharmaceutics and Biopharmaceutics*, 85, 162-169.
- KEIPER, F. & ATANASSOVA, A. 2020. Regulation of Synthetic Biology: Developments Under the Convention on Biological Diversity and Its Protocols. *Front Bioeng Biotechnol*, 8, 310.
- KHAMBHATI, K., BHATTACHARJEE, G., GOHIL, N., BRADDICK, D., KULKARNI, V. & SINGH, V. 2019. Exploring the Potential of Cell-Free Protein Synthesis for Extending the Abilities of Biological Systems. *Frontiers in Bioengineering and Biotechnology*, 7.
- KIGAWA, T., YABUKI, T., MATSUDA, N., MATSUDA, T., NAKAJIMA, R., TANAKA, A. & YOKOYAMA, S. 2004. Preparation of Escherichia coli cell extract for highly productive cell-free protein expression. *Journal of Structural and Functional Genomics*, 5, 63-68.
- KIM, D.-M. & SWARTZ, J. R. 2001. Regeneration of adenosine triphosphate from glycolytic intermediates for cell-free protein synthesis. *Biotechnology and Bioengineering*, 74, 309-316.
- KIM, H. C., KIM, K. S., KANG, T. J., CHOI, J. H., SONG, J. J., CHOI, Y. H., KIM, B. G. & KIM, D. M. 2015. Implementing bacterial acid resistance into cell-free protein synthesis for buffer-free expression and screening of enzymes. *Biotechnol Bioeng*, 112, 2630-5.
- KIM, T.-W., KEUM, J.-W., OH, I.-S., CHOI, C.-Y., KIM, H.-C. & KIM, D.-M. 2007. An economical and highly productive cell-free protein synthesis system utilizing fructose-1,6-bisphosphate as an energy source. *Journal of Biotechnology*, 130, 389-393.
- KIM, T.-W., KIM, D.-M. & CHOI, C.-Y. 2006a. Rapid production of milligram quantities of proteins in a batch cell-free protein synthesis system. *Journal of Biotechnology*, 124, 373-380.

- KIM, T. W., KEUM, J. W., OH, I. S., CHOI, C. Y., PARK, C. G. & KIM, D. M. 2006b. Simple procedures for the construction of a robust and cost-effective cell-free protein synthesis system. *J Biotechnol*, 126, 554-61.
- KIMPLE, M. E., BRILL, A. L. & PASKER, R. L. 2013. Overview of affinity tags for protein purification. *Current protocols in protein science*, 73, 9.9.1-9.9.23.
- KRINSKY, N., KADURI, M., SHAINSKY-ROITMAN, J., GOLDFEDER, M., IVANIR, E., BENHAR, I., SHOHAM, Y. & SCHROEDER, A. 2016. A Simple and Rapid Method for Preparing a Cell-Free Bacterial Lysate for Protein Synthesis. *PLoS One*, 11, e0165137.
- KRINSKY, N., KADURI, M., ZINGER, A., SHAINSKY-ROITMAN, J., GOLDFEDER, M., BENHAR, I., HERSHKOVITZ, D. & SCHROEDER, A. 2018. Synthetic Cells Synthesize Therapeutic Proteins inside Tumors. *Advanced Healthcare Materials*, 7, 1701163.
- KUNZ, P., ZINNER, K., MÜCKE, N., BARTOSCHIK, T., MUYLDERMANS, S. & HOHEISEL, J. D. 2018. The structural basis of nanobody unfolding reversibility and thermoresistance. *Scientific Reports*, 8, 7934.
- KWON, Y.-C. & JEWETT, M. C. 2015. High-throughput preparation methods of crude extract for robust cell-free protein synthesis. *Scientific Reports*, 5, 8663.
- LE, H. V. & TROTTA, P. P. 1991. Purification of secreted recombinant proteins from *Escherichia coli*. *Bioprocess Technol*, 12, 163-81.
- LEDERMAN, M. & ZUBAY, G. 1967. DNA-directed peptide synthesis I. A comparison of T2 and *Escherichia coli* DNA-directed peptide synthesis in two cell-free systems. *Biochimica et Biophysica Acta (BBA) - Nucleic Acids and Protein Synthesis*, 149, 253-258.
- LEVINE, M. Z., GREGORIO, N. E., JEWETT, M. C., WATTS, K. R. & OZA, J. P. 2019. *Escherichia coli*-Based Cell-Free Protein Synthesis: Protocols for a robust, flexible, and accessible platform technology. *J Vis Exp*.
- LI, H., HUANG, Y., WEI, Z., WANG, W., YANG, Z., LIANG, Z. & LI, Z. 2019. An oligonucleotide synthesizer based on a microreactor chip and an inkjet printer. *Scientific Reports*, 9, 5058.
- LI, J., WANG, H., KWON, Y.-C. & JEWETT, M. 2017. Establishing a high yielding *Streptomyces*-based cell-free protein synthesis system. *Biotechnology and Bioengineering*, 114.
- LIN, X., LI, Y., LI, Z., HUA, R., XING, Y. & LU, Y. 2020. Portable environment-signal detection biosensors with cell-free synthetic biosystems. *RSC Advances*, 10, 39261-39265.
- LIU, D. V., ZAWADA, J. F. & SWARTZ, J. R. 2005. Streamlining *Escherichia Coli* S30 Extract Preparation for Economical Cell-Free Protein Synthesis. *Biotechnology Progress*, 21, 460-465.
- LIU, H., SCHITTNY, V. & NASH, M. A. 2019. Removal of a Conserved Disulfide Bond Does Not Compromise Mechanical Stability of a VHH Antibody Complex. *Nano Letters*, 19, 5524-5529.
- LU, R., ZHANG, T., SONG, S., ZHOU, M., JIANG, L., HE, Z., YUAN, Y., YUAN, T., LU, Y., YAN, K. & CHENG, Y. 2019. Accurately cleavable goat β -lactoglobulin signal peptide efficiently guided translation of a recombinant human plasminogen activator in transgenic rabbit mammary gland. *Biosci Rep*, 39.

- MA, T., LI, Z. & WANG, S. 2019. Production of Bioactive Recombinant Reteplase by Virus-Based Transient Expression System in *Nicotiana benthamiana*. *Frontiers in Plant Science*, 10.
- MALAGON, F. 2013. RNase III is required for localization to the nucleoid of the 5' pre-rRNA leader and for optimal induction of rRNA synthesis in *E. coli*. *Rna*, 19, 1200-7.
- MANDI, N., SUNDARAM, K. R., TANDRA, S. K., BANDYOPADHYAY, S. & PADMANABHAN, S. 2010. Asn and asn: critical residues for in vitro biological activity of reteplase. *Adv Hematol*, 2010, 172484.
- MANOHAR, P. & RAMESH, N. 2019. Improved lyophilization conditions for long-term storage of bacteriophages. *Scientific Reports*, 9, 15242.
- MCSWEENEY, M. A. & STYCZYNSKI, M. P. 2021. Effective Use of Linear DNA in Cell-Free Expression Systems. *Frontiers in Bioengineering and Biotechnology*, 9.
- MEHTA, H. M., MALANDRA, M. & COREY, S. J. 2015. G-CSF and GM-CSF in Neutropenia. *Journal of immunology (Baltimore, Md. : 1950)*, 195, 1341-1349.
- MENG, Y., YANG, M., LIU, W. & LI, J. 2023. Cell-Free Expression of a Therapeutic Protein Serratiopeptidase. *Molecules*, 28, 3132.
- MERIVAARA, A., ZINI, J., KOIVUNOTKO, E., VALKONEN, S., KORHONEN, O., FERNANDES, F. M. & YLIPERTTULA, M. 2021. Preservation of biomaterials and cells by freeze-drying: Change of paradigm. *Journal of Controlled Release*, 336, 480-498.
- MHRA 2021. New guidance and information for industry from the MHRA. In: AGENCY, M. A. H. P. R. (ed.).
- MORITA, E. H., SAWASAKI, T., TANAKA, R., ENDO, Y. & KOHNO, T. 2003. A wheat germ cell-free system is a novel way to screen protein folding and function. *Protein science : a publication of the Protein Society*, 12, 1216-1221.
- MURPHY, T. W., SHENG, J., NALER, L. B., FENG, X. & LU, C. 2019. On-chip manufacturing of synthetic proteins for point-of-care therapeutics. *Microsystems & Nanoengineering*, 5, 13.
- NAEIMIPOUR, S., SHOJAOSADATI, S. A. & FAZELI, A. 2020. FTIR Investigation of Secondary Structure of Reteplase Inclusion Bodies Produced in *Escherichia coli* in Terms of Urea Concentration. *Iran J Pharm Res*, 19, 175-181.
- NAGARAJ, V. H., GREENE, J. M., SENGUPTA, A. M. & SONTAG, E. D. 2017. Translation inhibition and resource balance in the TX-TL cell-free gene expression system. *Synthetic Biology*, 2.
- NASA. 2018. *Apollo 8* [Online]. NASA. Available: https://www.nasa.gov/mission_pages/station/main/index.html [Accessed 20th January 2020].
- NATIONAL ACADEMIES OF SCIENCES, E. & MEDICINE 2018. *Biodefense in the Age of Synthetic Biology*, Washington, DC, The National Academies Press.
- NCBI 2023. PubChem Compound Summary for CID 16129704, Bivalirudin.
- NEB. 2020. *The Next Generation of Cell-Free Protein Synthesis* [Online]. New England Biolabs Incorporated. Available: <https://international.neb.com/tools-and-resources/feature-articles/the-next-generation-of-cell-free-protein-synthesis> [Accessed 15th May 2020].
- NIEß, A., FAILMEZGER, J., KUSCHEL, M., SIEMANN-HERZBERG, M. & TAKORS, R. 2017. Experimentally Validated Model Enables Debottlenecking of in Vitro

- Protein Synthesis and Identifies a Control Shift under in Vivo Conditions. *ACS Synthetic Biology*, 6, 1913-1921.
- NIH 2008. Alfimeprase. *Drugs R D*, 9, 185-90.
- NIRENBERG, M. 2004. Historical review: Deciphering the genetic code--a personal account. *Trends Biochem Sci*, 29, 46-54.
- NIRENBERG, M. W. & MATTHAEI, J. H. 1961. The dependence of cell-free protein synthesis in *E. coli* upon naturally occurring or synthetic polyribonucleotides. *Proc Natl Acad Sci U S A*, 47, 1588-602.
- NISHIMURA, K., MATSUURA, T., NISHIMURA, K., SUNAMI, T., SUZUKI, H. & YOMO, T. 2012. Cell-Free Protein Synthesis inside Giant Unilamellar Vesicles Analyzed by Flow Cytometry. *Langmuir*, 28, 8426-8432.
- NOIREAUX, V. & LIBCHABER, A. 2004. A vesicle bioreactor as a step toward an artificial cell assembly. *Proceedings of the National Academy of Sciences of the United States of America*, 101, 17669.
- NOIREAUX, V., MAEDA, Y. T. & LIBCHABER, A. 2011. Development of an artificial cell, from self-organization to computation and self-reproduction. *Proc Natl Acad Sci U S A*, 108, 3473-80.
- NOMOTO, M. & TADA, Y. 2018. Cloning-free template DNA preparation for cell-free protein synthesis via two-step PCR using versatile primer designs with short 3'-UTR. *Genes Cells*, 23, 46-53.
- NOTARANGELO, M., QUATTRONE, A., PIZZATO, M., MANSY, S. S. & TOPARLAK, Ö. D. 2021. Inexpensive and colorimetric RNA detection by *E. coli* cell-free protein synthesis platform at room temperature. *medRxiv*, 2021.11.29.21267025.
- OLENGINSKI, G. M., PIACENTINI, J., HARRIS, D. R., RUNKO, N. A., PAPOUTSIS, B. M., ALTER, J. R., HESS, K. R., BREWER, S. H. & PHILLIPS-PIRO, C. M. 2021. Structural and spectrophotometric investigation of two unnatural amino-acid altered chromophores in the superfolder green fluorescent protein. *Acta Crystallogr D Struct Biol*, 77, 1010-1018.
- PARDEE, K. 2018. Perspective: Solidifying the impact of cell-free synthetic biology through lyophilization. *Biochemical engineering journal*, 138, 91-97.
- PARDEE, K., GREEN, A. A., FERRANTE, T., CAMERON, D. E., DALEYKEYSER, A., YIN, P. & COLLINS, J. J. 2014. Paper-based synthetic gene networks. *Cell*, 159, 940-54.
- PARDEE, K., GREEN, A. A., TAKAHASHI, M. K., BRAFF, D., LAMBERT, G., LEE, J. W., FERRANTE, T., MA, D., DONGHIA, N., FAN, M., DARINGER, N. M., BOSCH, I., DUDLEY, D. M., O'CONNOR, D. H., GEHRKE, L. & COLLINS, J. J. 2016a. Rapid, Low-Cost Detection of Zika Virus Using Programmable Biomolecular Components. *Cell*, 165, 1255-1266.
- PARDEE, K., SLOMOVIC, S., NGUYEN, P. Q., LEE, J. W., DONGHIA, N., BURRILL, D., FERRANTE, T., MCSORLEY, F. R., FURUTA, Y., VERNET, A., LEWANDOWSKI, M., BODDY, C. N., JOSHI, N. S. & COLLINS, J. J. 2016b. Portable, On-Demand Biomolecular Manufacturing. *Cell*, 167, 248-259.e12.
- PÉDELACQ, J.-D., CABANTOUS, S., TRAN, T., TERWILLIGER, T. C. & WALDO, G. S. 2006. Engineering and characterization of a superfolder green fluorescent protein. *Nature Biotechnology*, 24, 79-88.

- PEREZ-PINERA, P., HAN, N., CLETO, S., CAO, J., PURCELL, O., SHAH, K. A., LEE, K., RAM, R. & LU, T. K. 2016. Synthetic biology and microreactor platforms for programmable production of biologics at the point-of-care. *Nature Communications*, 7, 12211.
- PERUZZI, J. A., JACOBS, M. L., VU, T. Q., WANG, K. S. & KAMAT, N. P. 2019. Barcoding Biological Reactions with DNA-Functionalized Vesicles. *Angewandte Chemie International Edition*, 58, 18683-18690.
- PETROS, S. 2008. Lepirudin in the management of patients with heparin-induced thrombocytopenia. *Biologics*, 2, 481-90.
- PETROV, A. S., BERNIER, C. R., HSIAO, C., OKAFOR, C. D., TANNENBAUM, E., STERN, J., GAUCHER, E., SCHNEIDER, D., HUD, N. V., HARVEY, S. C. & DEAN WILLIAMS, L. 2012. RNA–Magnesium–Protein Interactions in Large Ribosomal Subunit. *The Journal of Physical Chemistry B*, 116, 8113-8120.
- PIANTADOSI, C. A. 2003. *The Biology of Human Survival : Life and Death in Extreme Environments*, Cary, UNITED STATES, Oxford University Press, Incorporated.
- RAMPELOTTO, P. H. 2013. Extremophiles and extreme environments. *Life (Basel, Switzerland)*, 3, 482-485.
- REED, M., KERNDT, CC., NICOLAS, D. 2023. Alteplase. *StatPearls [Internet]*.
- ROSANO, G. L., MORALES, E. S. & CECCARELLI, E. A. 2019. New tools for recombinant protein production in Escherichia coli: A 5-year update. *Protein Sci*, 28, 1412-1422.
- ROSENBLUM, G. & COOPERMAN, B. S. 2014. Engine out of the chassis: cell-free protein synthesis and its uses. *FEBS Lett*, 588, 261-8.
- ROTHCHILD, L., LOFTUS, D., ADAMALA, K., SNYDER, J. & WILLIAMS, P. 2019. Astropharmacy. Project Proposal.
- ROTHSCHILD, L. 2020. An Astropharmacy. NASA Ames Research Center: NASA.
- ROTHSCHILD, L. J. & MANCINELLI, R. L. 2001. Life in extreme environments. *Nature*, 409, 1092-1101.
- RUDIKOFF, S. & PUMPHREY, J. G. 1986. Functional antibody lacking a variable-region disulfide bridge. *Proceedings of the National Academy of Sciences*, 83, 7875-7878.
- SACHSE, R., DONDAPATI, S. K., FENZ, S. F., SCHMIDT, T. & KUBICK, S. 2014. Membrane protein synthesis in cell-free systems: From bio-mimetic systems to bio-membranes. *FEBS Letters*, 588, 2774-2781.
- SACHSE, R., WÜSTENHAGEN, D., ŠAMALÍKOVÁ, M., GERRITS, M., BIER, F. F. & KUBICK, S. 2013. Synthesis of membrane proteins in eukaryotic cell-free systems. *Engineering in Life Sciences*, 13, 39-48.
- SADAT, A. & JOYE, I. J. 2020. Peak Fitting Applied to Fourier Transform Infrared and Raman Spectroscopic Analysis of Proteins. *Applied Sciences*, 10, 5918.
- SADEGHI, H. M. M., RABBANI, M., RISMANI, E., MOAZEN, F., KHODABAKHSH, F., DORMIANI, K. & KHAZAEI, Y. 2011. Optimization of the expression of reteplase in Escherichia coli. *Research in pharmaceutical sciences*, 6, 87-92.
- SAEKI, D., SUGIURA, S., KANAMORI, T., SATO, S. & ICHIKAWA, S. 2014. Microcompartmentalized cell-free protein synthesis in semipermeable microcapsules composed of polyethylenimine-coated alginate. *Journal of Bioscience and Bioengineering*, 118, 199-204.

- SALEHI, A. S., SMITH, M. T., BENNETT, A. M., WILLIAMS, J. B., PITT, W. G. & BUNDY, B. C. 2016a. Cell-free protein synthesis of a cytotoxic cancer therapeutic: Onconase production and a just-add-water cell-free system. *Biotechnol J*, 11, 274-81.
- SALEHI, A. S. M., SMITH, M. T., BENNETT, A. M., WILLIAMS, J. B., PITT, W. G. & BUNDY, B. C. 2016b. Cell-free protein synthesis of a cytotoxic cancer therapeutic: Onconase production and a just-add-water cell-free system. *Biotechnology Journal*, 11, 274-281.
- SANTOS, R., URSU, O., GAULTON, A., BENTO, A. P., DONADI, R. S., BOLOGA, C. G., KARLSSON, A., AL-LAZIKANI, B., HERSEY, A., OPREA, T. I. & OVERINGTON, J. P. 2017. A comprehensive map of molecular drug targets. *Nat Rev Drug Discov*, 16, 19-34.
- SATO, W., SHARON, J., DEICH, C., GAUT, N., CASH, B., ENGELHART, A. E. & ADAMALA, K. P. 2022. Akaby-Cell-free protein expression system for linear templates. *PLoS One*, 17, e0266272.
- SAWYERS, L., ANDERSON, C., BOYD, M. J., HESSEL, V., WOTRING, V., WILLIAMS, P. M. & TOH, L. S. 2022. Astropharmacy: Pushing the boundaries of the pharmacists' role for sustainable space exploration. *Research in Social and Administrative Pharmacy*, 18, 3612-3621.
- SCHEIN, C. H. 1989. Production of Soluble Recombinant Proteins in Bacteria. *Bio/Technology*, 7, 1141-1149.
- SCHWARZ, D., JUNGE, F., DURST, F., FRÖLICH, N., SCHNEIDER, B., RECKEL, S., SOBHANIFAR, S., DÖTSCH, V. & BERNHARD, F. 2007. Preparative scale expression of membrane proteins in Escherichia coli-based continuous exchange cell-free systems. *Nature Protocols*, 2, 2945-2957.
- SEOANE-VIAÑO, I., ONG, J. J., BASIT, A. W. & GOYANES, A. 2022. To infinity and beyond: Strategies for fabricating medicines in outer space. *International Journal of Pharmaceutics: X*, 4, 100121.
- SHELLEY, S. 2022. The Road Ahead for the Pharma Cold Chain. *BioPharm International*, 35, 31-34.
- SHIMIZU, Y., INOUE, A., TOMARI, Y., SUZUKI, T., YOKOGAWA, T., NISHIKAWA, K. & UEDA, T. 2001. Cell-free translation reconstituted with purified components. *Nature Biotechnology*, 19, 751-755.
- SHIRBAGHAEI, Z. & BOLHASSANI, A. 2016. Different applications of virus-like particles in biology and medicine: Vaccination and delivery systems. *Biopolymers*, 105, 113-132.
- SILVERMAN, A. D., KELLEY-LOUGHNANE, N., LUCKS, J. B. & JEWETT, M. C. 2019. Deconstructing Cell-Free Extract Preparation for in Vitro Activation of Transcriptional Genetic Circuitry. *ACS Synthetic Biology*, 8, 403-414.
- SITARAMAN, K., ESPOSITO, D., KLARMANN, G., LE GRICE, S. F., HARTLEY, J. L. & CHATTERJEE, D. K. 2004. A novel cell-free protein synthesis system. *Journal of Biotechnology*, 110, 257-263.
- SMITH, M. T., BERKHEIMER, S. D., WERNER, C. J. & BUNDY, B. C. 2014. Lyophilized Escherichia coli-based cell-free systems for robust, high-density, long-term storage. *BioTechniques*, 56, 186-193.
- SOLÁ, R. J. & GRIEBENOW, K. 2010. Glycosylation of therapeutic proteins: an effective strategy to optimize efficacy. *BioDrugs*, 24, 9-21.

- SONG, W. S., KIM, J.-H., CHOI, C.-M., LEE, W.-J. & YOON, S.-I. 2019. TLR5 binding and activation by KMRC011, a flagellin-derived radiation countermeasure. *Biochemical and Biophysical Research Communications*, 508, 570-575.
- SPIRIN, A. S., BARANOV, V. I., RYABOVA, L. A., OVODOV, S. Y. & ALAKHOV, Y. B. 1988. A continuous cell-free translation system capable of producing polypeptides in high yield. *Science*, 242, 1162.
- STARK, J. C., HUANG, A., NGUYEN, P. Q., DUBNER, R. S., HSU, K. J., FERRANTE, T. C., ANDERSON, M., KANAPSKYTE, A., MUCHA, Q., PACKETT, J. S., PATEL, P., PATEL, R., QAQ, D., ZONDOR, T., BURKE, J., MARTINEZ, T., MILLER-BERRY, A., PUPPALA, A., REICHERT, K., SCHMID, M., BRAND, L., HILL, L. R., CHELLASWAMY, J. F., FAHEEM, N., FETHERLING, S., GONG, E., GONZALZLES, E. M., GRANITO, T., KORITSARIS, J., NGUYEN, B., OTTMAN, S., PALFFY, C., PATEL, A., SKWERES, S., SLATON, A., WOODS, T., DONGHIA, N., PARDEE, K., COLLINS, J. J. & JEWETT, M. C. 2018. BioBits™ Bright: A fluorescent synthetic biology education kit. *Sci Adv*, 4, eaat5107.
- STECH, M., QUAST, R. B., SACHSE, R., SCHULZE, C., WÜSTENHAGEN, D. A. & KUBICK, S. 2014. A Continuous-Exchange Cell-Free Protein Synthesis System Based on Extracts from Cultured Insect Cells. *PLOS ONE*, 9, e96635.
- STOLLAR, E. J. & SMITH, D. P. 2020. Uncovering protein structure. *Essays Biochem*, 64, 649-680.
- TABOR, S. 2001. Expression using the T7 RNA polymerase/promoter system. *Curr Protoc Mol Biol*, Chapter 16, Unit16.2.
- TAKAHASHI, K., SATO, G., DOI, N. & FUJIWARA, K. 2021. A Relationship between NTP and Cell Extract Concentration for Cell-Free Protein Expression. *Life (Basel)*, 11.
- TANG, X. & PIKAL, M. J. 2004. Design of Freeze-Drying Processes for Pharmaceuticals: Practical Advice. *Pharmaceutical Research*, 21, 191-200.
- THE DEPARTMENT OF STATE, U. S. O. A. 1998. Space Station. TREATIES AND OTHER INTERNATIONAL ACTS SERIES 12927 ed. Washington, US.
- THOLE, A., FREY, D. & RAO, G. 2022. Purification challenges for the portable, on-demand point-of-care production of biologics. *Current Opinion in Chemical Engineering*, 36, 100802.
- THORING, L., DONDAPATI, S. K., STECH, M., WÜSTENHAGEN, D. A. & KUBICK, S. 2017. High-yield production of “difficult-to-express” proteins in a continuous exchange cell-free system based on CHO cell lysates. *Scientific Reports*, 7, 11710.
- THORING, L. & KUBICK, S. 2018. Versatile Cell-Free Protein Synthesis Systems Based on Chinese Hamster Ovary Cells. *Methods Mol Biol*, 1850, 289-308.
- TIMM, A. C., SHANKLES, P. G., FOSTER, C. M., DOKTYCZ, M. J. & RETTERER, S. T. 2016. Toward Microfluidic Reactors for Cell-Free Protein Synthesis at the Point-of-Care. *Small*, 12, 810-817.
- TONOOKA, T. 2020a. Freeze-Dried Cell-Free Protein Expression System in Microchambers Toward Point-of-Care Diagnostics. *2020 IEEE 33rd International Conference on Micro Electro Mechanical Systems (MEMS)*, 1036-1039.

- TONOOKA, T. 2020b. Microfluidic Device with an Integrated Freeze-Dried Cell-Free Protein Synthesis System for Small-Volume Biosensing. *Micromachines*, 12, 27.
- TWAIR, A., AL-OKLA, S., ZARKAWI, M. & ABBADY, A. Q. 2014. Characterization of camel nanobodies specific for superfolder GFP fusion proteins. *Molecular Biology Reports*, 41, 6887-6898.
- VISSER, N. V., HINK, M. A., BORST, J. W., VAN DER KROGT, G. N. M. & VISSER, A. J. W. G. 2002. Circular dichroism spectroscopy of fluorescent proteins. *FEBS Letters*, 521, 31-35.
- VOLOSHIN, A. M. & SWARTZ, J. R. 2005. Efficient and scalable method for scaling up cell free protein synthesis in batch mode. *Biotechnology and Bioengineering*, 91, 516-521.
- VOYVODIC, P. L., PANDI, A., KOCH, M., CONEJERO, I., VALJENT, E., COURTET, P., RENARD, E., FAULON, J.-L. & BONNET, J. 2019. Plug-and-play metabolic transducers expand the chemical detection space of cell-free biosensors. *Nature Communications*, 10, 1697.
- WANG, W. 2000. Lyophilization and development of solid protein pharmaceuticals. *International Journal of Pharmaceutics*, 203, 1-60.
- WANG, Y. & ZHANG, Y. H. P. 2009. Cell-free protein synthesis energized by slowly-metabolized maltodextrin. *BMC Biotechnology*, 9, 58.
- WANG, Z., LI, L., REN, G., DUAN, X., GUO, J., LIU, W., ANG, Y., ZHU, L. & REN, X. 2022. A comprehensive review on stability of therapeutic proteins treated by freeze-drying: induced stresses and stabilization mechanisms involved in processing. *Drying Technology*, 40, 3373-3388.
- WARFEL, K. F., WILLIAMS, A., WONG, D. A., SOBOL, S. E., DESAI, P., LI, J., CHANG, Y.-F., DELISA, M. P., KARIM, A. S. & JEWETT, M. C. 2023. A Low-Cost, Thermostable, Cell-Free Protein Synthesis Platform for On-Demand Production of Conjugate Vaccines. *ACS Synthetic Biology*, 12, 95-107.
- WAUDBY-WEST, R., PARCELL, B. J., PALMER, C. N. A., BELL, S., CHALMERS, J. D. & SIDDIQUI, M. K. 2021. The association between SARS-CoV-2 RT-PCR cycle threshold and mortality in a community cohort. *European Respiratory Journal*, 58, 2100360.
- WHITFIELD, C. J., BANKS, A. M., DURA, G., LOVE, J., FIELDSEND, J. E., GOODCHILD, S. A., FULTON, D. A. & HOWARD, T. P. 2020. Cell-free protein synthesis in hydrogel materials. *Chemical Communications*, 56, 7108-7111.
- WIEGAND, D. J., LEE, H. H., OSTROV, N. & CHURCH, G. M. 2018. Establishing a Cell-Free *Vibrio natriegens* Expression System. *ACS Synthetic Biology*, 7, 2475-2479.
- WILDING, K. M., HUNT, J. P., WILKERSON, J. W., FUNK, P. J., SWENSEN, R. L., CARVER, W. C., CHRISTIAN, M. L. & BUNDY, B. C. 2019. Endotoxin-Free *E. coli*-Based Cell-Free Protein Synthesis: Pre-Expression Endotoxin Removal Approaches for on-Demand Cancer Therapeutic Production. *Biotechnol J*, 14, e1800271.
- WILLIAMS, P. M., SHIVAKUMAR, T. & ANYANWU, V. 2022. Space Medicine and Countermeasures. *In-Space Manufacturing and Resources*.
- WINGFIELD, P. T. 2015. Overview of the purification of recombinant proteins. *Curr Protoc Protein Sci*, 80, 6.1.1-6.1.35.

- WOODY, R. W. 1995. [4] Circular dichroism. *Methods in Enzymology*. Academic Press.
- WOTRING, V. E. 2015. Medication use by U.S. crewmembers on the International Space Station. *Faseb j*, 29, 4417-23.
- WU, P. S., OZAWA, K., LIM, S. P., VASUDEVAN, S. G., DIXON, N. E. & OTTING, G. 2007. Cell-free transcription/translation from PCR-amplified DNA for high-throughput NMR studies. *Angew Chem Int Ed Engl*, 46, 3356-8.
- YANG, H., YANG, S., KONG, J., DONG, A. & YU, S. 2015. Obtaining information about protein secondary structures in aqueous solution using Fourier transform IR spectroscopy. *Nature Protocols*, 10, 382-396.
- YANG, S. O., NIELSEN, G. H., WILDING, K. M., COOPER, M. A., WOOD, D. W. & BUNDY, B. C. 2019. Towards On-Demand E. coli-Based Cell-Free Protein Synthesis of Tissue Plasminogen Activator. *Methods and Protocols*, 2.
- YARI, S., BEHZADIAN, F., ROUHANI NEJAD, H., MASOUMIAN, M. R. & KARIMI, M. 2017. Expression and Purification of Soluble form of Human Parathyroid Hormone (rhPTH1-34) by Trx Tag in E. coli. *Res-Mol-Med*, 5, 26-31.
- YU, C.-H., DANG, Y., ZHOU, Z., WU, C., ZHAO, F., SACHS, MATTHEW S. & LIU, Y. 2015. Codon Usage Influences the Local Rate of Translation Elongation to Regulate Co-translational Protein Folding. *Molecular Cell*, 59, 744-754.
- ZAMECNIK, P. C., FRANTZ, I. D., JR. & ET AL. 1948. Incorporation in vitro of radioactive carbon from carboxyl-labeled dl-alanine and glycine into proteins of normal and malignant rat livers. *J Biol Chem*, 175, 299-314.
- ZAWADA, J. F., YIN, G., STEINER, A. R., YANG, J., NARESH, A., ROY, S. M., GOLD, D. S., HEINSOHN, H. G. & MURRAY, C. J. 2011. Microscale to manufacturing scale-up of cell-free cytokine production—a new approach for shortening protein production development timelines. *Biotechnology and Bioengineering*, 108, 1570-1578.
- ZEMELLA, A., THORING, L., HOFFMEISTER, C. & KUBICK, S. 2015a. Cell-Free Protein Synthesis: Pros and Cons of Prokaryotic and Eukaryotic Systems. *ChemBioChem*, 16, 2420-2431.
- ZEMELLA, A., THORING, L., HOFFMEISTER, C. & KUBICK, S. 2015b. Cell-Free Protein Synthesis: Pros and Cons of Prokaryotic and Eukaryotic Systems. *ChemBioChem*, 16, 2420-2431.
- ZHANG, L., LIN, X., WANG, T., GUO, W. & LU, Y. 2021. Development and comparison of cell-free protein synthesis systems derived from typical bacterial chassis. *Bioresources and Bioprocessing*, 8, 58.
- ZHUO, X.-F., ZHANG, Y.-Y., GUAN, Y.-X. & YAO, S.-J. 2014. Co-expression of disulfide oxidoreductases DsbA/DsbC markedly enhanced soluble and functional expression of reteplase in Escherichia coli. *Journal of Biotechnology*, 192, 197-203.
- ZUBAY, G. 1973. IN VITRO SYNTHESIS OF PROTEIN IN MICROBIAL SYSTEMS. *Annual Review of Genetics*, 7, 267-287.
- ZUBAY, G. 1980. [77] The isolation and properties of CAP, the catabolite gene activator. *Methods in Enzymology*. Academic Press.

Supplementary information

Synthetic DNA fragments

> sfGFP_His

TAATACGACTCACTATAGGGAGACCACAACGGTTTCCCTCTAGAAATAATTT
TGTTAACTTTAAGAAGGAGATATACATATGCGTAAAGGCGAAGAGCTGTT
CACTGGTGTTCGTCCTATTCTGGTGGAACTGGATGGTGTGCAACGGTCAT
AAGTTTTCCGTGCGTGCGGAGGGTGAAGGTGACGCAACTAATGGTAAACTG
ACGCTGAAGTTCATCTGTACTACTGGTAAACTGCCGGTACCTTGGCCGACTC
TGGTAACGACGCTGACTTATGGTGTTCAGTGCTTTGCTCGTTATCCGGACCAT
ATGAAGCAGCATGACTTCTTCAAGTCCGCCATGCCGGAAGGCTATGTGCAG
GAACGCACGATTTCTTTAAGGATGACGGCACGTACAAAACGCGTGCGGAA
GTGAAATTTGAAGGCGATACCCTGGTAAACCGCATTGAGCTGAAAGGCATT
GACTTTAAAGAAGACGGCAATATCCTGGGCCATAAGCTGGAATACAATTTT
AACAGCCACAATGTTTACATCACCGCCGATAAACAAAAAAATGGCATTAA
AGCGAATTTTAAAATTCGCCACAACGTGGAGGATGGCAGCGTGCAGCTGGC
TGATCACTACCAGCAAAACACTCCAATCGGTGATGGTCCTGTTCTGCTGCCA
GACAATCACTATCTGAGCACGCAAAGCGTTCTGTCTAAAGATCCGAACGAG
AAACGCGATCATATGGTTCTGCTGGAGTTCGTAACCGCAGCGGGCATCACG
CATGGTATGGATGAACTGTACAAACACCACCACCACCACCACTGA

> Retepase_His

GTAAAACGACGGCCAGTGAATTCGAGCTCATATGAGCTACCAGGGCAACA
GCGATTGCTACTTCGGCAATGGCAGCGCCTATCGCGGCACCCACAGCCTGA
CCGAAAGCGGCGCCAGCTGCCTGCCGTGGAATAGCATGATCCTGATCGGCA
AAGTGTATACCGCCCAGAACCCGAGCGCGCAGGCGCTGGGTCTGGGTAAAC
ATAATTATTGTCGCAATCCGGATGGCGATGCGAAACCGTGGTGCCATGTGCT
GAAAAATCGCCGCTGACCTGGGAATATTGCGACGTGCCGAGCTGCAGCAC
CTGCGGCCTGCGTCAGTATAGCCAGCCGCAGTTCGCATTAAAGGCGGCCT
GTTTCGCGGACATTGCGAGCCATCCGTGGCAGGCGGCCATCTTCGCGAAACA
TCGCCGACGCCCGGGCGAACGCTTCCTGTGTGGCGGCATCCTGATTAGCAG
CTGCTGGATCTTAAGCGCGGCGCACTGCTTCCAGGAACGCTTCCC GCCGAT
CACCTGACCGTGATTCTGGGCCGCACCTACCGCGTGGTGCCGGGTGAAGAA
GAACAGAAATTCGAAGTGGA AAAAATACATCGTGCAAAAGAATTCGATGA
CGATACCTACGATAACGACATTGCCCTGCTGCAGCTGAAAAGCGATAGCAG

CCGCTGCGCCAGGAAAGCAGCGTGGTGCGCACCGTGTGTCTGCCGCCGGC
AGACCTGCAGCTGCCGGATTGGACCGAATGCGAACTGAGCGGCTATGGCAA
ACACGAAGCCCTGAGCCCGTTCTATAGCGAACGCCTGAAAGAAGCCCACGT
GCGCCTGTACCCGAGCAGCCGTTGCACCAGCCAGCACCTGCTGAACCGCAC
CGTGACCGACAACATGCTGTGCGCCGGCGACACCCGCGAGCGGTGGTCCTCA
AGCCAACCTGCATGACGCCTGCCAGGGCGACAGCGGCGGTCTCTGGTGTG
TCTGAACGACGGCCGCATGACCCTGGTGGGCATTATCAGCTGGGGCCTGGG
CTGCGGCCAGAAAGATGTGCCGGGCGTGTACACCAAAGTGACCAACTACCT
GGACTGGATTGCGGATAATATGCGCCCCGCATCATCACCATCACCACTAA

> **Entolimod** His

GTAAAACGACGGCCAGTGAATTCGAGCTCATATGGCACAGGTGATCAATAC
CAATAGCCTGAGCCTGCTGACCCAGAATAATCTGAATAAAAGCCAGAGCA
GCCTGAGCAGCGCGATTGAACGCCTGAGCAGCGGCCTGCGCATCAATAGCG
CCAAAGATGATGCGGCCGGCCAGGCCATTGCCAATCGCTTCACCAGCAATA
TTAAAGGCCTGACCCAGGCCAGCCGCAATGCCAATGATGGCATCAGCATTG
CGCAGACCACCGAAGGCGCGCTGAATGAAATCAATAATAATCTGCAGCGC
GTGCGGAACTGAGCGTGCAGGGCGACCAATGGCACCAATAGCGATAGCGA
TCTGAAAAGCATTTCAGGATGAAATCCAGCAGCGCCTGGAAGAAATCGATCG
CGTGAGCAATCAGACCCAGTTCAATGGCGTGAAAGTGCTGAGCCAGGATAA
TCAGATGAAAATTCAGGTGGGCGCGAATGATGGCGAAACCATCACCATCGA
TCTGCAGAAAATCGATGTGAAAAGCCTGGGCCTGGATGGCTTCAATGTGAA
TAGCCCGGGCATTAGCGGCGGCGGCGGCGGTATTCTGGATAGCATGGGCAC
CCTGATTAATGAAGATGCCGCCGCGGAAAAAAGCACCGCGAATCCGCT
GGCGAGCATTGATAGCGCGCTGAGCAAAGTGGATGCCGTGCGCAGCAGCCT
GGGCGCAATTCAGAATCGCTTCGATAGCGCCATTACCAATCTGGGCAATAC
CGTGACCAATCTGAATAGCGCCCGCAGCCGCATTGAAGATGCGGATTATGC
CACCGAAGTGAGCAATATGAGCAAAGCCCAGATTCTGCAGCAGGCCGGCA
CCAGCGTGCTGGCACAGGCAAATCAGGTGCCGCAGAATGTGCTGAGCCTGC
TGCGCCATCATCATCATCACCATTAA

> **G-CSF** His

GTAAAACGACGGCCAGTGAATTCGAGCTCATATGACCCCTCTGGGCCCTGC
AAGCAGCCTGCCGCAGAGCTTCTGCTGAAATGCCTGGAACAGGTGCGCAA
AATTCAGGGCGATGGCGCGGCGCTGCAGGAAAACTGTGTGCGACCTATAA
ACTGTGCCATCCGGAAGAAGTGGTGTGCTGGGCCATAGCCTGGGCATTCC
GTGGGCCCCGCTGAGCAGCTGCCCCGAGCCAAGCACTGCAGCTGGCGGGCTG
CCTGAGCCAGCTGCATAGCGGCCTGTTCTGTATCAGGGCCTGCTGCAGGCG

CTGGAAGGCATCAGCCCGGAACTGGGCCCCGACCCTGGATAACCCTGCAGCTG
GATGTGGCCGACTTCGCGACCACCATCTGGCAGCAGATGGAAGAACTGGGC
ATGGCCCCGGCGCTGCAGCCTACACAGGGCGCAATGCCGGCGTTCGCGAGC
GCATTCCAGCGCCGTGCCGGCGGTGTGCTGGTGGCAAGTCATCTGCAGAGC
TTCCTGGAAGTGAGCTATCGCGTGCTGCGCCATCTGGCGCAGCCGCATCATC
ATCATCACCATTA

> **Alfimeprase_His**

GAGCTCATATGAGCTTCCCGCAGCGCTATGTGCAGCTGGTGATCGTGGCCGA
TCATCGCATGAATACCAAATATAATGGCGATAGCGATAAAATCCGCCAGTG
GGTGCATCAGATTGTGAATACCATCAATGAAATCTATCGCCCCTGAATATC
CAGTTCACCCTGGTGGGCCTGGAAATCTGGAGCAATCAGGATCTGATCACC
GTGACCAGCGTGAGCCATGATACCCTGGCCAGCTTCGGCAATTGGCGCGAA
ACCGATCTGCTGCGCCGCCAGCGCCATGATAATGCCAGCTGCTGACCGCG
ATTGACTTCGATGGCGATAACCGTGGGCCTGGCGTATGTGGGCGGCATGTGCC
AGCTGAAACATAGCACCGGCGTGATCCAGGATCATAGCGCCATCAATCTGC
TGGTGGCGCTGACCATGGCGCATGAACTGGGCCATAATCTGGGCATGAATC
ATGATGGCAATCAGTGTCAATTGCGGGCGGAATAGCTGCGTGATGGCGGCGA
TGCTGAGCGATCAGCCGAGCAAACCTGTTTCAGCGATTGTAGCAAAAAAGATT
ATCAGACCTTCTGACCGTGAATAATCCGCAGTGTATCCTGAATAAACCGC
ATCATCATCATCACCATTAATAACTCGAGGGATCC

> **Teriparatide_His**

GAGCTCATATGAGCGTGAGCGAAATCCAGCTGATGCATAATCTGGGCAAAC
ATCTGAATAGCATGGAACGCGTGGAATGGCTGCGCAAAAAACTGCAGGAT
GTGCATAACTTCATCATCATCATCACCATTAATAACTCGAGGGATCC

> **NBS07_His**

AGATCTCGATCCCGCGAAATTAATACGACTCACTATAGGGAGACCACAACG
GTTTCCCTCTAGAAATAATTTTGTTTAACTTTAAGAAGGAGATATACATATG
CAGGTGCAGCTGCAGGAGTCTGGGGGAGGCTCGGTGCAGGCTGGAGGGTCT
CTGAGACTCTCCTGTGCAGCCTCTGGAAACACTCACATTACATTGGCCTGGT
TCCGCCAGGCTCCAGGGAAGGAGCGCGAGGGGGTTCGTTTTTATTTACACTA
GTACTGGTTACACATACTATTCCGACTCAGTGAAGGGCCGATTCACCATCTC
CCAAGACAACGCCAAGAACACGGTGTATCTGCAAATGGACAACCTGAAAC
CAGAGGACGCTGGCATGTACTACTGTGCAGCAGGACGCACCCGTAGTGTTCC

GACCTGGTGGCAGAATCGACCCCGGGGCATTTGATTACTGGGGCCAGGGGA
CCCAGGTCACCGTCTCCTCACACCACCACCACCACCACTGAACTCGAG

Plasmid maps

> sfGFP_His

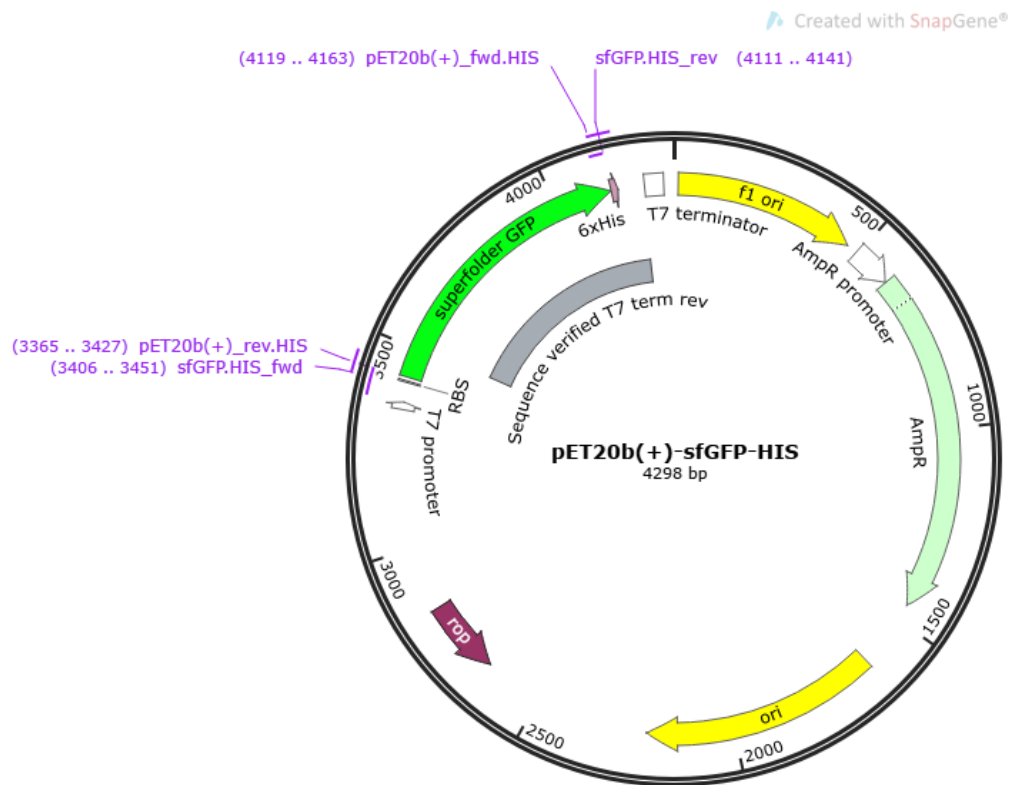


Figure S 1: Plasmid design for the pET20b-sfGFP-His DNA created using SnapGene. sfGFP sequence is highlighted in green and contains a C-terminal hexahistidine tag.

> Reteplase_His

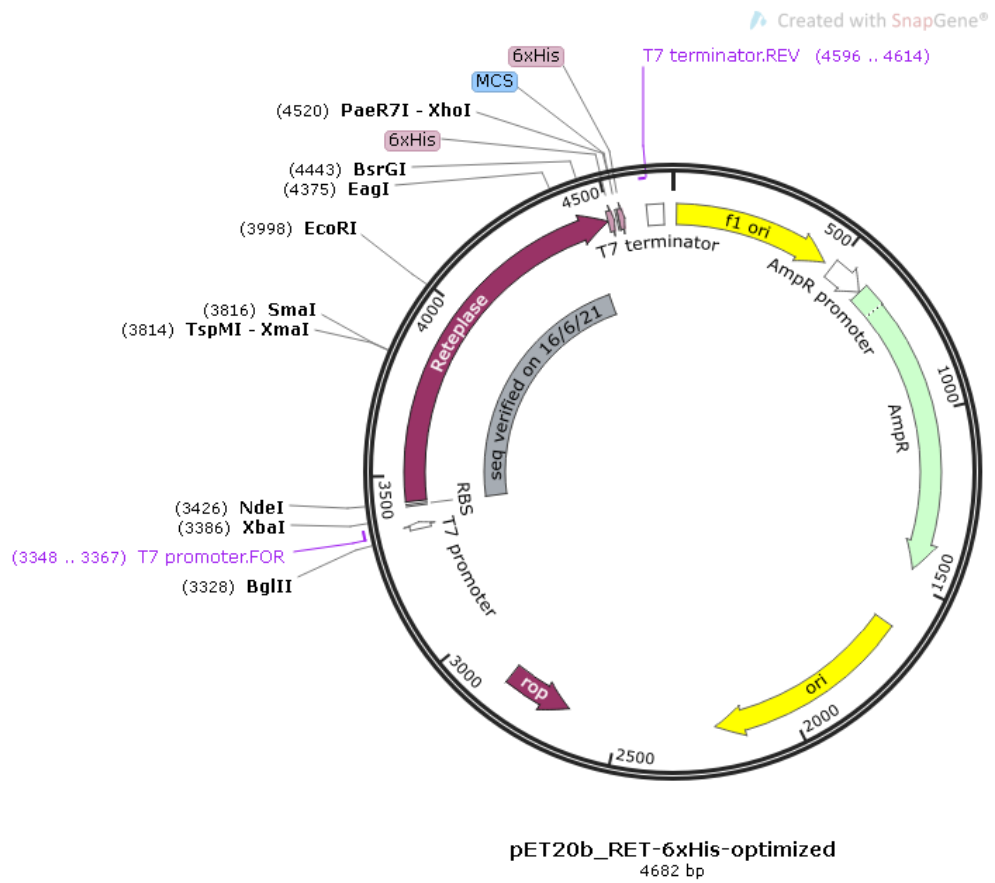


Figure S 2: Plasmid design for the pET20b-Reteplase-His DNA created using SnapGene. Reteplase sequence is highlighted in purple and contains a C-terminal hexahistidine tag.

> Entolimod_His

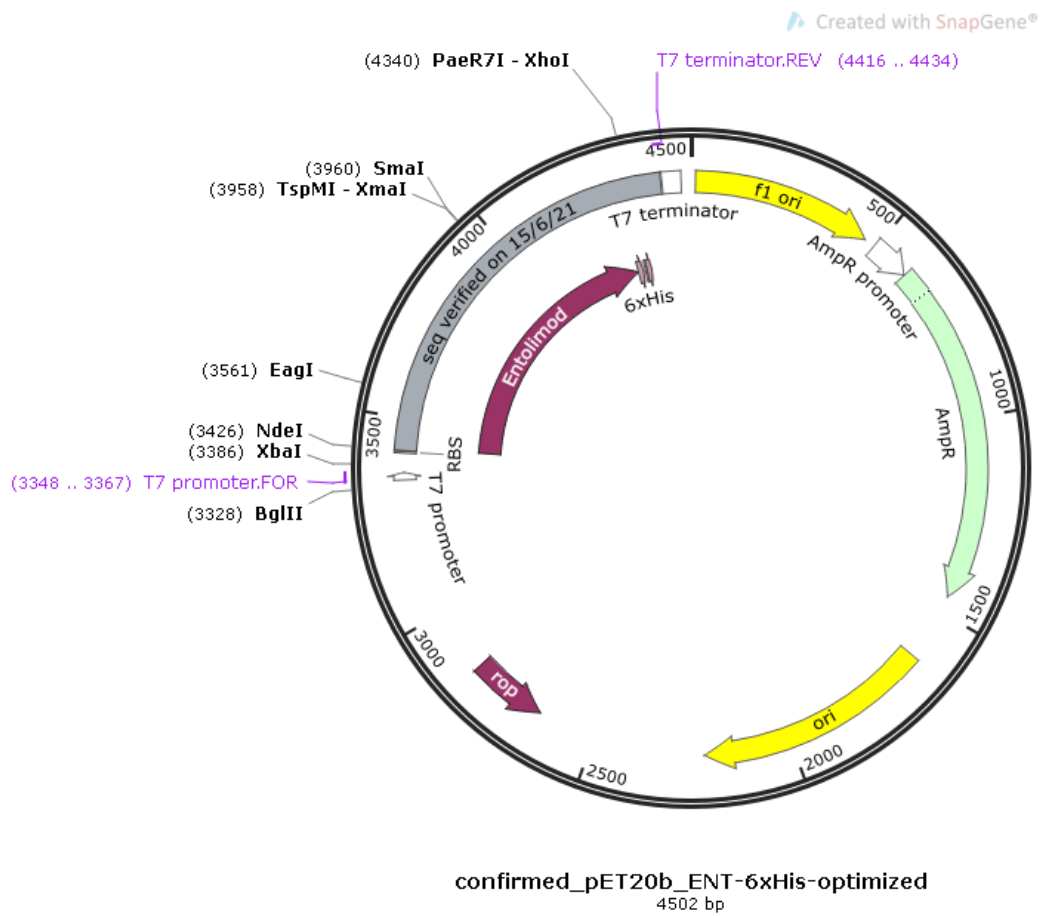


Figure S 3: Plasmid design for the pET20b-Ent-His DNA created using SnapGene. Entolimod sequence is highlighted in purple and contains a C-terminal hexahistidine tag.

> G-CSF_His

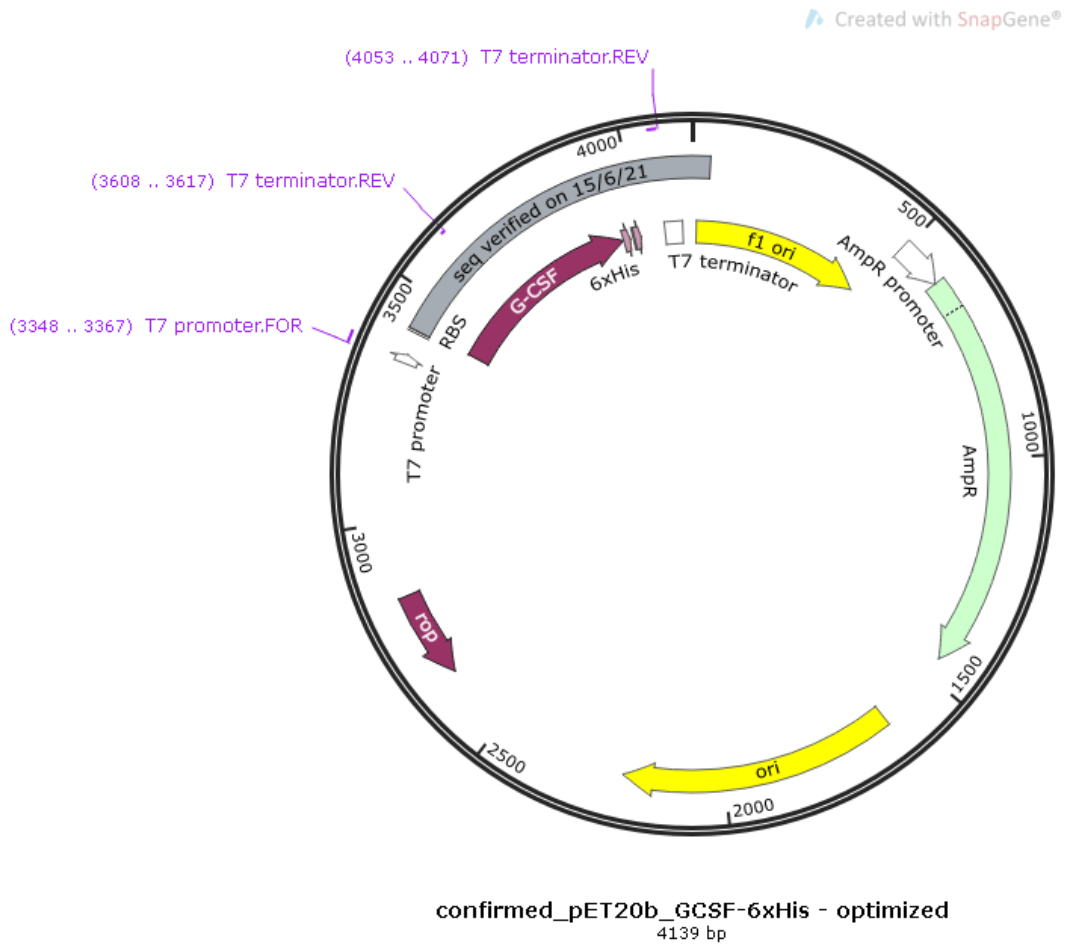


Figure S 4: Plasmid design for the pET20b-GCSF-His DNA created using SnapGene. G-CSF sequence is highlighted in purple and contains a C-terminal hexahistidine tag.

> Alfimeprase_His

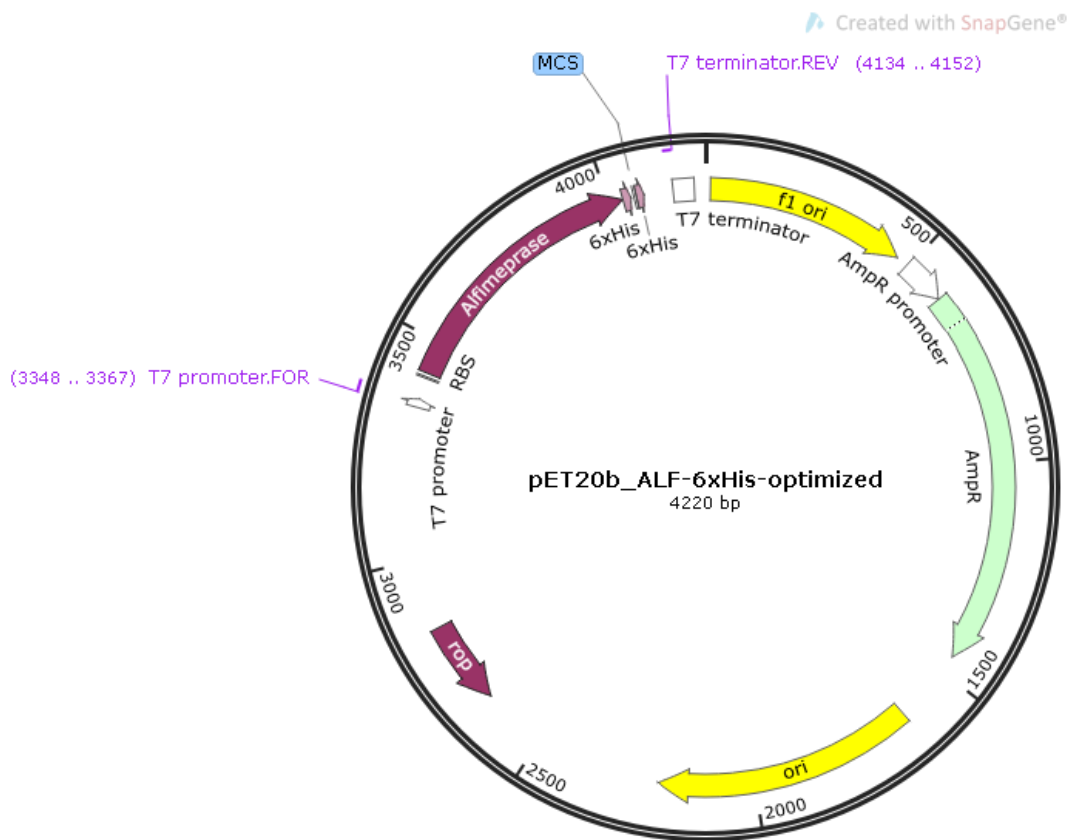


Figure S 5: Plasmid design for the pET20b-Alf-His DNA created using SnapGene. Alfimeprase sequence is highlighted in purple and contains a C-terminal hexahistidine tag.

> Teriparatide_His

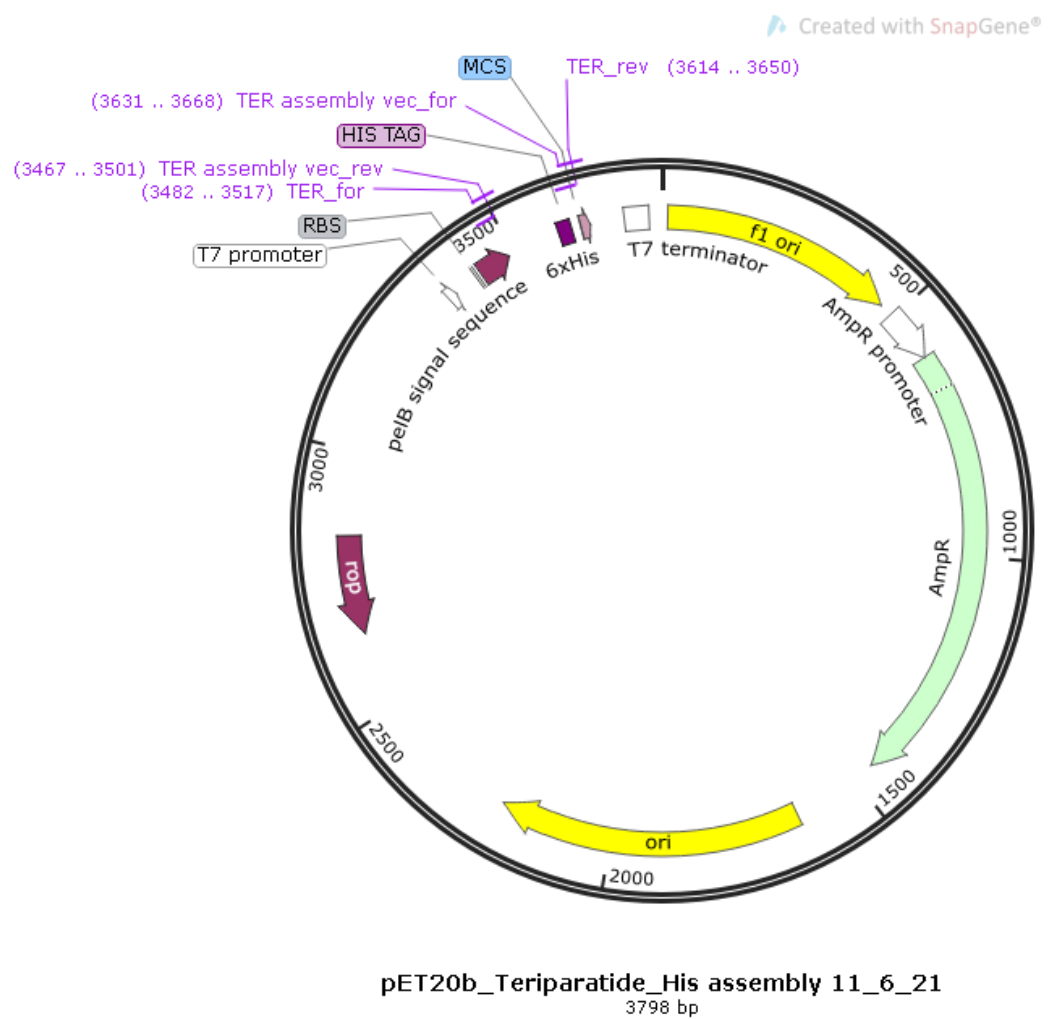


Figure S 6: Plasmid design for the pET20b-Ter-His DNA created using SnapGene. Teriparatide sequence is highlighted in purple and contains a C-terminal hexahistidine tag.

> NBS07_His

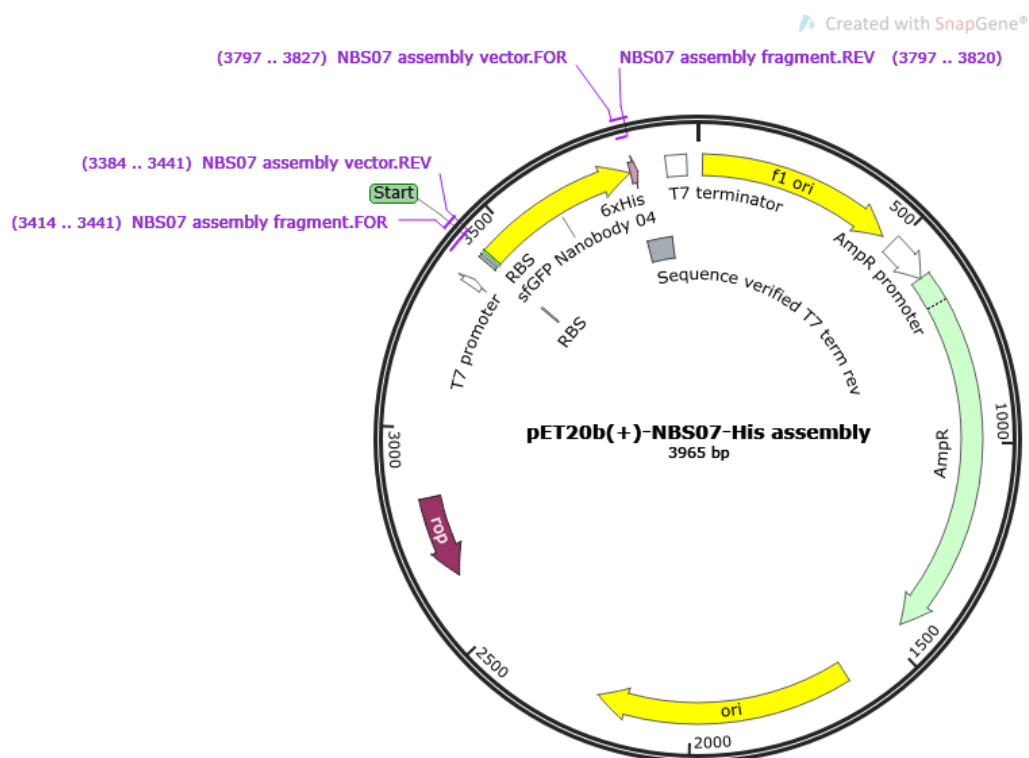
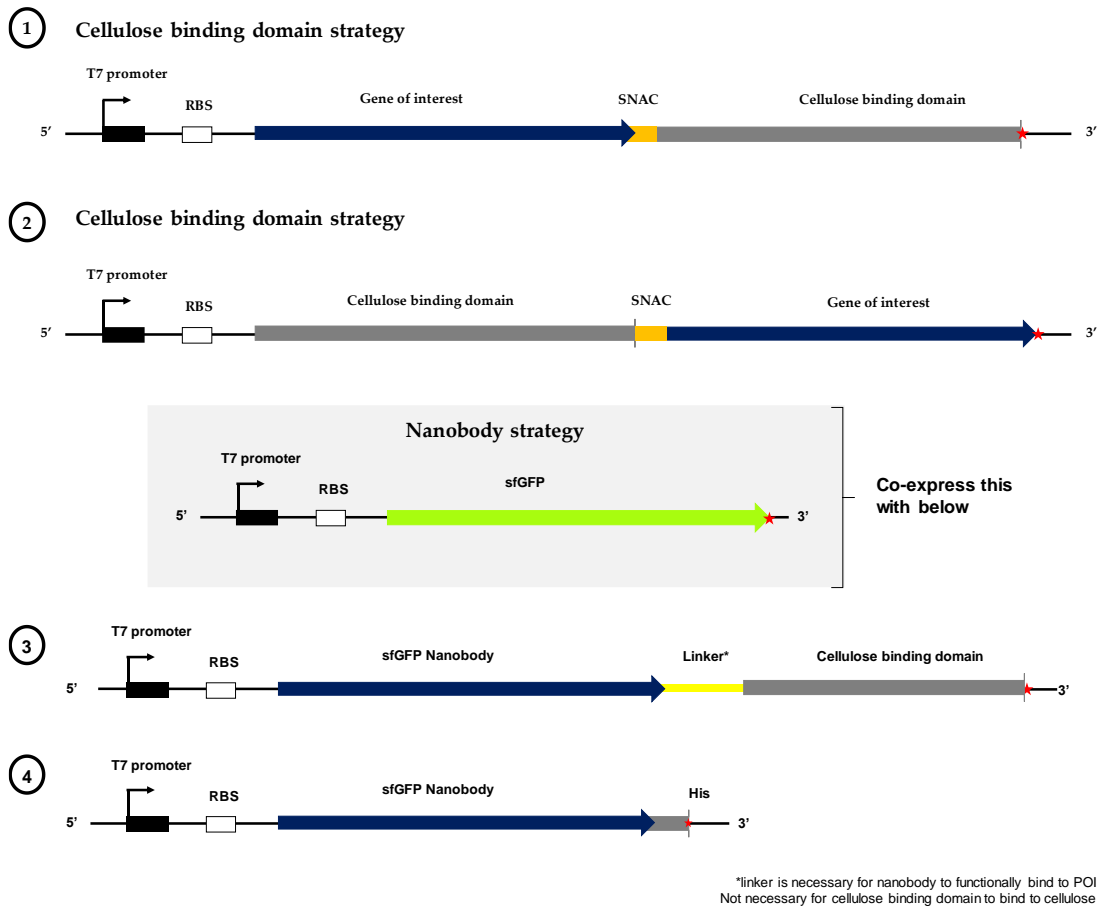


Figure S 7: Plasmid design for the pET20b-sfGFP-Nanobody07-His DNA created using Snapgene. The Nanobody sequence is highlighted in yellow and contains a C-terminal hexahistidine tag.

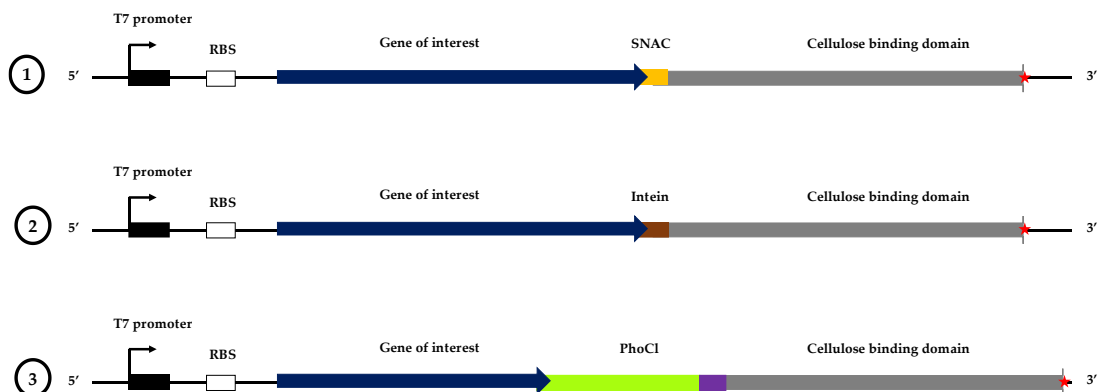
***In situ* purification templates (*In silico* designs)**

The cellulose binding domain strategy was considered for the immobilisation of cell-free produced proteins onto cellulose when carried out in the paper-based format. Similar to the pET system used for the above therapeutics and fluorescent reporter, the design contained an N-terminal T7 promoter and ribosome binding sequence. The cellulose binding domain was considered as an N-terminal or C-terminal tag for the gene of interest, separated by a SNAC tag (designs 1 and 2 below; further details on linkers and tags are provided in Figure S.8). The nanobody strategy was considered for *in situ* purification and quality control of cell-free produced target proteins. For the initial proof-of-concept experiments described in Chapter 6, sfGFP and its nanobody sfGFP-NBS-07 were co-expressed. To implement this strategy, the existing sfGFP gene was considered for co-expression with two nanobody designs. The first design involved a cellulose binding domain attached to the nanobody via a flexible linker (for above paper-based expression methods) and the second was a his-tagged nanobody construct, which was utilised in Chapter 6 (designs 3 and 4 below).



Cellulose binding domain linker strategies for *in situ* purification

In addition to the above *in silico* designs, three linkers were considered for connecting tags (such as the cellulose binding domain) and target protein(s). They were SNAC, Intein and PhoCl, chosen for their cleavage properties and ease of implementation for on-site and on-demand applications. The main features of these linkers are summarised in Figure S.8, where it is evident that each linker has equally advantageous and disadvantageous properties. Linker designs should be carefully chosen and implemented based on end application.





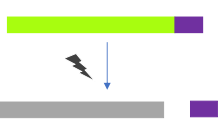
Linker	Cleavage	Scar?	Notes
SNAC 	-GSHHW- cleaves in the presence of NiCl ₂	NO	Buffer exchange required, need to get NiCl ₂ out
Intein 	Self-cleaves when temp/pH changes	NO	Random cleavage possible during expression, cleavage may not be very efficient. Overnight cleavage required!
PhoCl 	Cleaves in the presence of light (400nm) [Visual confirmation of expression]	YES	Buffer exchange potentially not require if wash is performed with final buffer after light. Regulatory issues due to scar, although an ideal feature for on-demand visualisation

Figure S 8: Linkers considered for the *in situ* purification designs, their methods of cleaving, remaining scars and points to consider

Room temperature measurements for stability studies

Room temperature stability studies were conducted on the lab bench, where the lab temperature was monitored every 30 minutes from August 2022 to June 2023, the time period in which all stability studies were conducted. The average temperature experienced by all samples were ~ 20°C, which falls within the room temperature range (Figure S.9). The temperature during winter months were significantly lower (~ 16°C) and summer months were significantly higher (~ 21°C). All other stability studies (at 40°C and 4°C) were conducted in a stability oven and fridge respectively.

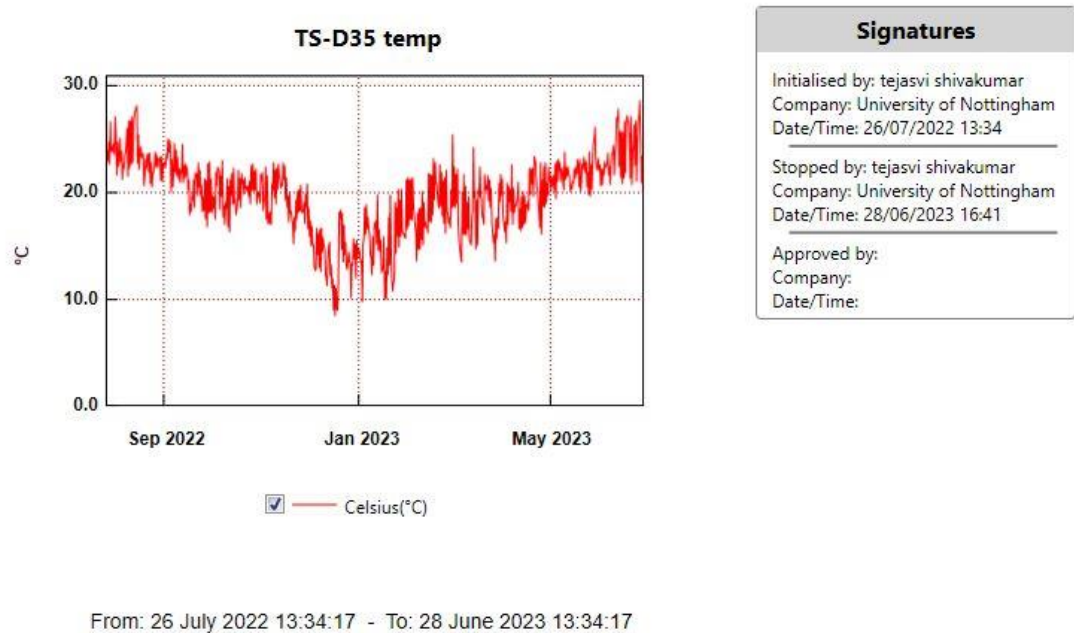


Figure S 9: Taken using the Lascar EL-21CFR-2-LCD Temperature & Humidity Data Logger, one reading taken every 30 minutes.

Impact of refrigeration on post-flight cell-free samples until for the VITA mission

Following the completion of the VITA mission, an astronaut will move the cube to the ISS fridge for sample storage until a return flight carries the cube back to Earth (also in a refrigerated format). Upon return of the experiment, several post-flight analyses will be performed, subject to intact sample integrity. To study and quantify the viability of post-cell-free-synthesised samples, a simulation of this operation was carried out. Cell-free reactions that produced sfGFP was immediately moved to the fridge upon reaction completion and fluorescence was quantified every month for four months (the maximum time in the fridge on the ISS). No significant difference was observed between the month 0 and month 4 samples, implying that sample integrity was preserved during this period (Figure S.10). It is important to note that this data confirms stability and viability only for sfGFP (as fluorescence implies stability and activity sfGFP). This experiment would need to be repeated for any other target protein, such as a therapeutic.

Fluorescence of cell-free synthesised sfGFP-His at 4°C over time

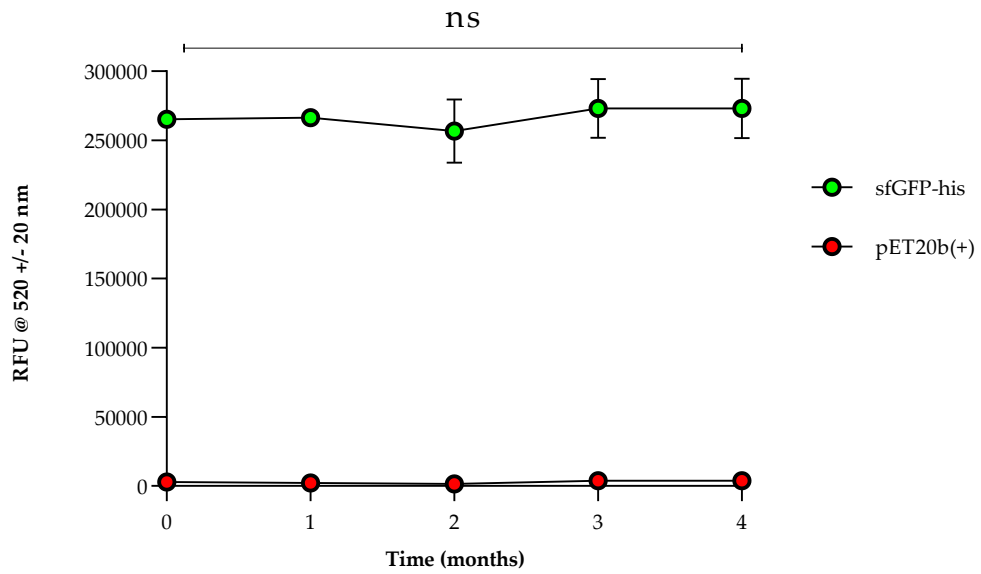


Figure S 10: Fluorescence of cell-free synthesised sfGFP-His at 4°C over 4 months. Fluorescence recordings were taken every month; experiments were performed in triplicates ($n = 3$); data are shown as mean \pm SD. Two-way repeated measures ANOVA was performed to test significance; P value $> 0.05 = ns$.